Universitat Autònoma de Barcelona

Aprofundiment en la relació estructura/funció de diverses metal·lotioneïnes (MTs) per analitzar els factors que determinen la seva especificitat metàl·lica

SÍLVIA PÉREZ RAFAEL

TESI DOCTORAL

PROGRAMA DE DOCTORAT EN QUÍMICA

Dirigida per:
ÒSCAR PALACIOS BONILLA
MERCÈ CAPDEVILA VIDAL

DEPARTAMENT DE QUÍMICA
FACULTAT DE CIÈNCIES

2013

4. CONCLUSIONS

4. Conclusions

Els resultats exposats en aquesta Tesi Doctoral ha permès arribar a un conjunt de conclusions, les quals s'exposen a continuació agrupades d'acord amb els objectius parcials proposats. Algunes de les conclusions que responen a l'objectiu principal (identificar els factors que determinen l'especificitat metàl·lica de les MTs) es troben incorporats a les conclusions parcials marcats en cursiva.

- **Comportament de les MTs de mol·lusc**

  - *Comportament de les MTs de* Helix pomatia

    - Els resultats obtinguts, tant *in vivo* com *in vitro*, permeten concloure que les dues isoformes d'MT, HpCdMT i HpCuMT, presenten unes especificitats metàl·liques extremes i completament oposades vers els ions metàl·lics divalents (Zn(II) i Cd(II)) i monovalents (Cu(I)):

    - HpCdMT es classifica com a Zn-tioneïna amb una especial preferència per enllaçar Cd(II), formant-se l'espècie Cd_6-HpCdMT.

    - La isoforma HpCuMT, presenta una gran preferència per enllaçar Cu(I) i, per tant, es classifica com una Cu-tioneïna.

    - El fet que totes dues isoformes tinguin una seqüència d'aminoàcids (aa) amb una elevada homologia, especialment pel que fa al nombre de Cys (aa coordinants) i les seves posicions, i alhora presentin especificitat metàl·liques completament oposades, permet concloure que *és el conjunt d'aa, els coordinants i els no coordinants, els que determinen l'especificitat metàl·lica en aquestes dues isoformes d'MT, i no només les Cys i les His*, com proposen molts autors.

    - Els resultats obtinguts amb la isoforma HpCuMT mutada, HpCuMTmut, on el residu d'His ha estat substituït per Ala, demostren que el comportament coordinant, tant *in vivo* com *in vitro*, és molt similar al de la forma nativa, HpCuMT, si bé presenta una especificitat metàl·lica enfront el Cu(I) molt més marcada que la forma nativa, augmentant l'estabilitat de l'espècie preferent Cu_{12}-MT. Aquests fets demostren que *el residu d'His no té un clar paper coordinant en HpCuMT però molt probablement és el responsable de l'alliberament de Cu(I)*, i per tant, pot ser una peça clau en la funció de HpCuMT com a donadora de Cu(I) a l'hemocianina en els rogòcits.

  - *Comportament de les MTs de* Cornu aspersum

    - El resultats obtinguts permeten concloure que les tres isoformes d'MT de C.aspersum (CaCdMT, CaCdCuMT i CaCuMT) tenen especificitats metàl·liques clarament diferents:

- La isoforma CaCdMT presenta una gran preferència per enllaçar els cations divalents Zn(II) i Cd(II), i s'ha classificat com a Zn-tioneïna, donant lloc a la formació de l'espècie Cd_6-CaCdMT, tant *in vivo* com *in vitro*.
- CaCuMT s'ha classificat com a Cu-tioneïna degut a la preferència per Cu(I). Es forma amb gran preferència el complex Cu_{12}-CaCuMT *in vivo*.
- La isoforma CaCdCuMT mostra un comportament intermedi entre les Zn- i les Cu-tioneïnes, si bé té una major preferència per enllaçar l'ió monovalent Cu(I).

- Un cop més, *la similitud seqüencial de les tres isoformes i la diversitat de comportaments en coordinar els ions metàl·lics fa palès l'important paper del conjunt d'aminoàcids per determinar la preferència metàl·lica*.

○ *Comportament de l'MT de* Megathura crenulata

- L'única MT descoberta en *M. cranulata* fins el moment, McMT, té un comportament, tant *in vivo* com *in vitro*, que indica que aquesta proteïna mostra una preferència metàl·lica intermèdia entre les Zn- i les Cu-tioneïnes, tot i mostrar una especial preferència per formar l'espècie Cd_6-McMT.
- El caràcter polivalent de McMT està d'acord amb el fet que una única MT hagi de fer els diferents papers per la qual sigui requerida (detoxificadora enfront de Cd(II) i homeòstasi de Zn(II) i Cu(I)).

○ *Comparació del comportament de les diferents MT dels mol·luscs* Helix pomatia, Cornu Aspersum *i* Megathura Crenulata

- Els resultats obtinguts, *in vivo* i *in vitro*, i l'estudi filogenètic de les diferents proteïnes de mol·luscs estudiades han permès diferenciar 3 grups, en base a la seva preferència metàl·lica: les classificades com a Zn-tioneïnes (CaCdMT i HpCdMT), les Cu-tioneïnes (HpCuMT i CaCuMT) i dues isoformes que tenen un comportament intermedi, la CaCdCuMT i la McMT.
- Els estudis filogenètics indiquen que HpCdMT i CaCdMT provenen d'un ancestre comú, explicant així l'elevada similitud en quant al comportament, formant les mateixes espècies M_6-MT (M= Zn, Cd).
- Comparant el comportament de les isoformes CaCuMT i HpCuMT, si bé totes dues han estat classificades com a Cu-tioneïnes, s'ha pogut concloure que CaCuMT té un caràcter més marcat de Cu-tioneïna que HpCuMT.
- L'estudi filogenètic indica que les isoformes CaCuMT, HpCuMT i CaCdCuMT provenen d'un ancestre comú, clarament segregat de la línea de les CdMT, en correspondència amb el comportament metàl·lic observat tant *in vivo* com *in vitro*.

➢ **Comportament de les dues isoformes d'MT de l'amfiox *Brianchostoma floridae*, BfMT1 i BfMT2**

- Les dues isoformes d'MT identificades al partir del genoma de *B.floridae*, BfMT1 i BfMT2, han mostrat diferències de comportament quan enllacen Zn(II), Cd(II) i Cu(I), però cap d'elles ha mostrat un clar caràcter ni de Zn- ni de Cu-tioneïna, tenint un comportament intermig.
- En comparar-les acuradament es pot concloure que la isoforma BfMT2 té un caràcter de Cu-tioneïna més marcat que no pas l'observat per a BfMT1.

➢ **Comportament de la cinquena isoforma d'MT del sistema d'MTs de la mosca *Drosophila melanogaster*, MtnE**

- L'estudi de les propietats coordinants de la cinquena isoforma en el sistema d'MT de *Drosophila melanogaster*, de la que es coneixien 4 isoformes amb un clar caràcter de Cu-tioneïna, indica que MTnE pertany al grup de les MntB-like si bé aquesta és la menys Cu-tioneïna de totes les isoformes prèviament descrites en aquest grup.

➢ **Obtenció dels paràmetres termodinàmics associats al desplaçament metàl·lic Zn(II)/Cd(II) en les formes Zn-MT de diverses metal·lotioneïnes mitjançant ITC**

- L'ITC ha permès determinar els paràmetres termodinàmics (ΔH, ΔS, K) associats al desplaçament metàl·lic Zn^{II}/Cd^{II} a partir de les formes Zn-MT de diverses MT de manera acurada i precisa, a partir d'un únic experiment.
- Les dades han permès confirmar que tots els processos de desplaçament metàl·lic són exotèrmics ($\Delta H < 0$), espontanis ($\Delta G < 0$) i amb constants de l'ordre de 10^5-10^6, indicatiu en conjunt de que el procés de desplaçament és termodinàmicament molt favorable.
- S'ha pogut observar una correlació entre el caràcter de Zn- i Cu-tioneïnes assignat a les MT estudiades i els valors de les K mesurades:
    - Com més gran és el caràcter de Zn-tioneïna, més gran és el valor de K, amb valors de l'ordre de 10^6.
    - Com més gran és el caràcter de Cu-tioneïna, menor és el valor de K, amb valors de l'ordre de 10^5.
- El comportament observat per ITC per a la majoria de les MT estudiades concorda de manera unívoca amb l'observat en la seva caracterització mitjançant altres tècniques habituals, com DC, UV-Vis i ESI-MS.

➢ **Estudi de l'evolució amb els temps de les preparacions Cd-MT mitjançant l'HPLC**

- La utilització de la cromatografia líquida d'exclusió per mides (SEC-HPLC) acoblada a diferents detectors (UV-Vis, ESI-MS i ICP-MS) ha permès monitoritzar l'evolució amb el temps de les diferents bioproduccions Cd-MT estudiades.
- Els estudis realitzats han permès demostrar l'existència d'aquest fenomen únicament en aquelles preparacions que compten amb la presència de lligands sulfur addicionals.
- S'ha pogut comprovar l'existència de diferents pics en els cromatogrames amb un contingut en Cd i S variable, indicant que les espècies Cd_xS_y-MT tenen una mida diferent de les Cd-MT.

- Els resultats han permès concloure que existeix una relació directa entre la presència d'espècies sulfurades, el caràcter de Cu-tioneïna de les MT, i l'evolució amb el temps de les espècies Cd-MT formades *in vivo*:
    - Com més marcat és el caràcter de Zn-tioneïna menor és la presència de sulfur addicional en les produccions Cd-MT i, per tant, no s'observa evolució amb el temps.
    - Com més marcat és el caràcter de Cu-tioneïna d'una MT, major és el seu contingut en S^{2-} i major és l'evolució amb el temps de les bioproduccions Cd-MT, observant-se pics cromatogràfics on bàsicament existeixen espècies Cd_xS_y-MT.

5. PROCEDIMENT EXPERIMENTAL I TÈCNIQUES UTILITZADES

5. Procediment experimental i tècniques utilitzades

En aquest apartat es fa un recull de les tècniques i procediments experimentals utilitzats en l'obtenció i caracterització de les proteïnes, així com d'altres propietats i comportaments exhibits per les metal·lotioneïnes, emprades en aquesta Tesi Doctoral.

Com a mesura de precaució per tal d'evitar focus de contaminació amb possibles ions metàl·lics, tot el material de vidre ha estat rentat inicialment amb HNO_3 20% (v/v) i posteriorment amb abundant aigua milliQ. Per a la utilització del material de plàstic no ha estat necessari prendre aquesta mesura de seguretat ja que consistia en material fungible d'un sol ús. En totes les experiències portades a terme s'ha utilitzat aigua milliQ i les solucions emprades han estat de qualitat espectroscòpica.

5.1. Obtenció i caracterització de la proteïna

Com ja s'ha esmentat al llarg d'aquest treball, totes les proteïnes emprades en tots els estudis i treballs que formen part d'aquesta Tesi Doctoral han estat biosintetitzades pel grup de recerca "Metal.lotioneïnes i xarxes de resposta a metalls", del Departament de Genètica de la Universitat de Barcelona, dirigit per la doctora Sílvia Atrian i Ventura, Catedràtica de Genètica de la Universitat de Barcelona. La tècnica utilitzada per a obtenir els complexos M-MT és l'anomenada de l'ADN recombinant (àmpliament explicada en l'**apartat 1.1.4 Mètodes d'obtenció**) que consisteix en la modificació de cèl·lules d'una soca del bacteri *E.coli* deficient en proteases, on s'introdueix un vector d'expressió que codifica l'MT desitjada. En tots els casos es realitza la síntesi recombinant d'aquests complexos en medis de cultiu cel·lular en presència d'un excés de l'ió metàl·lic desitjat, Zn(II), Cd(II) o Cu(II), per tal d'obtenir els corresponents complexos *in vivo* Zn-, Cd- i Cu-MT, respectivament. Després d'aquest procés, les preparacions metall-MT obtingudes es purifiquen i s'elueixen en tampó Tris-HCl 50 mM a pH 7.0. La producció, mitjançant enginyeria genètica, permet l'obtenció de proteïnes amb una puresa superior al 95% i unes concentracions força elevades (de l'ordre de 10^{-4}M).[70, 71] Cal esmentar que, si bé el coure que es coordina a les MTs presenta únicament estat d'oxidació +1, ja que Cu(II) oxida els tiolats cisteínics, la sal que s'introdueix en el medi de cultiu és $CuSO_4$. El pas de Cu(II) extracel·lular a Cu(I) intracel·lular és possible ja que les cèl·lules (en aquest cas d'*E.coli*) tenen mecanismes que permeten l'entrada de Cu(II) i no de Cu(I) i, un cop dins la cèl·lula, existeixen diversos mecanismes de reducció de Cu(II) que permeten la formació de complexos Cu^{I}-MT.

Seguidament es procedeix a la caracterització de les preparacions de M-MT (on M=Zn(II), Cd(II) i/o Cu(I)) principalment amb les següents tècniques: **i)** ICP-AES (espectroscòpia d'emissió atòmica amb plasma acoblat inductivament), per tal de quantificar la proteïna obtinguda i el contingut de metall present, per així conèixer la relació M/MT dels diferents ions metàl·lics en les corresponents preparacions; **ii)** ESI-MS (espectrometria de masses amb ionització per electrosprai) que aporta informació sobre la integritat de la cadena peptídica i la determinació del pes molecular d'aquesta quan l'anàlisi de les preparacions de Zn-MT es du a terme a pH 2.4 (en aquest pH els ions Zn(II) no poden enllaçar a l'MT, per tant, la forma apo-MT és l'única present en solució). Quan es du a terme l'enregistrament dels espectres d'ESI-MS a pH 7.0 aquests ens aporten informació sobre el nombre i l'estequiometria de les diferents espècies presents en solució; **iii)** DC (dicroïsme circular), emprada en l'estudi del plegament de la proteïna, aporta informació sobre el plegament de la proteïna al voltant del centre metàl·lic i la determinació de les absorcions amb la tècnica **iv)** absorció UV-Vis. Totes aquestes tècniques han estat també emprades per a caracteritzar els diferents complexos M-MT formats *in vitro,* obtinguts bàsicament a partir dels desplaçament metàl·lic de Zn(II) per Cd(II) o Cu(I) en els complexos Zn-MT *in vivo* i a partir del procés d'acidificació i posterior reneutral·lització de les bioproduccions Cd-MT.

A més, durant aquest treball s'han optimitzat i posat en marxa la utilització de noves metodologies per a l'estudi dels sistemes metall-MT que aporten informació addicional a l'obtinguda mitjançant les metodologies anteriorment esmentades: ITC (Isothermal Titration Calorimetry), en col·laboració amb el Dr. Francisco Javier Gómez Pérez de la Universitat Miguel Hernández de Elche (Elche); i cromatografia líquida d'exclusió molecular (SE-HPLC) acoblada als detectors d'UV-Vis, ESI-MS i ICP-MS, aquestes últimes realitzades en una breu estada predoctoral al centre de recerca del *LCABIE* (Laboratoire de Chemie Analytique, Bio-Inorganique et Environnement), de l'IPREM a Pau (França). La tècnica d'ITC ha estat emprada per a la determinació dels paràmetres termodinàmics associats a la reacció de desplaçament de Zn(II) per Cd(II) a partir de les bioproduccions de Zn-MT. Per altra banda, els experiments realitzats amb un sistema de separació de mostres (SE-HPLC) utilitzant tres sistemes de detecció diferents (UV-VIs, ICP-MS i ESI-MS) han estat molt útils en l'estudi de l'evolució amb el temps de les preparacions recombinants de les corresponents Cd-MT, permetent també la separació d'algunes de les diferents espècies presents en solució.

A continuació es detallen algunes de les característiques més importants de les tècniques anteriorment esmentades, així com les condicions experimentals emprades.

5.1.1. Espectroscòpia d'emissió atòmica amb plasma acoblat inductivament (ICP-AES)

Aquesta tècnica permet determinar simultàniament la quantitat de Zn, Cd i Cu present en les solucions proteiques, així com la concentració de S que, considerant la seqüència d'aminoàcids de la proteïna analitzada, permet quantificar la proteïna present en solució.

La metodologia utilitzada es basa en el mètode de quantificació mitjançant la interpolació en una recta patró. Totes les mostres s'han preparat prenent entre 50 i 200 µL de solució proteica i enrasant-les en matrassos aforats de 5 mL amb HNO_3 2 % (v/v). Les rectes de calibrat de S, Zn, Cd i Cu, entre 0 i 5 ppm de cadascun dels elements, s'han preparat a partir de patrons comercials de concentració 1000 ppm, diluint-los amb HNO_3 2 % (v/v). Aquest procediment s'ha anomenat en aquesta Tesi Doctoral "ICP-AES normal", ja que és la manera tradicional de quantificar les preparacions recombinants d'MTs.

Una variant d'aquesta metodologia, anomenada aquí "ICP-AES àcid", consisteix en afegir al matràs de 5 mL la proteïna prèviament acidificada i incubada amb $HClO_4$ concentrat (1:1 proteïna:àcid v/v) per tal d'eliminar els possibles ions àcid/làbils de sulfur presents en la solució en forma de $H_2S\uparrow$ (àcid sulfhídric gasós). D'aquesta manera, la concentració de sofre mesurada dependrà únicament de la quantitat de residus de cisteïna i metionina presents en la cadena polipeptídica de la proteïna. Finalment, es prepara una recta patró similar a la descrita per procediment d'"ICP-AES normal" però on es té en compte la presència de $HClO_4$ al 2 % (v/v).

Les determinacions de S, Zn, Cu i Cd s'han realitzat mitjançant l'espectrofotometre ICP Thermo Jarell Ash, model Polyscan 61E, dels Serveis Cientificotècnics de la UB. S'ha treballat a les longituds d'ona de 182.04, 213.85, 324.75 i 228.80 nm per analitzar S, Zn, Cu i Cd, respectivament. Cal esmentar aquí que l'aparell utilitzat i les limitacions d'aquesta tècnica analítica fan que l'error associat a la quantificació de S sigui molt gran, fins al punt de marcar l'error absolut en la quantificació de les mostres. Així, el límit de quantificació pel S, que és de 0.3 ppm en les condicions emprades, impedeix quantificar proteïnes amb concentracions inferiors a 1-2 µM.

Les anàlisis de les proteïnes mitjançant aquest procediment s'han dut a terme, com a mínim, per duplicat.

5.1.2. Espectrometria de masses ESI-TOF MS

L'espectrometria de masses amb ionització per electroesprai (ESI-MS) és una metodologia analítica que utilitza unes condicions d'ionització suaus de manera que manté intactes les espècies presents en solució, sense provocar fragmentació, i, en condicions òptimes, sense provocar la pèrdua dels ions metàl·lics dels complexos metall-MT. En el present treball s'ha utilitzat un equip que conté un analitzador de temps de vol (TOF) d'alta resolució, que

permet mesurar relacions m/z de manera molt acurada i per tant, una determinació de les espècies amb gran exactitud.

Així, la tècnica ESI-TOF MS permet identificar l'estequiometria de les espècies metall-MT presents en solució, tant el nombre d'espècies com el seu contingut metàl·lic, així com per donar una idea de la concentració/abundància relativa de les espècies. A més a més, el fet de poder acoblar una bomba d'HPLC prèvia a l'entrada de l'equip d'ESI-MS permet una elevada versatilitat tècnica, com, per exemple, treballar en diferents condicions de pH i solucions tampó, o utilitzar columnes separatives. Així, normalment les mostres s'han analitzat a dos valors de pH diferents: pH 7.0, en què les espècies metall-MT es mantenen inalterades; i pH 2.4, condicions en les quals el Zn (II) i el Cd(II) es descoordinen de la proteïna, observant-se així únicament les espècies Cu-MT (provinents de les formes Cu-MT i Zn,Cu-MT) i apo-MT (a partir de l'anàlisi de les formes Zn- i/o Cd-MT).

Els espectres de masses s'han enregistrat en un aparell Micro Tof-Q de Brucker del Servei d'Anàlisi Química (SAQ) de la UAB. L'equip s'ha calibrat amb una solució de NaI (200 ppm NaI en H_2O/isopropanol 1:1) i les mesures s'han realitzat sempre en condicions d'ionització de cations, ESI+. Les condicions experimentals per analitzar proteïnes amb metall divalents (Zn, Cd) han estat: 20 µL de proteïna injectada a través d'un llarg tub de PEEK (1.5 m x 0.18 mm i.d.) a 40 µL/min; voltatge del capil·lar de 5000 V; temperatura de la zona d'assecament (dry temp.) 90-110 ºC; gas d'assecament (dry gas) a 6 L/min; rang de m/z analitzat 800-2500. La fase mòbil consisteix en una mescla 95:5 d'acetat amònic 15 mM amb acetonitril, a pH 7.0. Les mostres amb coure han estat analitzades injectant 20 µL de proteïna a 40 µL/min; voltatge del capil·lar de 4000 V; temperatura de la zona d'assecament (dry temp.) 80 ºC; gas d'assecament (dry gas) a 6 L/min; rang de m/z analitzat 800-2500. La fase mòbil consisteix en una mescla 90:10 d'acetat amònic 15 mM amb acetonitril, a pH 7.0. Per l'anàlisi a pH àcid, les condicions utilitzades són les mateixes que les emprades en el cas de metalls divalents, excepte en la composició de la fase mòbil, que en aquest cas es tracta d'una mescla 95:5 d'àcid fòrmic i acetonitril a pH 2.4. Totes les mostres han estat injectades, com a mínim, per duplicat, per tal d'assegurar la reproductibilitat.

5.1.3 Espectroscòpia de dicroisme circular (DC)

La base de l'espectroscòpia de DC es troba en l'absorció de llum polaritzada per un cromòfor en solució òpticament actiu. Aquesta llum és d'una naturalesa especial per dos feixos de llum polaritzats circularment en sentits oposats i amb la mateixa fase, donant lloc a un feix de llum polaritzada en un pla. Per poder observar senyals de DC cal que hi hagi cromòfors que absorbeixin a les longituds d'ona analitzades, i a més a més, que aquests cromòfors siguin quirals. Així, cadascun dels cromòfors quirals presents en solució absorbiran de forma diferent en els dos feixos de llum polaritzats circularment. La diferent absorció dels dos feixos donarà lloc

a un senyal de DC en la longitud d'ona on absorbeix el cromòfor. Aquests senyals poden ser positius o negatius, en funció del feix que més s'absorbeixi. Si considerem que cadascun dels feixos circulars es representa per un coeficient d'extinció molar, Ɛ, tindrem dos valors, $Ɛ_e$ (llum polaritzada cap a l'esquerre) i $Ɛ_d$ (llum cap a la dreta). Així el fonament dels espectres de DC es troba en la diferència entre els valors dels dos coeficients d'extinció molar, $ΔƐ= Ɛ_e - Ɛ_d$, i en funció de la longitud d'ona de la radiació incident. Si bé els equips de DC mesuren un paràmetre anomenat elipticitat molar, aquest valor es pot transformar facilment en ΔƐ.

Bàsicament les bandes observades en els espectres de DC són de dos tipus: gaussianes (positives i negatives) o en forma de derivada (*exciton coupling*). Les de tipus gaussianes, que són les més habituals, indiquen l'existència d'un cromòfor quiral per cada màxim o mínim observat. S'ha de tenir en compte que, de forma general, apareixen bandes gaussianes prou definides i separades de les altres, i per tant, fàcilment identificables, però en molts dels casos, sobretot quan estem treballant amb una mescla de diferents espècies M-MT, és possible veure solapament de bandes de tipus gaussianes. Per altra banda, quan dos o més cromòfors similars que absorbeixen a longituds d'ona properes es troben connectats per enllaços de tipus σ, s'orienten de forma que existeix una interacció mútua entre ells. Apareixen així el que es denomina bandes de tipus *exciton coupling*, que modifica la banda gaussiana associada a cada cromòfor en una única banda corresponent a una forma de primera derivada fàcilment identificable.

D'aquesta manera, en el cas dels sistemes metall-MT, l'espectroscòpia de DC aporta informació sobre el plegament i l'entorn de coordinació de la proteïna al voltant dels centres metàl·lics, així com de la quiralitat de les espècies formades, essent la intensitat de les bandes dicroiques una mesura del grau de plegament o desestructuració de la proteïna. En les MTs, si bé els ions metàl·lics no són quirals per si mateixos, la coordinació a la proteïna, que sí que és quiral al estar formada de L-aminoàcids, provoca el que s'anomena transferència de quiralitat des de la proteïna al centre metàl·lic, de manera que els cromòfors M-SCys esdevenen quirals, i per tant, òpticament actius.

Val a dir que aquesta tècnica presenta certes limitacions a l'hora d'estudiar una mescla de compostos amb diferents estequiometries, entorns de coordinació i plegaments, molt freqüent en els estudis de les MTs, ja que un espectre de DC dóna una mesura global del sistema en estudi. Si bé un espectre per si sol és difícil d'interpretar degut a la seva complexitat, la comparació entre espectres enregistrats en diferents condicions (pH, concentració de metall, etc.) pot proporcionar una informació valuosa sobre el plegament de la proteïna al voltant dels centres metàl·lics a mida que es modifiquen aquestes condicions experimentals.

Els espectres de DC de les mostres s'han enregistrat en un espectropolarímetre Jasco-715 a 50 nm/min, 0.5 nm de resolució i utilitzant una cubeta de quars amb tap d'1 cm de pas de llum.

Com a blanc s'ha emprat una solució de la mateixa concentració en Tris-HCl que les mostres enregistrades. Finalment, els espectres d'absorció de DC han estat tractats amb el programa informàtic GRAMS/32.

5.1.4. Espectroscòpia d'absorció ultraviolat-visible (UV-Vis)

Aquesta tècnica, es basa en mesurar l'absorció de la llum (en el rang de l'UV-Vis, entre 190 i 800 nm) que passa a través d'una mostra en solució. En aquest cas, permet obtenir informació sobre la coordinació metàl·lica i sobre els aminoàcids de les proteïnes. És ben coneguda l'absorció de les cadenes peptídiques a longituds d'ona inferiors a 220 nm i l'absorció del aminoàcids aromàtics a 280 nm. També és sabut que la zona entre 220 i 500 nm és on s'observen les bandes de transferència de càrrega entre lligands i metalls o a l'inrevés quan s'analitzen complexos metàl·lics.

L'estudi de les MTs per aquesta espectroscòpia és molt particular. Una característica essencial en la caracterització espectroscòpica de les MTs és l'absència d'aminoàcids aromàtics en la majoria de proteïnes d'aquest tipus i que permet, per tant, relacionar les absorcions per sobre de 220 nm únicament amb la coordinació dels metalls a la proteïna. En general, les MTs coordinen els ions metàl·lics a través dels residus de Cys, és a dir, pels tiolats, de manera que totes les absorcions per sobre de 220 nm, en el cas de la coordinació a metal·lotioneïnes, correspondran forçosament a l'enllaç del metall amb el sofre cisteínic (S_{Cys}). També, el fet que la majoria d'ions metàl·lics que es coordinen a les MTs tinguin configuració electrònica d^{10} implica l'absència de bandes intermetàl·liques de tipus d-d. Per tant, en els espectres d'absorció UV-Vis s'observa, a banda de l'absorció de la cadena peptídica, les bandes de transferència de càrrega de lligand a metall (TCLM), les quals poden proporcionar informació sobre la naturalesa del cromòfor, el tipus de coordinació al voltant del centre metàl·lic. Si bé la informació aportada pels espectres d'UV-Vis directament no és molt rellevant, ja que generalment els espectres mostren bandes molt amples, l'evolució de l'absorció a determinades longituds d'ona (p.ex. en les valoracions de les Zn-MT amb Cd(II)) ens permet obtenir informació del sistema. També, quan es resten els espectres d'addicions consecutives (p. ex. restant a l'espectre enregistrat en afegir 6 eq Cd(II) el de 5 eq Cd(II), que expressem com a 6-5 Cd), es pot observar l'efecte provocat únicament per l'addició de l'equivalent considerat (en l'exemple, l'efecte del 6è Cd(II) afegit).

Pels espectres d'UV-Visible s'ha emprat la mateixa cubeta de quars amb tap d'1 cm de pas de llum i el mateix blanc que en el cas de les mesures de DC. Les mesures d'UV-Vis s'han realitzat en un espectrofotòmetre HP8453A de *diode array* amb 15 segons de temps d'integració, mesurant entre 200 i 800 nm. Els espectres enregistrats han estat tractats també amb el programa informàtic GRAMS/32.

5.2. Agents valorants de Cd(II) i Cu(I)

5.2.1. Solució de Cd(II)

Per a les valoracions de Zn-MT s'ha utilitzat una solució de $CdCl_2$, preparada a partir d'una solució estàndard de concentració 1000 ppm, diluint amb aigua MilliQ. La concentració de la solució final s'ha determinat per espectroscòpia d'absorció atòmica de flama.

5.2.2. Solució de Cu(I)

Per tal de valorar la proteïna amb coure(I) s'ha utilitzat una solució del complex $[Cu(CH_3CN)_4]ClO_4$ sintetitzat al laboratori. S'ha escollit aquest agent valorant atenent al fet que és una sal molt estable a l'oxidació per part de l'aire i a que l'anió ClO_4^- és feblement coordinant.

La síntesi del complex es duu a terme sota una atmosfera de nitrogen. Sobre una suspensió de 4.0 g de Cu_2O en 80 mL de CH_3CN s'hi addicionen lentament 24.6 mL de $HClO_4$ 4.6 M. La barreja resultant es deixa refluir a 100 °C sota agitació magnètica. El sòlid blanc que comença a precipitar es redissol ràpidament i la solució adquireix una tonalitat blau pàl·lid corresponent a la presència de traces de Cu(II). Un cop no s'observa gens de sòlid blanc es filtra la solució en calent. El filtrat es deixa refredar a temperatura ambient, després a la nevera i per últim al congelador tota la nit. Passat aquest temps es recullen els cristalls blancs de $[Cu(CH_3CN)_4]ClO_4$, es renten amb 3 porcions de 5-10 mL de Et_2O, s'assequen al buit i es guarden sota atmosfera d'argó al dessecador. Aquesta síntesi es basa en la publicada per Kubas, Monzyc i Crumbliss amb algunes modificacions.[178]

Finalment, la solució de Cu(I) utilitzada com a valorant s'ha preparat en atmosfera de N_2. El complex es dissol en una solució aquosa al 30 % en volum de CH_3CN. Abans d'utilitzar la solució s'ha de verificar l'absència d'ions Cu(II) en solució mitjançant mesures d'EPR (Espectroscòpia de resonància paramagnètica). La concentració de Cu(I) de la solució es determina per espectroscòpia d'absorció atòmica de flama. Per altra banda, els espectres d'EPR s'han realitzat amb un espectròmetre de ressonància paramagnètica electrònica Brucker ESP 300 E amb sistema criogènic de nitrogen líquid.

Un espectrofotòmetre d'absorció atòmica de flama Perkin Elmer 2100 ha estat emprat per relitzar les determinacions de concentració de Cu(I) i Cd(II) dels agents valorants. Els patrons de calibració han estat solucions estàndard de diferents concentracions de $CdCl_2$ i $CuCl_2$.

5.3. Calorimetria Isoterma de Titulació (ITC)

Tota reacció química porta associada l'alliberament o absorció d'energia calorífica, que és característica de la reacció en qüestió. Les tècniques calorimètriques es basen en la determinació

d'aquesta quantitat d'energia alliberada o absorbida en forma de calor. La Calorimetria Isoterma de Titulació[179] (normalment coneguda com a ITC, Isothermal Titration Calorimetry) és una tècnica calorimètrica ben coneguda que permet, a partir d'un únic experiment consistent en una valoració, determinar tots els paràmetres termodinàmics (constant, entalpia, entropia i estequiometria de la reacció en qüestió) que defineixen una interacció química.

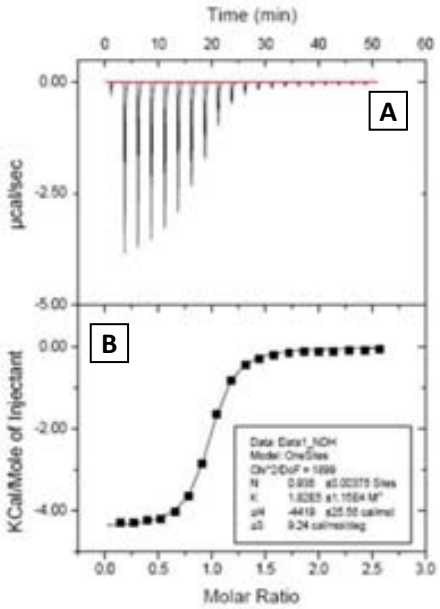

Fig. 90. Experiment d'ITC seguint l'enllaç del lligand a la proteïna (A). Les tres variables (N estequiometria, constant d'equilibri d'enllaç K i la entalpia de interacció, ΔH) resultat després de determinar el millor ajust a les dades de la isoterma obtinguda experimentalment (B).

La tècnica d'ITC funciona en condicions isotèrmiques, on les dues cubetes de què disposa l'aparell, referència i mostra, estan a la mateixa temperatura, escollida per l'usuari. Quan a la cubeta de la mostra es realitza l'addició d'un agent valorant, aquesta cubeta pateix un escalfament o refredament degut al canvi de calor associat a la reacció que té lloc dins d'ella. Aquest canvi de calor depèn del signe de l'entalpia de la reacció, una certa quantitat d'energia en forma de calor serà absorbida (si la reacció és endotèrmica, ΔH>0) o alliberada (si la reacció és exotèrmica, ΔH<0). La quantitat de calor necessària per mantenir les dues cubetes a la mateixa temperatura es pot mesurar perfectament i de manera molt acurada. Quan el sistema torna a l'equilibri, es pot realitzar una altra addició de valorant i mesurar el canvi de calor provocat per la nova addició. El conjunt d'addicions dóna lloc al termograma (**Fig. 90A**), que és un conjunt de pics, l'àrea dels quals està directament relacionada amb la quantitat de calor alliberada (pics negatius) o absorbida (pics positius). El tractament del termograma, tenint en compte l'àrea dels pics, la concentració i la quantitat de l'agent valorant, i la concentració inicial de la proteïna o molècula valorada, dóna lloc a la isoterma de valoració, on es relaciona l'energia associada a l'addició de valorant en funció de la relació molar entre l'agent valorant i el valorat (**Fig. 90B**). A partir de les dades així representades s'obtenen, mitjançant un tractament matemàtic que ajusta els valors experimentals a algun dels models teòrics preestablerts (utilitzant el mateix software proporcionat amb l'equip), els valors de la constant associada al procés, el canvi d'entalpia i d'entropia de la reacció, així com el punt d'equivalència o estequiometria de la reacció (N).

En l'estudi de les MTs presentat en aquesta treball s'ha emprat l'ITC com a metodologia per a determinar els paràmetres termodinàmics associats a la reacció de desplaçament metàl·lic de Zn(II) per Cd(II) en diferents preparacions recombinants Zn-MT, en condicions anàlogues a les utilitzades en les valoracions amb Cd(II) seguides per DC, UV-Vis i ESI-MS.

L'addició de Cd(II) a una solució Zn-MT provoca el desplaçament dels ions Zn(II) inicialment coordinats a la proteïna per donar lloc a les espècies Cd-MT fins a la saturació d'aquesta, moment a partir del qual l'addició de més Cd(II) no provoca cap efecte sobre la proteïna, i per tant, cap canvi de calor.

$$Zn_x\text{-MT} + y\ Cd^{2+} \rightarrow Cd_y\text{-MT} + x\ Zn^{2+}$$

Així, en la reacció descrita, la constant associada serà la constant d'afinitat aparent (K_{af}), i la resta de paràmetres (ΔH i ΔS) són els associats al bescanvi de Zn(II) per Cd(II). El valor N calculat a partir de les dades d'ITC pot aportar informació sobre l'estequiometria de l'espècie més afavorida termodinàmicament o sobre el punt de saturació de l'MT estudiada. El conjunt de paràmetres termodinàmics permet també calcular el valor de l'energia lliure de Gibbs (ΔG), ja sigui a partir de la constant o dels valors d'entalpia i entropia:

$$\Delta G = RT \ln K \qquad \Delta G = \Delta H - T\,\Delta S$$

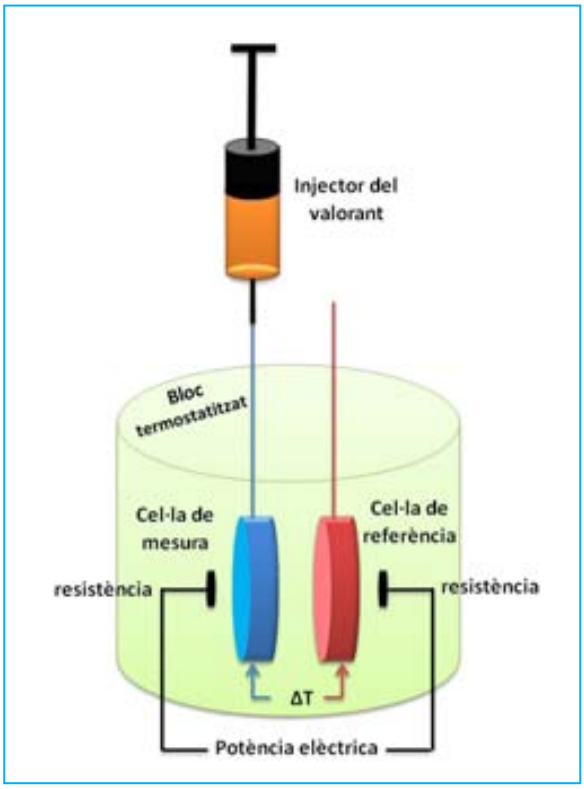

Fig. 91. Representació esquemàtica dels components essencials de l'aparell d'ITC utilitzat.

Els experiments d'ITC que es mostren en aquesta Tesi han estat realitzats en un equip marca MicroCal® model VP-ITC. Aquest equip consta de dues cel·les calorimètriques (la de referència i la de mesura) situades dins d'un bloc, una camisa, termostatitzat a la temperatura desitjada (l'escollida per a realitzar l'experiència) que es manté constant (**Fig. 91**). La cel·la de referència ha d'estar plena de solució tampó que conté la mostra (en el nostre cas solució de tampó Tris-HCl 50 mM a pH 7.0), mentre que la solució de la macromolècula que es vol valorar (aquí una solució de la Zn-MT corresponent) s'allotja en la cel·la de mesura. Per la seva banda, la ssolució de l'agent valorant (solució de Cd(II)) s'introdueix a la xeringa externa de què disposa l'equip. Aquesta xeringa d'injecció, que s'introdueix dins la cel·la de mesura, esta sotmesa a un moviment de rotació a velocitat constant (i modulable), i permet fer les addicions seqüencials de volums coneguts de la solució valorant a la cel·la de la mostra, alhora que manté la solució el més homogènia possible mitjançant l'agitació de la solució.

Les cel·les (de mesura i de referència) porten adossades unes resistències que permeten controlar i mantenir la temperatura desitjada. Actualment, la majoria dels instruments existents

al mercat disposen de l'anomenat "sistema de compensació de potencia", que confereix a l'equip una elevada sensibilitat, permetent mesurar canvis de calors molt petites. Aquest és un dels motius de la recent aplicació d'aquest tipus de tècniques en la determinació dels paràmetres termodinàmics en sistemes biològics, fins ara difícil d'estudiar. L'instrument monitoritza constantment la temperatura de cadascuna de les cel·les i envia més o menys potència elèctrica a la resistència adossada a cada cel·la calorimètrica fins que la diferència de temperatura entre elles es nul·la (exactament a la mateixa temperatura). En aquest moment, la potencia elèctrica enviada a cada cel·la és idèntica i, per tant, la diferència en la potència elèctrica és nul·la també, dQ/dt=0.

Com a metodologia de treball en tots els experiments d'ITC realitzats en aquesta Tesi Doctoral, la solució de Zn-MT de concentració 10-12 µM s'introdueix en la cel·la de mesura (d'un volum fix i perfectament conegut al voltant de 1.4 mL), i la solució de metall valorant (en una concentració adequada amb l'experiment que es vol realitzar, en aquest cas, aproximadament 1000 µM) s'introdueix en la xeringa externa fins a un volum màxim de 300 µL. Es realitzen addicions seqüencials, d'entre 2 i 15 µL cadascuna, de l'agent valorant fins que la concentració total de Cd(II) en la cel·la de mesura sigui suficient com per saturar tots els centres d'unió de la proteïna. Com a qualsevol tècnica calorimètrica, l'observable monitoritzat serà la quantitat d'energia en forma de calor, Q_i, que s'absorbeix o s'allibera després de l'addició de cada volum de lligand, V_{inj}, a temperatura i pressió constants.

És important esmentar que a l'hora de dissenyar un experiment d'ITC s'han de tenir en compte algunes consideracions:

a) Optimització de les concentracions a utilitzar de cada reactiu. No només és important per evitar possibles processos d'agregació i precipitació o interaccions no desitjades, sino també per tal de trobar les condicions òptimes d'anàlisi dels senyals obtinguts, que dependran del grau d'afinitat de la interacció. Pel que fa a les concentracions de la macromolècula, aquestes es determinen a partir del paràmetre "c", que és la resultant del producte entre l'afinitat predita (obtinguda a partir d'un experiment d'ITC previ, a partir de la bibliografia existent pel sistema a estudiar o per altres previsiblement similars) i la concentració total de la macromolècula (en el nostre cas la metal·lotioneïna, MT), on c=K·[MT]. El valor òptim per c estaria entre 10 i 1000. Així en el cas de les MTs on el valor de K_a generalment varia al voltant de 10^6 M^{-1}, s'empra una concentració de entre 10-15 µM minimitzant la quantitat de proteïna emprada i optimitzant al màxim el senyal obtingut per ITC. També és important tenir en compte que un "fitting" (ajust) correcte dels resultats requereix una saturació del senyal i el màxim de punts possibles. Pels sistemes amb una elevada afinitat, la millor opció és utilitzar una concentració baixa d'agent

valorant, ja que això permet evitar una saturació del sistema en un estadi massa inicial i, per tant, obtenint una isoterma amb molt poques dades.

b) Una vegada la calor de dilució control (valoració del lligand dins la solució tampó) ha estat restada de la valoració, la entalpia i la saturació haurien d'aproximar-se al 0.

c) La composició de les solucions de l'agent valorant i la macromolècula valorada han de ser el més semblants possible. Sovint, petites diferències en la composició de les solucions, degudes a diferents raons com el co-solvent, sals o pH, provoquen processos no desitjats que causen canvis de calor emmascarant o interferint en la determinació de la interacció que es desitja estudiar. Per tal d'evitar aquesta interferència, és recomanable, quan es treballa amb un sistema nou, fer un "blanc", un experiment d'ITC on es comprova que l'addició de l'agent valorant sobre el buffer o viceversa no provoca cap interacció massa intensa, produïnt canvis de calor considerables, i assegurar-se així que els senyals de la calor obtingudes en la valoració desitjada són principalment degudes al sistema en estudi.

d) Evitar la presència de bombolles d'aire a les cel·les. És molt important eliminar les bombolles d'aire de les cel·les de referència i de mesura per dos motius principals: perquè el volum de mostra continguda sigui el més precís possible; i per facilitar que la mostra es pugui homogeneïtzar fàcilment i recuperi la temperatura fixada amb rapidesa, fet que es veuria alterat per la presència de gas. Amb l'objectiu d'evitar la presència de gas a les solucions utilitzades, cal que aquestes hagin estat prèviament desgasades (mitjançant ultrasons normalment). En introduir les solucions a les cel·les corresponents, és convenient realitzar moviments ràpids cap amunt i cap a baix de l'agulla utilitzada per introduir la mostra, fregant les parets de la cel·la per tal d'eliminar les bombolles de gas presents a la cel·la provocades per la introducció de la solució.

e) Purgar la solució d'agent valorant de la xeringa d'injecció, buidant i omplint el seu contingut com a mínim una vegada. Fet això, es netegen les restes de solució d'agent valorant que queden en la cànula d'injecció amb una gassa per tal d'evitar errors en la mesura i finalment es col·loca la xeringa d'injecció en la cel·la de la mostra.

Des del punt de vista instrumental, hi ha un conjunt de paràmetres que es poden optimitzar i modular per tal d'obtenir el màxim de rendiment de cada experiment. Els més importants, i que cal establir prèviament abans d'iniciar l'experiment, són:

1- El número d'injeccions i els volums d'agent valorant que s'injectaran. S'han de tenir un conjunt de precaucions prèvies per cada sistema que es pretén estudiar, depenent principalment de si l'afinitat entre el valorant i la biomolècula és alta o baixa, tenint sempre com a premissa

que és desitjable observar senyals el més intenses possibles, però sense saturar el detector, i molts punts experimentals per tal de poder fer un bon ajustament a la isoterma obtinguda. Així, per sistemes que tenen desprendiments o absorcions de calor dèbils, obtenint-se senyals poc intenses, és preferible tenir menys número d'injeccions però amb una intensitat adequada, i per tant, s'utilitzaria un volum d'agent valorant més gran o una concentració de l'agent valorant major. I de manera inversa, per sistemes que tenen una gran afinitat, els volums de valorant seran inferiors. Altres paràmetres que poden afectar a l'afinitat, i per tant, el volum d'agent valorant, són la variació de la concentració de la macromolècula, la temperatura de l'experiment (depenent de la capacitat calorífica de l'enllaç del sistema), i l'alteració del pH o de la força iònica del medi tamponat.

2- El temps d'estabilització entre cada injecció de l'agent valorant. Degut a que després de cada injecció el sistema ha de tenir suficient temps per tornar a l'equilibri, a la línea base, abans de realitzar la següent addició de valorant, és important donar prou temps entre injeccions consecutives. En cas que el temps no sigui suficient, hi ha el perill de que es solapin els senyals i que les dades obtingudes no siguin útils. També un temps entre injeccions massa gran fa que l'experiment sigui excessivament llarg i comporti una despesa de temps innecessària per a l'operador.

3- La primera injecció sempre és errònia. En introduir la xeringa d'injecció dins la cel·la de mesura habitualment succeeix que, per difusió, una petita quantitat de la dissolució de la xeringa passa a la solució de mostra, de manera que la quantitat injectada en la primera addició no és la correcta. És una limitació pròpia del sistema i no es pot corregir fàcilment, per la qual cosa, és recomanable que la primera injecció sigui del volum mínim, 2 µL, tenint en compte que aquesta dada posteriorment serà descartada.

4- La temperatura de l'experiment ha de ser l'adequada. Si bé el rang de treball dels equips és molt ampli, entre 2 i 80 °C, la temperatura habitual de treball és de 25 °C. Tanmateix, és recomanable escollir una temperatura que coincideixi amb la utilitzada en altres experiments complementaris al d'ITC (enllaç, cinètica, etc) duts a terme amb el nostre sistema lligand-macromolècula per poder comparar els resultats. Tot i això, cal tenir en compte que mitjançant l'equació de Van't Hoff, és possible calcular el valor de la constant d'equilibri per qualsevol temperatura un cop es coneix el valor de la constant a una temperatura determinada i el valor d'entalpia de la reacció.

5- La velocitat d'agitació de la xeringa ha de ser tinguda en compte. L'agitació és necessària per a una adequada mescla de l'agent valorant amb la macromolècula durant la valoració, alhora que facilita arribar a l'equilibri de manera més ràpida. Però una agitació massa

vigorosa pot afectar als senyals obtinguts, augmentat el soroll de manera considerable. Normalment la velocitat d'agitació òptima és de 15 rpm. També cal tenir en consideració que algunes proteïnes es desestabilitzen per una agitació massa ràpida, per tant, la velocitat d'agitació s'haurà d'adequar quan el sistema ho requereixi.

Tenint en compte totes les consideracions descrites fins ara, les mesures d'ITC realitzades es van realitzar a 25 °C en el mode de valoració directa (la solució de metall continguda a la xeringa). Cal dir que la concentració de les diferents solucions d'MT, així com el volum d'injecció, varia en funció de cada proteïna, tenint en compte la seva longitud i el contingut en residus de Cys de cadascuna d'elles. De forma general, la concentració de l'MT corresponent dins la cel·la de mesura ha tingut un valor de 10-15 µM i la de la solució metàl·lica al voltant de 1000 µM. El volum d'injecció ha estat de 5-8 µL, corresponent aproximadament a 0.3-0.5 eq de Cd(II)/mol de proteïna, amb un interval de temps entre les diferents injeccions que varia entre 250 i 400 s, depenent de la intensitat dels pics. Totes les solucions van ser tamponades amb Tris-HCl 50 mM a pH 7.0. Finalment, pel que fa a l'agitació, s'escull una agitació de 15 rpm, prou suau (Low feat back) per homogeneïtzar el sistema sense provocar pertorbacions del mateix.

Les experiències amb la tècnica d'ITC presentades en aquest treball s'han realitzat en dos localitzacions diferents però amb el mateix model d'equip: al Parc Científic de la Universitat de Barcelona, al servei de calorimetria dirigit pel Doctor Rafel Probens; i al laboratori del Dr. Francisco Javier Gomez Pérez, del Departament de Química Física de la Universidad Miguel Hernández, Elx. Les mesures calorimètriques es realitzen en uns calorímetres de titulació VP-ITC MicroCal, i l'ajustament de les dades experimentals s'ha dut a terme amb el software MicroCal Origin versió 7.0.

5.4. Tècniques acoblades a SE-HPLC (Size Exclusion-High Performance Liquid Chromatography)

Amb la finalitat d'estudiar i/o monitoritzar l'evolució de les preparacions que contenen lligands sulfur addicionals, identificats en algunes de les preparacions recombinants Cd-MT (**Apartat 3.5. de Resultats i discussió**), a més d'intentar fer una separació de les espècies de tipus Cd-S^{2-}-MT de les Cd-MT, es va dissenyar una metodologia de treball que consisteix, a grans trets, en utilitzar un sistema de separació de les mostres (HPLC) amb un tipus de columna que no alteri les mostres (exclusió per mides). Com a sistemes de detecció s'han emprat tres tipus diferents (**Il·lustració 2**): UV-Vis, que habitualment es troba incorporat amb els sistemas d'HPLC; ICP-MS, que permet monitoritzar els àtoms de la majoria d'elements, especialment els metalls, amb uns límits de detecció molt baixos; i ESI-MS, que permet identificar les espècies presents en solució al llarg del temps. Cal dir que una part important d'aquests experiments s'han dut a

terme durant una estada breu de 3 mesos i en col·laboració amb el grup de recerca de la Dra. Joanna Szpunar i el Dr. Ryszard Lobinski, del *LCABIE* (Laboratoire de Chemie Analytique, Byo-Inorganique et Environnement), a l'IPREM del CNRS de Pau, França.

Es va decidir utilitzar un sistema de separació basat en columnes d'exclusió per mides (size exclusion, SE-HPLC) perquè és una tècnica àmpliament utilitzada per a l'estudi de les MTs ja que, a diferència d'altres tipus de separació, no altera els clústers metàl·lics metall-MT, alhora que permet un fàcil acoblament a diferents sistemes de detecció.

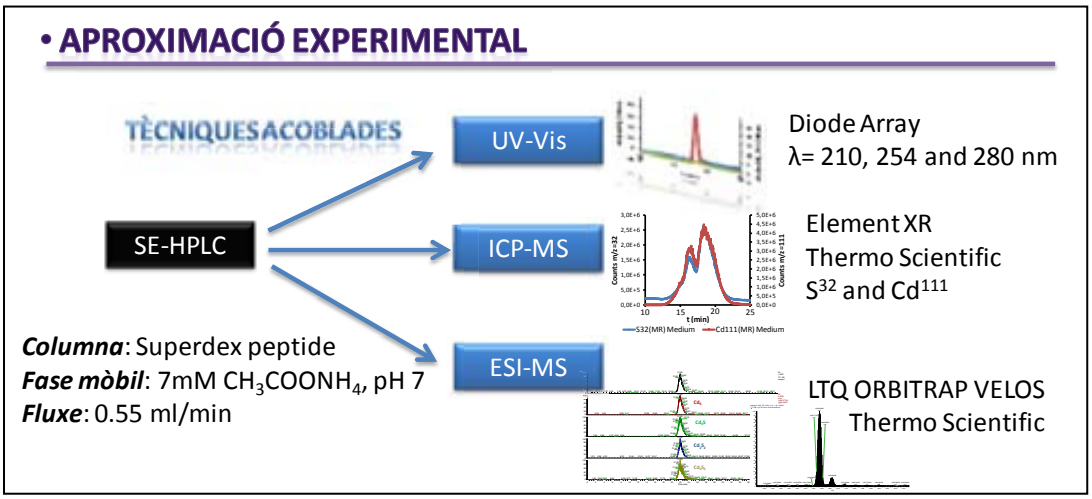

Il·lustració 1. Esquema de l'aproximació experimental duta a terme per a l'estudi i monitorització de la evolució amb el temps de les diferents preparacions recombinants de Cd-MT.

La separació cromatogràfica de les mostres Cd-MT, obtingudes en les preparacions recombinants en medis suplementats amb Cd(II), s'han dut a terme mitjançant la columna d'exclusió molecular Superdex Peptide 10/300 GL (GE Healthcare), amb un rang d'exclusió entre 100 i 7000 Da, connectada a una bomba d'HPLC, Sèrie 1200 (Agilent Technologies), equipada amb un automostrejador i un detector de diode array, controlat tot pel programa Compass. S'han injectat alíquotes de 100 µL de la mostra (de diferent concentració depenent del sistema de detecció al que es trobi acoblat) i eluïdes amb una solució tampó d'acetat amònic 7 mM i pH 7.5, amb un flux de 0.55 mL/min.

Quan s'ha utilitzat l'acoblament SE-HPLC-UV-Vis, on el detector d'UV-Vis és de tipus diode array i correspon al mòdul que forma part del equip d'HPLC, a la sortida de la columna s'ha monitoritzat on-line l'absorbància de l'eluat. S'enregistrent els valors a 210, 254 i 280 nm, corresponents a absorcions de la cadena peptídica, de l'enllaç Cd-S_{Cys} i de la presència d'espècies Cd-S^{2-}-MT, respectivament. Finalment les dades obtingudes són exportades i tractades amb el programa EXCEL 2007, de Microsoft Office.

Les mesures d'ICP-MS en l'acoblament SE-HPLC-ICP-MS, es duen a terme en l'instrument d'alta resolució Element XR, de Thermo Scientific. Es monitoritzen dos elements: Cd, mitjançant les masses 111 i 113; i S, mitjançant la massa 32. Aquest darrer element, que acostuma a donar

lloc a senyals amb molt soroll, i per tant límits de detecció molt alts, és el responsable de la utilització de l'equip d'alta resolució, ja que l'alt grau d'interferències observades en un aparell convencional, bàsicament degudes a la presència inevitable d'O_2, no permet fer un seguiment del S als nivells de concentració de les mostres utilitzades. Per tal d'acoblar les dues tècniques, SE-HPLC i ICP-MS, cal fer una divisió del flux (*split*) del 50 %, mitjaçant un divisor *splitter*, a la sortida de l'HPLC, abans d'introduir-ho al detector d'ICP-MS, donat que massa volum de líquid pot interferir en el bon funcionament de l'equip, bàsicament en la nebulització del líquid introduït. Així, igual que en el cas de les dades obtingudes per UV-Vis, els resultats de l'anàlisi per ICP-MS també van ser exportades i representades amb el programa EXCEL 2007, de Microsoft Office.

Finalment, en l'acoblament SE-HPLC-ESI-MS s'empra l'instrument d'ESI-MS LTQ ORBITRAP VELOS, de la marca Thermo Scientific, equipat amb un sistema d'analitzador de trampa lineal orbitalària que permet enregistrar espectres en condicions d'alta resolució. L'acoblament esmentat requereix la utilització d'una segona bomba just a l'entrada de l'ESI-MS (Model de bomba 33, Harvard Apparatus, South Natick, MA) per l'addició de metanol a la solució que surt de la columna, mitjançant un tub de PEEK, a un flux de 0.1 mL/min. Posteriorment també s'ha requerit d'un segon mòdul divisor de flux per reduir el cabal d'entra a l'aparell d'ESI-MS fins a 0.005 mL/min per tal de permetre la correcta ionització de la mostra.

La calibració de l'espectrometre de masses es realitza amb una mescla de cafeïna (195.08765), el pèptid MRFA (524.26499) i el polímer Ultramark (*m/z* 1221.99063). La font d'ionització opera en mode positiu a 3.2 kV, la temperatura de vaporització de la mostra és de 120 °C i la temperatura del capil·lar de 280 °C. El gas portador, N_2, s'utilitza a 20 mL/min i l'auxiliar a 5 (unitats arbitràries). La mostra s' introdueix per infusió a 5 μL/min i es monitoritza el rang de *m/z* de 1300-2000 unitats.

El control de l'aparell i el tractament de les dades es fa a través d'un PC amb el software XCalibur™.

6. BIBLIOGRAFIA

[1] M. Margoshes, B. Vallee, *J. Am. Chem. Soc.*, 1957, **79**, 4813-4814.

[2] J.H.R. Kägi, M. Nordberg, *Experientia Supplementum Metallothionein I*, vol. 34, Birkhäuser Verlag, Basel, 1979.

[3] J.H.R. Kägi, Y. Kojima, *Experientia Supplementum Metallothionein II*, vol. 52, Birkhäuser Verlag, Basel, 1987.

[4] K.T. Suzuki, N. Imura, M. Kimura, *Metallothionein III*, Biological Roles and Medical Implications, Birkhäuser Verlag, Basel, 1993.

[5] C.D. Klassen, *Metallothionein IV*, Birkhäuser Verlag, Basel, 1999.

[6] A. Sigel, H. Sigel, R.K.O. Sigel, *Metal ions in life Sciences Metallothioneins and Related Chelators*, vol. 5, RSC Publishing, Cambridge, 2009.

[7] M.J. Stillman, C.F. Shaw III, K.T. Suzuki, *Metallothioneins. Synthesis, Structure and Properties of Metallothioneins Phytochelatins and Metal-Thiolate Complexes*, VCH Publishers Inc, New York, 1992.

[8] J.F. Riordan, B.L. Vallee, *Methods in Enzymology Metallobiochemistry Part B Metallothionein and Related Molecules*, vol. 205, Academic Press, San Diego, 1991.

[9] M. Vašák, J.H.R. Kägi, in: R.B. King (Ed.) *Encyclopedia of Inorganic Chemistry*, vol. 4, John Wiley and Sons, Chichester, 1994, 2229-2241.

[10] P. González-Duarte, in: J.A. McCleverty, T.J. Meyer (Eds.), *Comprehensive Coordination Chemistry*, vol. 8, Elsevier, Amsterdam, 2003, 213-228.

[11] Ò. Palacios, S. Atrian, M. Capdevila, *JBIC*, 2011, **16**, 991-1009.

[12] M. Capdevila, R. Bofill, O. Palacios, S. Atrian, *Coord. Chem. Rev.*, 2011, **256**, 46-62.

[13] B. Gold, H. Deng, R. Bryk, D. Vargas, D. Eliezer, J. Roberts, X. Jiang, C. Nathan, *Nat. Chem. Bio.*, 2008, **4**, 609-616.

[14] http://www.bioc.unizh.ch/mtpage/intro.html

[15] http://www.expasy.org/cgi-bin/lists?metallo.txt

[16] M.J. Stillman, *Coord. Chem. Rev.*, 1995, **144**, 461-511.

[17] L. Villarreal, *Tesi doctoral*, Dept. Química, Universitat Autònoma de Barcelona, 2005.

[18] N. Romero-Isart, M. Vašák, *J. Inorg. Biochem.*, 2002, **88**, 388-396.

[19] E. Carpenè, G. Andreani, G. Isani, *J. Trace Elem. Med. Biol.*, 2007, **21**, 35-39.

[20] N. Darby, T. Creighton, *Methods Mol. Biol.*, 1995, **40**, 219-252.

[21] Y. Yang, W. Maret, B.L. Vallee, *Prod. Natl. Acad. Sci. U.S.A.*, 2001, **98**, 5556-5559.

[22] A. Krezel, W. Maret, *J. Biol. Inorg. Chem.*, 2008, **13**, 401-409.

[23] M. Vašák, in: *J. F. Riordan, B.L. Vallee (Eds.)*, Metallobiochemistry Part B, Metallothionein and Related Molecules, Methods in Enzymology, vol. 205, Academic Press, San Diego, 1991, 452-458.

[24] W. Maret, *Biometals*, 2009, **22**, 149-157.

[25] Y. Lia, W. Maret, *J. Anal. At., Spectrom.*, 2008, **23**, 1055-1062.

[26] W. Maret, *Exp. Gerontol.*, 2008, **43**, 363-369.

[27] Y.J. Kang., *Exp. Biol. Med.,* 2006, **231**, 1459-1467.

[28] C. Montoliu, P. Monfort, J. Carrasco, Ò. Palacios, M. Capdevila, J. Hidalgo, V. Felipo, *J. Neurochem.*, 2000, **75**, 266-273.

[29] P. Coyle, J.C. Philcox, L.C. Carey, A.M. Rofe, *Cell. Mol. Life. Sci.*, 2002, **59**, 627-647.

[30] C.D. Klassen, J. Liu, S. Choudhuri, *Annu. Rev. Pharmacol. Toxicol.*, 1999, **39**, 267-294.

[31] R. D. Palmiter, *Proc. Nat. Acad. Sci. U .S. A.*¸1998, **95**, 8428-8430.

[32] B.A. Masterms, E.J. Kelly, C.J. Quaife, C.J. Brinster, R.D. Palmiter, *Proc. Natl. Acad. Sci. USA.*, 1994, **91**, 584-588.

[33] F. Trinchella, M. Riggio, S. Filosa, M.G. Volpe, E. Parisi, R. Scudiero, *Comp. Biochem. Physiol. C Toxicol. Pharmacol.,* 2006, **144**, 272-278.

[34] J.C. Amiard, C.S. Amiard-Triquet, B.J. Pellerin, P.S. Rainbow, *Aquat. Toxicol.*, 2006, **76**, 160-202.

[35] E. Moltó, E. Bonzón-Kulichenko, A. del Arco, D.M. López-Alañón, O. Carrillo, N. Gallardo, A. Andrés, *Gene*, 2005, **361**, 140-148.

[36] Z.B. Yang, Y.L. Zhao, N. Li, J. Yang, *Arch. Environ. Contam. Toxicol.*, 2007, **52**, 222-228.

[37] J.H. Kägi, *Methods Enzymol.*, 1991, **205**, 613-626.

[38] F. Haq, M. Mahoney, J. Koropatnick, *Mutat. Res.*, 2003, **533**, 211-226.

[39] C.A. Blindauer, P.J. Sadler, *Acc. Chem. Res.*, 2005, **38**, 62-69.

[40] D.R. Winge, L.T. Jensen, C. Srinivasan, *Curr. Opin. Chem. Biol.*, 1998, **2**, 216-221.

[41] H. Shen, H. Qin, J. Guo, *Nutr. Res.*, 2008, **28**, 406-413.

[42] W. Maret, *J. Chromatogr. B*, 2009, **877**, 3378-3383.

[43] W. Maret, *Biochemistry.*, 2004, **43**¸3301-3309.

[44] W. Maret, G. Heffron, H. A. Hill, D. Djuricic, L.J. Jiang, B. L. Vallee, *Biochemistry*, 2002, **41**, 1689-1694.

[45] W. Maret, *J. Nutr.*¸2003, **133**, 1460-1462.

[46] W. Feng, J. Cai, W.M. Pierce, R.B. Franklin, W. Maret, F.W. Benz, Y.J. Kang¸ *Biochem. Biophys. Res. Commun.*, 2005, **332**, 853-858.

[47] S.G. Bell, B.L. Vallee, *ChemBioChem*, 2009, **10**, 55-62.

[48] A.O. Udom, F.O. Bradly, *Biochem. J.*, 1980, **187**, 329-335.

[49] J.R. Prohaska, A.A. Gybina, *J. Nutr.*, 2004, **134**, 1003-1006.

[50] A. Formigari, P. Irato, A. Santon, *Comp. Biochem. Physiol. C Toxicol. Pharmacol.*, 2007, **146**, 443-459.

[51] M. Valko, C.J. Rhodes, J. Moncol, M. Izakovic, M. Mazur, *Chemico-Biological Interactions*, 2006, **160**, 1-40.

[52] A. Viarengo, B. Burlando, N. Ceratto, I. Panfoli, *Cell. Mol. Biol.*, 2000, **46**, 407-417.

[53] A.R. Quesada, R.W. Byrnes, S.O. Krezoski, D.H. Petering, *Arch. Biochem. Biophys.*, 1996, **334**, 241-250.

[54] J.S. Lazo, Y. Kondo, D. Dellapiazza, A.E. Michalska, K.H. Choo, B.R. Pitt, *J. Biol. Chem.,* 1995, **270**, 5506-5510.

[55] T.M. Buttke, P.A. Sandstrom, *Immunol. Today*, 1994, **15**, 7-10.

[56] J.H. Beattie, A.M. Wood, A.M. Newman, I. Bremner, K.H. Choo, A.E. Michalska, J.S. Duncan, P. T Trayhurn, *Prod. Natl. Acad. Sci. U S A*, 1998, **95**, 358-363.

[57] R. Nath, D. Kumar, T. Li, P.K. Singal, *Toxicology*, 2000, **155**, 17-26.

[58] M. Ø. Pedersen, R. Jensen, D.S. Pedersen, A.D. Skjolding, C. Hempel, L. Maretty, M. Penkowa, *BioFactors*, 2009, **35**, 315-325.

[59] Y. Kondo, J.M. Rusnak, D.G. Hoyt, C.E. Settineri, B.R. Pitt, J.S. Lazo, *Mol. Pharmacol.*, 1997, **52**, 195-201.

[60] Y. Irie, W.M. Keung, *Biochem. Biophys. Res. Commun.*, 2001, **282**, 416-420.

[61] G. Meloni, V. Sonois, T. Delaine, L. Guilloreau, A. Gillet, J. Teissie, P. Faller, M. Vašák, *Nat. Chem. Biol.*, 2008, **4**, 366-372.

[62] Y. Nishiyama, S. Nakayama, Y.Okada, K.S. Min, S. Onosaka, K. Tanaka, *Chem. Pharm.Bull.*, 1990, **38**, 2112-2117.

[63] F.J. Kull, M.F. Reed, T.E. Elgren, T.L. Ciardelli, D.E. Wilcox, *J. Am. Chem. Soc.*, 1990, **112**, 2291-2298.

[64] Y. Okada, N. Ohta, S. Iguchi, Y. Tsuda, H. Sasaki, T. Kitagawa, M. Yagyu, K.S. Min, S. Onosaka, K. Tanaka, *Chem. Pharm. Bull.*, 1986, **34**¸ 986-998.

[65] H.J. Hartman, Y.J. Li, U. Weser, *Biometals*, 1992, **5**, 187-191.

[66] Y.J. Li, U. Weser, *Inorg. Chem.*, 1992, **31**, 5526-5533.

[67] A.K. Sewell, L.T. Jensen, J.C. Erikson, R.D. Palmiter, D.R. Winge, *Biochemistry*, 1995, **34**, 4740-4747.

[68] Y. Okada, K. Tanaka, J. Sawada, Y. Kikuchi, en: M.J. Stillman, C.F. Shaw III, K.T. Suzuki (Eds.), Metallothioneins Synthesis, Structure and Properties of Metallothioneins, Phytochelatins and Metal-Thiolate Complexes, VCH Publishers Inc, New York, 1992, 195.

[69] N. Cols, *Tesi Doctoral*, Dept. Genètica, Universitat de Barcelona, 1996.

[70] M. Capdevila, N. Cols, N. Romero-Isart, R. Gonzàlez-Duarte, S. Atrian, P. Gonzàlez-Duarte, *Cell. Mol. Life Sci.*, 1997, **53**, 681-688.

[71] N. Cols, N. Romero-Isart, M. Capdevila, B. Oliva, P. Gonzàlez-Duarte, R. Gonzàlez-Duarte, S. Atrian, *J. Inorg. Biochem.*, 1997, **68**, 157-166.

[72] R. Bofill, M. Capdevila, S. Atrian, *Metallomics*, 2009, **1**, 229-234.

[73] M. J. Cismowski, P.C. Huang, *Biochemistry*, 1991, **30**, 6626-6632.

[74] M. J. Cismowski, S.S. Narula, I.M. Armitage, M.L. Chernaik, P.C. Huang, *J. Biol. Chem.*, 1991, **226**¸ 24390-24397.

[75] C.W. Cody, P.C. Huang, *Biochemistry*¸1993, **32**, 5127-5131.

[76] C.W. Cody, P.C. Huang, *Biochem. Biophys. Res. Commun.*, 1994, **202**, 954-959.

[77] N. Romero-Isart, N. Cols, M. Termansen, J.L. Gelpí, R. González-Duarte, S. Atrian, M. Capdevila, P. González-Duarte, *Eur. J. Biochem.*, 1999, **259**, 519-527.

[78] R. Bofill, R. Orihuela, M. Romagosa, J. Domènech, S. Atrian, M. Capdevila, *FEBS J.,* 2009, **276**, 7040-7056.

[79] C.A. Blindauer, M.D. Harrison, J.A. Parkinson, A.K. Robinson, J.S. Cavet, N.J. Robinson, P.J. Sadler, *Proc. NAtl. Acad. Sci. USA*, 2001, **98**, 9593-9598.

[80] M.J. Daniels, J.S. Turner-Cavet, R. Selkirk, H.Z. Sun, J.A. Parkinson, P.J. Sadler, N.J. Robinson, *J. Biol. Chem.*, 1998, **273**, 22957-22961.

[81] T.A. Smith, K. Lerch, K.O. Hodgson, *Inorg. Chem.*, 1986, **25**, 4677-4680.

[82] P.A. Cobine, R.T. McKay, K. Zanger, C.T. Dameron, I.M. Armitage, *Eur. J. Biochem.*, 2004, **271**, 4213-4221.

[83] V. Calderone, B. Dolderer, H.J. Hartmann, H. Echner, C. Luchinat, C. Del Bianco, S. Mangani, U. Weser, *Proc. Natl. Acad. Sci. U. S. A.*, 2005, **102**, 51-56.

[84] I. Bertini, H.J. Hartmann, T. Klein, G. Liu, C. Luchinat, U. Weser, *Eur. J. Biochem.*, 2000, **267**, 1008-1018.

[85] C.W. Peterson, S.S. Narula, I.M. Armitage, *FEBS lett.*, 1996, **379**, 85-93.

[86] P.C. Jocelyn, *Eur. J. Biochem.*, 1967, **2**, 327-331.

[87] L. Villarreal, L. Tio, S. Atrian, M. Capdevila, *Arch. Biochem. Bioph*., 2005;**435**, 331-335.

[88] M. Capdevila, J. Domènech, A. Pagani, L. Tio, L. Villarreal, S. Atrian, *Angew. Chem. Int. Ed.*, 2005, **44**, 4618-4622.

[89] R. Orihuela, F. Monteiro, A. Pagani, M. Capdevila, S. Atrian, *Chem. Eur. J.*, 2010, **16**, 12363-12372.

[90] J. Domènech, Ò. Palacios, L. Villarreal, P. González-Duarte, M. Capdevila, S. Atrian, *FEBS Lett.*, 2003, **533**, 72-78.

[91] L. Tío, L. Villarreal, S. Atrian, M. Capdevila, *J. Biol. Chem.*, 2004, **279**, 24403-24413.

[92] R. N. Reese, D. R. Winge, *J. Biol. Chem.*, 1988, **263**, 12832-12835.

[93] D. N. Weber, F. Shall III, D. H. Petering, *J. Biol. Chem.*, 1987, **262**, 6962-6964.

[94] R. N. Reese, R. M. Mehra, E. B. Tarbet, D. R. Winge, *J. Biol. Chem.*, 1988, **263**, 4186-4192.

[95] D. R. Winge, C. T. Dameron, R. K. Mehra, dins: *Metallothioneins*, M. J. Stillman, F. C. Shaw III, K. T. Suzuki, 1992, **11**, 257-270.

[96] R.N. Reese, C.A. White, D.R. Winge, *Plant Physiol.*, 1992, **98**, 225-229.

[97] G. Mir, J. Domènech, G. Huguet, W. Guo, P. Golsbrough, S. Atrian, M. Molinas, *J. Exp. Bot*., 2004, **55**, 2483-2493.

[98] X. Wan, E. Freisinger, *Inorg. Chem*., 2013, **52**, 785-792.

[99] T. Huber, E. Freisinger, *Dalton Trans*., 2013, **42**, 8878-8889.

[100] T.J. Park, S.Y. Lee, N.S. Heo, T.S. Seo, *Angew. Chem. Int. Ed.*, 2010, **49**, 7019-7024.

[101] N. Krumov, S. Oder, I. Perner-Nochta, A. Angelov, C. Posten, *J. Biotechnol.*, 2007, **132**¸ 481-486.

[102] B. A. Fowler, C.E. Hildebrand, T. Kojima, M. Webb, *Experientia Supp.,* 1987, **52**, 19-22.

[103] J. H. R. Kägi, A.Schäffer, *Biochemistry,* 1988, **27**, 8509-8515.

[104] B.A. Binz, H.R. Kagi, Dins: *Metallothionein IV,* Birkhäuser Verlag, 1999, **7-13.**

[105] Ò. Palacios, *Tesi Doctoral*, Dept. Química, Universistat Autònoma de Barcelona, 2003.

[106] A. Pagani, L. Villarreal, M. Capdevila, S. Atrian, *Mol. Microbiol.*, 2007, **63**, 256-269.

[107] M. Capdevila, O. Palacios, S. Atrian, *Bioinorg. Chem. Appl*, 2010, 1-6, doi:10.1155/2010/541829.

[108] R. Orihuela, *Tesi Doctoral*, Dept. Química, Universistat Autònoma de Barcelona, 2008.

[109] L. Villarreal, L. Tío, M. Capdevila, S. Atrian, *FEBS J.*, 2006, **273**, 523-535.

[**110**] http://wwwd.unizh.ch/~mtpage/classif.html.

[111] C.J. Quaife, S.D. Findley, J.C. Erikson, G.J. Froelick, E.J. Kelly, B.P. Zambrowicz, R.D. Palmiter, *Biochemistry*, 1994, **33**, 7250-7259.

[112] L. Liang, K. Fu, D.K. Leee, R.J. Sobieski, T. Dalton, G.K. Andrews, *Mol. Rep. Dev.*, 1996, **43**, 25-37.

[113] D. Egli, J. Domènech, A. Selvaraj, K. Balamurugan, H. Hua, M. Capdevila, O. Georgiev, W. Schaffner, S. Atrian, *Genes to Cells*¸ 2006, **11**, 647-658.

[114] S.S. Narula, M. Brouwer, Y. Hua, I.M. Armitage, *Biochemistry*, 1995, **34**, 620-631.

[115] M. Valls, R. Bofill, R. González-Duarte, P. González-Duarte, M. Capdevila, S. Atrian, *J. Biol. Chem.*, 2001, **276**, 32835-32843.

[116] K. Lerch, D. Ammer, R. Olafson, *J. Biol. Chem.*, 1982, **257**, 2420-2426.

[117] R. Riek, B. Prêcheur, Y. Wang, E.A. Mackay, G. Wider, P. Güntert, A. Liu, J.H. Kägi, K. Würthrich, *J. Mol. Biol*, 1999, **291**, 417-428.

[118] N. Ceratto, F. Dondero, J.W. Van de Loo, B. Burlando, A. Vilarengo, *Comp. Biochem. Physiol*. *C*, 2002, **131**, 217-222.

[119] M. Höckner, R. Dallinger, S.R. Stüzerbaum, *J. Biol. Inorg. Chem*, 2011, **16**, 1057-1065.

[120] V.C-H. Liao, J. Dong, J.H. Freedman, *J. Biol.Chem.*, 1982, **257**, 2420-2426.

[121] K. Maruyama, R. Hori, T. Nishihara, *Eisei Kagaku*, 1986, **32**, 22-27.

[122] W. Ponder, D.R. Lindberg, *Phylogeny and Evolution of the Mollusca* CA: University of California Press, 2008, 1-488.

[123] G. Rosenberg, *Evolution*, 1996, **50 (2)**, 682-693.

[124] G.M. Barker, dins: Barker GM (Eds.) Biology of terrestrial molluscs, CAB International, 2001, Wallingford, 1-146.

[125] M. Capdevila, S. Atrian, *J. Biol. Inorg. Chem.*, 2011, **16**, 991-1009.

[126] L. Vergani, in *Metal ions in Life Sciences: Metallothioneins and Related Chelators*, ed. A. Sigel, H. Sigel, and R.K.O. Sigel, RSC Publishing, cambridge, U.K., 2009, vol. 5, pp. 199-238.

[127] K.M. Jörger, I. Stoger, Y. Kano, H. Fukuda, T. Knebelsberger, M. Schrodl, *BMC Evol. Biol.*, 2010, **10**, 323.

[128] R. Dallinger, *Comp. Biochem. Physiol.*, 1996, **113c**, 125-133.

[129] B. Lieb, *Comp. Biochem. Physiol*. *C*, 2003, **134**, 131-137.

[130] R. Dallinger, B. Berger, A. Bauer-Hilty, *Mol. Cell. Biochem.*, 1989, **85**, 135-145.

[131] F. Hispard, D. Schuler, A. de Vaufleury, R. Schifler, P.M. Badot, R. Dallinger, *Environ. Toxicol. Chem.*, 2008, **27**, 1533-1542.

[132] L. Vergani, M. Gattarola, C. Borghi, F. Dondero, A. Viarengo, *FEBS J.,* 2005, **272**, 6014-6023.

[133] B. Berger, P. E. Hunziker, *Biochem. J.,* 1995, **311**, 951-957.

[134] M. Chabicovsky, H. Niederstatätter, *Toxicol. Appl. Pharm.,* 2003, **190**, 25-36.

[135] B. Berger, R. Dallinger, *Biochem. J.,* 1997, **328**, 219-224.

[136] R. Dallinger, B. Berger, *Nature,* 1997, **388**, 237-238.

[137] R. Dallinger, M. Chabicovsky, *Am. J. Phydiol. Regul. Integr. Comp. Physiol.*, 2005, **289**, 1185-1195.

[138] P. M. Gehrig, C. You, R. Dallinger, *Prot. Sci.,* 2000, **9**, 395-402.

[139] R. Dallinger, B. Berger, *Eur. J. Biochem.,* 1993, **216**, 739-746.

[140] R. Dallinger, Y. Wang, *Eur. J. Biochem.,* 2001, **68**, 4126-4133.

[141] M. Höckner, K. Stefanon, A. de Vaufleury, F. Monteiro, S. Pérez-Rafael, O. Palacios, M. Capdevila, S. Atrian, R. Dallinger, *Biometals*, 2011, **24**, 1079-1092.

[142] http://www. bioc.unizh.ch/mtpage/trees.html

[143] M. Schubert, H. Escriva, J. Xavier-Neto, V. Laudet, *TRENDS Ecol. Evol.,* 2006, **5**, 269-277.

[144] C. Cañestro, S. Bassham, J.H. Postlethwait, *Genome Biol.*, 2003, **4**, 208.

[145] N. H. Putnam, T. Butts, D.E. Ferrier, R.F. Furlong, U. Hellsten, et al., *Nature*, 2008, **19**, 1064-1071.

[146] https://scripps.ucsd.edu/news/2456

[147] M. Vašák, G. Meloni, *J. Biol. Inorg. Chem.*, 2011, **16**, 1067-1078.

[148] J.C. Gutierrez, F. Amaro, S. Diaz, P. de Francisco, L.L. Cubas and A. Martí-González, *J. Biol. Inorg. Chem.*, 2011, **16**, 1025-1034.

[149] B. Dolderer, H.J. Hartman and U. Weser, dins: *Metal ions in Life Sciences: Metallothioneins and Related Chelators,* ed. A. Sigel, H. Sigel, and R.K.O. Sigel, RSC Publishing, Cambridge, U.K., 2009, **5**, 83-106.

[150] S. Atrian, dins *Metal ions in Life Sciences: Metallothioneins and Related Chelators,* ed. A. Sigel, H. Sigel, and R.K.O. Sigel, RSC Publishing, Cambridge, U.K., 2009, **5**, 155-181.

[151] K. Balamurugan and Schaffner W., dins *Metal ions in Life Sciences: Metallothioneins and Related Chelators,* ed. A. Sigel, H. Sigel, and R.K.O. Sigel, RSC Publishing, Cambridge, U.K., 2009, **5**, 31-49.

[152] L. Atanesyan, V. Günther, S.E. Celniker, O. Georgiev, W. Schaffner, *J. Biol. Inorg. Chem.*, 2011, **16**, 1047-1056.

[153] M. Guirola, Y. Naranjo, M. Cadevila, S. Atrian, *J. Inorg. Biochem.*, 2011, **105**¸ 1050-1059.

[154] A. Pagani, L. Villarreal, M. Capdevila, S. Atrian, *Mol.Microbiol.*, 2007, **63**, 256-269.

[155] P.M. Gehrig, C. You, R. Dallinger, C. Gruber, M. Brouwer, J.H.R. Kägi, P.E. Hunziker, *Prot. Sci.*, 2000, **9**, 395-402.

[156] N. Cols, N. Romero-Isart, M. Capdevila, B. Oliva, P. Gonzàlez-Duarte, R. Gonzàlez-Duarte, S. Atrian, *J. Inorg. Biochem*, 1997, **68**, 157-166.

[157] R. Orihuela, J. Domènech, R.Bofill, C. You, E.A. Mackay, J.H.R. Kägi, M.Capdevila, S.Atrian, *J. Biol. Inorg. Chem.,* 2008, **13**, 801-812.

[158] A. Pagani, L. Villarreal, M. Capdevila, S. Atrian, *Mol. Microbiol.* 2007, **63**, 256-269.

[159] R. Orihuela, F. Monteiro, A. Pagani, M. Capdevila, S. Atrian, *Chem. A Eur. J.*, 2010, **16**, 2363-2372.

[160] E.W. Milles, *Methods Enzymol.*, 1977, **47**, 431-442.

[161] V.L. Mendoza, R.W. Vachet, *Anal. Chem.*, 2008, **80**, 2895-2904.

[162] R. Bofill, R. Orihuela, M. Romagosa, J. Domenech, S. Atrian, et al., *FEBS J.*, 2009, **276**, 7040-7056.

[163]R. Orihuela, F. Monteiro, A. Pagani, M. Capdevila, S. Atrian, *Chem. A Eur. J.*, **(2010)**, 16, 2363-2372.

[164] A. Pagani, L. Villarreal, M. Capdevila, S. Atrian, *J. Mol. Microbiol*, 2007, **63**, 256-269.

[165] M. Valls, R. Bofill, N. Romero-Isart, R. González-Duarte, J. Abian, M. Carrascal, P. Gonzalez-Duarte, M. Capdevila, S. Atrian, *FEBS Lett.*, 2000, **467**, 189-194.

[166] Z.Xiao, G. Weed, *Nat. Prod. Rep.*, 2012, **27**, 768-789

[167] A.M. Sparla, J. Overnell, *Biochem. J.*, 1990. **267**(2), 39-540.

[168] Y. J. Wang, et al., *Eur. J. Biochem*., 1994. **225**(1), 449-457.

[169] C. Ruiz, J. Mendieta, A.R. Rodriguez, *Anal. Chim. Acta*, 1995. **305**(1-3),285-294.

[170] M. A. Namdarghanbari, et al., *J. Inorg. Biochem.*, 2010. **104**(3): p. 224-231.

[171] D.E. Wilcox, *Inorg. Chim. Acta*, 2008, **361**, 857-867.

[172] D. Chu, Y. Tang, W. Cao, *Thermochim. Acta*, 2000, **352/353**, 205-212.

[173] Y. Huan, D. chu, Y. Tnag, W.Cao, *Acta Physico-Chim Sinica*, 2000, **16**, 764-768.

[174] E. Chekmeneva, R. Prohens, J. M. Díaz-Cruz, C. Ariño, M. Esteban, *Anal. Biochem.*, 2008, **375**, 82-89.

[175] E. Chekmeneva, R. Prohens, J. M. Díaz-Cruz, C. Ariño, M. Esteban, *Environ. Sci. Technol.*, 2008, **42**, 2860-2886.

[176] E. Artells, Ò. Palacios, M. Capdevila, S. Atrian, *Metallomics*, 2013, DOI: 10.1039/c3mt00123g.

[177] E. Artells, Ò. Palacios, M. Capdevila, S. Atrian, *Biochem J.*, 2013 submited.

[178] G.J. Kubas, B. Monzyk, A.L. Crumbliss, *Inorg. Synt.*, 1979, **19**, 90-92.

[179] http://www.jove.com/video/2796/isothermal-titration-calorimetry-for-measuring-macromolecule-ligand

7. ANNEX

7.1. ANNEX D'EXPERIMENTS: CARACTERITZACIÓ DE LES DIFERENTS MTs ESTUDIADES

7.1.1. Caracterització de les isoformes d'MT del cargol *Helix pomatia*

Làmina 7.1.1.1. Valoració de Zn_6-HpCdMT *in vivo* amb Cd(II).

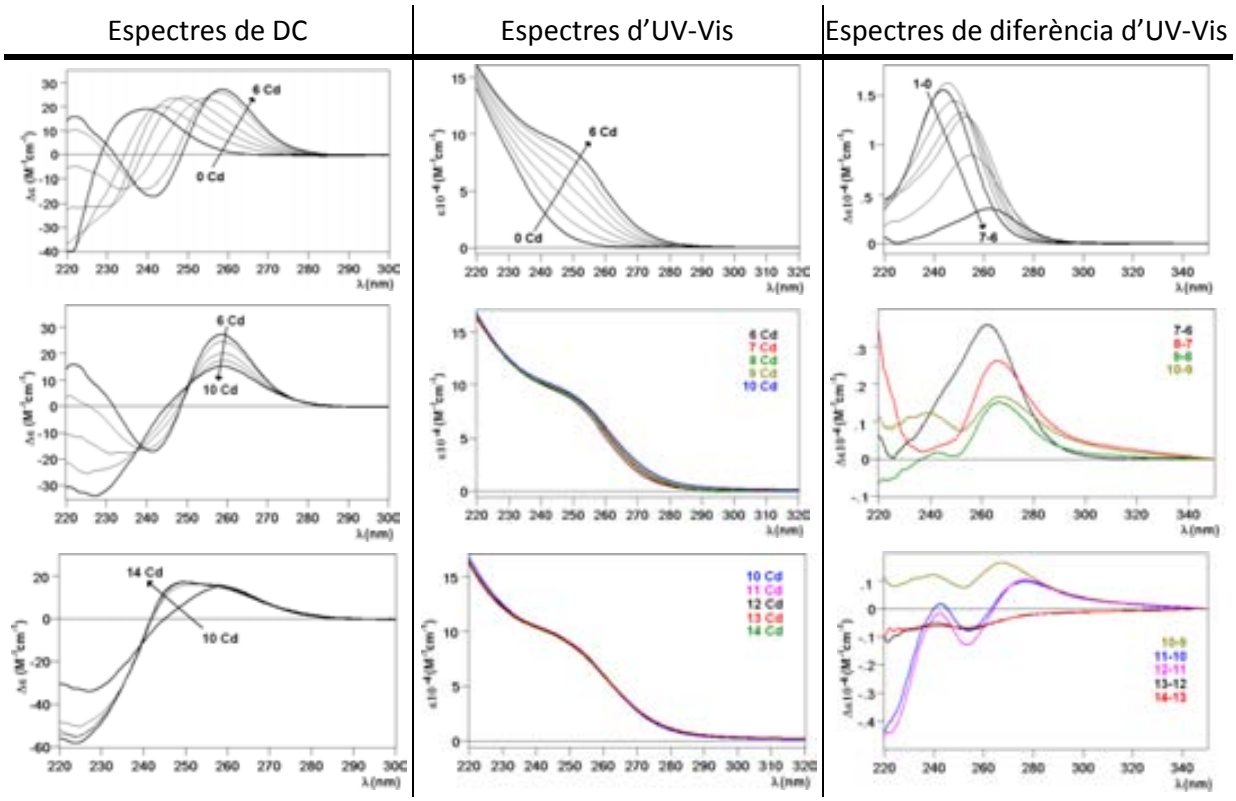

Fig. 1. Espectres de DC, UV-Visible i diferència d'UV-Visible enregistrats en la valoració d'una solució 15,08 µM de Zn_6-HpCdMT amb Cd(II) a pH 7 i 25 °C.

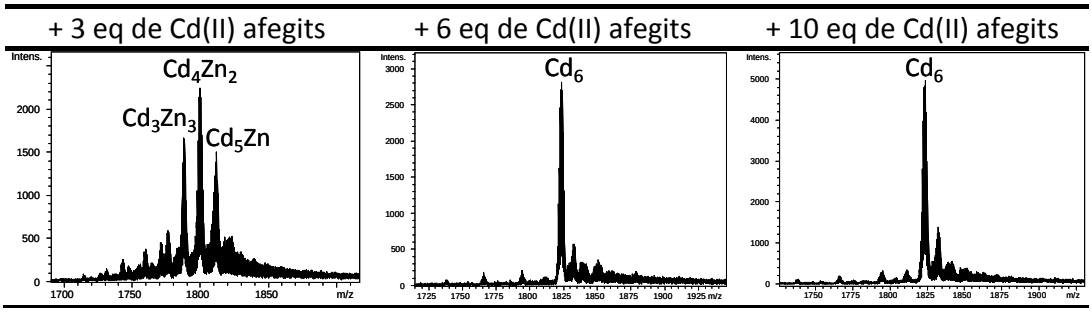

Taula 1. Espectres d'ESI-MS obtinguts després d'addicionar 3, 6 i 10 eq de Cd(II) a una solució 15,08 µM de Zn_6-HpCdMT a pH 7 i 25 °C.

Làmina 7.1.1.2. Acidificació i posterior reneutral·lització de Cd_6-HpCdMT *in vivo*.

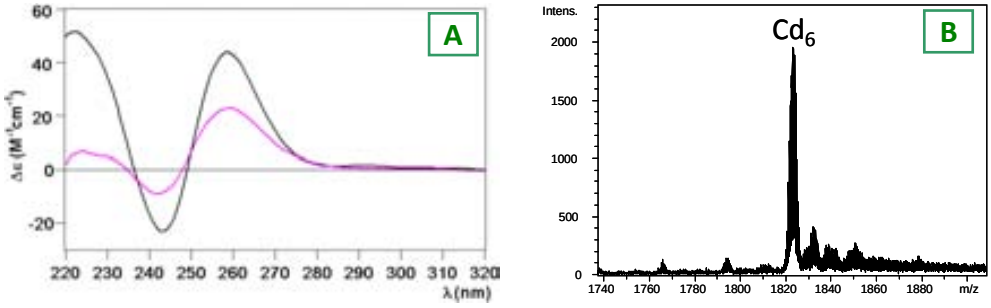

Fig. 2. Espectre de DC (**A, rosa**) i d'ESI-MS (**B**) obtinguts després d'acidificar a un valor de pH per sota d'1 i posteriorment reneutral·litzant a pH 7 una solució 14,99 µM de Cd_6-HpCdMT *in vivo* (**A, negre**) a 25 °C.

Làmina 7.1.1.3. Valoració de Zn_6-HpCdMT *in vivo* amb Cu(I).

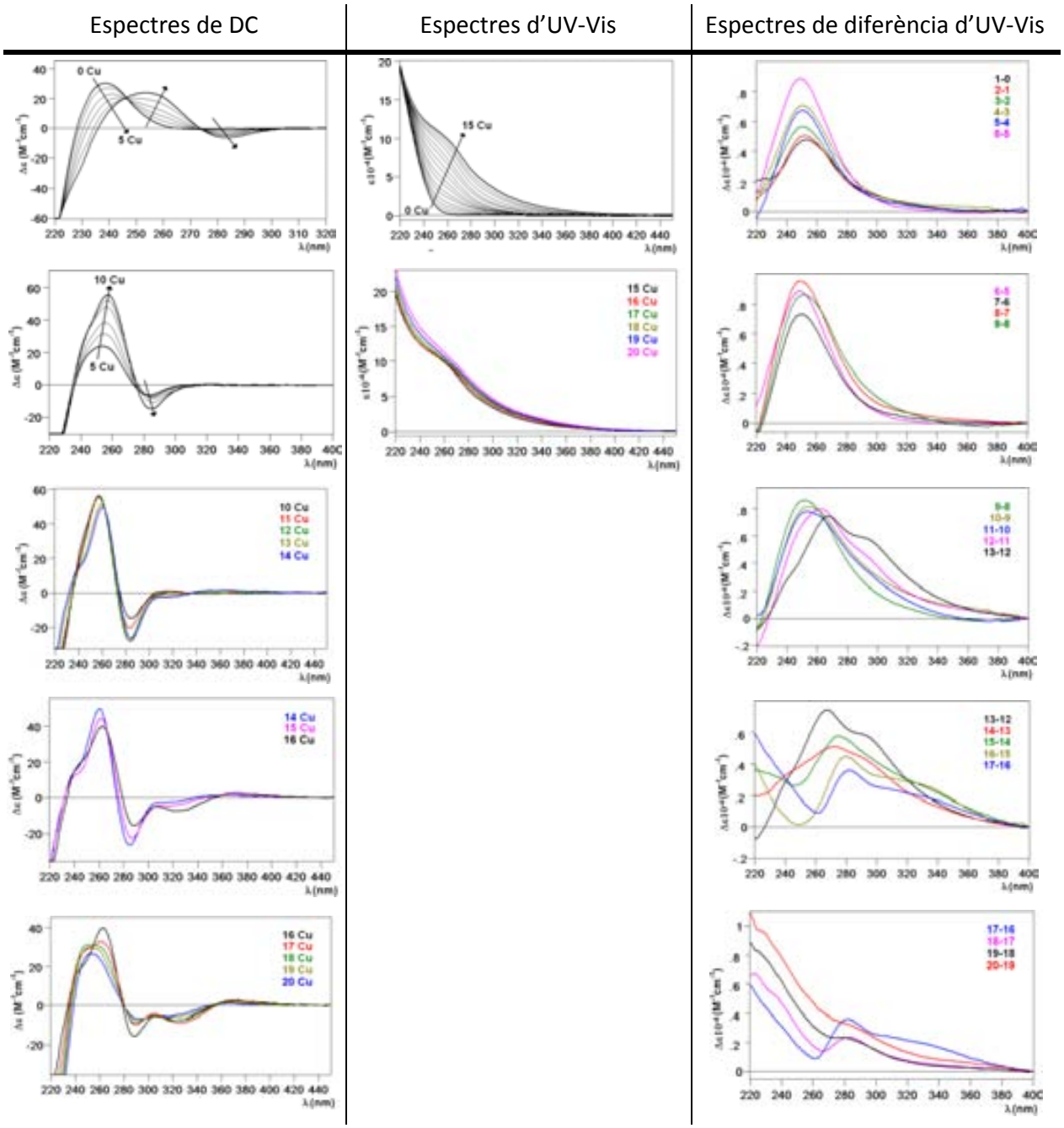

Fig. 3. Espectres de DC, UV-Visible i diferència d'UV-Visible enregistrats en la valoració d'una solució 14,98 µM de Zn_6-HpCdMT amb Cu(I) a pH 7 i 25 °C.

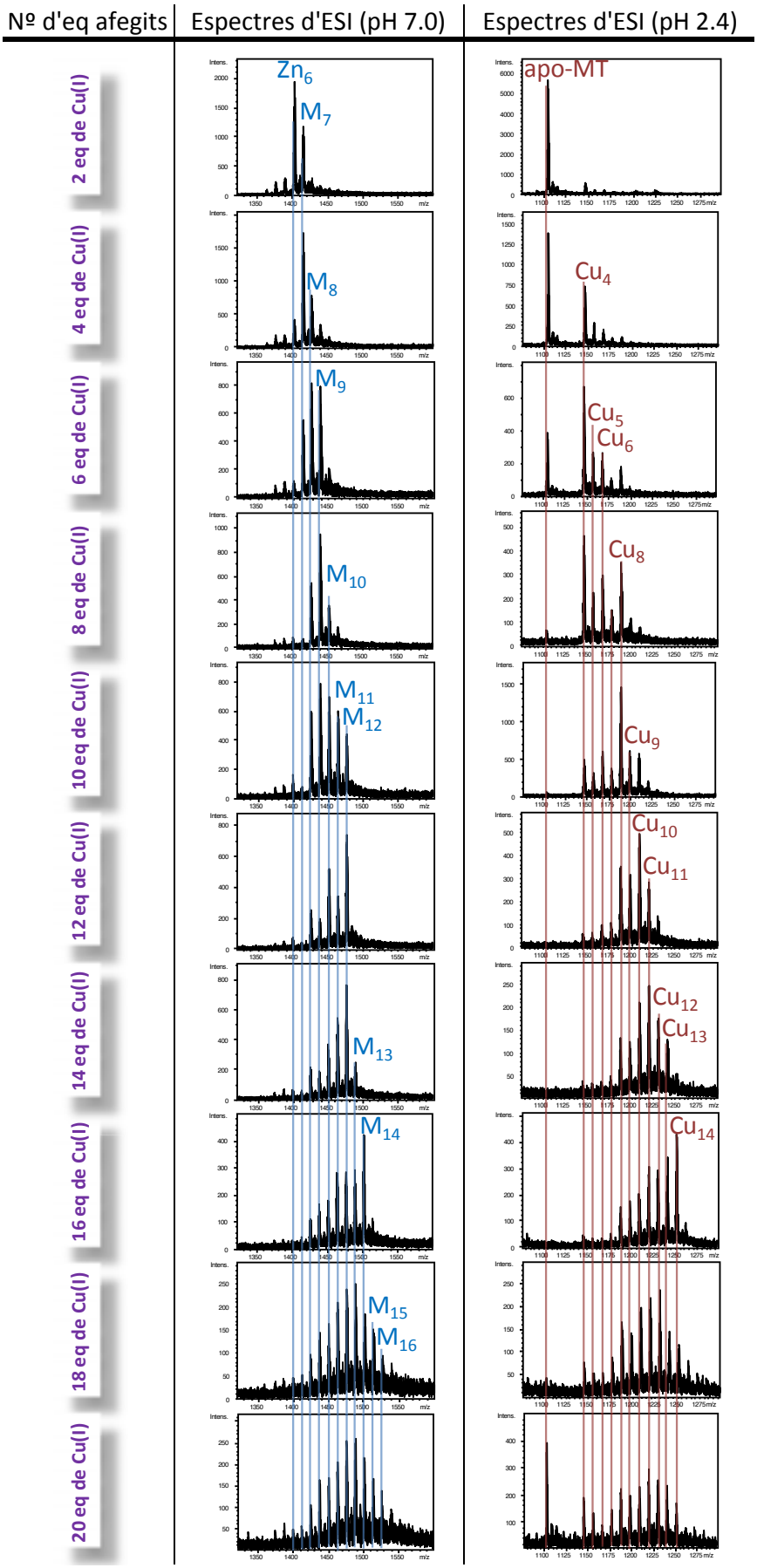

Taula 2. Espectres d'ESI-MS enregistrats a pH 7.0 i 2.4, cada 2 eq de Cu(I) afegits, en la valoració d'una solució 14,98 µM de Zn_6-HpCdMT.

Làmina 7.1.1.4. Valoració de Zn-HpCuMT *in vivo* amb Cd(II).

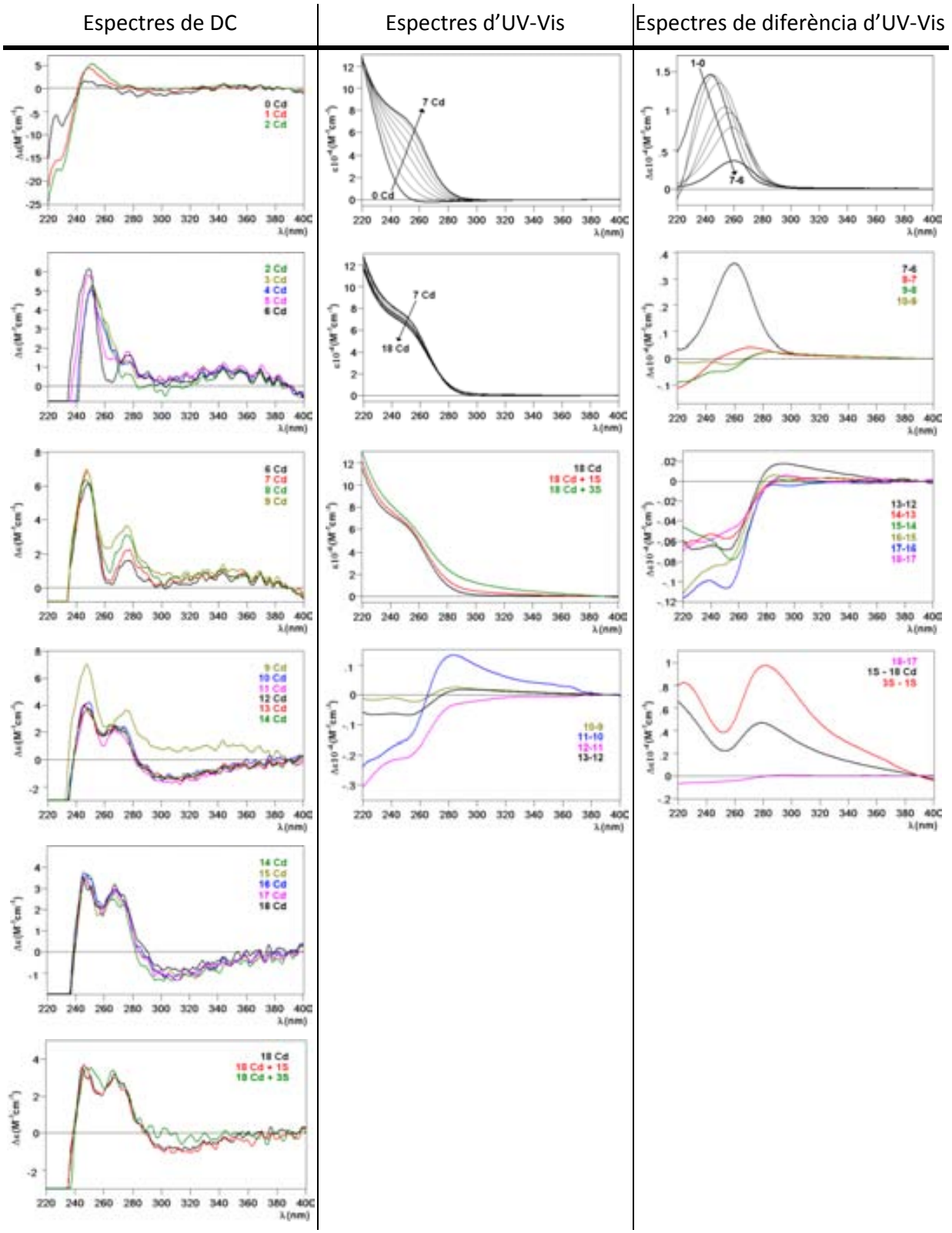

Fig. 4. Espectres de DC, UV-Visible i diferència d'UV-Visible enregistrats en la valoració d'una solució 14,09 µM de Zn-HpCuMT *in vivo* (Tipus 3) amb Cd(II) a pH 7 i 25 °C.

Làmina 7.1.1.5. Acidificació i posterior reneutral·lització de Cd-HpCuMT *in vivo*.

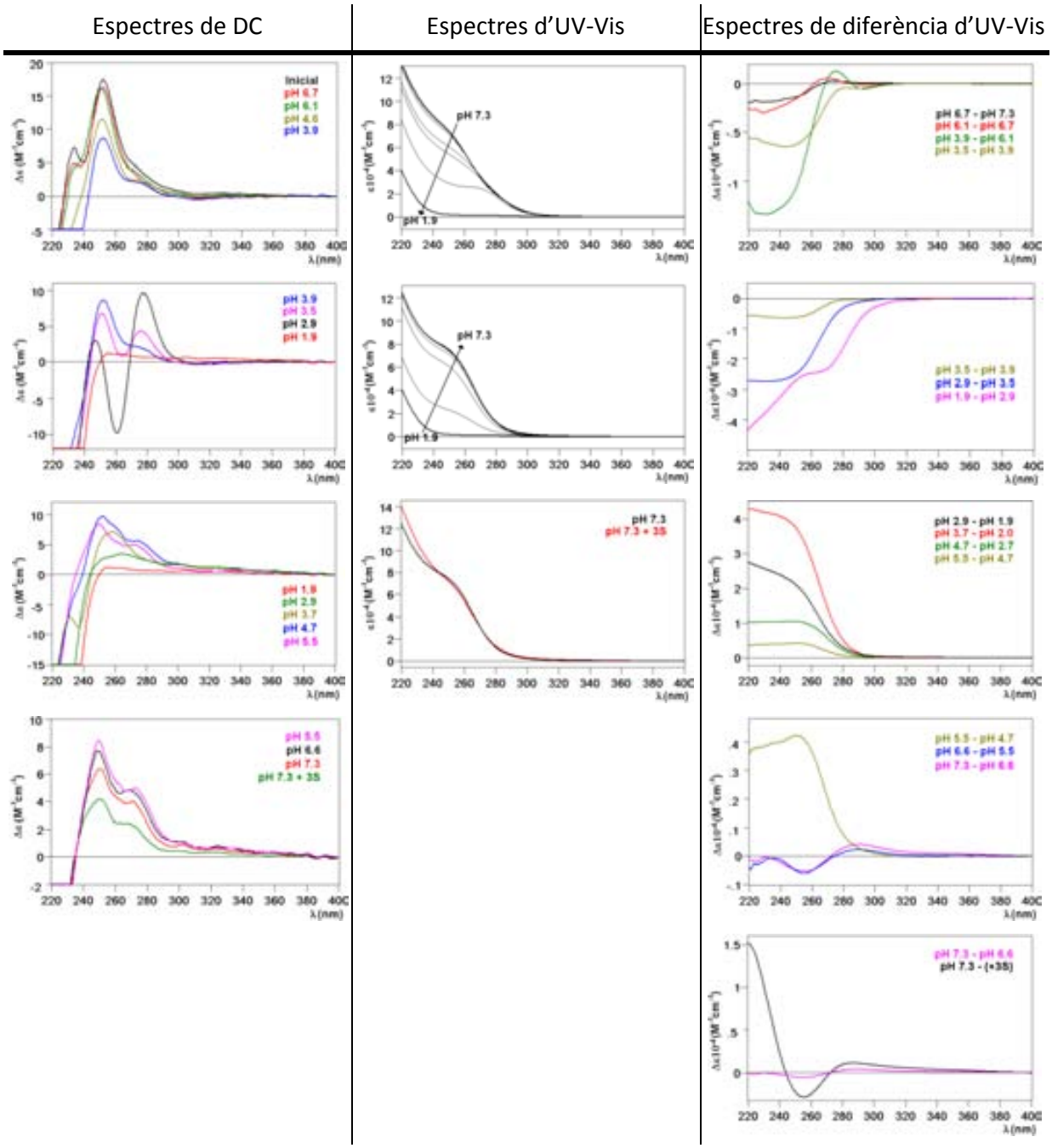

Fig. 5. Espectres de DC, UV-Visible i diferència d'UV-Visible enregistrats en el procés d'acidificació/reneutral·lització i finalment addició de 3 eq de Na_2S a una solució 13,12 µM de Cd-HpCuMT *in vivo* (Tipus 1) a pH 7 i 25 °C.

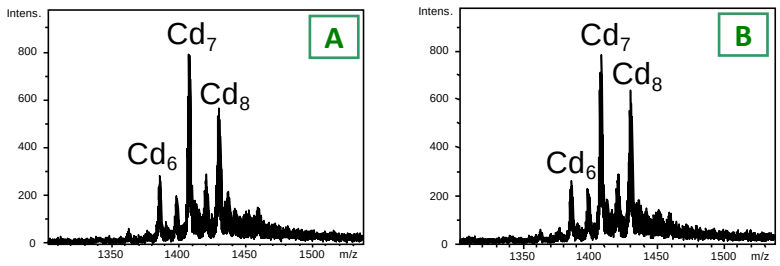

Fig. 6. Espectres d'ESI-MS enregistrats al final de l'estudi de acidificació/reneutral·lització de Cd-HpCuMT (**A**) (Tipus 1) i després d'afegir 3 eq de S^{2-} (**B**).

Làmina 7.1.1.6. Valoració de Zn-HpCuMT *in vivo* amb Cu(I).

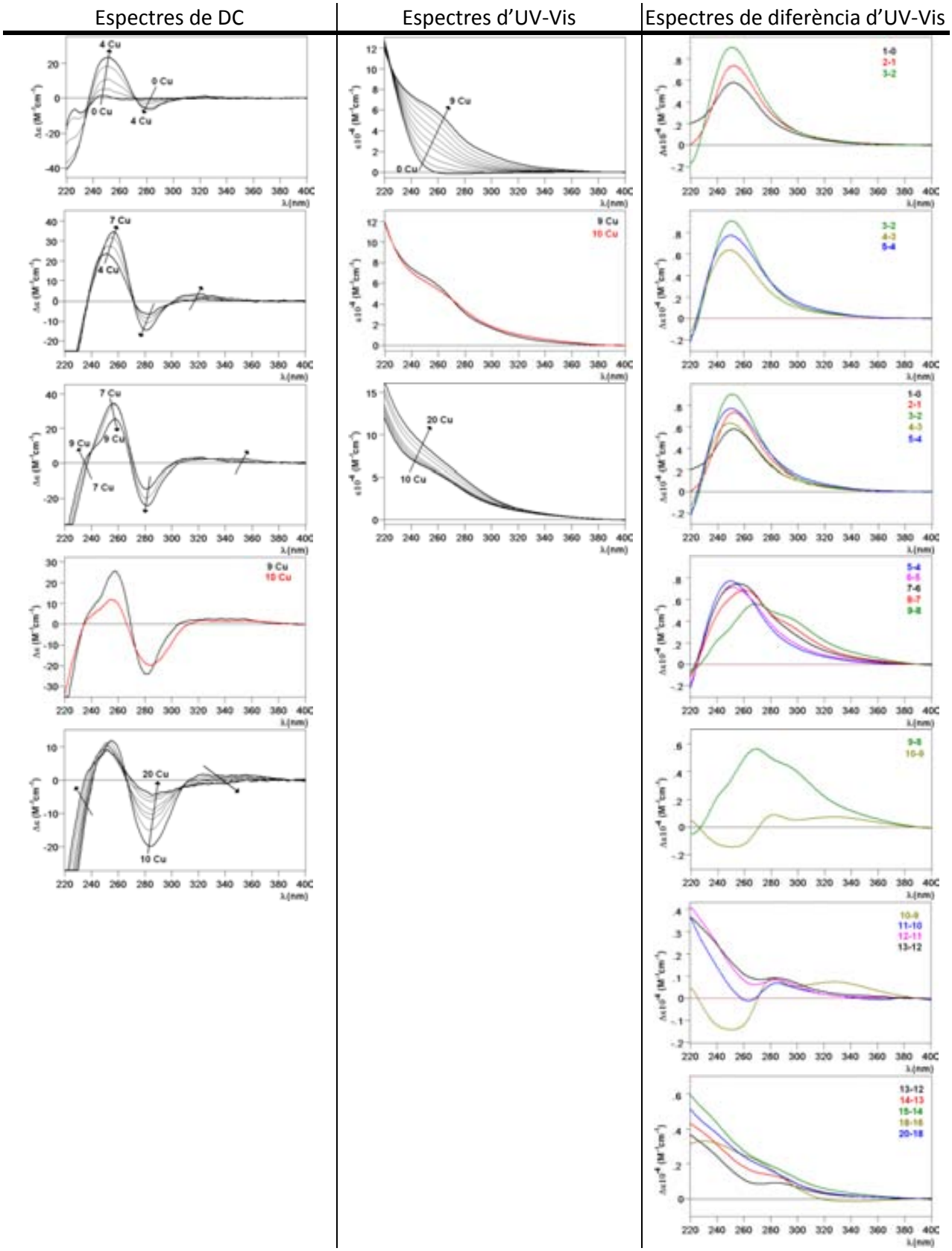

Fig. 7. Espectres de DC, UV-Visible i diferència d'UV-Visible enregistrats en la valoració d'una solució 12,13 µM de Zn-HpCuMT (Tipus 1) amb Cu(I) a pH 7 i 25 °C.

Làmina 7.1.1.7. Valoració de Cu-HpCuMT *in vivo* amb Cu(I).

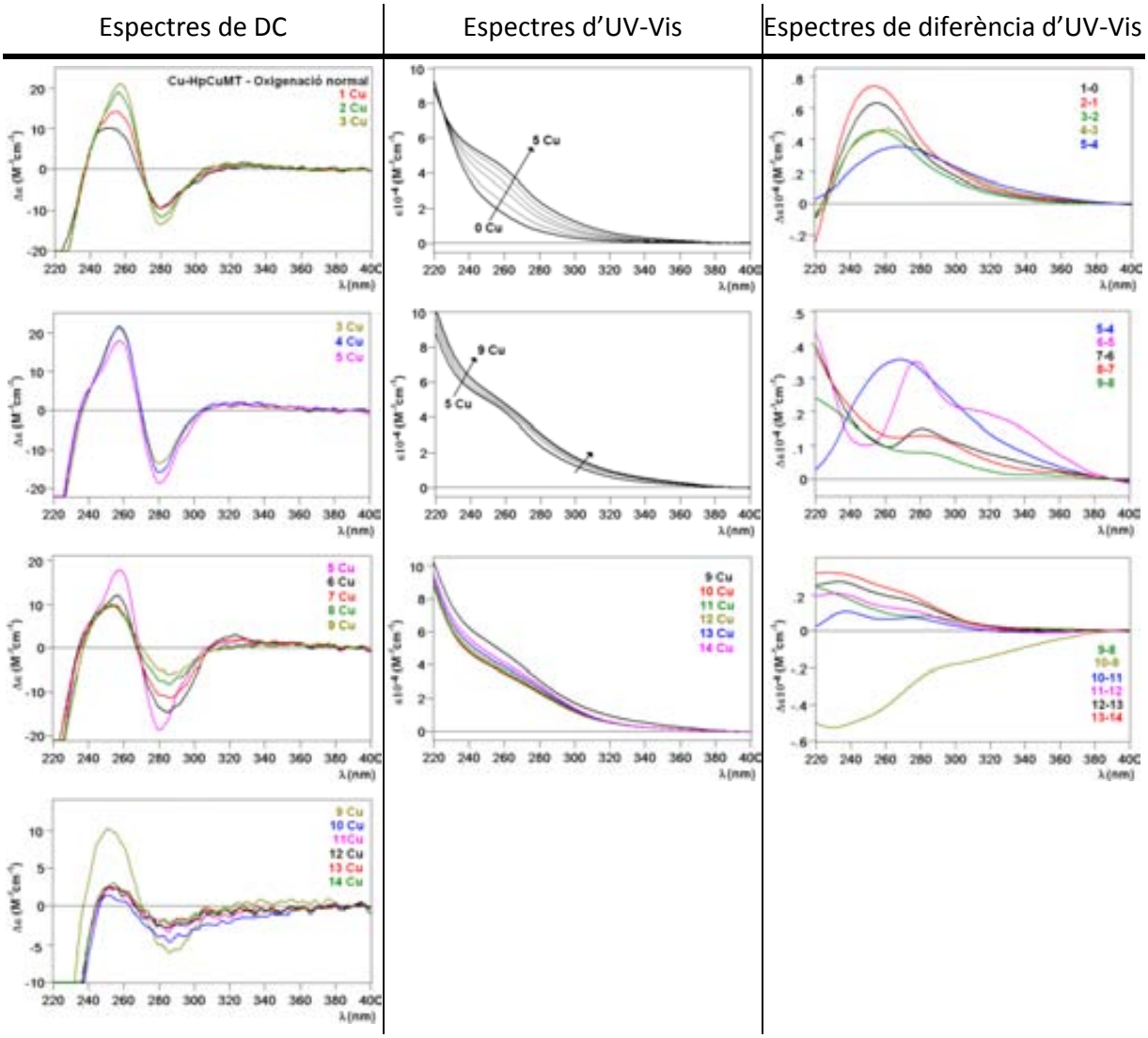

Fig. 8. Espectres de DC, UV-Visible i diferència d'UV-Visible enregistrats en la valoració d'una solució 13,20 µM de Cu-HpCuMT *in vivo* (baixa oxigenació) amb Cu(I) a pH 7 i 25 °C.

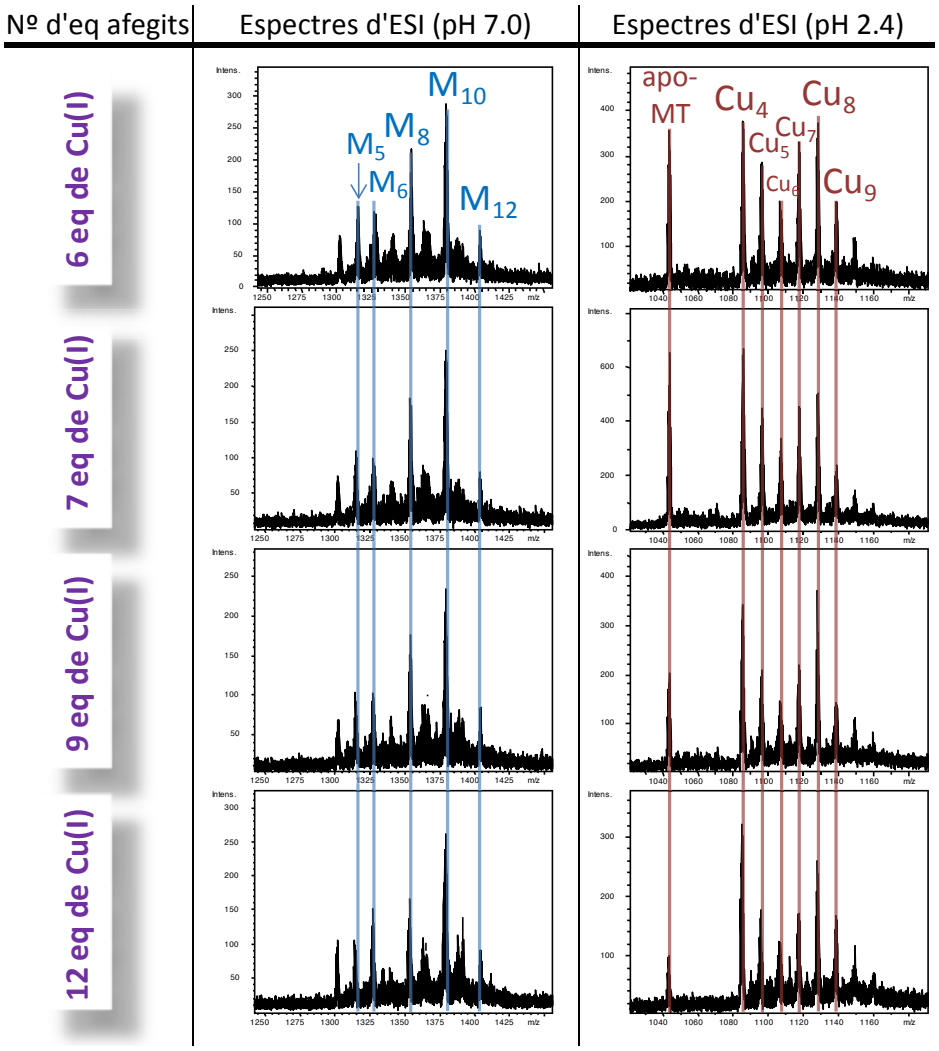

Taula 3. Espectres d'ESI-MS, enregistrats a pH 7.0 i 2.4, corresponents a la valoració d'una solució 13,20 µM de Cu-HpCuMT *in vivo* (baixa oxigenació) amb 6, 7, 9 i 12 eq de Cu(I).

Làmina 7.1.1.8. Valoració de Zn-HpCuMTmut *in vivo* amb Cd(II).

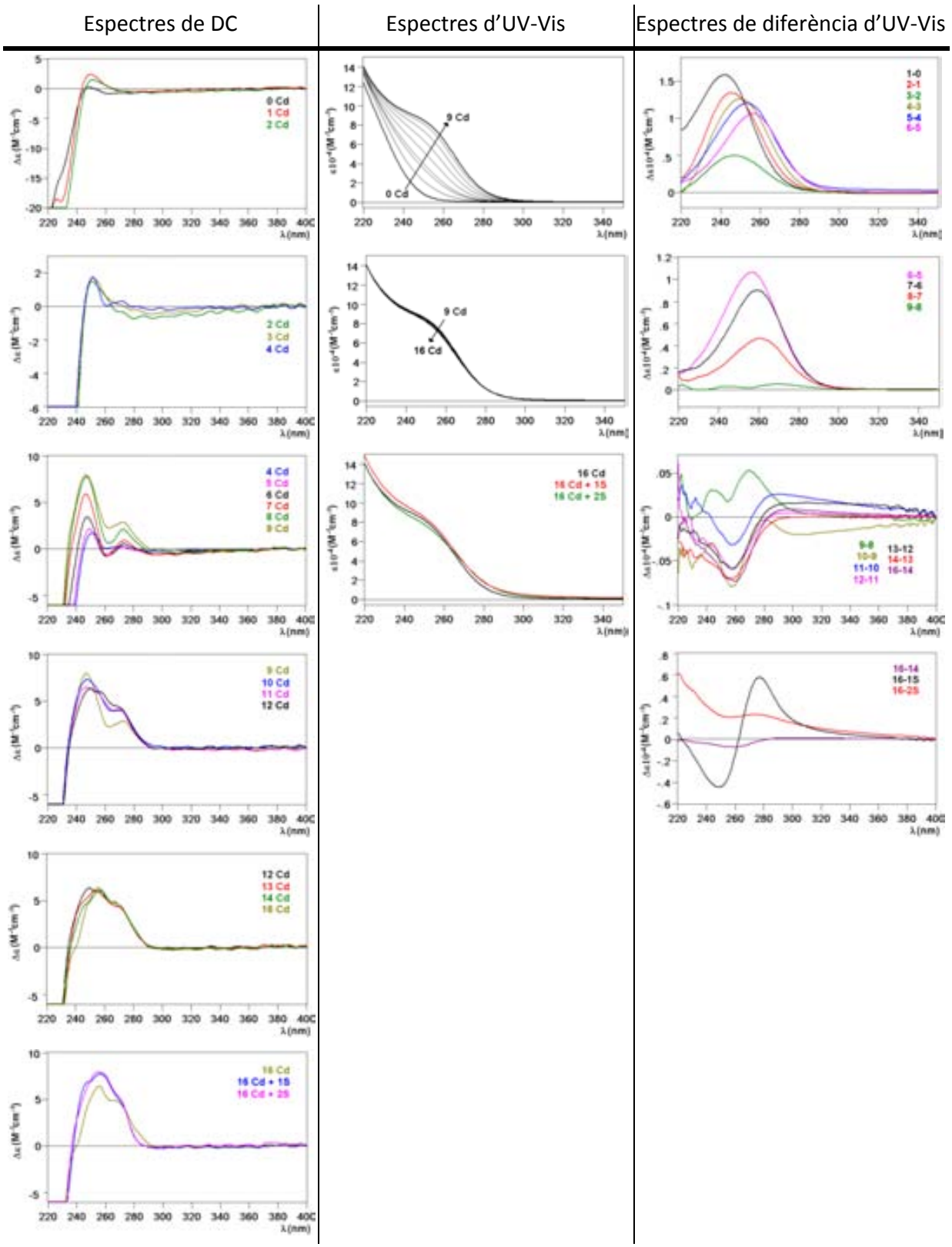

Fig. 9. Espectres de DC, UV-Visible i diferència d'UV-Visible enregistrats en la valoració d'una solució 14,50 µM de Zn-HpCuMTmut *in vivo* amb Cd(II) a pH 7 i 25 °C.

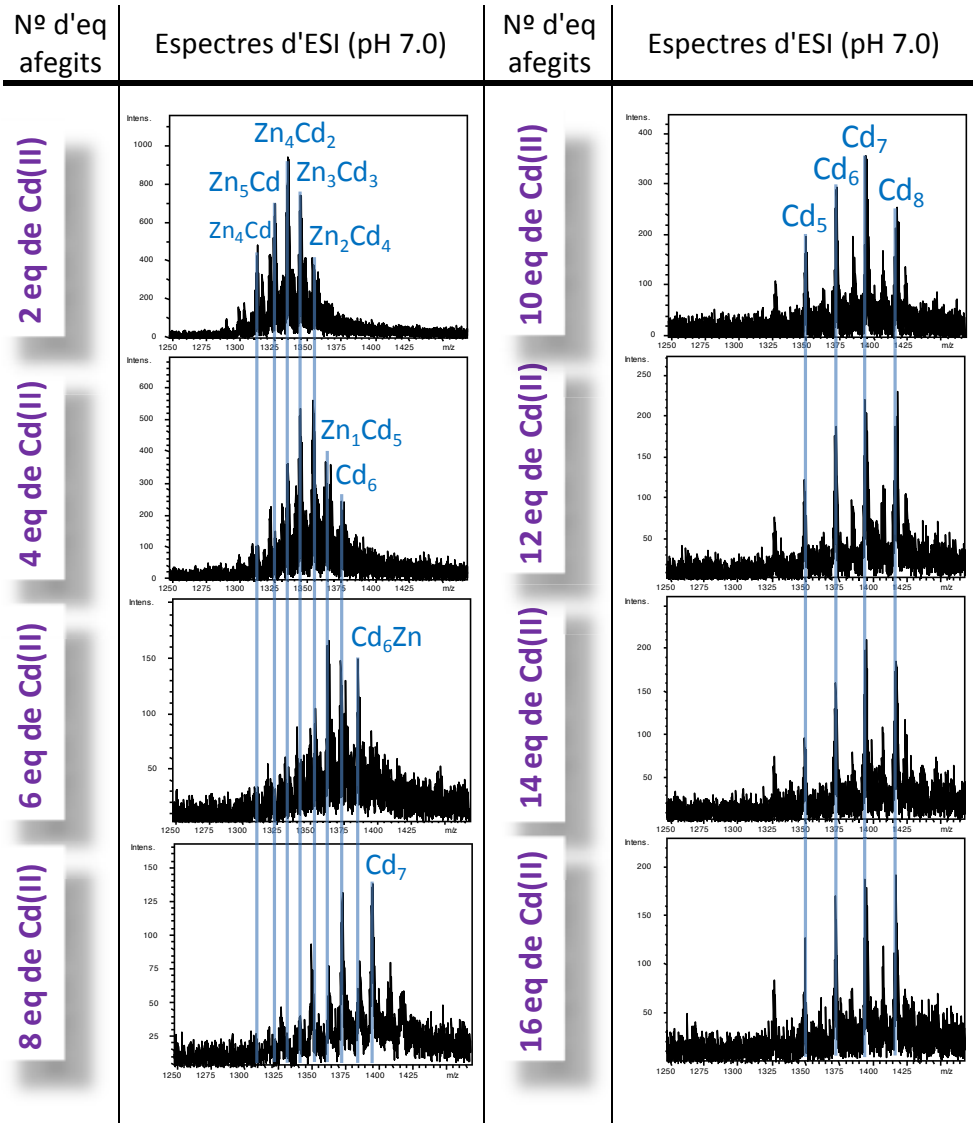

Eq. Cd(II)	Espectre	Especies
16 + 2S	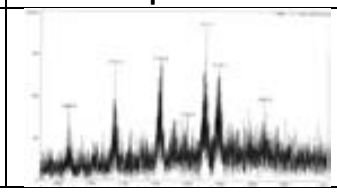	$Cd_8 > Cd_8S > Cd_7 > Cd_6 > Cd_9S > Cd_5$

Fig. 10. Espectres d'ESI-MS obtinguts després addicionar diferents números d'eq de Cd(II) i de S^{2-} a una solució 14,50 µM de Zn-HpCuMTmut a pH 7 i 25 °.

Làmina 7.1.1.9. Acidificació i posterior reneutral·lització de la Cd-HpCuMTmut *in vivo*.

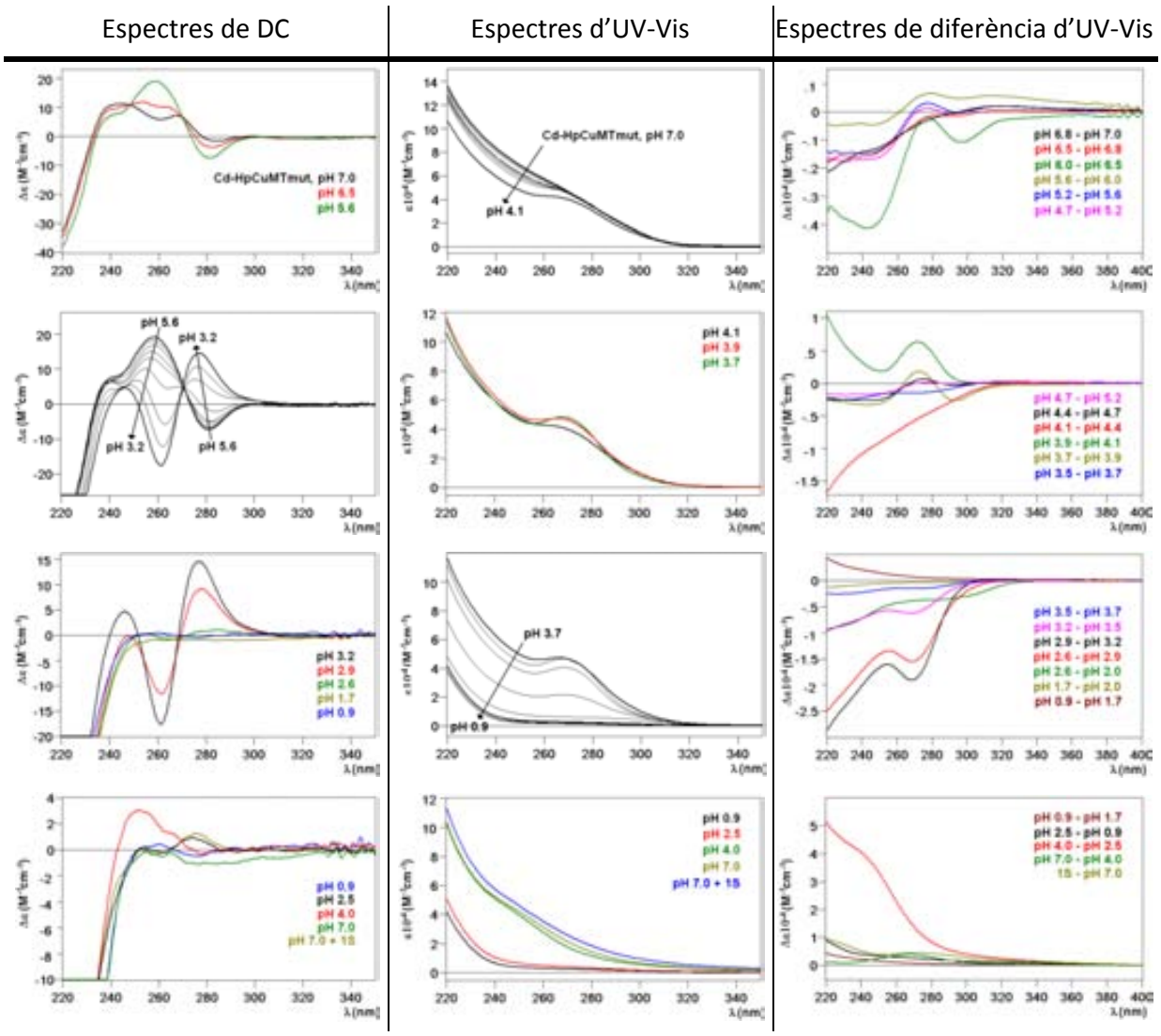

Fig. 11. Espectres de DC, UV-Visible i diferència d'UV-Visible enregistrats en el procés d'acidificació/reneutral·lització i finalment addició de 3 eq de Na_2S a una solució 13,12 µM de Cd-HpCuMTmut *in vivo* a pH 7 i 25 °C

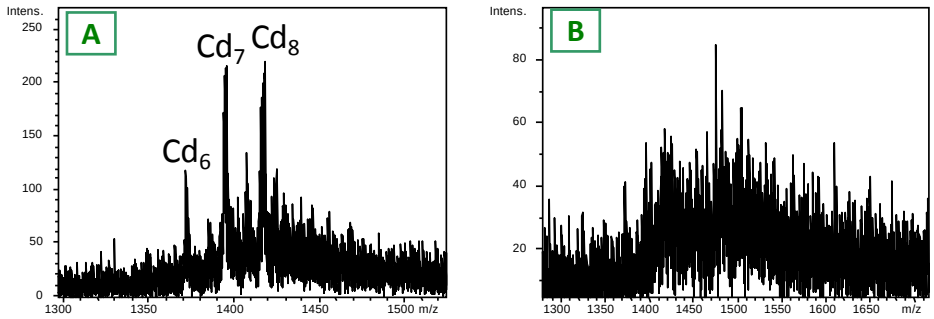

Fig. 12. Espectres d'ESI-MS enregistrats al final de l'estudi de acidificació/reneutral·lització de Cd-HpCuMTmut (**A**) i després d'afegir 1 eq de S^{2-} (**B**).

Làmina 7.1.1.10. Valoració amb Cu(I) de Zn-HpCuMTmut *in vivo.*

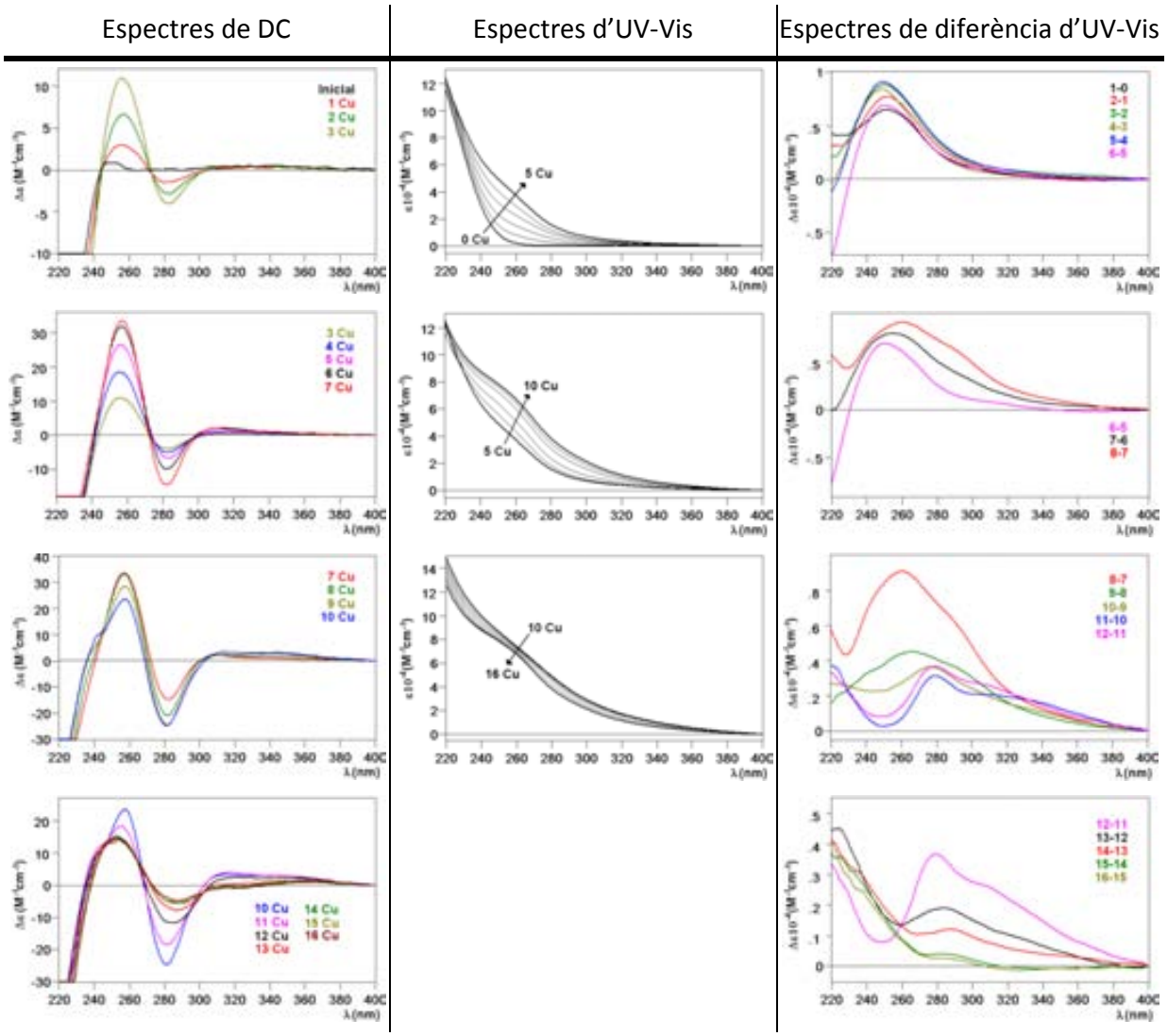

Fig. 13. Espectres de DC, UV-Visible i diferència d'UV-Visible enregistrats en la valoració d'una solució 12,20 µM de Zn-HpCuMTmut *in vivo* amb Cu(I) a pH 7 i 25 °C.

7.1.2. Caracterització de les isoformes d'MT del cargol *Cornu aspersum*

Làmina 7.1.2.1. Valoració de Zn_6-CaCdMT *in vivo* amb Cd(II).

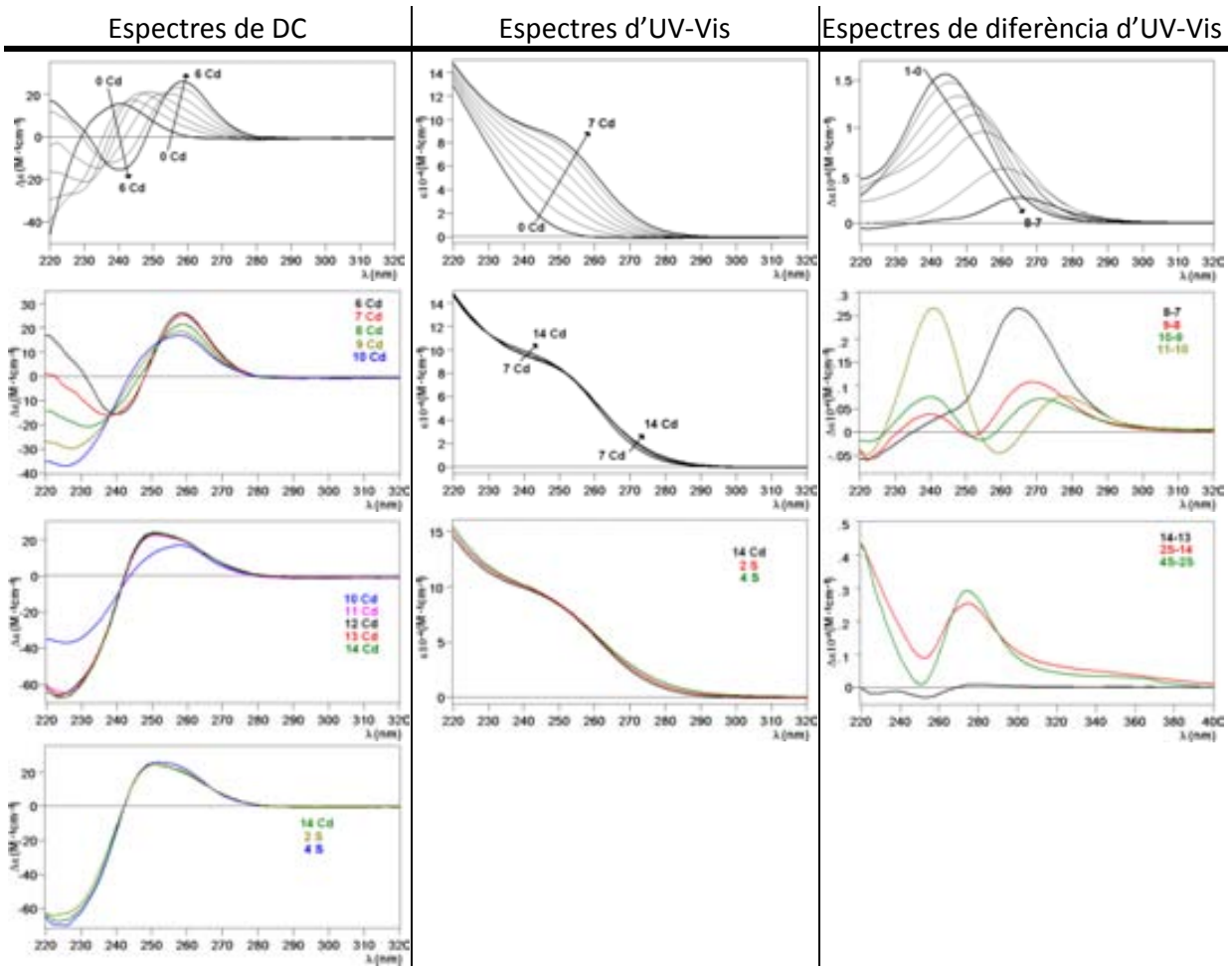

Fig. 14. Espectres de DC, UV-Visible i diferència d'UV-Visible enregistrats en la valoració d'una solució 16,42 µM de Zn_6-CaCdMT *in vivo* amb Cd(II) a pH 7 i 25 °C.

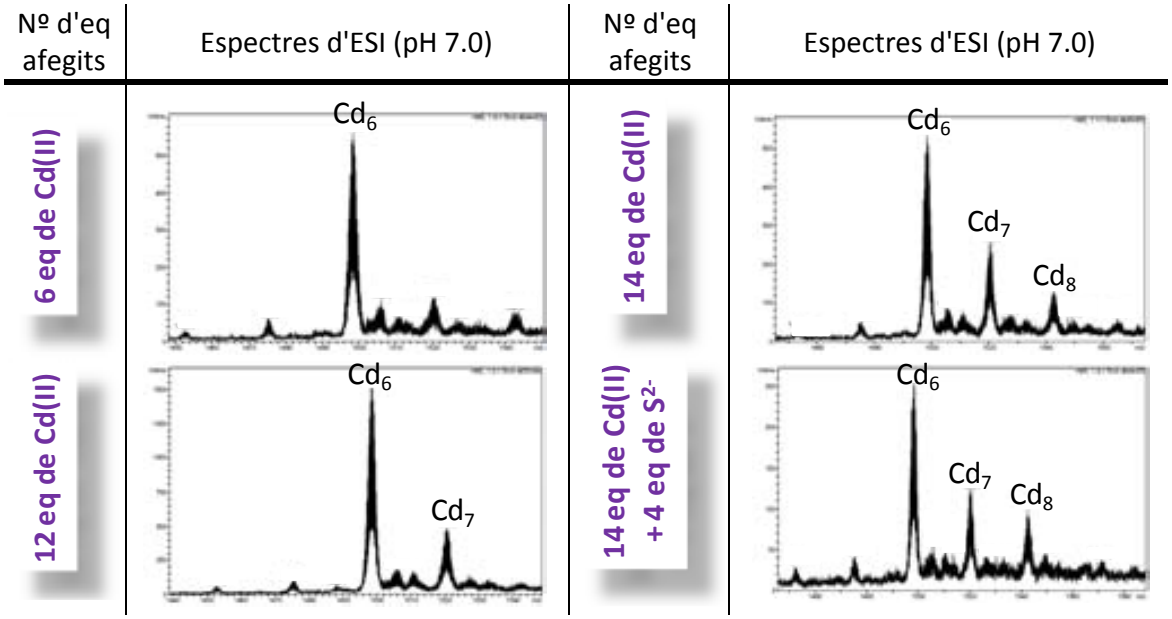

Fig. 15. Espectres d'ESI-MS obtinguts després d'addicionar diferents números d'eq de Cd(II) a una solució 16,42 µM de Zn-CaCdMT a pH 7 i 25 °.

Làmina 7.1.2.2. Valoració de Zn-CaCdCuMT *in vivo* amb Cd(II).

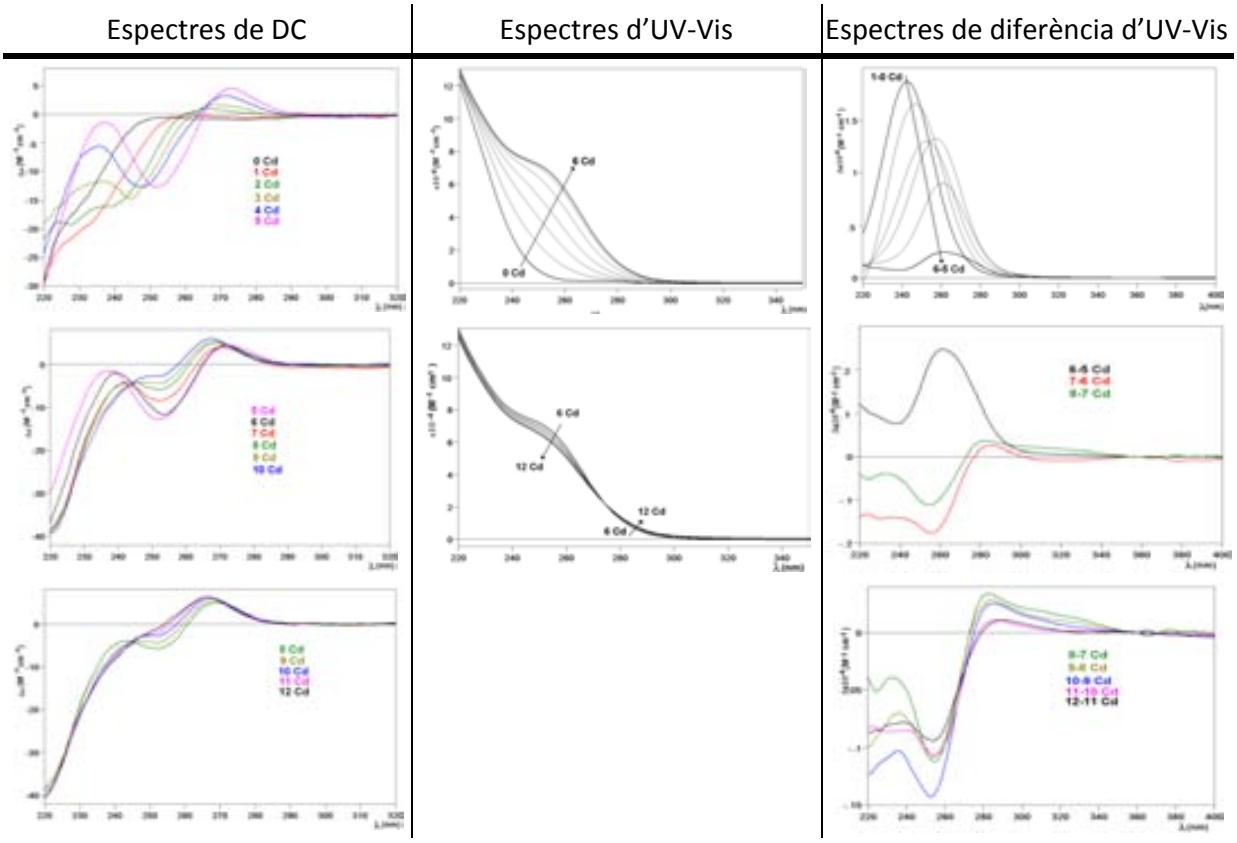

Fig. 16. Espectres de DC, UV-Visible i diferència d'UV-Visible enregistrats en la valoració d'una solució 15,35 µM de Zn-CaCdCuMT *in vivo* amb Cd(II) a pH 7 i 25 °C.

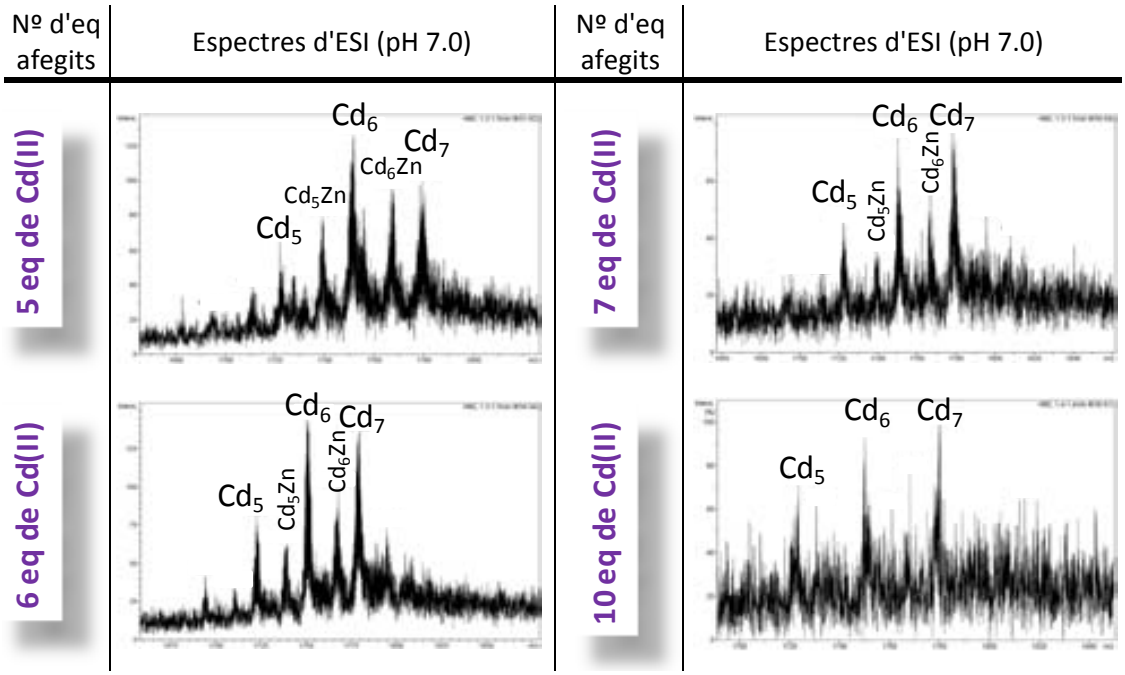

Fig. 17. Espectres d'ESI-MS obtinguts després d'addicionar diferents números d'eq de Cd(II) a una solució 15,35 µM de Zn-CaCdCuMT a pH 7 i 25 °C.

Làmina 7.1.2.3. Valoració de Zn-CaCuMT *in vivo* amb Cd(II).

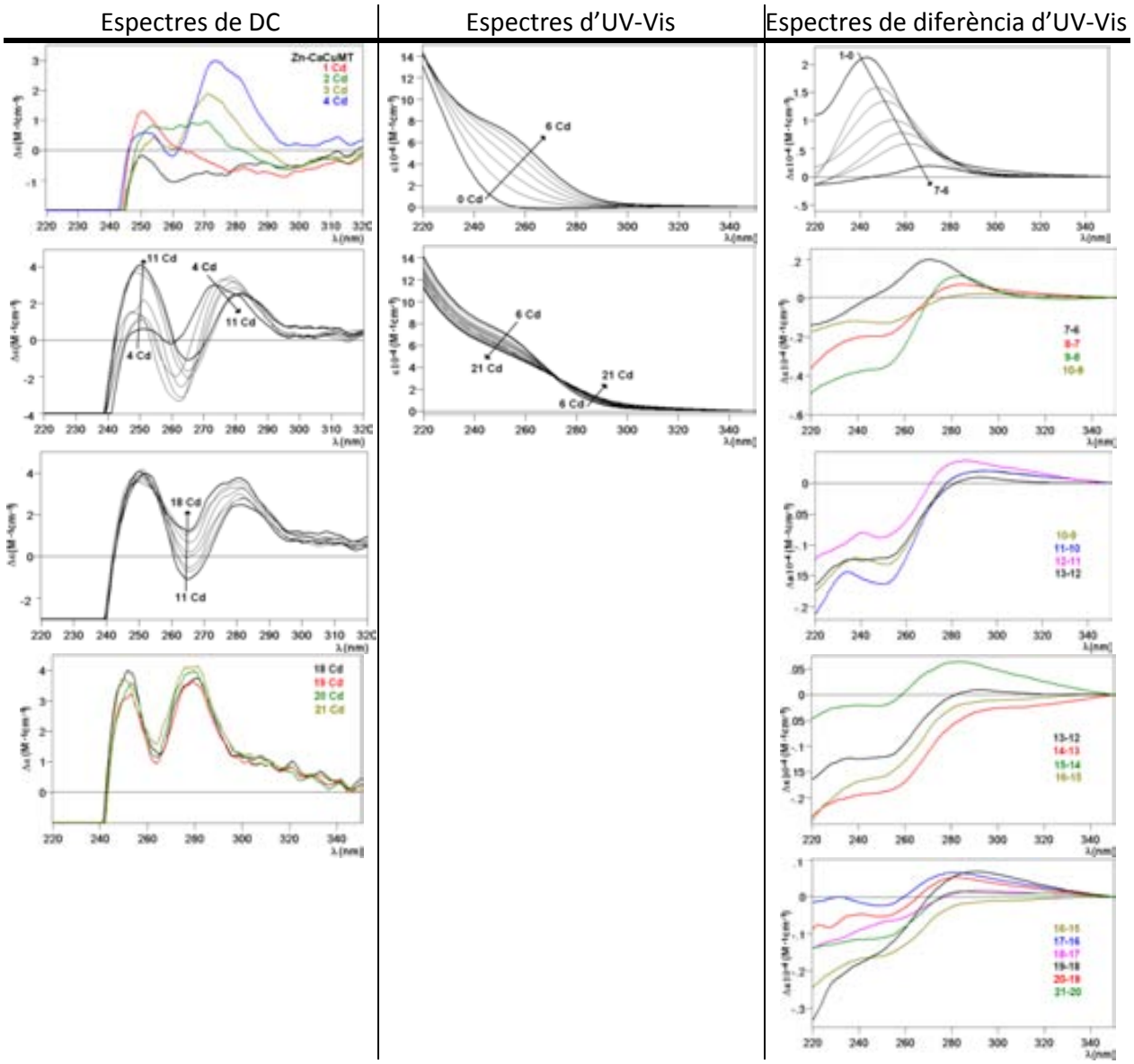

Fig. 18. Espectres de DC, UV-Visible i diferència d'UV-Visible enregistrats en la valoració d'una solució 14,90 µM de Zn-CaCuMT *in vivo* amb Cd(II) a pH 7 i 25 °C.

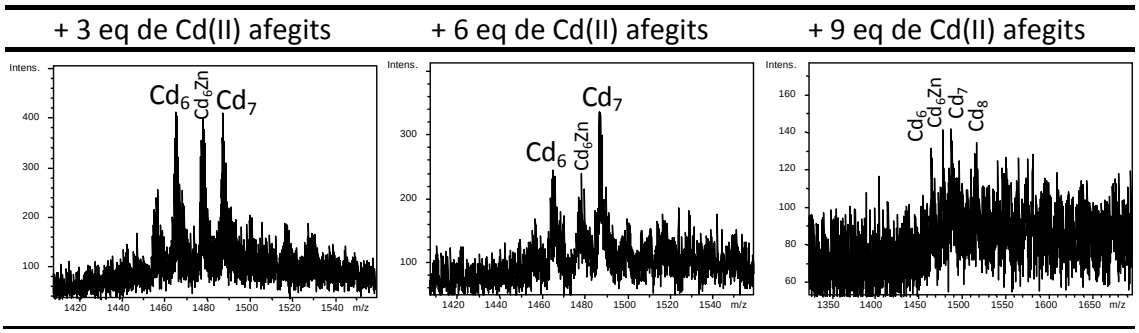

Taula 4. Espectres d'ESI-MS obtinguts després d'addicionar 3, 6 i 9 eq de Cd(II) a una solució 14,90 µM de Zn-CaCuMT a pH 7 i 25 °C.

Làmina 7.1.2.4. Valoració de Zn_6-CaCdMT *in vivo* amb Cu(I).

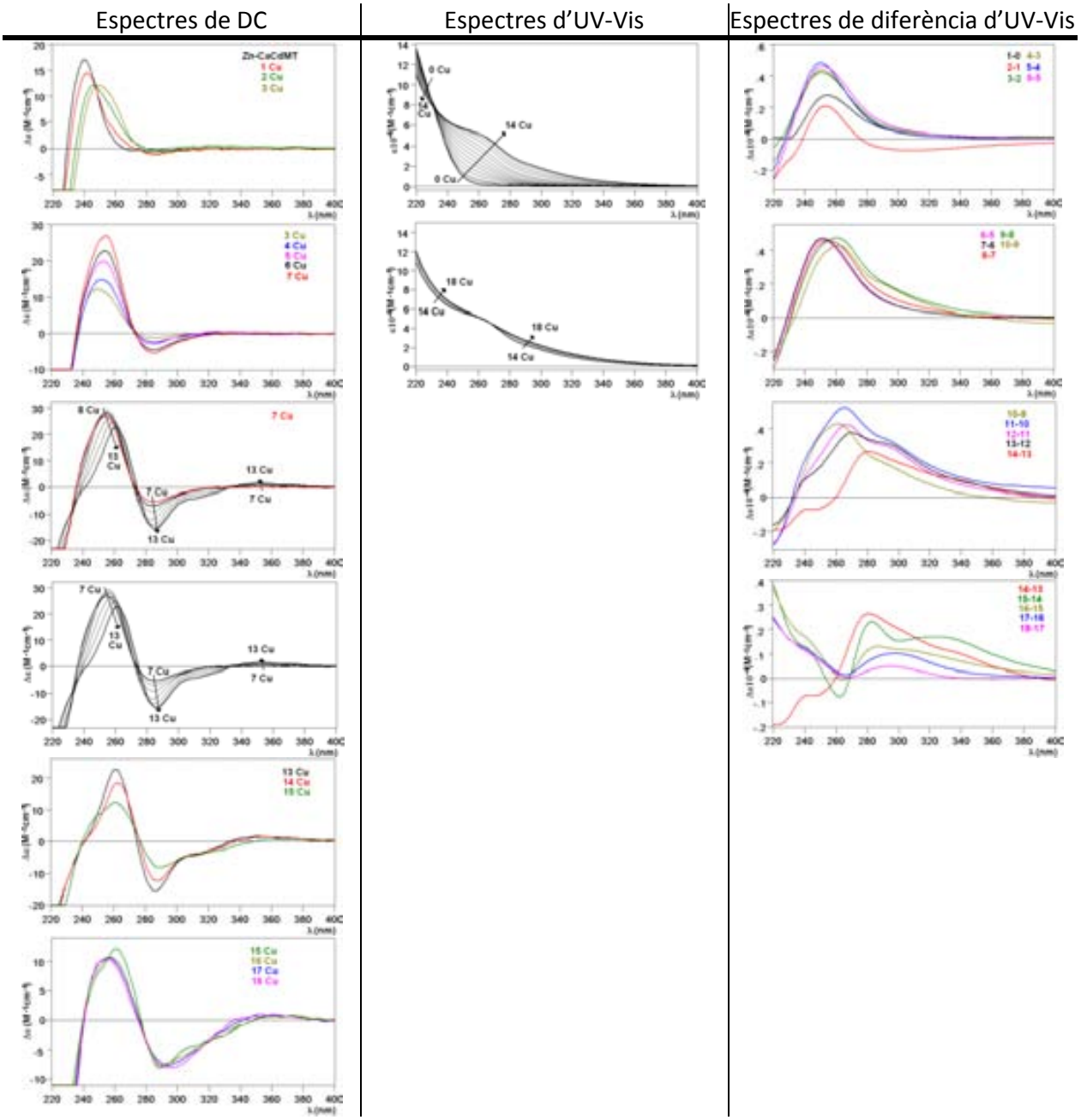

Fig. 19. Espectres de DC, UV-Visible i diferència d'UV-Visible enregistrats en la valoració d'una solució 15,71 µM de Zn_6-CaCdMT *in vivo* amb Cu(I) a pH 7 i 25 °C.

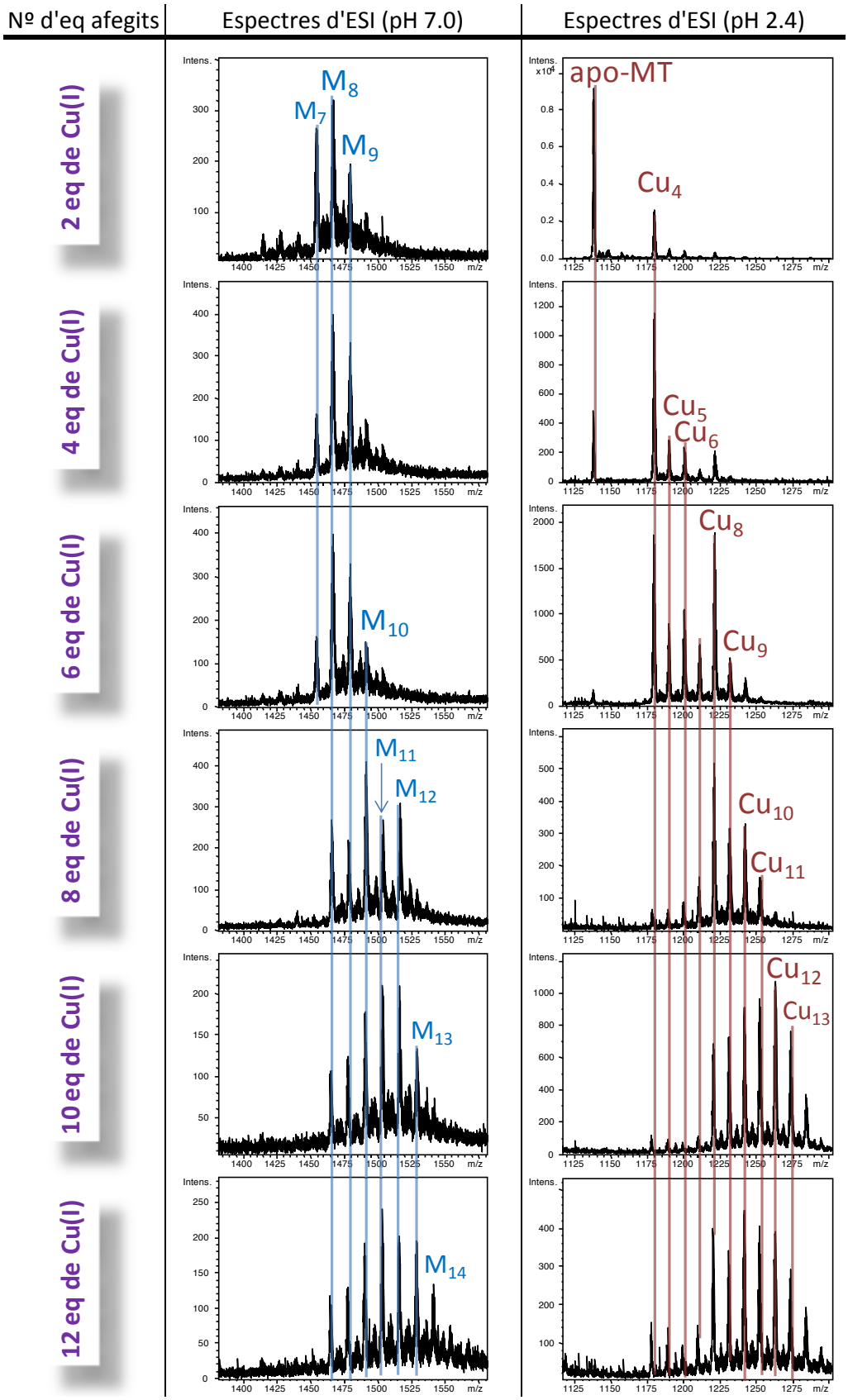

Taula 5. Espectres d'ESI-MS enregistrats a pH 7.0 i 2.4, cada 2 eq de Cu(I) afegits en la valoració d'una solució 15,71 µM de Zn_6-CaCdMT.

Làmina 7.1.2.5. Valoració de Zn-CaCdCuMT *in vivo* amb Cu(I).

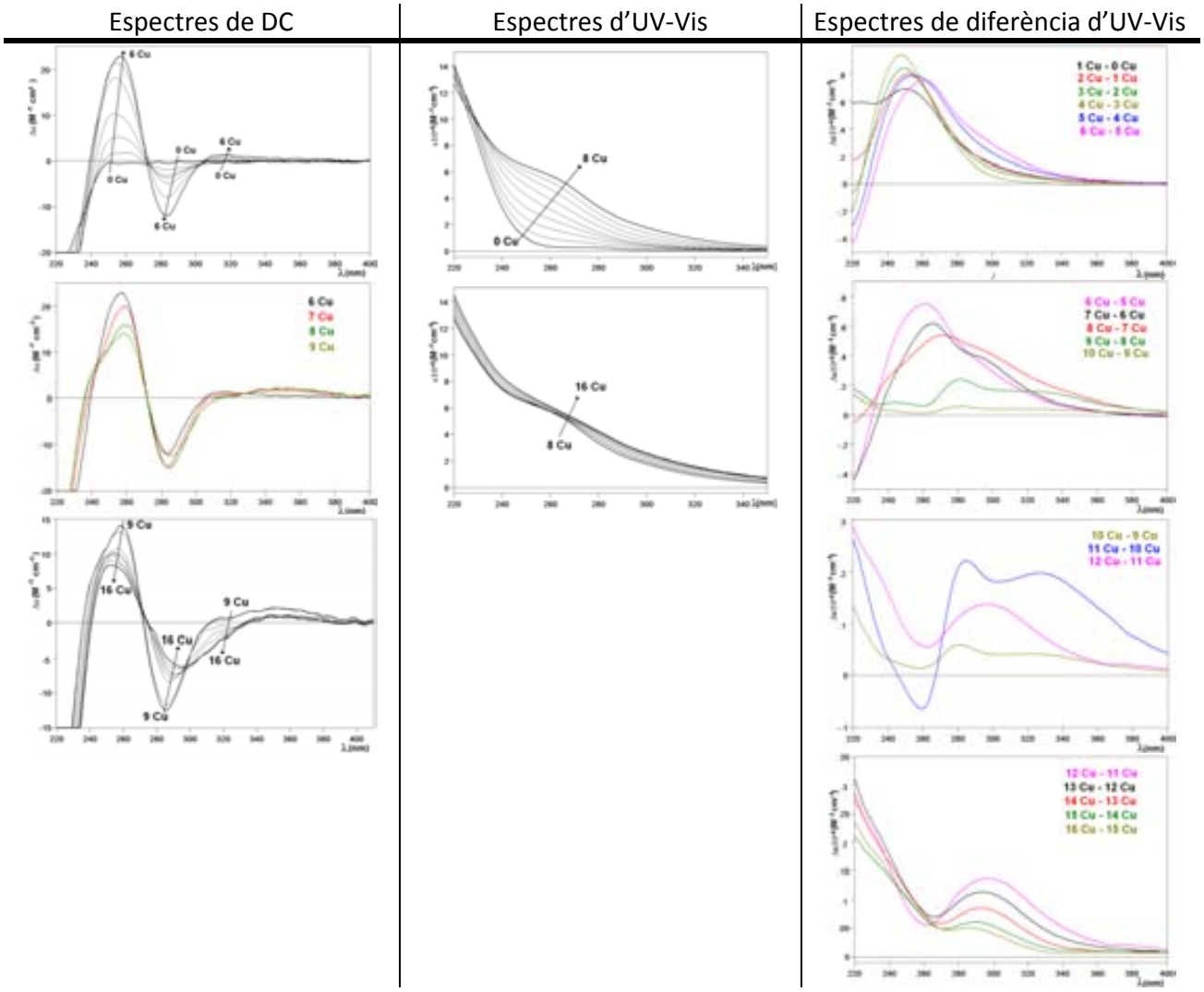

Fig. 20. Espectres de DC, UV-Visible i diferència d'UV-Visible enregistrats en la valoració d'una solució 15,34 µM de Zn-CaCdCuMT *in vivo* amb Cu(I) a pH 7 i 25 °C

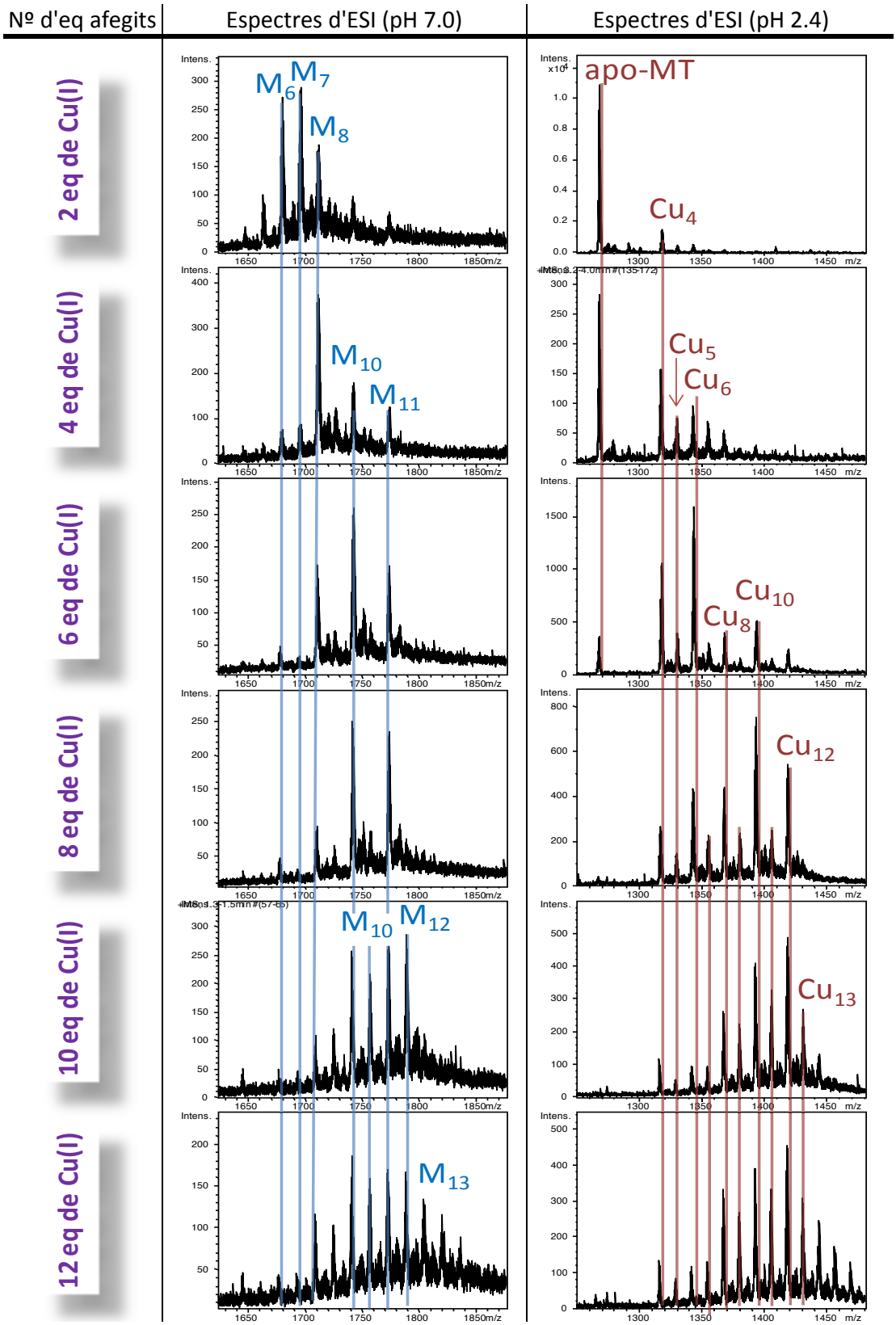

Taula 6. Espectres d'ESI-MS enregistrats a pH 7.0 i 2.4, cada 2 eq de Cu(I) afegits en la valoració d'una solució 15,34 µM de Zn-CaCdCuMT.

Làmina 7.1.2.6. Valoració de Zn-CaCuMT *in vivo* amb Cu(I).

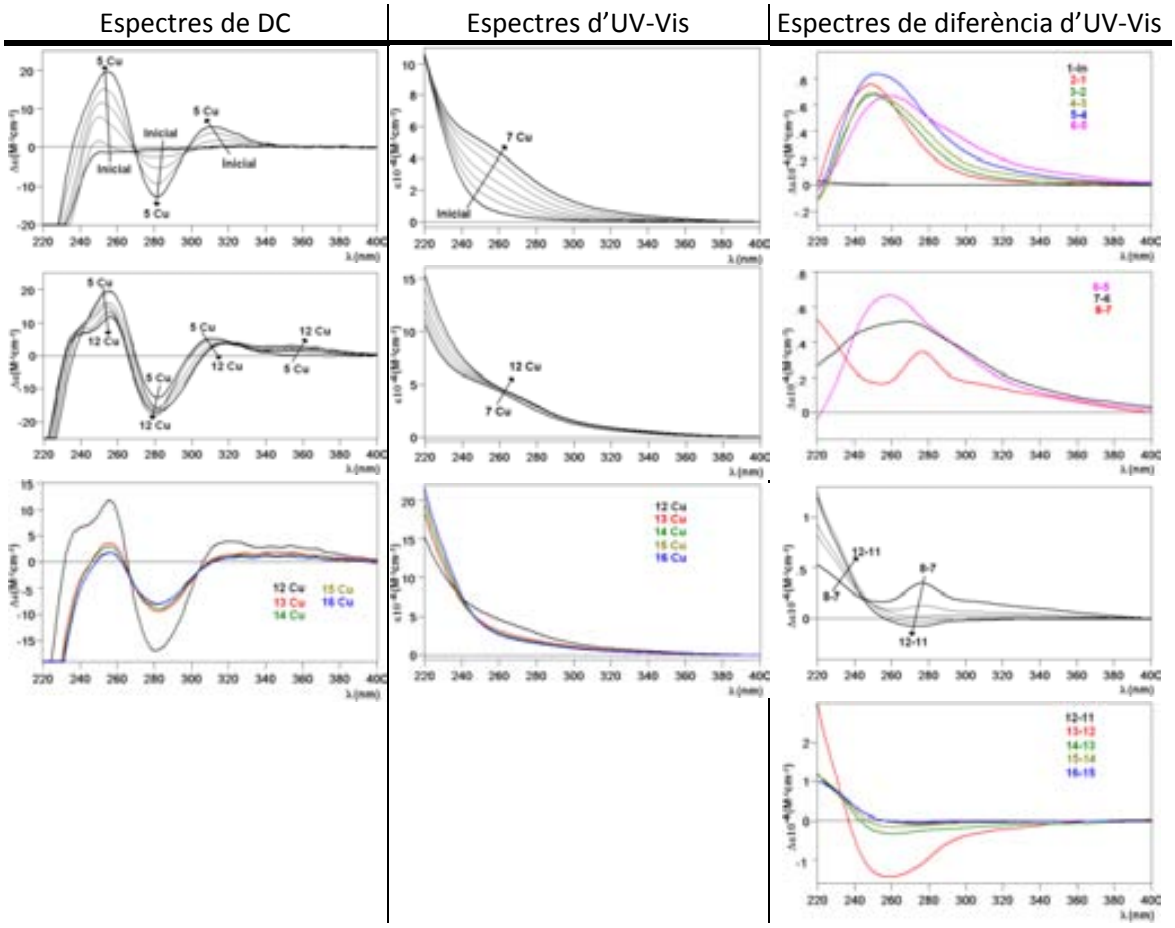

Fig. 21. Espectres de DC, UV-Visible i diferència d'UV-Visible enregistrats en la valoració d'una solució 15,088 µM de Zn-CaCuMT *in vivo* amb Cu(I) a pH 7 i 25 °C.

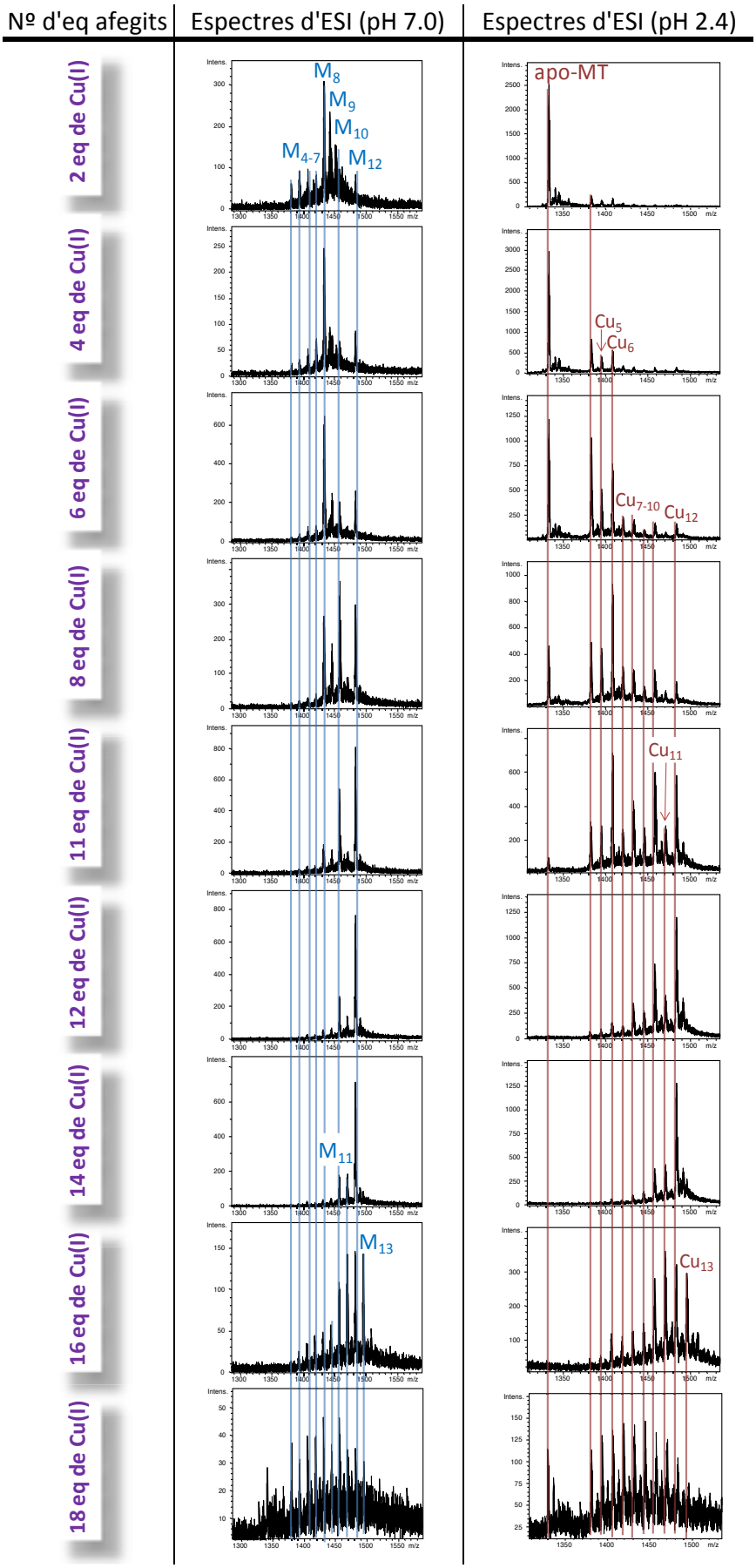

Taula 7. Espectres d'ESI-MS enregistrats a pH 7.0 i 2.4, cada 2 eq de Cu(I) afegits en la valoració d'una solució 15,08 µM de Zn-CaCuMT.

7.1.3. Caracterització de la MT del barretet marí *Megathura crenulata*

Làmina 7.1.3.1. Valoració de Zn-McMT *in vivo* amb Cd(II).

Espectres de DC	Espectres d'UV-Vis	Espectres de diferència d'UV-Vis

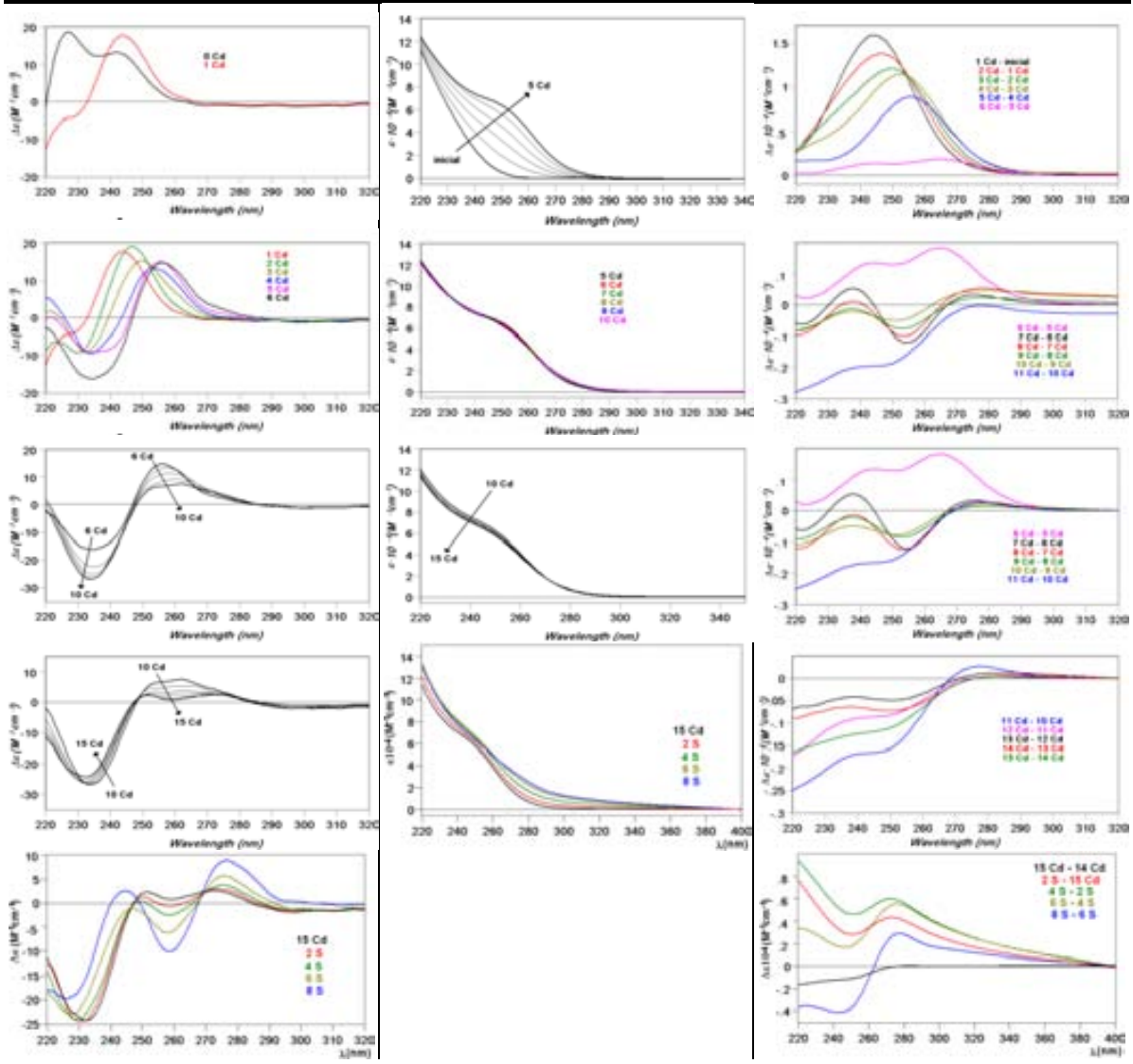

Fig. 22. Espectres de DC, UV-Visible i diferència d'UV-Visible enregistrats en la valoració d'una solució 15,335 µM de Zn-McMT *in vivo* amb Cd(II) a pH 7 i 25 °C

Nº d'eq afegits	Espectres d'ESI (pH 7.0)	Nº d'eq afegits	Espectres d'ESI (pH 7.0)
3 eq de Cd(II)	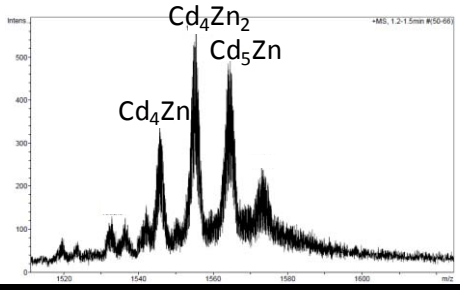	**6 eq de Cd(II)**	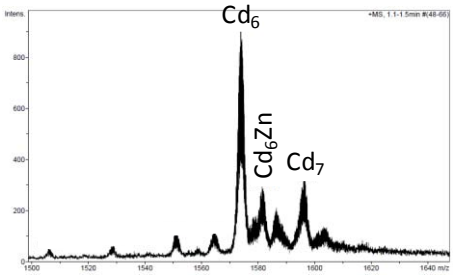
10 eq de Cd(II)	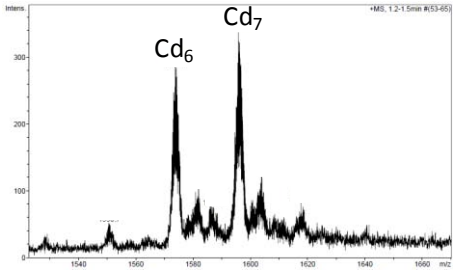	**15 eq de Cd(II)**	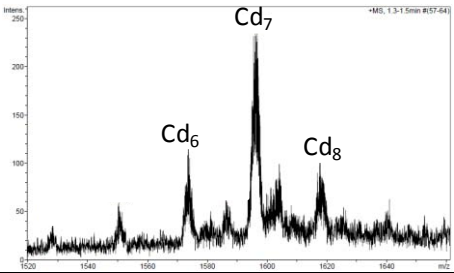
15 eq de Cd(II) + 6 S^{-2}	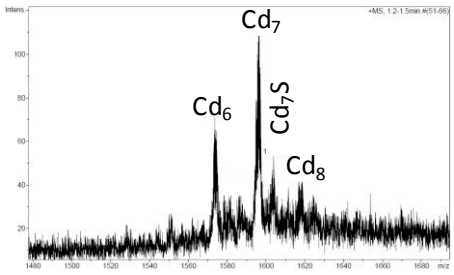	**15 eq de Cd(II) + 8 S^{-2}**	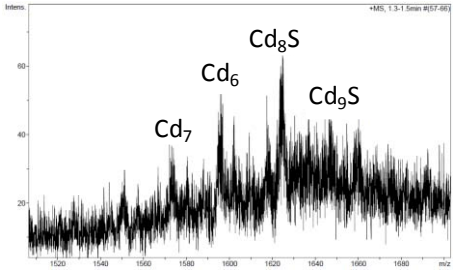

Taula 8. Espectres d'ESI-MS obtinguts després d'addicionar diferent quantitats d'eq de Cd(II) i S^{2-} a una solució 15,335 µM de Zn-McMT a pH 7 i 25 °C

7.1.4. Caracterització de les isoformes d'MT de l'amfiox *Brianchostoma floridae*

Làmina 7.1.4.1. Reacció de Zn-BfMT1 *in vivo* amb el reactiu DEPC (pirocarbonat de dietil).

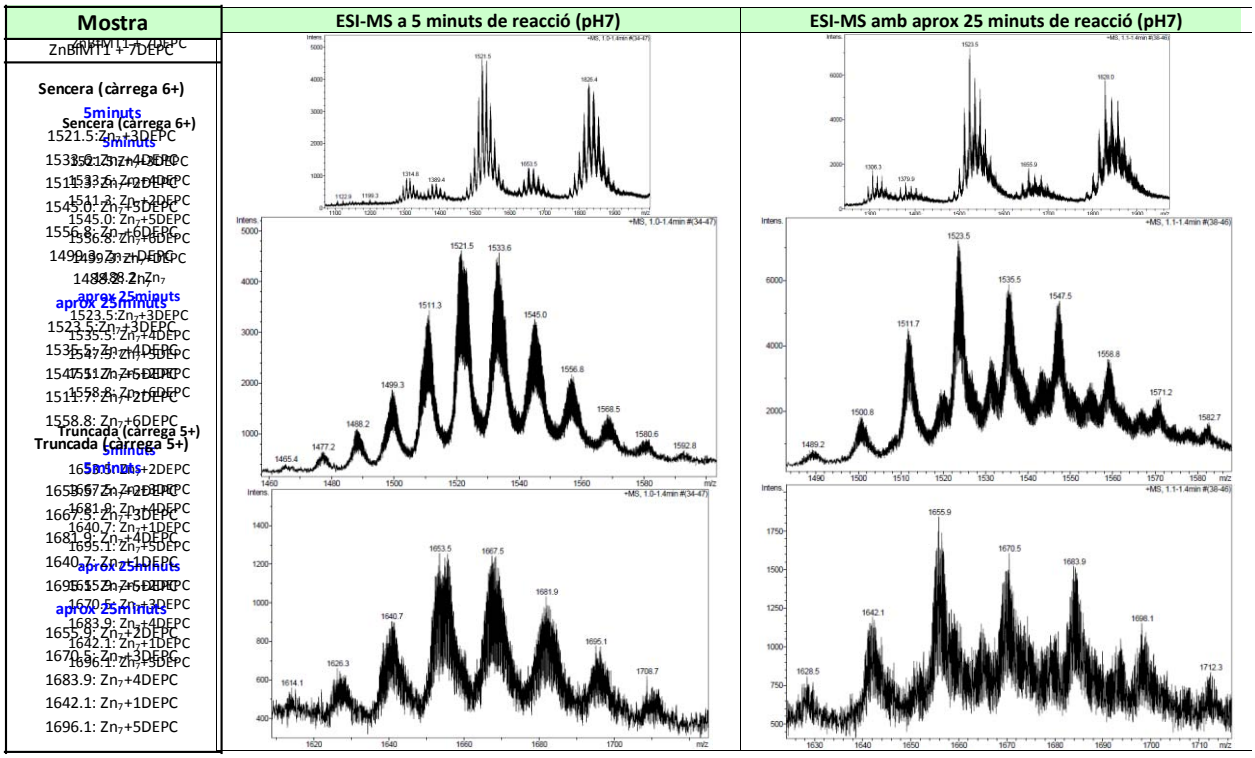

Fig. 23. Espectres d'ESI-MS enregistrats en diferents estadis de la reacció de ZnBfMT1 *in vivo* amb el reactiu DEPC (pirocarbonat dietil).

Làmina 7.1.4.2. Valoració de ZnBfMT1 *in vivo* amb Cd(II)

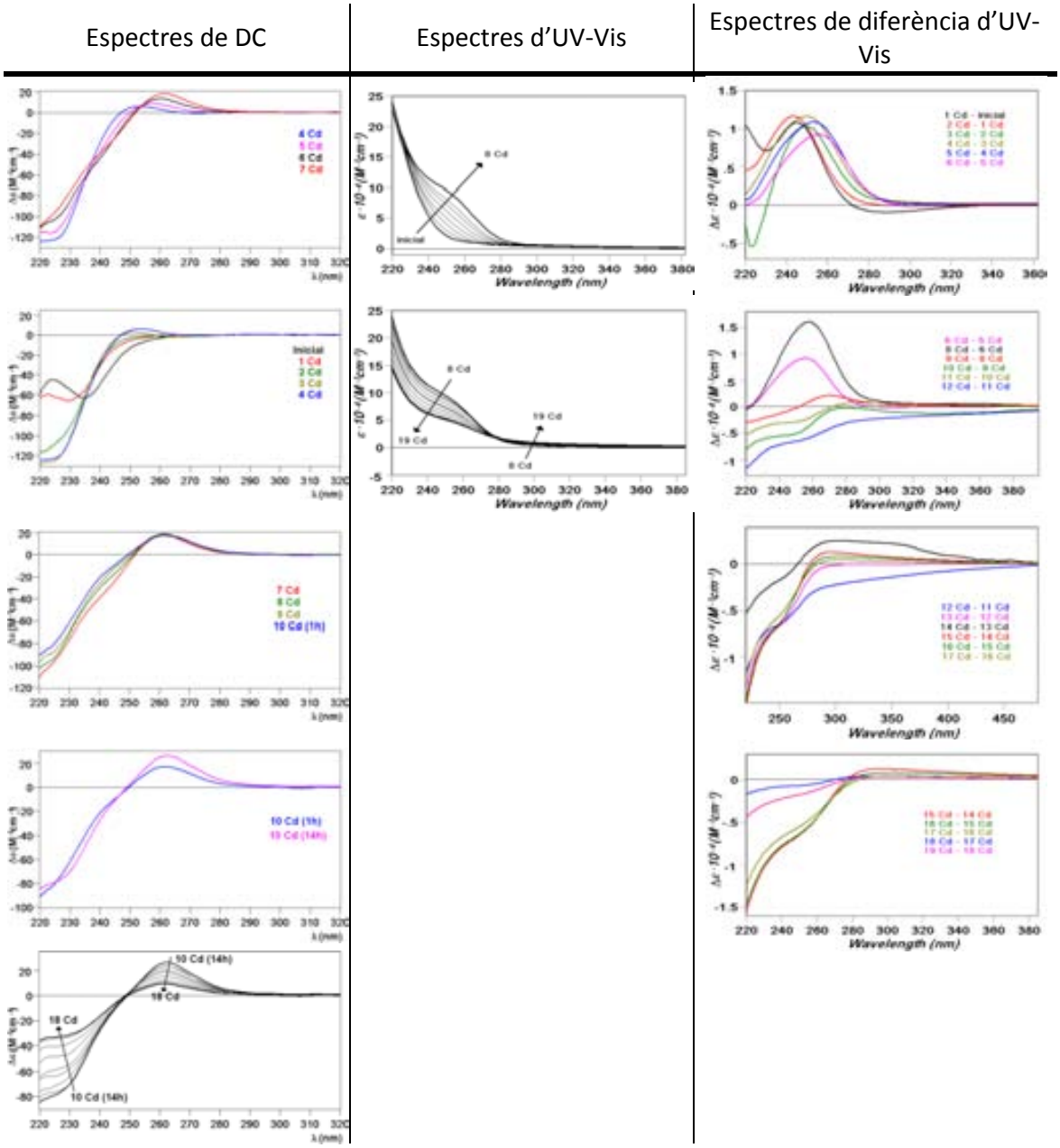

Fig. 24. Espectres de DC, UV-Visible i diferència d'UV-Visible enregistrats en la valoració d'una solució 10,12 µM de Zn-BfMT1 *in vivo* amb Cd(II) a pH 7 i 25 °C.

Nº d'eq afegits	Espectres d'ESI (pH 7.0)	Nº d'eq afegits	Espectres d'ESI (pH 7.0)
4 eq de Cd(II)	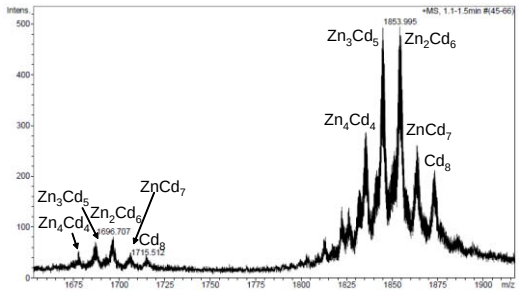	**8 eq de Cd(II)**	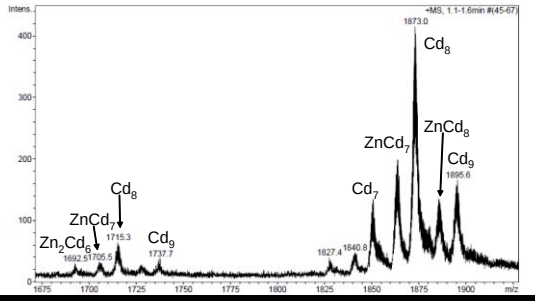
12 eq de Cd(II)	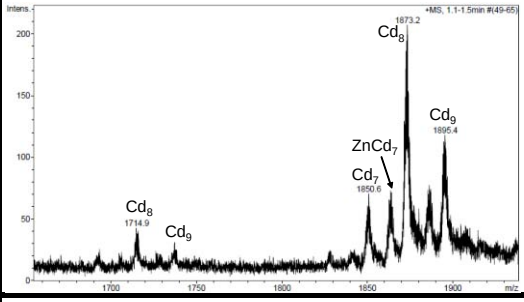	**16 eq de Cd(II)**	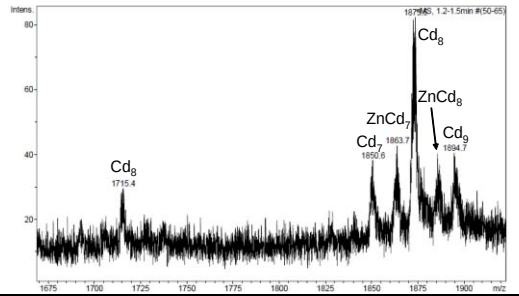
19 eq de Cd(II)	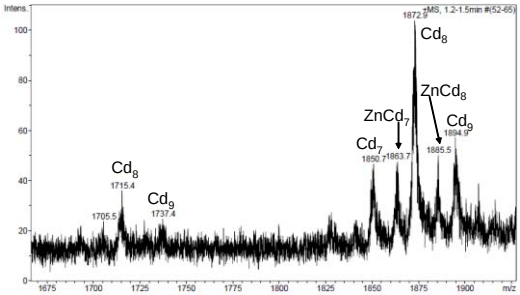		

Taula 9. Espectres d'ESI-MS obtinguts després addicionar diferent quantitats d'eq de Cd(II) i S^{2-} a una solució 10,12 µM de Zn-BfMT1 a pH 7 i 25 °C.

Làmina 7.1.4.3. Acidificació i posterior reneutral·lització de la Cd-BfMT1 *in vivo*.

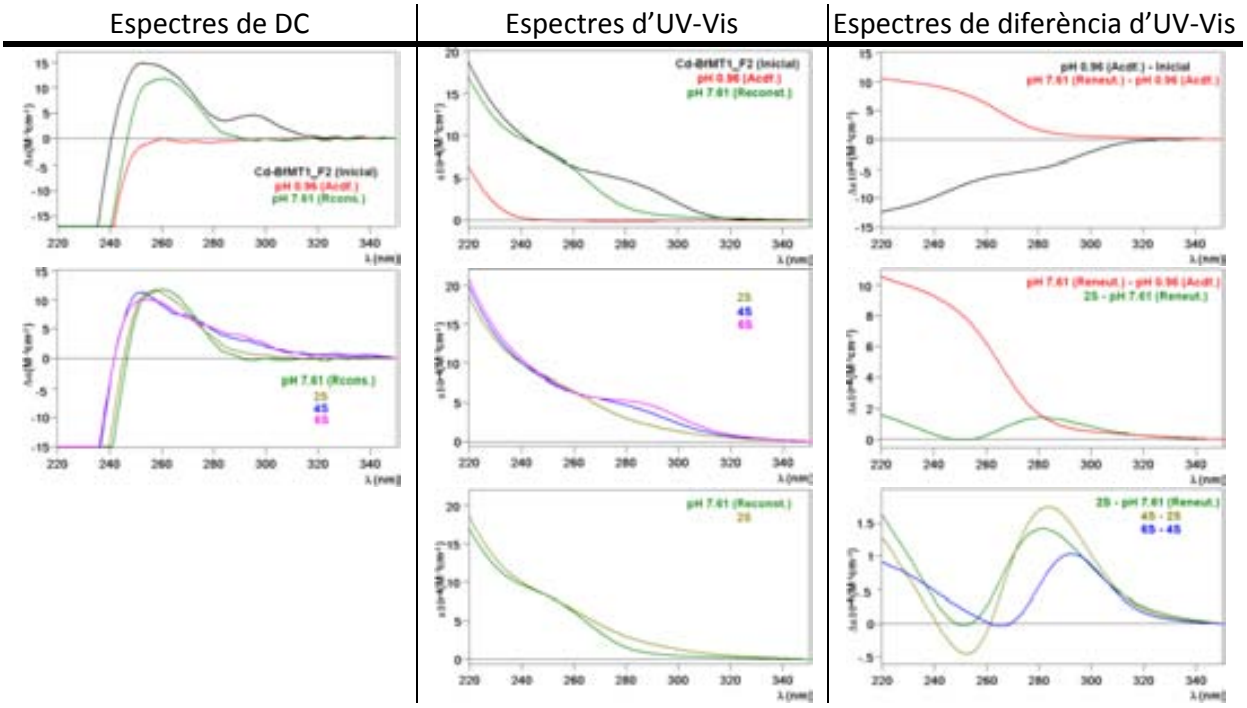

Fig. 25. Espectres de DC, UV-Visible i diferència d'UV-Visible enregistrats en el procés d'acidificació/reneutral·lització i finalment addició de Na_2S a una solució 10,05 µM de Cd-BfMT1 *in vivo* a pH 7 i 25 °C

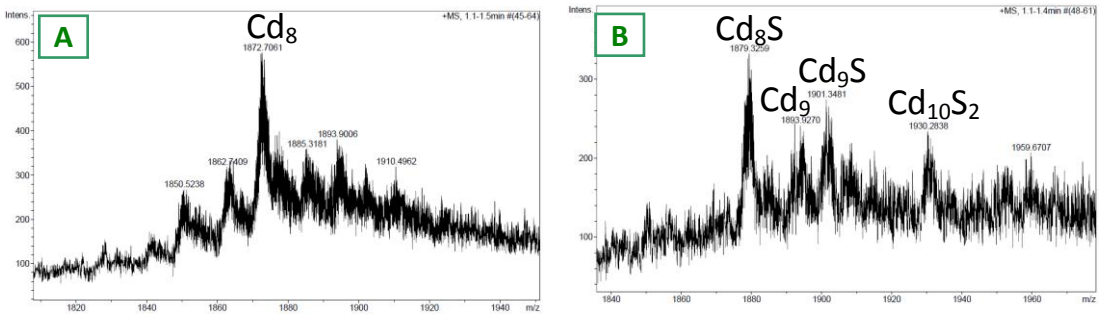

Fig. 26. Espectres d'ESI-MS enregistrats al final de l'estudi de acidificació/reneutral·lització de Cd-BfMT1 (**A**) i després d'afegir 4 eq de S^{2-} (**B**).

Làmina 7.1.1.4. Valoració de ZnBfMT2 *in vivo* amb Cd(II)

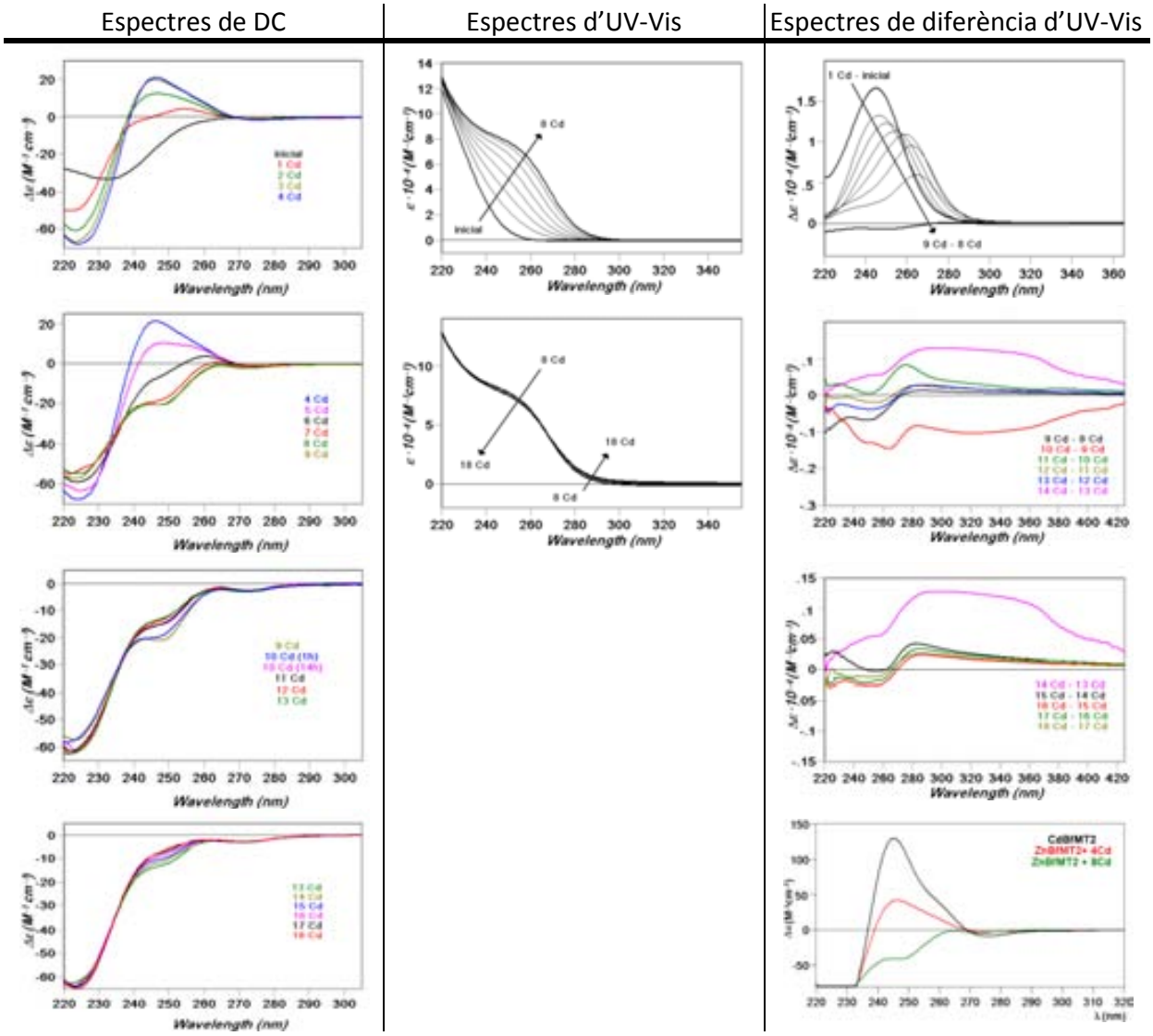

Fig. 27. Espectres de DC, UV-Visible i diferència d'UV-Visible enregistrats en la valoració d'una solució 11,30 µM de Zn-BfMT2 *in vivo* amb Cd(II) a pH 7 i 25 °C

Nº d'eq afegits	Espectres d'ESI (pH 7.0)	Nº d'eq afegits	Espectres d'ESI (pH 7.0)
4 eq de Cd(II)	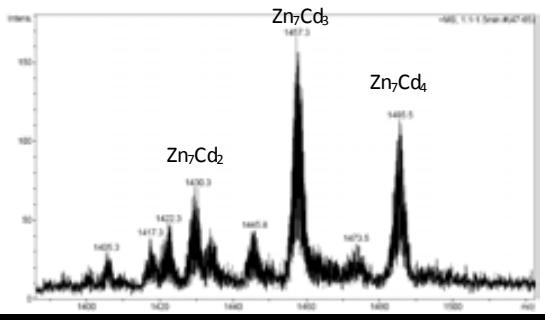	**8 eq de Cd(II)**	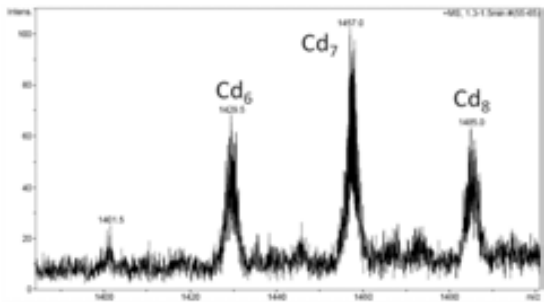
12 eq de Cd(II)	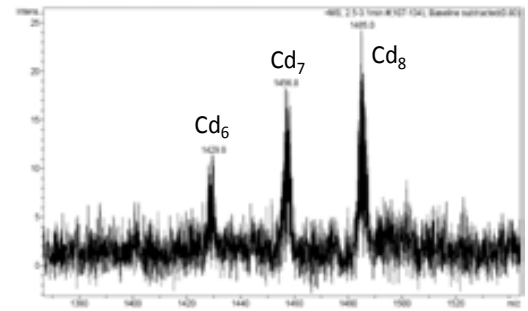	**16 eq de Cd(II)**	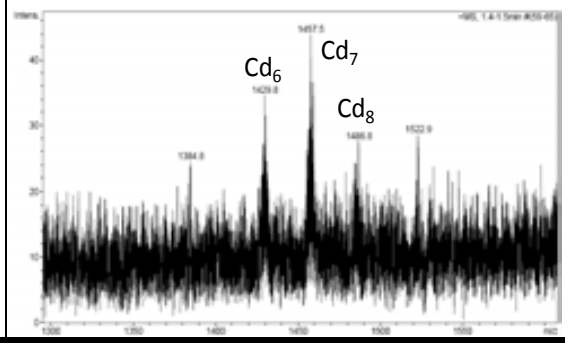

Taula 10. Espectres d'ESI-MS obtinguts després addicionar diferent quantitats d'eq de Cd(II) a una solució 11,30 µM de Zn-BfMT2 a pH 7 i 25 °C

Làmina 7.1.4.5. Acidificació i posterior reneutral·lització de la Cd-BfMT1 *in vivo*.

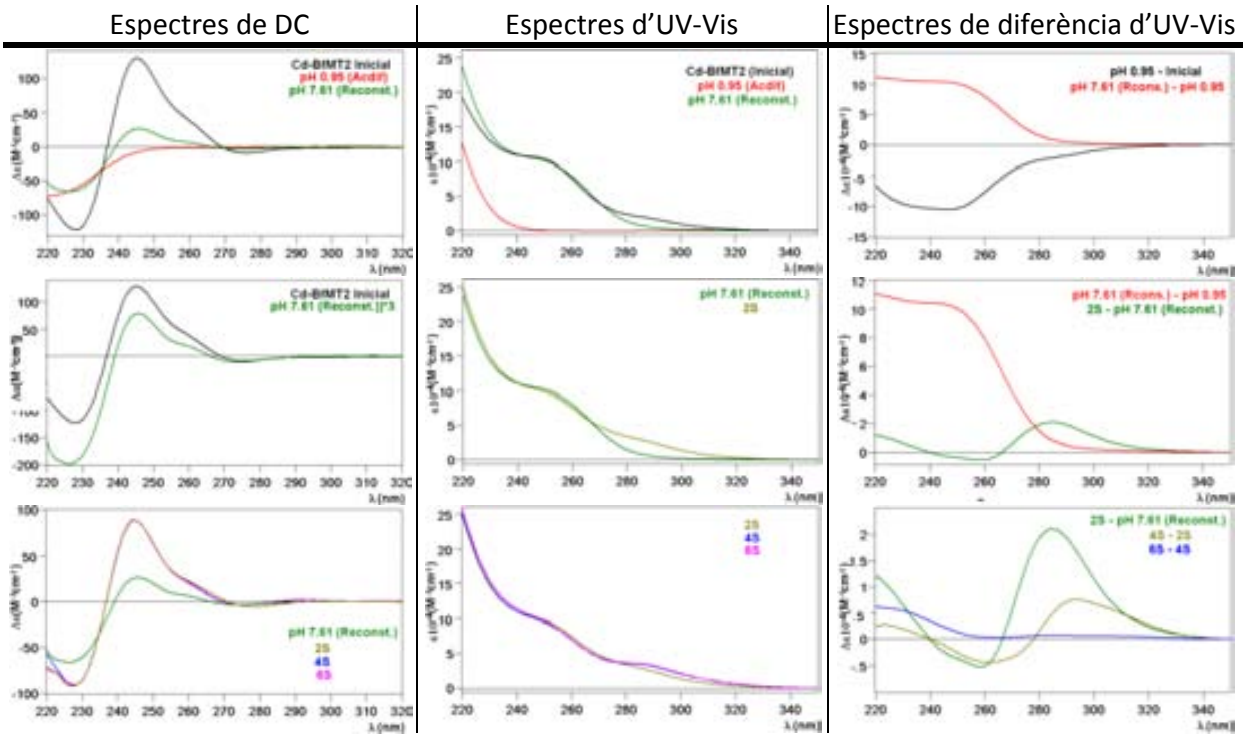

Fig. 28. Espectres de DC, UV-Visible i diferència d'UV-Visible enregistrats en el procés d'acidificació/reneutral·lització i finalment addició de Na_2S a una solució 10,10 µM de Cd-BfMT2 *in vivo* a pH 7 i 25 °C

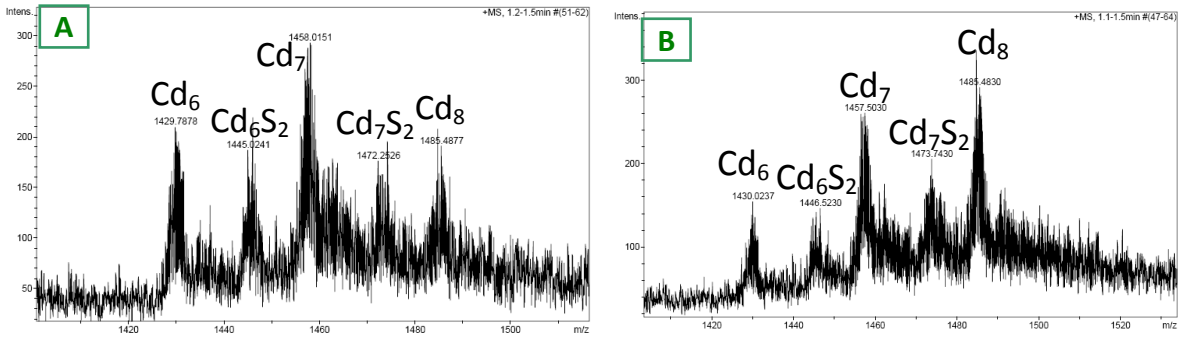

Fig. 29. Espectres d'ESI-MS enregistrats al final de l'estudi de acidificació/reneutral·lització de Cd-BfMT2 (**A**) i després d'afegir 4 eq de S^{2-} (**B**).

Làmina 7.1.4.6. Valoració de ZnBfMT1 *in vivo* amb Cu(I)

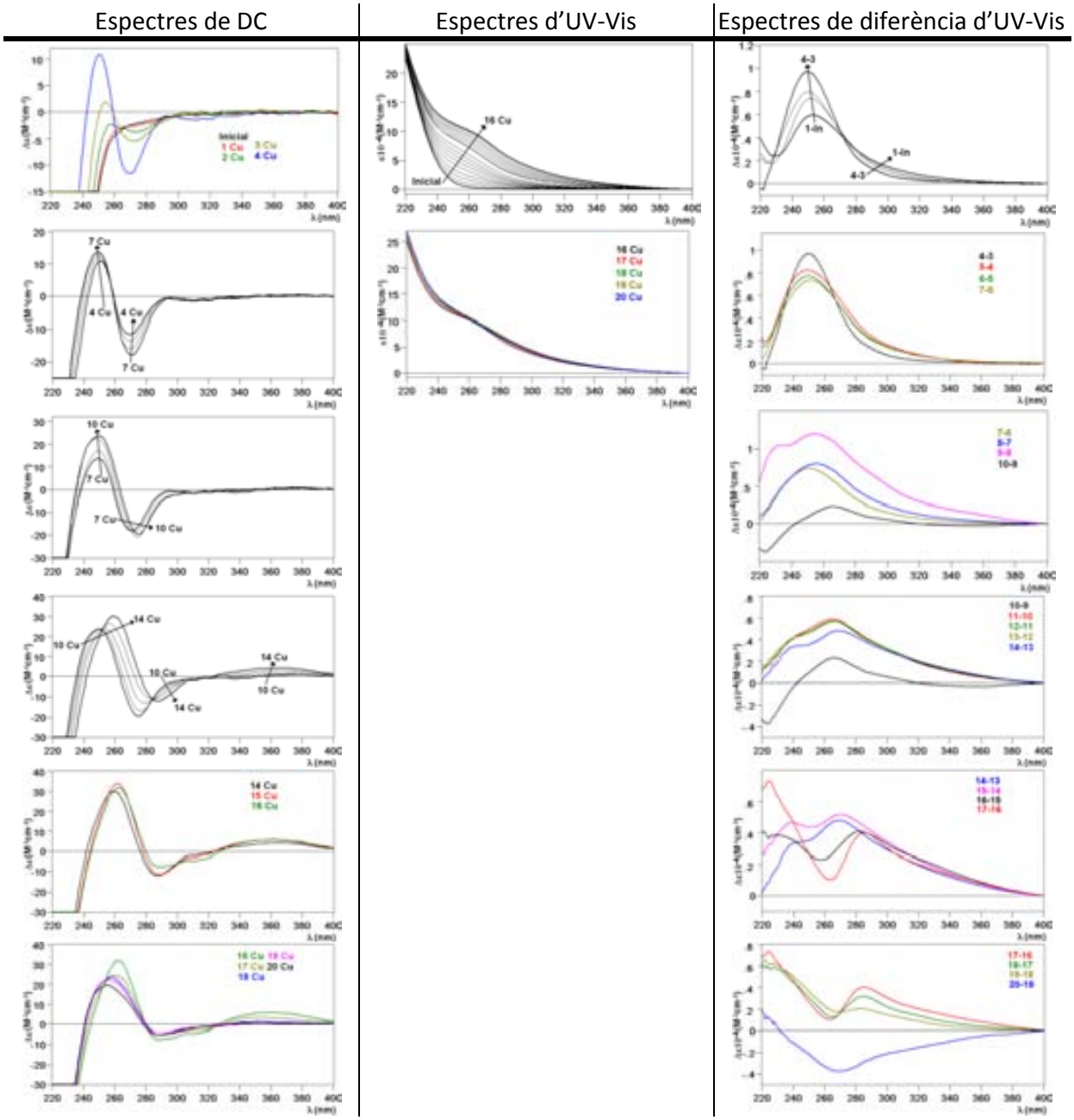

Fig. 30. Espectres de DC, UV-Visible i diferència d'UV-Visible enregistrats en la valoració d'una solució 11,83 µM de Zn-BfMT1 *in vivo* amb Cu(I) a pH 7 i 25 °C.

Eq de Cu(I) afegits	pH 7.0	pH 2.4
2 eq	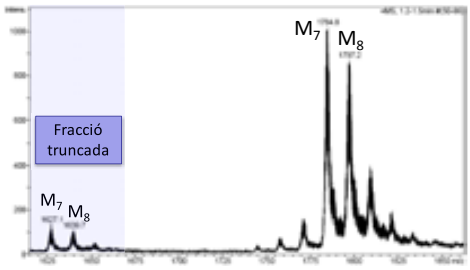	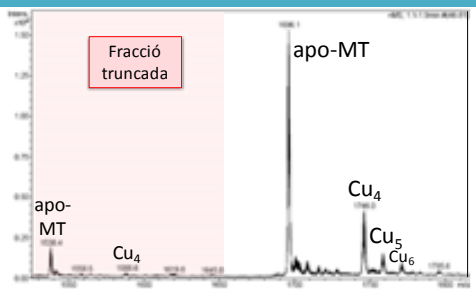
4 eq	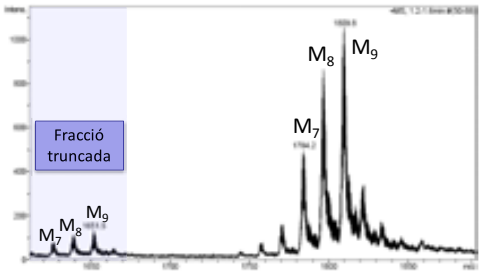	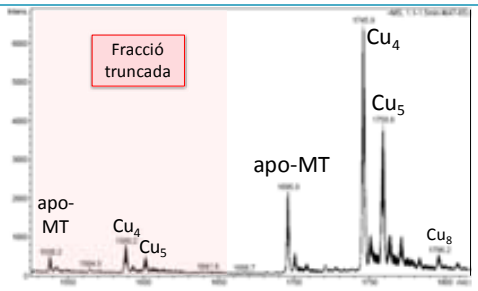
6 eq	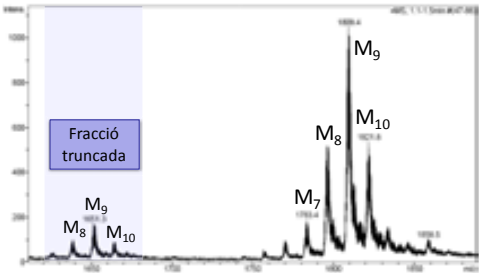	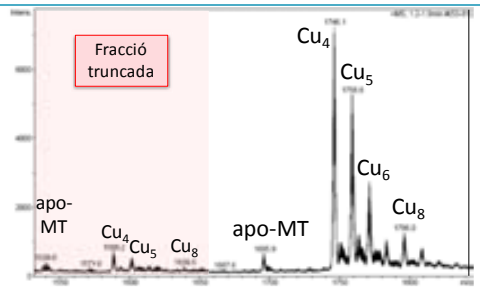
8 eq	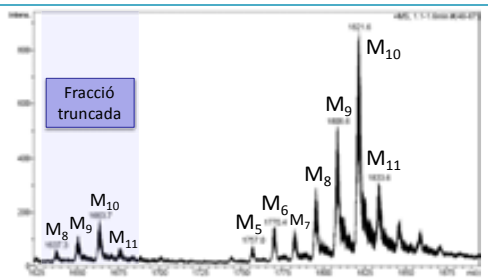	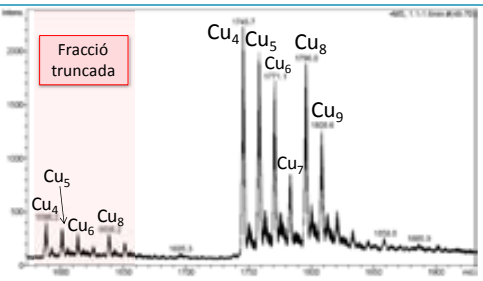
10 eq	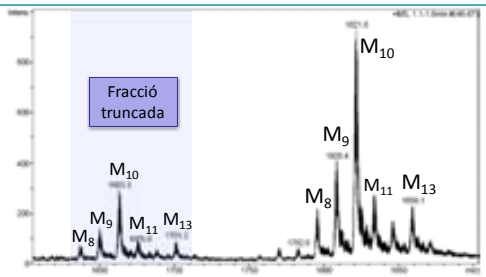	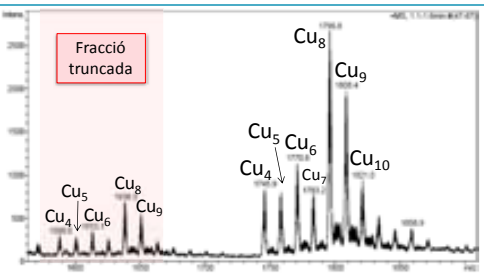
12 eq	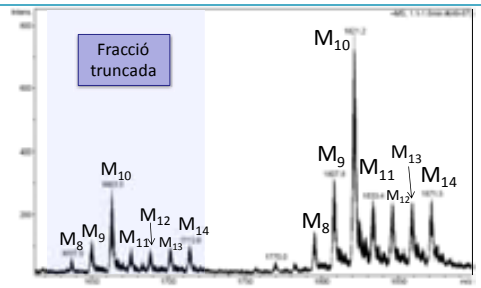	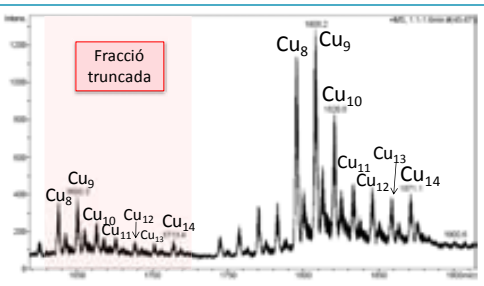

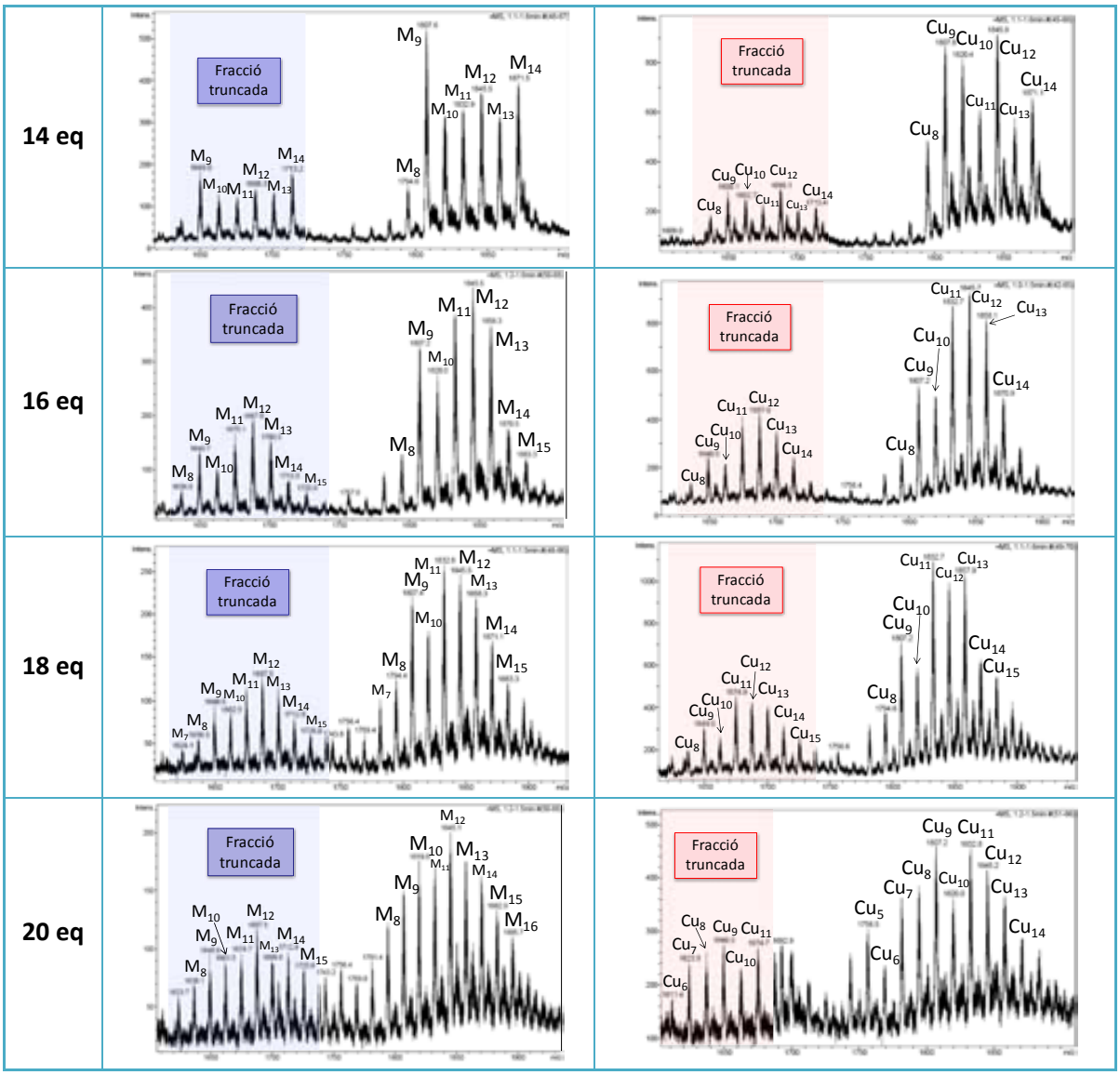

Taula 11. Espectres d'ESI-MS enregistrats a pH 7.0 i 2.4, cada 2 eq de Cu(I) afegits en la valoració d'una solució 11,83 µM de Zn-BfMT1.

7.1.5. Caracterització de la cinquena isoforma d'MT de *Drosophila melanogaster*

Làmina 7.1.5.1. Acidificació de Cd-MtnE *in vivo*.

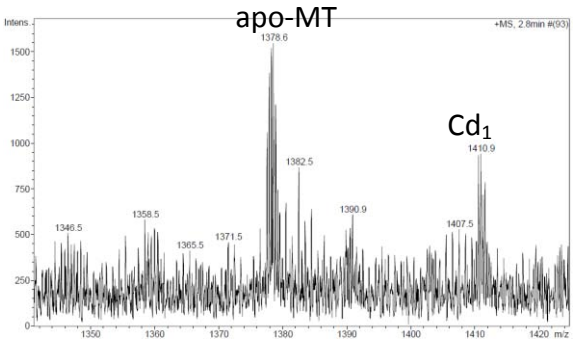

Fig. 31. Espectre d'ESI-MS de la mostra Cd-MtnE *in vivo* enregistrat a pH 2.4.

7.2. ARTICLES PUBLICATS

I. ARTICLE 1:

Shaping mechanisms of metal specificity in a family of metazoan metallothioneins: evolutionary differentiation of mollusc metallothioneins

BMC Biology, **(2011)**, 9:4.

Palacios et al. BMC Biology 2011, 9:4
http://www.biomedcentral.com/1741-7007/9/4

BMC Biology
incorporating Journal of Biology

RESEARCH ARTICLE Open Access

Shaping mechanisms of metal specificity in a family of metazoan metallothioneins: evolutionary differentiation of mollusc metallothioneins

Òscar Palacios[1], Ayelen Pagani[2], Sílvia Pérez-Rafael[1], Margit Egg[3], Martina Höckner[3], Anita Brandstätter[4], Mercè Capdevila[1], Sílvia Atrian[2], Reinhard Dallinger[3*]

Abstract

Background: The degree of metal binding specificity in metalloproteins such as metallothioneins (MTs) can be crucial for their functional accuracy. Unlike most other animal species, pulmonate molluscs possess homometallic MT isoforms loaded with Cu^{+} or Cd^{2+}. They have, so far, been obtained as native metal-MT complexes from snail tissues, where they are involved in the metabolism of the metal ion species bound to the respective isoform. However, it has not as yet been discerned if their specific metal occupation is the result of a rigid control of metal availability, or isoform expression programming in the hosting tissues or of structural differences of the respective peptides determining the coordinative options for the different metal ions. In this study, the Roman snail (*Helix pomatia*) Cu-loaded and Cd-loaded isoforms (HpCuMT and HpCdMT) were used as model molecules in order to elucidate the biochemical and evolutionary mechanisms permitting pulmonate MTs to achieve specificity for their cognate metal ion.

Results: HpCuMT and HpCdMT were recombinantly synthesized in the presence of Cd^{2+}, Zn^{2+} or Cu^{2+} and corresponding metal complexes analysed by electrospray mass spectrometry and circular dichroism (CD) and ultra violet-visible (UV-Vis) spectrophotometry. Both MT isoforms were only able to form unique, homometallic and stable complexes (Cd_6-HpCdMT and Cu_{12}-HpCuMT) with their cognate metal ions. Yeast complementation assays demonstrated that the two isoforms assumed metal-specific functions, in agreement with their binding preferences, in heterologous eukaryotic environments. In the snail organism, the functional metal specificity of HpCdMT and HpCuMT was contributed by metal-specific transcription programming and cell-specific expression. Sequence elucidation and phylogenetic analysis of MT isoforms from a number of snail species revealed that they possess an unspecific and two metal-specific MT isoforms, whose metal specificity was achieved exclusively by evolutionary modulation of non-cysteine amino acid positions.

Conclusion: The Roman snail HpCdMT and HpCuMT isoforms can thus be regarded as prototypes of isoform families that evolved genuine metal-specificity within pulmonate molluscs. Diversification into these isoforms may have been initiated by gene duplication, followed by speciation and selection towards opposite needs for protecting copper-dominated metabolic pathways from nonessential cadmium. The mechanisms enabling these proteins to be metal-specific could also be relevant for other metalloproteins.

Background

Metallothioneins (MTs) constitute a superfamily of genetically polymorphic cysteine (Cys)-rich polypeptides that bind, with high affinity, closed-shell metal ions such as Zn^{2+}, Cd^{2+}, Cu^{+} and others [1,2]. In many organisms they play multiple roles. By serving as principal cellular stores for Zn^{2+} and Cu^{+} they warrant the supply of these essential trace elements in growth and rescue processes and, by their high sequestration power, they shield cell components from deleterious bonding by highly reactive metals such as Cd^{2+} and overabundant Zn^{2+} and Cu^{+} [3,4]. In addition, they are also thought to serve as quenchers of free radicals [5,6]. In most animal species examined different MT isoforms show poor or

* Correspondence: reinhard.dallinger@uibk.ac.at
[3]Institute of Zoology and Center of Molecular Biosciences Innsbruck (CMBI), University of Innsbruck, Technikerstraße 25, A-6020 Innsbruck, Austria
Full list of author information is available at the end of the article

no appreciable differentiation and specialization in their functions and metal-binding preferences [7,8], although variations in metal selectivity between MT domains exist in some cases [9-11]. As a consequence, the metal composition of most native metal-MT complexes is very often remarkably promiscuous [12,13]. Occasionally, apparent metal specificity results from a disproportional oversupply of a certain metal ion, due to particular physiological conditions such as metabolic trace element disorders [14] or cellular overload due to metal exposure [15]. In such cases, this metal ion occupies all the binding sites of an MT molecule which would otherwise form heterometallic complexes. However, true metal specificity requires an exclusive binding preference for a certain metal to an MT peptide due to its innate structural configuration.

Understanding how MTs and other metalloproteins achieved metal specificity through evolution is a key question in the study of their structure/function relationship [2,16]. Among molluscs, pulmonate snails provide an optimal system with which to study the determinants of metal MT specificity in metazoans. Molluscs comprise a range of economically, medically and ecologically significant species and represent one of the most successful animal phyla, having been able to colonize nearly every habitat on earth [17]. Some gastropod molluscs - particularly from the subclass of pulmonate snails - feature MT isoforms that can be isolated from their tissues as homometallic complexes with either Cd^{2+} or Cu^{+} [18-21]. Hence, one isoform isolated from Cd-exposed Roman snails (*Helix pomatia*) exhibited an exclusive metal complement of six equivalents of Cd^{2+} per mol of protein [22], whereas another isoform from the same species contained 12 equivalents of Cu^{+} [23]. It has been proposed that these two pulmonate MT isoforms serve metal specific tasks related to cadmium detoxification [24-26] or homeostatic copper regulation [27]. Only recently, a third MT isoform, recovered as a mixed Cd^{2+}- and Cu^{+}-containing complex has been detected in a terrestrial pulmonate but, due to its low abundance, this isoform is probably less important to the snail's metal metabolism [21].

So far, all pulmonate MT isoforms have been obtained as native metal-MT complexes purified from snail tissues, where they are primarily involved in the metabolism of the metal ion species bound to the respective isoform [18,19]. Therefore, it cannot yet be discerned if their specific metal occupation is the result of a rigid control of metal availability, an isoform expression programming in the hosting cells and tissues or of structural differences of the respective peptides determining the coordinative options for the different metal ions. The aim of the present investigation was, therefore, to use the metal-specific snail MTs as model molecules and to test which of the above determinants contributes to the metal specificity in the snail MT system. To this end, the two metal-specific *H. pomatia* (Hp) MT isogenes (*HpCdMT* and *HpCuMT*) were expressed in two different heterologous environments - bacteria and yeast - in order to test their metal binding and functional capacities independent of their native environments. HpCdMT and HpCuMT were recombinantly synthesized in *Escherichia coli* in the presence of zinc, cadmium and copper and the features of the formed metal complexes compared by optical, chiroptical and mass spectrometric analyses; both isoforms were compared for their functional competence in yeast MT-knockout cells. Furthermore, cell- and tissue-specific expression of the two MT isogenes in the snail was scrutinized by *in situ* hybridization techniques and their expression regulation pattern was assessed by real-time polymerase chain reaction (PCR). Finally, the phylogenetic radiation of the gastropod MT family cluster inside the mollusc phylum was assessed and evaluated. Overall, our data provide an unprecedented analysis of the mechanisms determining, at different levels, the specificity of functions of paralogous MTs, suggesting clues to how these could have been achieved through evolution.

Results

Analysis of recombinant HpCdMT and HpCuMT metal complexes reveals sequence-determined specialization of metal binding

Recombinant expression of *HpCdMT* and *HpCuMT* in metal-exposed *E. coli* cells was expected to reveal their *in vivo* binding ability for zinc, cadmium and copper, independent of which is the natively coordinated metal ion.

Binding of Zn^{2+} and Cd^{2+} by HpCdMT

Mass spectrometric analysis documents that recombinant synthesis of HpCdMT in *E. coli* cultured in Cd^{2+} or Zn^{2+}-enriched media led to the production of only a single species with a fixed content of either six equivalents of cadmium or zinc (Figure 1a and 1b). The two metal complexes - Cd_6-HpCdMT and Zn_6-HpCdMT - display optical spectra with steep rises of absorbance below 270 nm and below 240 nm which is typical of tetrahedral bonding of both metal ions to multiple thiolate ligands (Figure 2a and 2c). The metal-to-sulphur linkages also manifest themselves by the intense positive and negative circular dichroism (CD) bands associated with the absorption envelopes (Figure 2b and 2d). These signals arise in part from the dissymmetric excitonic interactions of the sulphur-based transitions in pairs of doubly coordinated metal-connecting cysteine residues (of bridging thiolate ligands), thereby signifying the collective bonding of Cd^{2+} or Zn^{2+} in oligonuclear metal

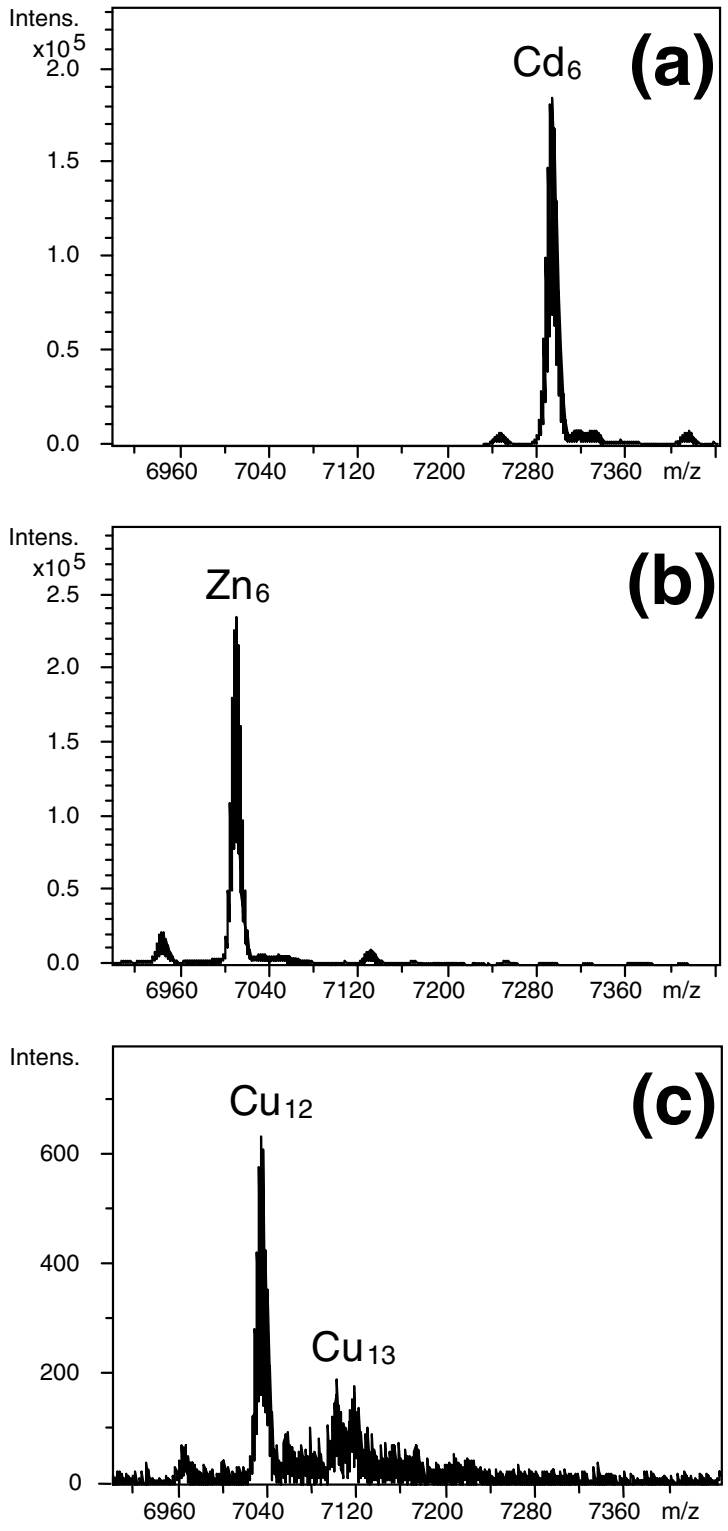

Figure 1 Deconvoluted electrospray ionization time-of-flight mass spectography spectra of the different metal-metallothionein (MT) complexes recombinantly synthesized: (a) HpCdMT obtained in Cd-enriched medium; (b) HpCdMT produced in Zn-enriched medium; and (c) HpCuMT synthesized in Cu-enriched medium under low aeration conditions. Inductively coupled plasma atomic emission spectroscopy (ICP-AES) analysis of these preparations indicated a respective mean content of 6.2 Cd/MT in (a) and 5.8 Zn/MT in (b) for HpCdMT and of 12.2 Cu/MT for HpCuMT in (c).

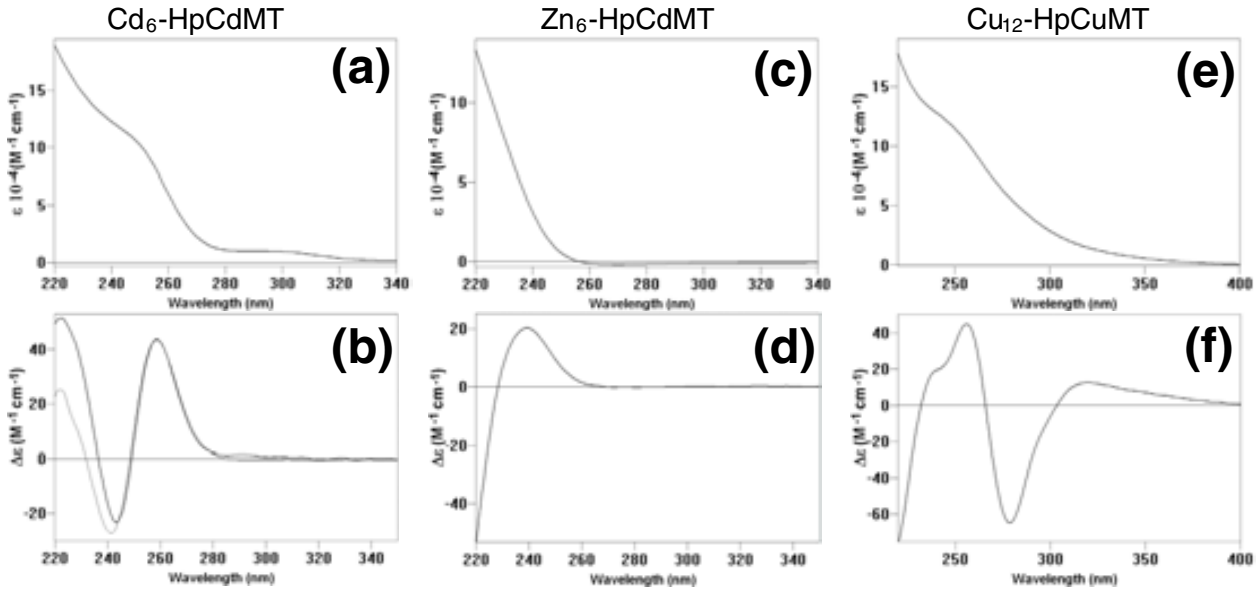

Figure 2 Ultra violet-*vis* absorption (a, c and e) and circular dichroism (CD (b, d and f) spectra of the following single species recombinantly synthesized in the corresponding metal-enriched media (Cd^{2+}, Zn^{2+}, and Cu^{2+}): Cd_6-HpCdMT (a, b), Zn_6-HpCdMT (c, d) and Cu_{12}-HpCuMT (e, f). Panel (b) also encloses (thin line) the CD spectra of the Cd_6-HpCdMT species prepared *in vitro* by addition of 6 Cd^{2+} equivalents to Zn_6-HpCdMT. MT, metallothionein.

thiolate complexes [28-30]. The spectral features of the recombinant Cd_6-HpCdMT product are indistinguishable from those of the native Cd_6-HpCdMT previously isolated from the tissue of Cd-exposed Roman snails [23]. They also reappear when, at neutral pH, the full complement of six equivalents of Cd^{2+} is added *in vitro* to the metal-free protein apo-HpCdMT [22] or when Zn^{2+} is replaced in recombinant Zn_6-HpCdMT by exposure to the much more firmly binding Cd^{2+} (Figure 2b). Thus, in both *in vivo* and *in vitro*, the structure of the protein product of the *HpCdMT* gene is seen to direct bonding of Cd^{2+} in a single energetically favoured complex fitting its supposed role of shielding the snail tissue from this highly toxic metal ion [20,24].

Binding of Cu^+ by HpCuMT

The recombinant expression of *HpCuMT* in *E. coli* cultures grown in Cu^{2+}-enriched medium led to the formation of homometallic Cu_{12}-HpCuMT as an essentially single molecular species (Figure 1c), equivalent to the native complex purified earlier from snail tissue [23]. The absorption spectra display a progressive rise below 350 nm with a broad shoulder centred at 250 nm (Figure 2e) and in CD positive and negative ellipticity bands (Figure 2f). These features match qualitatively and quantitatively those seen in mammalian Cu_{12}-MT prepared *in vitro* by adding 12 equivalents of the acetonitrile complex of Cu^+ to native MT from rabbit and are attributable to the formation of oligonuclear Cu^+ thiolate complexes in trigonal coordination geometry [31]. A molecular species with the same composition and spectral properties was attained *in vitro* by saturating at acidic pH the recombinant, metal-free, apo-HpCuMT peptide with Cu^+ using $[Cu(CH_3CN)_4]ClO_4$ as a titrating agent. As previously observed [23], this homometallic recombinant product is sensitive to atmospheric O_2. The recombinant complex was formed as a single product only when the bacteria were grown under low aeration conditions [32]. At normal oxygenation the same culture produced a heterometallic mixture of several Cu,Zn-HpCuMT species ranging from M_4 to M_{12}-HpCuMT (where M = Zn + Cu) and with spectroscopic features clearly different from those of Cu_{12}-HpCuMT. *In vitro* addition of Cu^+ to these species in the form of $[Cu(CH_3CN)_4]ClO_4$ (see above) also failed to transform these products into the homometallic single form.

Complexes of HpCdMT and HpCuMT with non-cognate metal partners

In contrast to the single, well-defined MT species resulting from the recombinant expression of the *HpCdMT* and *HpCuMT* genes in cultures enriched with their cognate metal partners, only poorly defined products were obtained when the partners were interchanged (Figure 3). Thus, expression of the *HpCdMT* gene in the presence of copper resulted in mixtures of heterometallic Zn, Cu-HpCdMT species of varying metal-to-protein

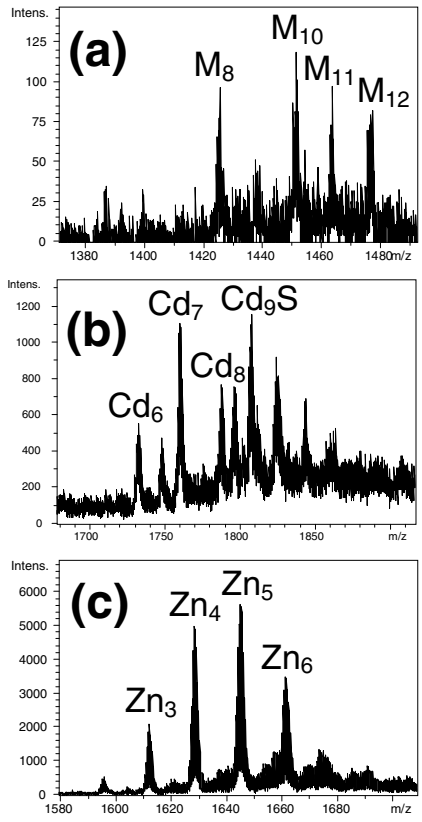

Figure 3 Electrospray ionization (ESI) time-of-flight mass spectroscopy (MS) spectra of the different metal-metallothionein (MT) complexes obtained when recombinantly synthesizing the MT peptides with their 'non-cognate' metal ion. (a) HpCdMT produced in Cu-enriched medium and; HpCuMT in (b) Cd- and (c) Zn-enriched media, where M stands for Zn+Cu, due to the difficulty of ESI-MS to discriminate between these two metal ions. For the Zn and Cd-enriched preparations, the MS spectra show the +4 charge state (intensity *vs* m/z) obtained for each preparation, while in the protein produced in a Cu-enriched medium, the MS spectrum shows the +5 charge state (intensity *vs* m/z). inductively coupled plasma atomic emission spectroscopy (ICP-AES) analysis of these preparations indicated a mean content of 0.8 Zn/MT and 7.7 Cu/MT for HpCdMT in (A); 7.8 Cd/MT in (B) and 4.8 Zn/MT in (C) for HpCuMT.

stoichiometry, when grown under normal and low aeration conditions. In the first case, their metal complement varied from three to seven equivalents and in the second from eight to 12 equivalents (Figure 3a). The CD spectra of the mixtures (not shown) displayed signals typical of oligonuclear Cu^{+}-thiolate bonding but varied in shape and amplitudes in different preparations.

The recombinant synthesis of HpCuMT in Cd^{2+}-enriched cultures led to mixtures of a number of Cd-HpCuMT species with a Cd content ranging from six to more than nine equivalents and also including a sulphide-containing Cd_9S-HpCuMT complex (Figure 3b). The CD spectra of these mixtures (not shown) displayed spectropolarimetric features arising at less than 270 nm from oligonuclear Cd-thiolate complexes and close to 280 nm from sulphide bonding to the Cd-thiolate clusters [33]. In a parallel way, the production of HpCuMT in zinc (Zn)-enriched media yielded mixtures of Zn-containing species ranging from Zn_3 to Zn_7-HpCuMT, with the different forms varying in abundance and in different preparations (Figure 3c). The CD spectra were indicative of Zn-thiolate coordination but differed widely in intensity (data not shown).

Therefore, these two MTs behave in accordance with their high metal specificity when recombinantly synthesized by bacteria grown in cultures enriched with the non-cognate metal. The HpCdMT isoform thus rendered several mixed Zn, Cu-MT complexes of different stoichiometries when biosynthesized in a Cu-rich medium. Following an equivalent behaviour, the HpCuMT isoform produced a mixture of species of different stoichiometry when synthesized by bacteria grown on Zn- or Cd-supplemented media. The classification of MTs according to the metal-binding behaviour shown when recombinantly synthesized in cultures enriched with different metals and the correspondence of this classification with other 'metal-specificity' criteria, have been fully reviewed [34].

Stability of the Cd_6-HpCdMT and Cu_{12}-HpCuMT complexes is documented by their metal exchange inertness

In order to study the lability/inertness of the recombinantly synthesized Cd_6-HpCdMT and Cu_{12}-HpCuMT species and their propensity to exchange their preferentially bound metal ions, an equimolar mixture of these two complexes was allowed to stand for 20 h at 25°C (Figure 4). The invariant electrospray ionization-mass spectrometry (ESI-MS) spectra recorded just after mixing and 20 h later demonstrate that the integrity and individuality of these two species was maintained for a long period of time, which confirms that both metal-HpMT complexes possess an exceptionally high stability and exhibit a persistence attributable to their metal binding specificity.

Transformation of HpCdMT and HpCuMT in yeast MT-knockout cells confirms metal-specific roles

In order to advance from metal-specific folding to metal-specific function, the particular performance of the two snail MT isoforms was compared by complementation studies in another heterologous system. Hence, yeast cells deficient in their endogenous MTs (yeast *Cup1* and *Crs5* knockout cells) were transformed with complimentary DNAs (cDNAs) coding for HpCdMT, HpCuMT, mouse MT1, yeast Cup1 and yeast Crs5 and their growth was examined for Cu^{2+} and Cd^{2+} tolerance. When these cells were grown at increasing Cu^{2+} concentrations in the

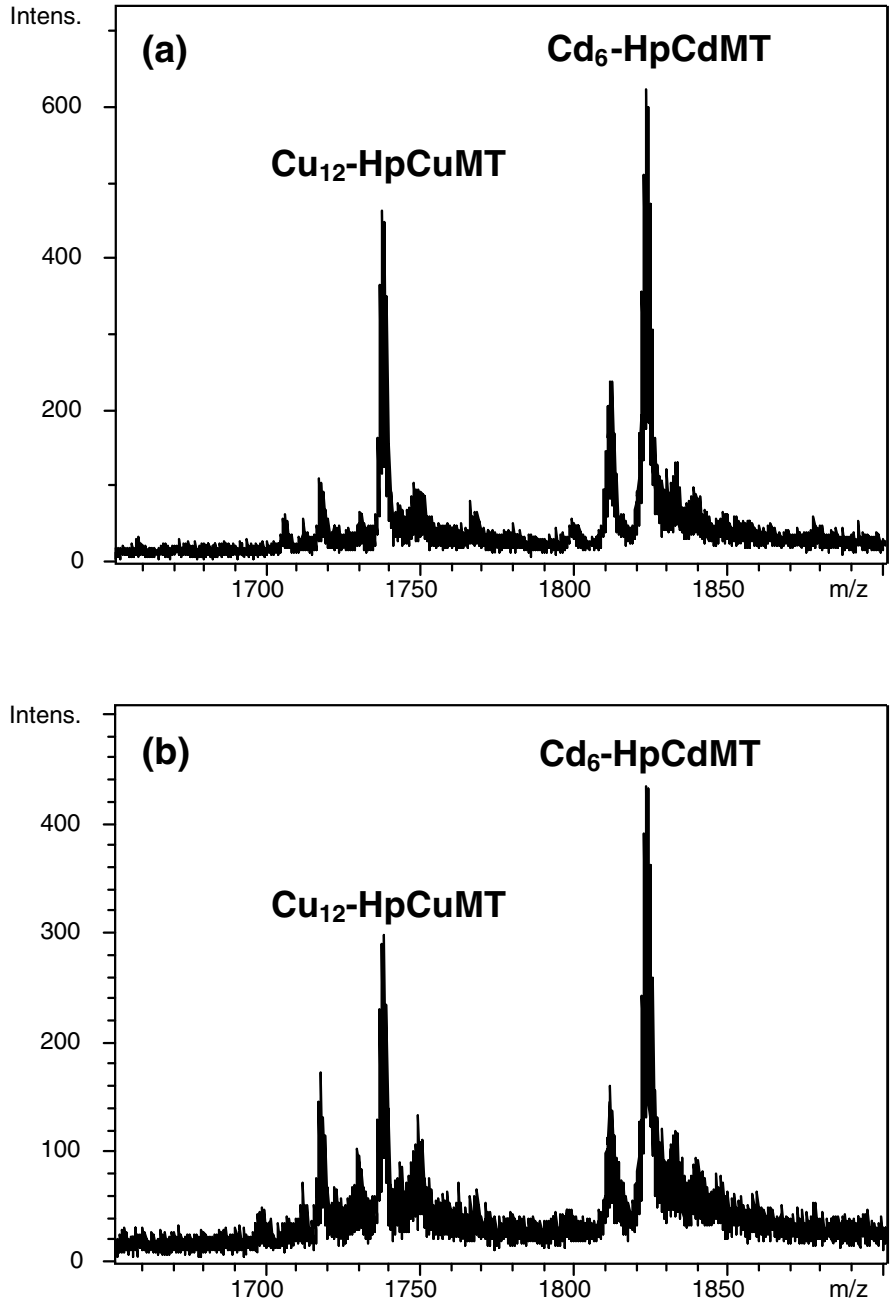

Figure 4 Electrospray ionization (ESI) time-of-flight mass spectroscopy (MS) spectra of an equimolar mixture of recombinant Cd_6-HpCdMT and Cu_{12}-HpCuMT, recorded at (a) *t* = 0 and (b) *t* = 20 h, showing that no metal exchange occurs between the two HpMT isoforms at 25°C. MT, metallothionein.

medium (Figure 5a), the highest copper tolerance was observed for the strain transformed with yeast *Cup1*, followed by the strain transformed with the HpCuMT cDNA. The strain transformed with HpCdMT cDNA gave no evidence of tolerating copper at all.

In marked contrast, when the cells were grown in media with increasing concentrations of Cd^{2+}, tolerance was greatest in the strain transformed with the endogenous yeast *Crs5* which reflects the known preference of this yeast MT for divalent metal ions [32]. The second best was the strain transformed with the cDNA for HpCdMT showing a Cd^{2+} detoxification capacity that was also much better than that of the cells transformed with the cDNA coding for the mouse MT1 isoform, which natively binds

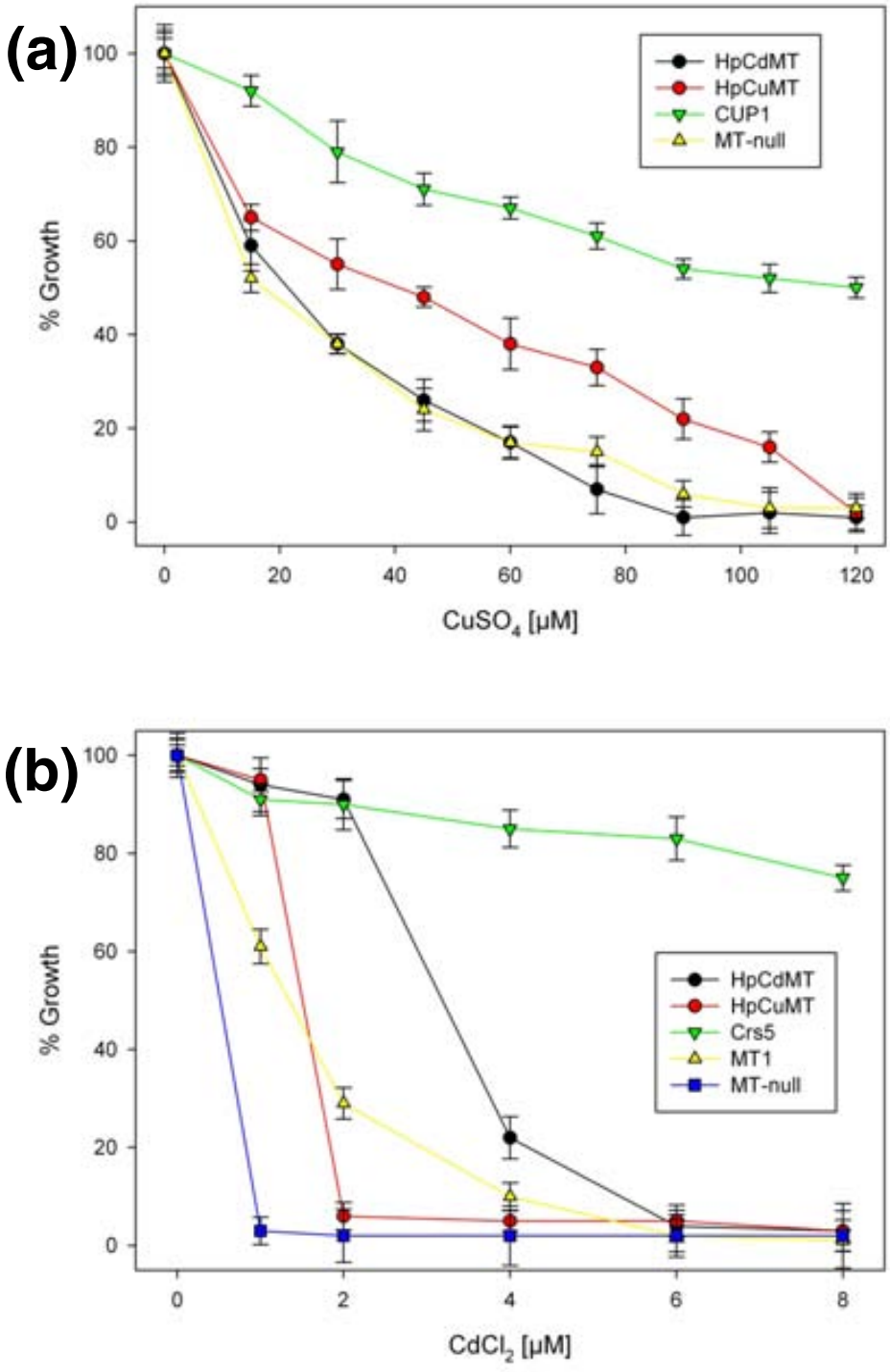

Figure 5 (a) Copper and (b) cadmium tolerance evaluated by phenotype rescue on DTY4 [metallothionein (MT) deficient] yeast cells. Metal tolerance of each DTY4 strain transformed with different MTs, as indicated in the side boxes, is shown as a percentage of the growth rate exhibited in a non-metal-supplemented medium. Cup1 and Crs5 are the two yeast MTs, and MT1 stands for the mouse MT1 isoform.

either Zn^{2+}, Cd^{2+} or Cu^{+}. The strain carrying cDNA for HpCuMT showed almost the same high sensitivity to Cd^{2+} as the MT-null knockout cells (Figure 5b).

These results show that the two snail MT isoforms also assume metal-specific roles in a heterologous eukaryotic environment (yeast), in accordance with their metal-specific binding preferences revealed by their synthesis in recombinant prokaryotic systems. Significantly, the total equivalence between the features of the metal-MT complexes synthesized in these two hosts (bacteria and yeast) has recently been demonstrated for both cadmium and copper, using the Cup1 MT as a model system [35].

In pulmonate snails, CdMT and CuMT isoforms are products of cell-specific expression

In the midgut gland of the snail *Helix pomatia*, the Cd-specific isoform (HpCdMT) is synthesized in all cell types of this organ (Figure 6a) and is also produced in the epithelial cells of foot, gut and kidney [24]. In contrast, the messenger RNA (mRNA) coding for HpCuMT is located only in one cell type, the so-called rhogocytes (Figure 6b), which are present in the midgut gland, and in many other organs, and have been shown to be the sites of hemocyanin synthesis [27]. Consequently, both metal-specific MT isoforms can be recovered natively from the snail midgut gland (Figure 6c).

Pulmonate MT isoform genes display metal-specific transcription patterns

The pattern of metal-specific transcriptional induction of MT isogenes was examined in two pulmonate species: in *H. pomatia*, the subject of this work, and in *Cantareus aspersus* because, in this species, a third and so far unknown MT isogene (here called *Cd/CuMT*; Figure 7b) has been reported [21]. The product of this gene also seems to occur in other pulmonate snails, as first reported in this work (see below). The effect of metal supplementation in the feed of the snails upon transcription was evaluated by measurement of the mRNA copy number. For both species, the expression of the *CdMT* genes was highly responsive to cadmium exposure (Figure 7a and 7b). While Cd^{2+} increased the number of transcripts of the *CdMT* genes in both species at concentrations as low as 0.45 μmol Cd^{2+}/g dry weight (in the feed), no statistically significant enhancement was observed in *H. pomatia* for a more than a 10-times higher amount of Zn^{2+} (6.93 μmol Zn^{2+}/g dry feed weight; Figure 7a). In Cu^{2+} a significant increase of the mRNA copies of the HpCdMT gene was seen only at an effective concentration of 5.05 μmol/g dry weight in the feed (Figure 7a). In contrast to the *CdMT* genes, no significant metal-dependent enhancement of mRNA copy number - at least at the metal concentrations assayed - was observed for the *CuMT* and *Cd/CuMT* genes of the two species (Figure 7a and 7b). These induction patterns are totally in accordance with the constitutive expression of the *CuMT* gene in rhogocytes [27], whereas the much higher inducible expression of the *CdMT genes* in epithelial cells supports the view that the product of this gene plays a role in Cd^{2+} sequestration and detoxification [24-26]. In addition, CdMT may also serve other biological functions, very likely in the form of the Zn^{2+} complex for *H. pomatia*, as suggested and discussed elsewhere [36].

HpCdMT and HpCuMT as prototypes of isoform families which have evolved metal specificity in pulmonate snails by modulation of non-cysteine amino acid positions

HpCdMT and HpCuMT can be considered as prototypes of a series of orthologous genes also present, except from *H. pomatia*, in other pulmonate snails. Within molluscs, gastropods and pulmonate snails, in particular, have evolved three MT gene subfamilies, two of them comprising isoforms with a homometallic composition [20,22,23] and distinct metal binding behaviour and functional specificities for either Cd^{2+} or Cu^{+} [18 - 21, 23; and this work]. Figure 8 shows an alignment of the, so far identified, MT sequences from pulmonate gastropods, including the secondarily aquatic species *Biomphalaria glabrata*. Throughout, two of the three MT isoforms are alignable with and can thus be assimilated to the known *H. pomatia* isoforms HpCdMT and HpCuMT [18]. The third sequence, the Cd/CuMT isoform first observed in the terrestrial garden snail (*Cantareus aspersus*), has been recovered from native sources as a simultaneously Cu^{+} and Cd^{2+}-containing complex [21] and has been identified in other species too (see Figure 8). However, this isogene is transcribed at low constitutive levels, as it is not inducible by metals at all (Figure 4b) and thus hardly detectable at the protein level. It may, therefore, be only of circumstantial importance for the metal metabolism in its host. However, its discovery is critical for the understanding of the diversification of MTs in this group of organisms.

The three isoform types share strictly conserved Cys positions in their primary structure, confirming the fundamental importance of the sulphur atoms provided by these residues for metal complex and metal thiolate cluster formation, irrespective of the metal species involved. Besides Cys, a few other amino acid positions, either on the N-terminal tail of the peptides or in the direct neighbourhood of Cys residues, show conserved positions through the members of the three isoform subfamilies (Figure 8). In contrast, there is significant variability across the three isoform types for the non-cysteine amino acid residues interspersed between the conserved positions. This suggests that the different

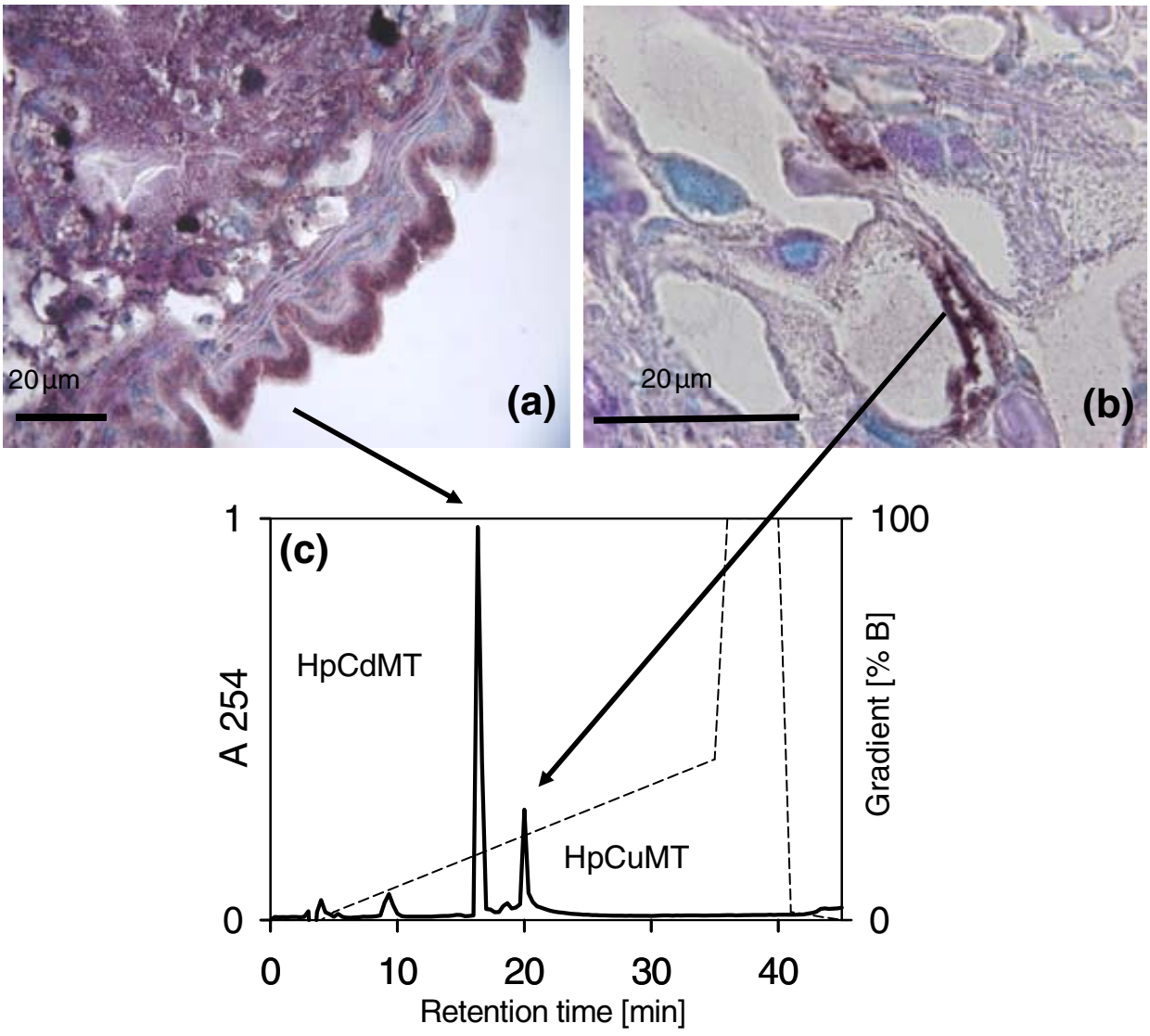

Figure 6 Cell-specific visualizuation of HpCdMT and and HpCuMT mRNA, and isolation of both native expressed isoforms from snail midgut gland tissue. *In situ* hybridization (dark violet precipitations) of (a) HpCdMT messenger RNA (mRNA) in midgut gland cells and (b) HpCuMT mRNA in rhogocytes from midgut gland of cadmium-exposed *Helix pomatia*. (c) Reverse-phase high-performance liquid chromatogram of purified homogenate supernatants from midgut gland of cadmium-exposed *H. pomatia* snails, showing by the arrows the HpCdMT and HpCuMT isoforms originating from the different cell types, as characterized in references [18] and [19]. MT, metallothionein.

metal specificities of the isoforms were achieved by gene duplication and subsequent speciation by evolutionary modulation of these non-coordinating amino acid positions. Moreover, the alignment pattern shows that the similarity between the members of the CuMT and the Cd/CuMT isoform families is clearly higher than that observed between those and the CdMT isoforms (Figure 8, Table 1).

A nucleotide-based neighbour-joining tree shows that pulmonate MT isoform subfamilies are assembled in three distinct branches and are thus clearly distinguishable from all other mollusc forms represented by the group of Bivalvia (Figure 9). This suggests that the differentiation into these isoforms has been an evolutionary process which, within molluscs, remained restricted essentially to pulmonate snails. The protein distance analysis tree (Figure 10) confirms the close relationship between the CuMT and Cd/CuMT isoforms (Table 1), which apparently evolved from a common ancestor that gave rise to the differentiation of the Cu-specific and the less metal-specific Cd/CuMT gene subfamilies, clearly segregated from the CdMT gene subfamily. On the other hand, the three

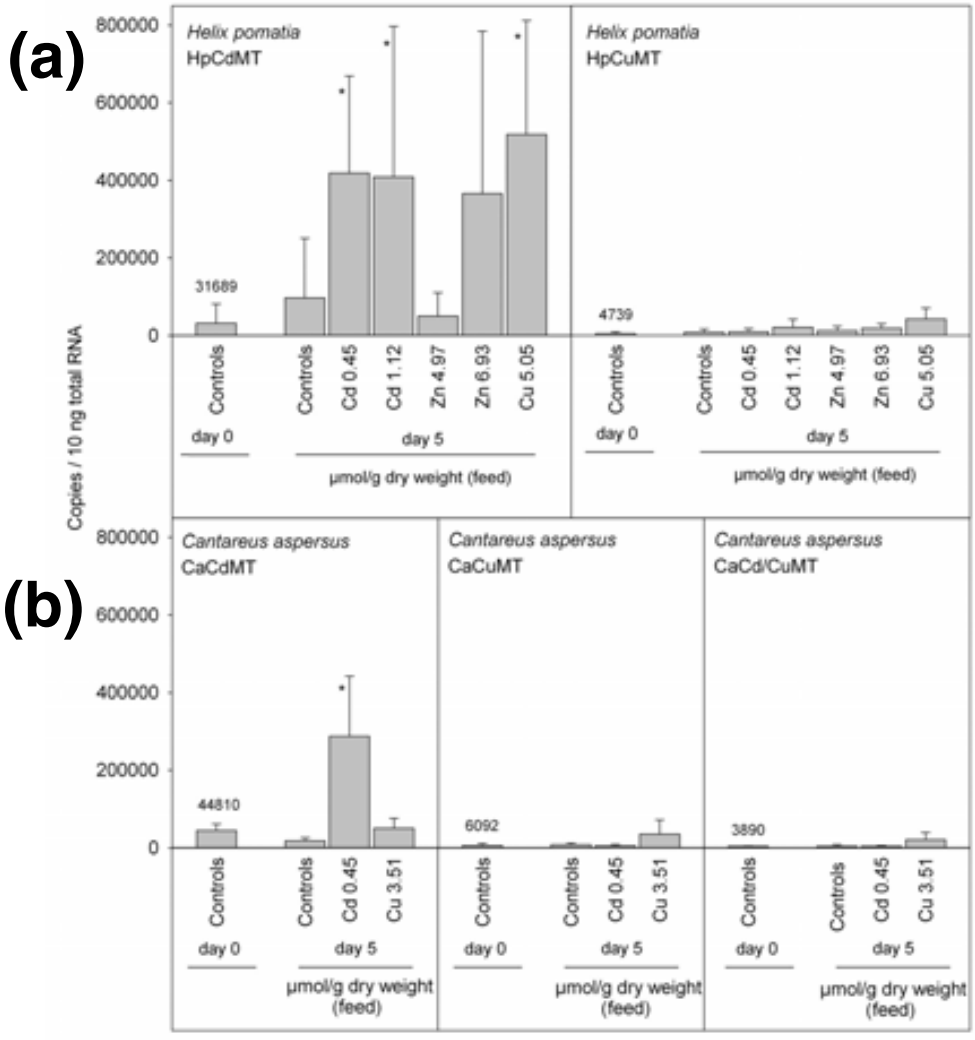

Figure 7 Real-time detection polymerase chain reaction (copy number/10 ng total RNA) of messenger RNA (mRNA) of *Helix pomatia* HpCdMT and HpCuMT (a) and *Cantareus aspersus* CaCdMT, CaCuMT and CaCd/CuMT (b). Respective mRNA concentrations (copy numbers/10 ng total RNA) were measured in midgut gland tissue of control (unexposed) snails at the beginning of the experiments and of controls, as well as metal-exposed snails, after a feeding period of 5 days. For each bar, means and standard deviations are shown ($n = 5$). Asterisks above bars designate significant deviations (*T*-test, $P \leq 0.05$) from control animals at the beginning of the experiment. For controls, copy numbers are specified above bars. Respective metal concentrations in the feed are shown below each bar, expressed as µmol metal/g dry weight of feed. MT, metallothionein.

pulmonate MT subfamilies share a common root with all other gastropod MTs (Figures 9 and 10).

Discussion

In MTs, metal binding and metal exchange reactions are mainly governed by the coordination chemistry of thiolate bonding with closed-shell metal ions such as Zn^{2+}, Cd^{2+}, Cu^{+} [12]. To be more precise, the relative order of *in vitro* metal binding affinities of apo-MT peptides, as well as the order of displacement capacity of each heavy metal ion within a metal-MT complex (Hg(II) > Cu(I) ~ Ag(I) > Cd(II) > Pb(II) > Co(II) > Zn(II)), follow the rules established for metal-thiolate and metal-sulphide low-molecular mass complexes [37]. However, the assumption that these 'inorganic chemistry' rules are the unique responsible of the metal-MT complex properties would lead to the conclusion that MT polypeptides sharing the same number and position of Cys residues would exhibit equivalent metal binding behaviour. However, this is essentially untrue, as firmly demonstrated in this work for the snail MT system. MT metal specificity is a subject of vivid, current debate [16], as to a larger

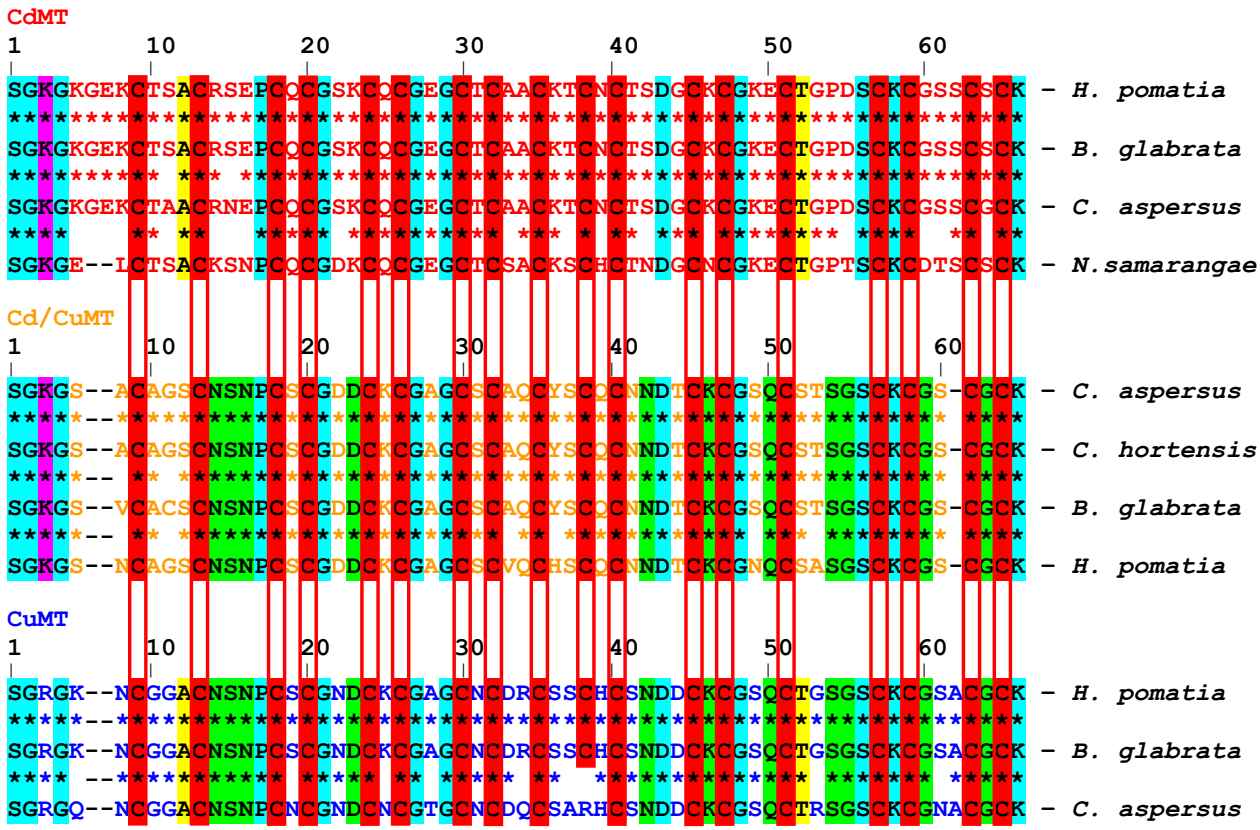

Figure 8 Amino acid sequence alignments of terrestrial and freshwater pulmonate snail metallothioneins [MTs; CdMT, CuMT and Cd/CuMT]. Protein or nucleotide sequences were obtained from GenBank and are specified in the legend of Figure 9. Conserved cysteine (cys) positions shared by all isoform families are shaded in red. Conserved non-cys amino acid positions are shaded as follows: blue, shared by all three isoform families; yellow, shared by the CdMT and the CuMT families; pink, shared by the CdMT and Cd/CuMT families; green, shared by the Cd/CuMT and the CuMT families. Asterisks between two sequences indicate identity; Cys residues are marked in bold. For abbreviations of species names see legend of Figure 9.

Table 1 Comparative protein Blast analysis of pulmonate metallothionein (MT) isoform families*

	Score†	E-value†	Identities	Positives
CdMT versus CuMT				
Helix pomatia	65.1	8e-17	57%	73%
Cantareus aspersus	59.3	5e-15	52%	68%
Biomphalaria glabrata	65.1	8e-17	57%	73%
CdMT versus Cd/CuMT				
H. pomatia	57.8	2e-14	53%	65%
C. aspersus	58.2	1e-14	55%	68%
B.glabrata	56.2	4e-14	55%	67%
CuMT versus Cd/CuMT				
H. pomatia	79.3	5e-21	75%	87%
C. aspersus	72.0	7e-19	67%	81%
B. glabrata	75.1	9e-20	73%	84%

*Protein BLAST calculation (blastp algorithm, NCBI tools) for testing similarities between the three pulmonate MT isoform subfamilies, exemplified by CdMT, CuMT and Cd/CuMT from *H. pomatia*, *C. aspersus* and *B. glabrata*.

or lesser extent, all MTs show a degree of metal specificity in native and/or *in vivo* environments. In this case, metal specificity is understood to be the set of determinants that eventually leads a given MT peptide to natively discriminate among metal ions, thus allowing the formation of particular metal complexes and the performance of the biological function for which they were selected. To date, major factors claimed to explain metal-MT specificity in live systems are protein sequence optimization, metal ion availability and/or metal-responsive transcription programming [2].

The structural features of the resulting MT complexes with different metal ion species arise from the equilibrium between kinetic and thermodynamic requirements [29], so that they converge to a stoichiometric ratio that reflects their energetically most stable state [38]. Hence, the observation by ESI-MS of metal-MT species synthesized in *in-vivo* environments, either

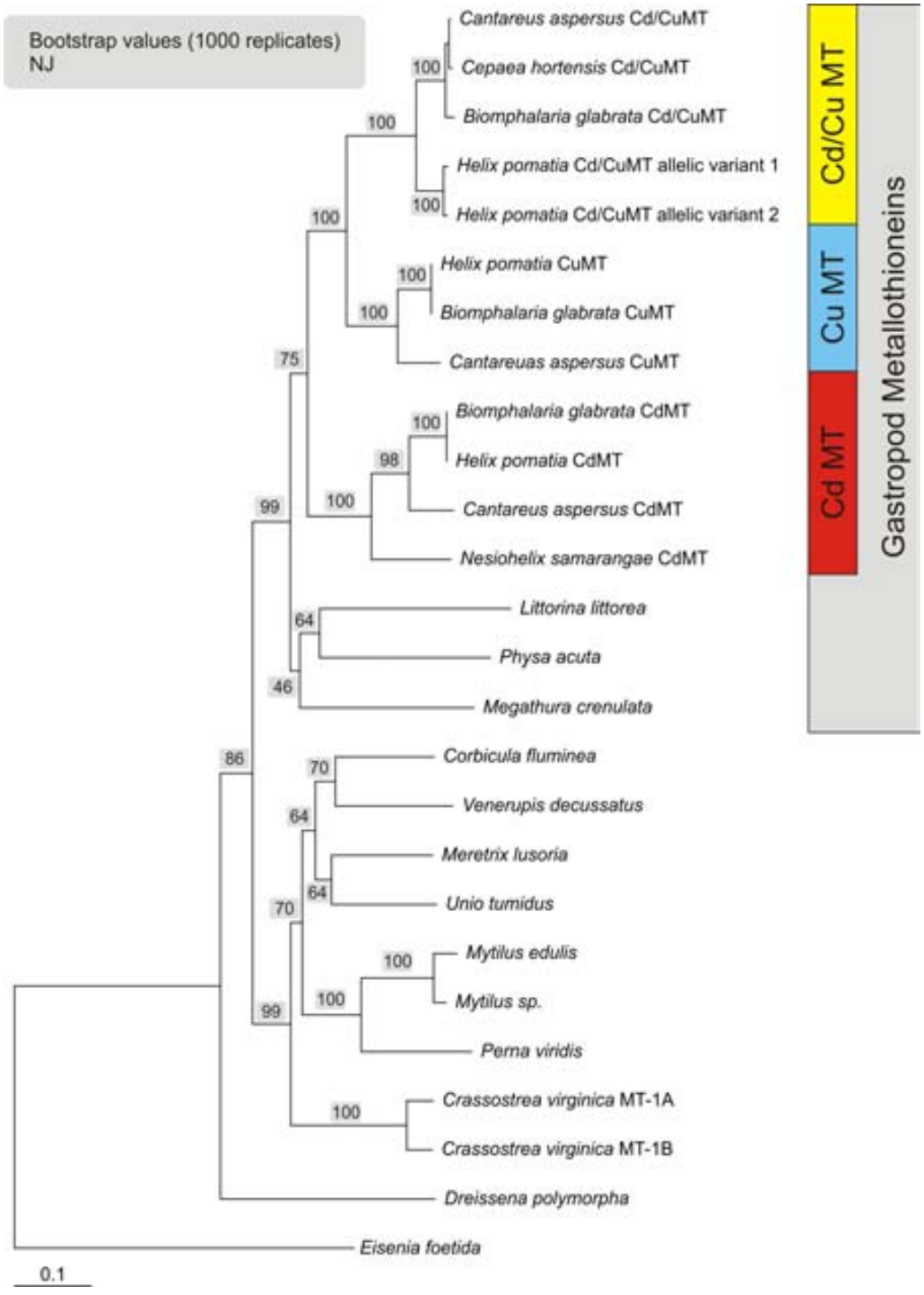

Figure 9 Nucleotide-based neighbour-joining tree of mollusc metallothioneins (MTs) comprising mussels and gastropods, with *Eisenia foetida* MT used as out-group. Pulmonate MTs appear grouped in separate clusters of metal-specific subfamilies (CuMTs, Cd/CuMTs and CuMTs). Accession numbers of GenBank entries used were as follows: *Helix pomatia* CdMT (HpCdMT), AAK84863 and AF399740; *H. pomatia* CuMT (HpCuMT), AAK84864 and AF399741. *Biomphalaria glabrata* CdMT, ACS91928 and GQ205374; *B. glabrata* CuMT, ACS91927 and GQ205373; *B. glabrata* Cd/CuMT, ACS91929 and GQ205375; *Cantareus aspersus* CdMT, ABL73910 and EF152281; *C. aspersus* CuMT, ABM55268 and EF178297; *C. aspersus* Cd/CuMT, ABM92276 and EF206312; *Nesiohelix samarangae* CdMT, ACC17831 and EU437399; *Megathura crenulata* MT, AY102647; *Littorina littorea* MT, AY034179; *Mytilus edulis* MT-10, AJ007506 and EF140765; *Crassostrea virginica* MT-1A, AY331697; *C. virginica* MT-1B, AY331699; *Meretrix lusoria* MT, AY525635; *Perna viridis* MT-2, F092972; *Dreissena polymorpha* MT, DPU67347; *Unio tumidus* MT, EF185127; *Corbicula fluminea* MT, EF185126; *Eisenia foetida* MT, AK236886.

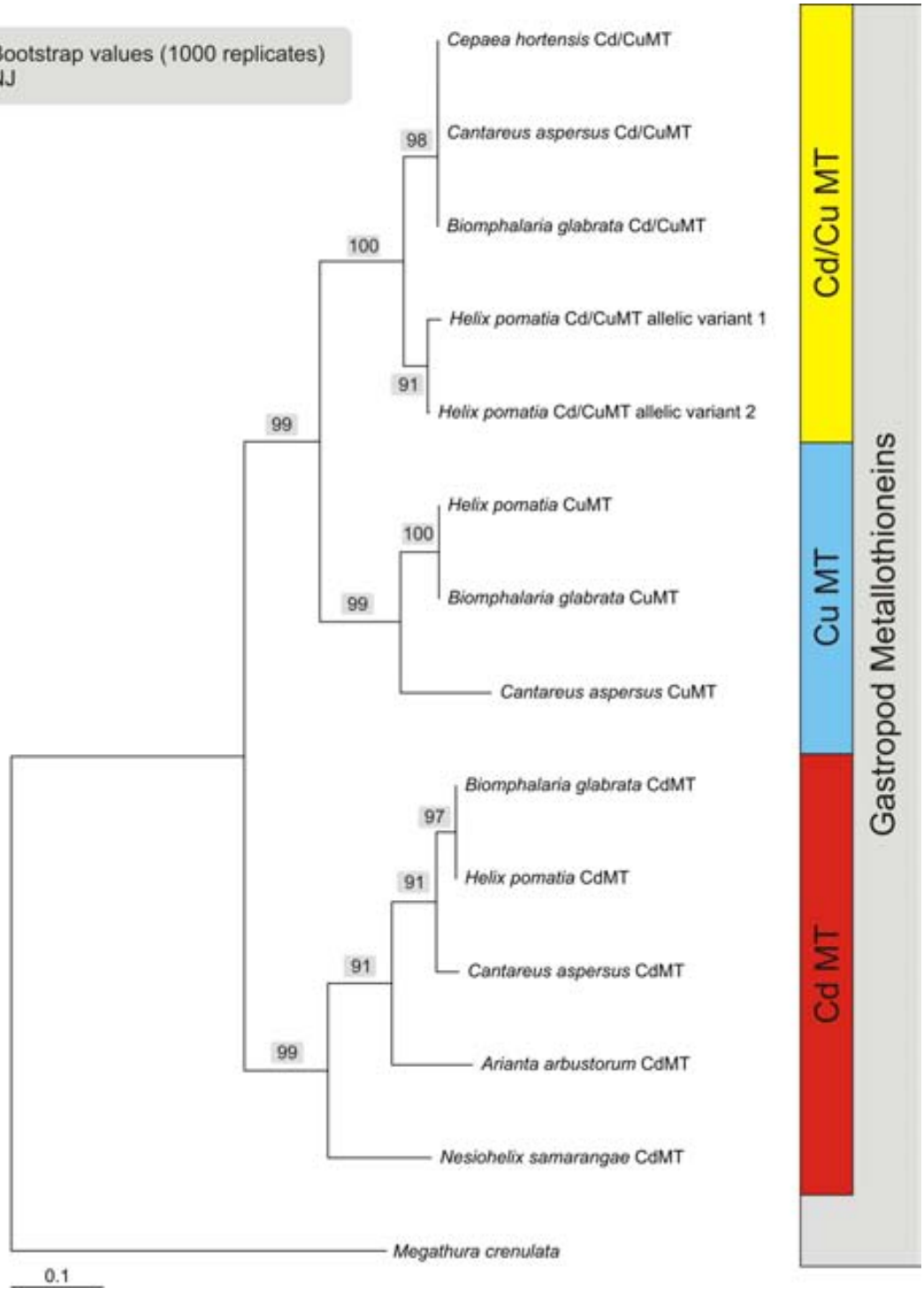

Figure 10 Amino acid sequence-based neighbour-joining tree of pulmonate metallothionein (MT) subfamilies represented in clusters of Cd/CuMTs, CuMTs and CdMTs, with *Megathura crenulata* MT as out-group . Accession numbers of GenBank entries are as indicated in the legend of Figure. 9.

native or recombinant, allows one to read the propensity of the respective peptides to form metal complexes that are uniquely defined from a stoichiometric and thermodynamic point of view [2,23,34]. In combination with spectroscopic studies, this leads to a clear appraisal of the distinctness of a MT metal specificity, as exemplified in the present work. It can, therefore, be concluded that the homometallic and unique composition of the complexes formed by HpCdMT and HpCuMT with their cognate metal species upon isolation from recombinant cultures (Figure 1) reflects the innate metal specificity of the two isoforms, rather than being the result of an occasional association with metal ions governed by their intracellular or environmental availability. This is confirmed by the poor metal-binding behaviour of the same isoforms confronted with their non-cognate metal ions (Figure 3) and by the inertness of the two complexes, Cd_6-HpCdMT and Cu_{12}-HpCuMT, to exchange metal ions (Figure 4). Such metal ion exchange processes have repeatedly been reported in MTs [39] and would be reasonable to expect [12].

The complete sequential identity of Cys residues and the high degree of conserved positions for other amino acids shared among the three isoform families (Figure 8) suggest, along with their nearly equal size, that metal-specific differentiation of pulmonate snail MTs must have been initiated by gene duplication events, followed by modulatory speciation of amino acid residues located between the cysteine positions. Gene duplication seems to be a common mechanism driving the evolutionary differentiation of MT isoform in animals and is documented for MTs of *Drosophila melanogaster*, among others [40], and the mussel *Crassostrea gigas* [41]. Once duplicated, such genes are free to independently generate mutations, upon which selective forces can then act towards evolution of specific features [42]. The example of pulmonate snail MTs also proves that the evolutionary variation of non-cysteine residues can impose a metal-specific character on to the coordination chemistry of a MT peptide. At present, it is not known how this is achieved at a structural level. However, it must be supposed that, due to their particular position in the sequence and chemical nature of their side-chains, non-cysteine amino acids constrain the sulphur ligands provided by the conserved Cys positions to assume only one of several theoretically possible spatial coordination foldings. Determination of the three dimensional structure of the Cd_6-HpCdMT and Cu_{12}-HpCuMT complexes is actually in progress which may unveil the detailed structural basis of the metal specificity of the two HpMT isoforms.

Cell-specific expression may also contribute to enhancing distinct metal-related functionality [2]. Roman snails, for example, synthesize HpCuMT exclusively in rhogocytes (Figure 6b), the modified cells of mesodermal origin found in virtually all connective tissues of mollusc organs [43]. Since they are also the sites of hemocyanin synthesis [44], it was suggested that HpCuMT functions as a Cu^+ reservoir/donor for the nascent hemocyanin [27]. The constitutive expression of *HpCuMT* (Figure 7) and the exclusive preference of this isoform for Cu^+ (Figure 6c) support this presumed function. The supposed incorporation of Cu^+ into the structure of hemocyanin must occur under reducing conditions, which is also consistent with the high susceptibility of native Cu_{12}-HpCuMT complexes to oxidization [20,23] and the fact that homometallic Cu_{12}-HpCuMT synthesis is only achieved in low-aerated recombinant cultures (this work). The apparent connection between the tasks of Cu-specific MT isoforms and their presence in organisms with Cu-depending hemocyanins is reminiscent of the situation reported for decapod crustaceans [45,46]. In these animals, concentrations of Cu-MT complexes fluctuate with the metabolic state and the hemocyanin levels during the moulting cycle [47,48]. Cu-specific MTs are also observed in organisms of other kingdoms, especially in fungi [49-51], where their role may be connected to the synthesis of the Cu-containing enzyme tyrosinase, as in *Neurospora crassa* [52].

After exposure of Roman snails to Cd^{2+}, virtually all of this metal in the digestive tissues was bound to HpCdMT (20) in a similar manner as for CdMT isoforms of other snail species [53]. Consistently, in the Roman snail, HpCdMT is produced in digestive and excretory tissues [24] (Figure 6a), where the corresponding gene is selectively upregulated by Cd^{2+} exposure (Figure 7). This suggests that absorption of toxic Cd^{2+} from the surrounding substrate via the alimentary tract may constitute a particular physiological challenge, exacerbated by the evolutionary transition of gastropods to terrestrial life [36]. Moreover, the sensitivity to Cd^{2+} of important Cu-dominated metabolic pathways [54-56] and Zn-dependent enzymes [57] could have been the basis of the generation of a specific MT isoform devoted to Cd^{2+} detoxification in these animals. Our data also demonstrate the ready formation of homometallic complexes of HpCdMT with Zn^{2+}, which may be a consequence of the comparable coordination preferences of these two d^{10} metal ions. The much weaker bonding of Zn^{2+} [58] to this isoform, however, does not prevent the peptide from functioning as a most effective Cd^{2+} sequestration agent. In the presence of Zn^{2+} and the absence of Cd^{2+}, the HpCdMT isoform is expressed only at low basal concentrations (Figure 7) and, as in the case of mammalian MTs [59], is thought to serve other functions [36].

Conclusion

Overall, the present study, together with the extensive body of evidence provided by our previous work, suggests that the pair of the metal-specific *H. pomatia* MT isoforms (HpCdMT and HpCuMT) can be regarded as the prototype of a series of paralogous forms present in pulmonate gastropods. In these organisms, divergent evolution by gene duplication, with subsequent modulation of non-cysteine amino acid positions and a cell specific occurrence and gene expression regulation, has led to the complete separation of their metal-binding preference, cell-specific occurrence, expression regulation and functionality. This resulted in genuine CdMTs becoming inducible forms specializing in the global protection of the organism from the non-essential toxic element Cd and in genuine CuMTs becoming constitutive forms supplying the essential element Cu. Our findings provide experimental evidence and possible answers to how metallotproteins in general, and MTs specifically, were able to achieve partial or complete specificity in their metal binding behaviour and functionality.

Methods

Animals and metal exposure

Roman snails (*H. pomatia* L.) were obtained from a commercial dealer (Exoterra, Dillingen, Germany). Garden snails (*C. aspersus*) were provided by the Department of Chrono-Environment, University of Franche-Comté, Besançon, France. All animals were reared under laboratory conditions (20°C, 80% humidity, 12:12 h photoperiod) at the Institute of Zoology in Innsbruck, Austria. Twenty-five snails from each species were split equally into five groups and fed over a period of 5 days on metal-enriched lettuce (*Lactuca sativa*). Metal loading of feed was achieved by soaking salad leaves in a corresponding metal salt solution ($CdCl_2$ in H_2O, with 1 and 3 mg Cd^{2+} L^{-1}; $ZnCl_2$ in H_2O, with 5 and 10 mg Zn^{2+} L^{-1}; $CuCl_2$, with 10 mg Cu^{2+} L^{-1}) [60]. Resulting metal ion concentrations in the salad feed were as follows (means ± standard deviation, n = 5): Cd^{2+}, 0.45 ± 0.11 and 1.12 ± 0.23 μmol g^{-1} dry weight; Cu^{2+}, 3.51 ± 0.73 or 5.05 ± 0.97 μmol g^{-1} dry weight; Zn^{2+}, 4.97 ± 3.42 and 6.93 ± 0.89 μmol g^{-1} dry weight). These concentrations range from physiologically to moderately elevated levels and are, therefore, representative for what could be the natural conditions encountered by snails. At days 0 and 5, RNA was extracted from the small midgut gland tissue aliquots (~10 mg fresh weight) of at least three animals and processed for cDNA synthesis as detailed below.

For *in-situ*-hybridization of HpCdMT isoform mRNAs, five individuals of *H. pomatia* were exposed over 14 days to a concentration of 14.97 μmol Cd g^{-1} dry weight. At the end of the exposure period, animals were sacrificed and their organs (midgut gland, midgut, kidney, mantle and foot) used for *in-situ*-hybridization analysis as described below.

Metal analyses

Metal-enriched salad samples were oven-dried at 60°C for several days. Dried samples (snail tissues: 50-100 mg dry weight; salad samples: 100 - 500 mg dry weight) were wet-digested in screw-capped polypropylene tubes (Greiner, Kremsmünster, Austria) with a mixture of HNO_3 (suprapure; Merck, Darmstadt, Germany) and distilled water (1:1) by heating at 70°C for several days. At the end of digestion, a few drops of H_2O_2 were added to the heated samples. The remaining solutions were diluted to a known volume with distilled water and analysed for metal concentrations (Cd, Zn, Cu) either by flame (model 2380 instrument, Perkin Elmer, Massachusetts, USA) or graphite furnace atomic absorption spectrophotometry (Hitachi Z-8200) with polarized Zeeman background correction (Hitachi, Tokyo, Japan).

Real-time detection PCR

RNA sampling for real-time detection PCR was done in control snails and animals exposed to metals over a 5 day period (see above). This time range was chosen because, in pulmonate snails, maximal induction of the *CdMT* gene by Cd^{2+} is reached only after several days. Total RNA was isolated from the homogenized midgut gland tissue of *H. pomatia* and *C. aspersus* individuals (Ultra Turrax T25, IKA Maschinenbau, Staufen, Germany) and quantified after DNaseI digestion (Fermentas, St Leon-Rot, Germany) by means of RiboGreen® RNA Quantitation Kit (Molecular Probes, OR, USA) with calibration curves derived from RNA standards using a fluorescence plate reader (Molecular Devices, CA, USA). Of total RNA, 450 ng was applied for cDNA synthesis using *RevertAid™ H Minus M-MuLV Reverse Transcriptase* (Fermentas) with hexamer primers in a 50 μL approach. Quantification of **the** RNA copy number was performed on a 7500 real-time PCR (RT-PCR) instrument from Applied Biosystems (CA, USA) using the Power SYBR Green approach (Applied Biosystems). Calibration curves from amplicon plasmids were used for copy number analysis for each of the MT isoforms involved, using primers designed with the Primer Express 3.0 software (Applied Biosystems) based on the known cDNA sequences for MT isoforms published in GenBank (*H. pomatia* HpCdMT and HpCuMT, accession numbers: AF399740 and AF399741, respectively; *C. aspersus* CaCdMT, CaCuMT and CaCd/CuMT, accession numbers: EF152281, EF178297, and EF206312). PCR primers used were as follows: HpCdMT: sense primer, 5'AAAGTGCACCTCAGCTTGCA 3'; antisense primer: 5'

GCAGGCGGCACA TGTACAG 3'; amplicon length, 85 bp. HpCuMT: sense primer, 5' CCTTGCAGCTGTGGT AACGA 3'; antisense primer, 5' CAAGAACTG-CATCGGTCACAA 3'; amplicon length, 65 bp; CaCdMT: sense primer, 5' GCCGCCTGTAAGACTTGCA 3'; antisense primer: 5' CACG CCTTGCCACACTTG 3'; amplicon length, 56 bp. CaCuMT: sense primer, 5' AACAGCA ACCCTTGCAACTGT 3'; antisense primer, 5' CGAG-CACTGCATTGATCACAA 3'; amplicon length, 74 bp. CaCd/CuMT: sense primer, 5' TGTGGAGCCGGCT GTTCT 3'; antisense primer, 5' CAGGTGTCATTGTTG-CATTGG 3'; amplicon length, 59 bp. Optimal primer concentrations were determined by means of dissociation curves established for each primer pair. Two microlitres of cDNA were applied for RT detection PCR in a 20-μL approach (1x Power SYBR Green PCR Mastermix, 1x U-BSA, 900 mM sense primer, 300 mM antisense primer for HpCdMT and HpCuMT; 300 mM sense and 900 mM antisense primer for CaCdMT; 900 mM for sense and antisense primer for CaCuMT; 99 mM sense and 300 mM antisense primer for CaCd/CuMT). The PCR conditions were as follows: 50°C, 2 min; 95°C, 10 min; 40 repeats of 95°C, 15 s; and 60°C, 1 min.

In situ hybridization techniques

Cell- and tissue-specific expression of both HpMT isoforms was demonstrated by *in situ* hybridization (ISH). Construction of digoxigenin-11-UTP-labelled sense and antisense RNA probes for ISH of both MT isoform mRNAs, as well as ISH, antibody exposure and staining of parafomaldehyde-phosphate buffered saline (PBS)-fixed paraffin sections (5 μm) from tissues (midgut gland, midgut, kidney, mantle and foot) of control and metal-exposed animals were performed exactly as described previously [24]. Control sections (exposed to either hybridization antisense or sense probes) were treated and incubated in the same way as samples but without anti-digoxigenin-alkaline phosphatase antibodies. For microscopy, all sections were embedded in Entellan (Merck) [24].

Construction of the recombinant expression vectors for wild-type Roman snail MT isoforms

The *H. pomatia* coding regions for both MT isoforms were amplified by PCR using the respective cDNAs synthesized during a previous investigation as a template [24]. In order to facilitate their in frame cloning into the pGEX-4T1 expression vector (Amersham GE Healthcare Bio-Sciences AB, Uppsala, Sweden), *Bam*HI and *Sal*I restriction sites were generated just before the anti-thymocyte globulin (ATG) and after the stop codon. The oligonucleotides used for these PCR amplifications were: 5' ACAGGATCCGGACGAGGAAAGAACTGC 3' and 5' ATTGGATCCGGGAAAG GAAAAGGAGAAA AGTG 3' as HpCuMT and HpCdMT upstream primers, and 5' AGGCGTCGACTTGTCGTTTATTTGCAG 3' and 5' ATGCGTCGACTTGTCCTGC GGTTACT 3' as the HpCuMT and HpCdMT downstream primers. 35-cycle PCR reactions were performed under the following conditions: 94°C 30 s, 55°C 30 s and 72°C 30 s, using Deep Vent (New England Biolabs, Massachusetts, USA) thermostable DNA polymerase. PCR products were isolated from 2% agarose gels, digested with *Bam*HI-*Sal*I restriction enzymes (New England Biolabs) and cloned into the corresponding sites of pGEX-4T-1, for glutathione-S-transferase (GST)-MT fusion protein synthesis. The product resulting after purification was used in the second PCR as reverse megaprimer together with the forward primer mentioned earlier. In the final amplification product, the desired mutation had been introduced and the flanking restriction sites (*Bam*HI and *Sal*I) allowed the cloning in frame in pGEX-4T-1. Prior to the protein synthesis assays, all the DNA constructs were confirmed by automatic DNA sequencing (ABI 370, Perkin Elmer Life Sciences), using BigDye Terminator (Applied Biosystems). DH5α was the *E. coli* host strain used for cloning and sequencing purposes and, thereafter, the expression plasmids were transformed into the *E. coli* protease-deficient strain BL21 for recombinant protein overexpression.

Recombinant synthesis and purification of the metal-HpMT complexes

All HpMT metal complexes analysed in this work were biosynthesized in 2-L Erlenmeyer cultures of the corresponding transformed *E. coli* cells grown in LB medium with 100 mg mL^{-1} ampicillin and the following metal supplements: 300 μM $ZnCl_2$ or $CdCl_2$ for the zinc- or cadmium-rich media, or 500 μM $CuSO_4$ for the copper-rich medium. Copper cultures were performed under two aeration conditions (high and low aeration) as previously described [32]. GST-MT synthesis was induced with isopropyl-1-thio-β-D-galactopyranoside at a final concentration of 100 mM 30 min before the addition of the metal solution. After a 2.5 h-induction, cells were harvested by centrifugation. In order to prevent oxidation of the metal-HpMT complexes, argon was bubbled in all the steps of the purification following cell disruption.

For protein purification, cells were re-suspended in ice-cold PBS (1.4 M NaCl, 27 mM KCl, 101 mM Na_2HPO_4, 18 mM KH_2PO_4)-0.5% v/v β-mercaptoethanol, disrupted by sonication and centrifuged at 12,000 *g* for 30 min. The recovered supernatant was used to purify the GST-HpMT polypeptides by batch affinity chromatography with glutathione sepharose 4B (GE Healthcare, Buckinghamshire, UK) incubating the mixture with gentle agitation for 60 min at room temperature. After three washes in PBS and, since the GST-HpMT fusions include a

thrombin recognition site, this protease was added (10 μ per mg of fusion protein) and digestion was carried out overnight at 23°-25°C. This allowed separation of the GST fragment of the fusion proteins, which remained bound to the gel matrix from the metal-HpMT portions that were eluted together with thrombin. Therefore, the eluate was concentrated using Centriprep Concentrators (Amicon; Millipore, MA, USA) with a cut-off of 3 kDa and subsequently fractionated using fast protein liquid chromatography (FPLC), through a Superdex-75 column (GE Healthcare) equilibrated with 50 mM Tris-HCl, pH 7.0, and run at 1 mL min^{-1}. Fractions were collected and analysed for protein content by their absorbance at 254 nm. Aliquots of the protein-containing FPLC fractions were analysed by 15% SDS-PAGE and stained by Coomassie Blue. HpMT-containing samples were pooled and stored at -70°C until further use. Due to the specific recombinant expression conditions, the three synthesized snail MT isoforms contained one additional amino acid residue (G) at their N-termini in relation to the native isoforms previously isolated [20]. These modifications do not interfere with the metal-binding capacity, as previously shown for both vertebrate [61] and invertebrate [8] MT isoforms.

Analysis of recombinantly expressed and *in vitro* prepared metal-HpMT complexes

The recombinantly expressed metal-MT complexes were analysed for element composition (S, Zn, Cd and Cu) by inductively coupled plasma atomic emission spectroscopy (ICP-AES) on a Polyscan 61E spectrometer (Thermo Jarrell Ash Corporation, MA, USA) at appropriate wavelengths (S, 182.040 nm; Zn, 213.856 nm; Cd, 228.802 nm; Cu, 324.803 nm), either under 'conventional' (dilution with 2% HNO_3 (v/v)) or under 'acidic' (incubation in 1 M HCl at 65°C for 5 min) conditions [62]. MT concentration in the recombinant preparations was calculated from the acidic ICP sulphur measurements, thus assuming the only contribution to their S content was that made by the HpCuMT and HpCdMT peptides. Protein concentrations were confirmed by standard amino acid analysis performed on an Alpha Plus Amino acid Autoanalyzer (Pharmacia LKB Biotechnology, Uppsala, Sweden) after sample hydrolysis in 6 M HCl (22 h at 110°C). Ser, Lys and Gly contents were used to extrapolate sample concentrations.

CD spectroscopy was performed using a model J-715 spectropolarimeter (JASCO, Gross-Umstadt, Germany) equipped with a computer (J-700 software, JASCO). Measurements were carried out at a constant temperature of 25°C maintained by a Peltier PTC-351 S apparatus (TE Technology Inc, MI, USA). Electronic absorption was measured on an HP-8453 diode-array ultra violet (UV)-vis spectrophotometer (GMI Inc, MN, USA), using 1-cm capped quartz cuvettes, and correcting for the dilution effects by means of the GRAMS 32 software (Thermo Fisher Scientific Inc, MA, USA).

Molecular mass determination was performed by electrospray ionization mass spectrometry equipped with a time-of-flight analyser (ESI-TOF MS) using a Micro Tof-Q Instrument (Brucker Daltonics GmbH, Bremen, Germany) calibrated with NaI (200 ppm NaI in a 1:1 H_2O: isopropanol mixture), interfaced with a Series 1100 HPLC pump (Agilent Technologies, CA, USA) equipped with an autosampler, both controlled by the Compass Software. The experimental conditions for analysing proteins with divalent metals (Zn, Cd) were: 20 μL of the sample were injected through a PEEK long tube (1.5 m × 0.18 mm i.d.) at 40 μL/min under the following conditions: capillary-counterelectrode voltage, 5.0 kV; desolvation temperature, 90-110°C; dry gas 6 L/min. Spectra were collected throughout an m/z range from 800 to 2000. The proteins that contain copper were analysed injecting 20 μL of the sample at 30 μL/min; capillary-counterelectrode voltage, 4.0 kV; desolvation temperature, 80°C; m/z range from 800 to 2000. The liquid carrier was a 90:10 mixture of 15 mM ammonium acetate and acetonitrile, pH 7.0. For the analysis at acidic pH the conditions used were the same as those used in the analysis of the case for divalent metals, except in the composition of the carrier liquid which, in this case, was a 95:5 mixture of formic acid and acetonitrile at pH 2.4. All samples were injected at least in duplicate to ensure reproducibility. In all cases, molecular masses were calculated according to the reported method [63].

Metal replacement titrations were performed by adding the corresponding metal ions (Cd^{2+} or Cu^{+}) at equivalent molar ratios to the recombinant Zn-HpMT complexes. Titrations were carried out following previously described procedures [64,65]. The resulting *in vitro* complexes were analysed by UV-Vis and CD spectroscopy as well as mass spectrometry. All assays were carried out in an Ar atmosphere and the pH for all experiments remained constant throughout, without the addition of any extra buffers.

Metal tolerance complementation assays in transformed yeast MT-knockout cells

The *Saccharomyces cerevisiae* DTY4 strain (*MATα, leu2-3, 112his3$^{\Delta}$1, trp1-1, ura3-50, gal1, cup1::URA3*) was used for metal tolerance complementation assays. This strain is characterized by a total MT deficiency due to *cup1* disruption and *Crs5* truncation [66].

The cDNAs coding for the different MTs assayed - the two snail MT isoforms (snail HpCdMT and snail HpCuMT), the two yeast MTs (Cup1 and Crs5) and the mouse MT1 - were ligated into the *Bam*HI/*Pst*I sites of the yeast vector p424, which contains TRP1 for selection,

the constitutive GPD (glyceraldehyde-3-phosphate dehydrogenase) promoter for heterologous gene expression, and the CYC1 (cytochrome-c-oxidase) transcriptional terminator [67]. The recombinant p424 vectors were introduced into the DTY4 cells using the lithium acetate procedure [68]. Transformed cells were selected according to their capacity to grow in synthetic complete medium (SC) without Trp and Ura.

For metal tolerance tests, transformed yeast cells were initially grown in selective SC-Trp-Ura medium at 30°C and 220 rpm until saturation. These cells were then diluted to OD_{600} 0.01 and used to re-inoculate tubes with 3 mL of fresh medium supplemented with $CuSO_4$ added at 15, 30, 45, 60, 75, 90 and 105 μM final concentrations or $CdCl_2$ at 1, 2, 4, 6 and 8 μM final concentrations. These cultures were allowed to grow for 18 h and the final OD_{600} was recorded and plotted as a percentage of the OD_{600} reached by the culture grown without metal supplement. For each concentration, and each kind of transformation, two replicas were run.

MT sequence alignment and phylogenetic analyses

MT amino acid sequences used for pulmonate MT alignments were derived mostly from amino acid sequence files or translated cDNA open reading frame sequences published in GenBank (http://www.ncbi.nlm.nih.gov/Tools/; see accession numbers in the legend to Figure 9). The editing and alignment were done manually in combination with ClustalX software Version 2.0.9 [69]. For phylogenetic analyses, nucleotide sequences of the coding region of mollusc MT cDNAs or MT genes as well as protein primary sequences were used as published in GenBank (for accession numbers see legend of Figure 9). Phylogenetic reconstructions we performed with neighbour-joining [70] using the computer program PAUP* (version 4). The robustness of the phylogenetic hypothesis was tested by bootstrapping (1000 replicates) [71].

Abbreviations

ATG: anti-thymocyte globulin; CD: circular dichroism; cDNA: complimentary DNA; ESI: electrospray ionization; FPLC: fast protein liquid chromatography; GPD: glyceraldehyde-3-phosphate dehydrogenase; GST: glutathione-S-transferase; Hp: *Helix pomatia*; ICP-AES: inductively coupled plasma atomic emission spectroscopy; ISH: *in situ* hybridization; GPD: glyceraldehyde-3-phosphate dehydrogenase; mRNA: messenger RNA; MS: mass spectrometry; MT: metallothionein; PBS: phosphate buffered saline; RT-PCR: real time polymerase chain reaction; SC: synthetic complete medium.

Acknowledgements

This work was supported by the Spanish Ministerio de Ciencia y Tecnología grants BIO2009-12513-C02-01 to SA, BIO2009-12513-C02-02 to MC and project No. P19782-B02 from the Austrian Science Foundation to RD. Collaboration between the Spanish and Austrian research groups was financed by the 'Acciones Integradas' grants HU2006-0027 (Spain) and ES 02/2007 (Austria). SPR received a pre-doctoral fellowship from the Department de Química, Universitat Autònoma de Barcelona. Authors from the University of Innsbruck are members of the 'Centre of Molecular Biosciences Innsbruck'. The authors from the Universitat Autònoma de Barcelona (UAB) and Universitat de Barcelona (UB) are members of a 'Grups de Recerca de la Generalitat de Catalunya' (2009SGR-1457). We thank the Serveis Cientificotècnics of UB (GC-FPD, ICP-AES, DNA sequencing) and the Servei d'Anàlisi Química of UAB (CD, UV-vis, ESI-MS) for allocating instrument time to us.

Author details

[1]Departamento Química, Faculty Ciències, Universitat Autònoma de Barcelona, E-08193 Cerdanyola del Vallès, Barcelona, Spain. [2]Departamento Genètica, Faculty Biologia, Universitat de Barcelona, Avenida Diagonal 645, E-08028 Barcelona, Spain. [3]Institute of Zoology and Center of Molecular Biosciences Innsbruck (CMBI), University of Innsbruck, Technikerstraße 25, A-6020 Innsbruck, Austria. [4]Division of Genetic Epidemiology, Department of Medical Genetics, Molecular and Clinical Pharmacology, Innsbruck Medical University, Austria.

Authors' contributions

ÒP, AP, and SPR carried out the recombinant expression studies, participating in the construction of the expression vectors, the synthesis and characterization of the corresponding metal complexes, and also performed the yeast complementation experiments. ME and MH performed quantitative Real-Time PCR experiments and in situ hybridization, and carried out most of the sequencing work of MT cDNAs from different pulmonate snail species. AB calculated and established the phylogenetic trees. MC and SA designed the study together with RD, supervised recombinant DNA and recombinant protein experiments, yeast complementation studies, as well as analytical, spectrometric and spectrophotometric work, and contributed to the drafting of the manuscript. RD supervised and participated in molecular sequencing and Real-Time PCR as well as in situ hybridization, and performed chromatography and Reversed-Phase HPLC. He was responsible for the protein alignments and assisted in calculation of phylogenetic trees. He designed the study together with MC and SA, and drafted the manuscript. All authors read and approved the final manuscript.

Received: 3 December 2010 Accepted: 21 January 2011
Published: 21 January 2011

References

1. Sigel A, Sigel H, Sigel RKO: *Metal ions in Life Sciences; v 5: Metallothioneins and Related Chelators* Cambridge: Royal Society of Chemistry; 2009, 1-514.
2. Blindauer CA, Leszczyszyn OI: **Metallothioneins: unparalleled diversity in structures and functions for metal ion homeostasis and more.** *Nat Prod Rep* 2010, **27**:720-741.
3. Klaassen CD, Liu J, Choudhuri S: **Metallothionein: An intracellular protein to protect against cadmium toxicity.** *Ann Rev Pharmacol Toxicol* 1999, **39**:267-294.
4. Egli D, Yepiskoposyan H, Selvaraj A, Balamurugan K, Rajaram R, Simons A, Multhaup G, Mettler S, Vardanyan A, Georgiev O, Schaffner W: **A family knockout of all four *Drosophila* metallothioneins reveals a central role in copper homeostasis and detoxification.** *Mol Cell Biol* 2006, **26**:2286-2296.
5. Palmiter RD: **The elusive function of metallothioneins.** *Proc Natl Acad Sci USA* 1998, **95**:8428-8430.
6. Davis SR, Cousins RJ: **Metallothionein expression in animals: a physiological perspective on function.** *J Nutr* 2000, **130**:1085-1088.
7. Chen P, Muñoz A, Nettesheim D, Shaw CF-III, Petering DH: **Stoichiometry and cluster specificity of copper binding to metallothionein: homogeneous metal clusters.** *Biochem J* 1996, **317**:395-402.
8. Egli D, Domenech J, Selvaraj A, Balamurugan K, Hua H, Capdevila M, Georgiev O, Schaffner W, Atrian S: **The four members of the *Drosophila* metallothionein family exhibit distinct yet overlapping roles in heavy metal homeostasis and detoxification.** *Genes to Cells* 2006, **11**:647-658.
9. Stillman MJ, Zelazowski AJ: **Domain specificity of Cd^{2+} and Zn^{2+} binding to rabbit liver metallothionein2.** *Biochem J* 1989, **262**:181-188.
10. Li H, Otvos JD: **^{111}Cd NMR studies of the domain specificity of Ag^{+} and Cu^{+} binding to metallothionein.** *Biochemistry* 1996, **35**:13929-13936.
11. Tio L, Villarreal L, Atrian S, Capdevila M: **Functional differentiation in the mammalian metallothionein gene family. Metal binding features of Mouse MT4 and comparison with its paralog MT1.** *J Biol Chem* 2004, **279**:24403-24413.

12. Kägi JHR, Kojima Y: **Chemistry and biochemistry of metallothionein.** In *Metallothionein II*. Edited by: Kägi JHR,Kojima Y. Basel: Birkhäuser Verlag; 1987:25-61, Exp Suppl 52..
13. Vasák M: **Standard isolation procedure for metallothionein.** *Meth Enzymol* 1991, **205**:41-44.
14. Lerch K, Johnsen GF, Grushoff PS, Sternlieb I: **Canine hepatic lysosomal copper protein: identification as metallothionein.** *Arch Biochem Biophys* 1985, **243**:108-114.
15. Overnell J: **Occurrence of cadmium in crabs (*Cancer pagurus*) and the isolation and properties of cadmium metallothionein.** *Environ Hlth Perspect* 1986, **65**:101-105.
16. Waldron KJ, Robinson NJ: **How do bacterial cells ensure that metalloproteins get the correct metal?** *Nature Rev Microb* 2010, **6**:25-35.
17. Ponder W, Lindberg DR: *Phylogeny and Evolution of the Mollusca* CA: University of California Press; 2008, 1-488.
18. Dallinger R, Berger B, Hunziker PE, Birchler N, Hauer C, Kägi JHR: **Purification and primary structure of snail metallothionein. Similarity of the N-terminal sequence with histones H4 and H2A.** *Eur J Biochem* 1993, **216**:739-746.
19. Berger B, Dallinger R, Gehrig P, Hunziker PE: **Primary structures of a copper-binding metallothionein from mantle tissue of the terrestrial gastropod *Helix pomatia*.** *L Biochem J* 1997, **328**:219-224.
20. Dallinger R, Berger B, Hunziker PE, Kägi JHR: **Metallothionein in snail Cd and Cu metabolism.** *Nature* 1997, **388**:237-238.
21. Hispard F, Schuler D, deVaufleury A, Scheifler R, Badot PM, Dallinger R: **Metal distribution and metallothionein induction after cadmium exposure in the terrestrial snail *Helix aspersa* (gastropoda, pulmonata).** *Environ Toxicol Chem* **27**:1533-1542, 208.
22. Dallinger R, Wang Y, Berger B, Mackay EA, Kägi JHR: **Spectroscopic characterization of metallothionein from the terrestrial snail, *Helix pomatia*.** *Eur J Biochem* 2001, **268**:4126-4133.
23. Gehrig PM, You C, Dallinger R, Gruber C, Brouwer M, Kägi JHR, Hunziker PE: **Electrospray ionization mass spectrometry of Zn, Cd and Cu metallothioneins: evidence for metal-binding cooperativity.** *Prot Sci* 2000, **9**:395-402.
24. Chabicovsky M, Niederstaetter H, Thaler R, Hödl E, Parson W, Rossmanith W, Dallinger R: **Localization and quantification of Cd- and Cu-specific metallothionein isoform mRNA in cells and organs of the terrestrial gastropod *Helix pomatia*.** *Toxicol Appl Pharmacol* 2003, **190**:25-36.
25. Chabicovsky M, Klepal W, Dallinger R: **Mechanisms of cadmium toxicity in terrestrial pulmonates: programmed cell death and metallothionein overload.** *Environ Toxicol Chem* 2004, **23**:648-655.
26. Manzl C, Krumschnabel G, Schwarzbaum PJ, Dallinger R: **Acute toxicity of cadmium and copper in hepatopancreas cells from the Roman snail (*Helix pomatia*).** *Comp Biochem Physiol C* 2004, **138**:45-52.
27. Dallinger R, Chabicovsky M, Hödl E, Prem C, Hunziker P, Manzl C: **Copper in *Helix pomatia* (Gastropoda) is regulated by one single cell type: differently responsive metal pools in rhogocytes.** *Am J Physiol* **189**: R1185-R1195, 205.
28. Vasák M, Kägi JHR, Hill HAO: **Zinc(II), cadmium(II) and mercury(II) thiolate transitions in metallothionein.** *Biochemistry* 1981, **20**:2852-2856.
29. Willner H, Vasák M, Kägi JHR: **Cadmium-thiolate clusters in metallothionein: spectrometric and spectropolarimetric features.** *Biochemistry* 1987, **26**:6287-6292.
30. Willner H, Bernhard WR, Kägi JHR: **Optical properties of metallothioneins. Origin of the optical properties of mammalian metallothioneins.** In *Metallothioneins, Synthesis, Structure and Properties of Metallothioneins, Phytochelatins and Metal-Thiolate Complexes*. Edited by: Stillman MJ, Shaw CF, Suzuki KT. New York: VCH Publishers; 1992:128-143.
31. Presta A, Rae Green A, Zelazowski A, Stillman MJ: **Copper binding to rabbit liver metallothionein: formation of a continuum of Copper(I)-thiolate stoichiometric species.** *Eur J Biochem* 1885, **227**:226-240.
32. Pagani A, Villarreal L, Capdevila M, Atrian S: **The *Saccharomyces cerevisiae* Crs5 metallothionein metal-binding abilities and its role in the response to zinc overload.** *Mol Microbiol* 2007, **63**:256-269.
33. Capdevila M, Domènech J, Pagani A, Tío L, Villarreal L, Atrian S: **Zn- and Cd-metallothionein recombinant species from the most diverse phyla may contain sulfide (S^{2-}) ligands.** *Angew Chem Int Ed Engl* 2005, **44**:4618-4622.
34. Bofill R, Capdevila M, Atrian S: **Independent metal-binding features of recombinant metallothioneins convergently draw a step gradation between Zn- and Cu-thioneins.** *Metallomics* 2009, **1**:229-234.
35. Orihuela R, Monteiro F, Pagani A, Capdevila M, Atrian S: **Evidence of native metal-(S^{2-})-MT complexes confirmed by the analysis of Cup1 divalent metal ion binding properties.** *Chem A Eur J* **16**:12363-12372, 210.
36. Egg M, Höckner M, Brandstätter A, Schuler D, Dallinger R: **Structural and bioinformatic analysis of the Roman snail Cd-Metallothionein gene uncovers molecular adaptation towards plasticity in coping with multifarious environmental stress.** *Mol Ecol* 2009, **18**:2426-2443.
37. Nielson KB, Atkin CL, Winge DR: **Distinc Metal-binding Configurations in Metallothioneins.** *J Biol Chem* 1985, **260**:5342-5350.
38. Stillman MJ, Rae Green A, Gui Z, Fowle D, Presta PA: **Circular dichroism, emission, and exafs studies of Ag(I), Cd(II), Cu(I), and Hg(II) binding to metallothioneins and modelling the metal binding site.** In *Metallothionein*. Edited by: Klaassen C. Basel: Birkhäuser Verlag; 1999:23-35, Vol IV.
39. Otvos JD, Engeseth HR, Nettesheim DG, Hilt CR: **Interprotein metal exchange reactions of metallothionein.** *Experientia Suppl* 1987, **52**:171-178.
40. Maroni G, Wise J, Young JE, Otto E: **Metallothionein gene duplications and metal tolerance in natural populations of *Drosophila melanogaster*.** *Genetics* 1987, **117**:739-744.
41. Tanguy A, Moraga D: **Cloning and characterization of a gene coding for a novel metallothionein in the Pacific Oyster *Crassostrea gigas* (CgMT2): a case of adaptive response to metal-induced stress?** *Gene* 2001, **273**:123-130.
42. Kondrashov FA, Kondrashov AS: **Role of selection in fixation of gene duplications.** *J Theoret Biol* 2006, **239**:141-151.
43. Haszprunar G: **The molluscan rhogocyte (pore-cell, Blasenzelle, cellule nucale), and its significance for ideas on nephridial evolution.** *J Mollus Stud* 1996, **62**:185-211.
44. Albrecht U, Keller H, Gebauer W, Markl J: **Rhogocytes (pore cells) as the site of hemocyanin biosynthesis in the marine gastropod *Haliotis tuberculata*.** *Cell Tissue Res* 2001, **304**:455-462.
45. Brouwer M, Whaling P, Engel DW: **Copper-Metallothioneins in the American Lobster, *Homarus americanus*: Potential role as Cu(I) donors to apohemocyanin.** *Environ Hlth Persp* 1986, **65**:93-100.
46. Narula SS, Brouwer M, Hua Y, Armitage IM: **Three-dimensional solution structure of *Callinectes sapidus* metallothionein-1 determined by homonuclear and heteronuclear magnetic resonance spectroscopy.** *Biochemistry* 1995, **34**:620-631.
47. Engel DW, Brouwer M: **Metal regulation and molting in the blue crab, *Callinectes sapidus*: Metallothionein function in metal metabolism.** *Biol Bull* 1987, **173**:239-251.
48. Engel DW, Brouwer M: **Short-term metallothionein and copper changes in blue crabs at ecdysis.** *Biol Bull* 1991, **180**:447-452.
49. Butt TR, Sternberg EJ, Gorman JA, Clark P, Hamer D, Rosenberg M, Crooke ST: **Copper Metallothionein of yeast, structure of the gene, and regulation of expression.** *Proc Natl Acad Sci USA* 1984, **81**:3332-3336.
50. Münger K, Lerch K: **Copper Metallothionein from the fungus *Agaricus bisporus*: chemical and spectroscopic properties.** *Biochemistry* 1985, **24**:6751-6756.
51. Beltramini M, Lerch K: **Primary structure and spectroscopic studies of *Neurospora* copper Metallothionein.** *Environ Hlth Persp* 1986, **65**:21-27.
52. Lerch K: **Copper metallothionein, a copper-binding protein from *Neurospora crassa*.** *Nature* 1980, **284**:368-370.
53. Dallinger R, Berger B, Bauer-Hilty A: **Purification of cadmium-binding proteins from related species of terrestrial helicidae (Gastropoda, Mollusca): a comparative study.** *Mol Cell Biochem* 1989, **85**:135-145.
54. Münger K, Lerch K, Tschierpe HJ: **Metal accumulation in *Agaricus bisporus*: Influence of Cd and Cu on growth and tyrosinase activity.** *Cell Mol Life Sci* 1982, **38**:1039-1041.
55. Brouwer M, Bonaventura C, Bonaventura J: **Metal ion interactions with *Limulus polyphemus* and *Callinectes sapidus* hemocyanins: stoichiometry and structural and functional consequences of calcium(II), cadmium(II), zinc(II), and mercury(II) binding.** *Biochemistry* 1983, **22**:4713-4723.
56. Bubacco L, Rocco GP, Salvato B, Beltramini M: **The binding of Cd(II) to the hemocyanin of the Mediterranean crab *Carcinus maenas*.** *Arch Biochem Biphys* 1993, **302**:78-84.

57. Ngo HTT, Gerstmann S, Frank H: **Subchronic effects of environment-like cadmium levels on the bivalve *Anodonta anatina* (Linnaeus 1758): III. Effects on carbonic anhydrase activity in relation to calcium metabolism.** *Toxicol Environ Chem* 2010, **92(10)**:1029-0486.
58. Vasak M, Kägi JHR: **Spectroscopic properties of metallothionein.** In *Metal Ions in Biological Systems*. Edited by: Sigel H. New York: Marcel Dekker; 1983:213-273, Vol 15.
59. Haq F, Mahoney M, Koropatnick J: **Signalling events for metallothionein induction.** *Mutat Res* 2003, **533**:211-226.
60. Dallinger R, Chabicovsky M, Berger B: **Isoform-specific quantification of metallothionein in the terrestrial gastropod *Helix pomatia* I. Molecular, biochemical, and methodical background.** *Environ Toxicol Chem* 2004, **23**:890-901.
61. Cols N, Romero-Isart N, Capdevila M, Oliva B, Gonzàlez-Duarte P, Gonzàlez-Duarte R, Atrian S: **Binding of excess cadmium(II) to Cd_7-metallothionein from recombinant mouse Zn_7-metallothionein 1. UV-VIS absorption and circular dichroism studies and theoretical location approach by surface accessibility analysis.** *J Inorg Biochem* 1997, **68**:157-166.
62. Bongers J, Walton CD, Richardson DE, Bell JU: **Micromolar protein concentrations and metalloprotein stoichiometries obtained by inductively coupled plasma. Atomic emission spectrometric determination of sulphur.** *Anal Chem* 1988, **60**:2683-2686.
63. Fabris D, Zaia J, Hathout Y, Fenselau C: **Retention of thiol protons in two classes of protein zinc ion coordination centers.** *J Am Chem Soc* 1996, **118**:12242-12243.
64. Capdevila M, Cols N, Romero-Isart N, González-Duarte R, Atrian S, González-Duarte P: **Recombinant synthesis of mouse Zn_3-α and Zn_4-α metallothionein 1 domains and characterization of their cadmium(II) binding capacity.** *Cell Mol Life Sci* 1997, **53**:681-688.
65. Bofill R, Palacios O, Capdevila M, Cols N, González-Duarte R, Atrian S, González-Duarte P: **A new insight into the Ag^+ and Cu^+ binding sites in the metallothionein β domain.** *J Inorg Biochem* 1999, **73**:57-64.
66. Longo VD, Gralla EB, Valentine JS: **Superoxide dismutase activity is essential for stationary phase survival in *Saccharomyces cerevisiae*.** *J Biol Chem* 1996, **271**:12275-12280.
67. Mumberg D, Müller R, Funk M: **Yeast vectors for the controlled expression of heterologous proteins in different genetic backgrounds.** *Gene* 1995, **156**:119-122.
68. Stearns T, Ma H, Botstein D: **Manipulating yeast genome using plasmid vectors.** *Methods Enzymol* 1990, **185**:280-297.
69. Larkin MA, Blackshields G, Brown NP, Chenna R, McGettigan PA, McWilliam H, Valentin F, Wallace IM, Wilm A, Lopez R, *et al*: **Clustal W and Clustal X version 2.0.** *Bioinformatics* 2007, **23**:2947-2948.
70. Saitou N, Nei M: **The neighbour-joining method: a new method for reconstructing phylogenetic trees.** *Mol Biol Evol* 1987, **4**:406-425.
71. Felsenstein J: **Confidence limits on phylogenies: an approach using the bootstrap.** *Evolution* 1985, **39**:783-791.

doi:10.1186/1741-7007-9-4
Cite this article as: Palacios *et al.*: Shaping mechanisms of metal specificity in a family of metazoan metallothioneins: evolutionary differentiation of mollusc metallothioneins. *BMC Biology* 2011 **9**:4.

II. ARTICLE 2:

The role of histidine in a copper-specific metallothionein

ZAAC, **(2013)**, 639, 1356-1360

DOI: 10.1002/zaac.201300053

The Role of Histidine in a Copper-Specific Metallothionein

Sílvia Pérez-Rafael,[a][‡] Ayelen Pagani,[b,c][‡] Òscar Palacios,[a] Reinhard Dallinger,[d] Mercè Capdevila,*[a] and Sílvia Atrian[b]

Keywords: Metallothioneins; Histidine; Cu-thionein; *Helix pomatia*; Copper

Abstract. Metallothioneins achieve metal binding specificity by modulation of their amino acid sequences through evolution. Non-coordinating residues seem to play a key role in this function, and among them histidine may be of particular importance. Here we report how this residue regulates Cu^{I} binding to a highly copper specific isoform, the CuMT of the snail *Helix pomatia*, by analysis of the recombinant complexes yielded by a constructed mutant where this residue has been changed to an alanine.

Introduction

Metallothioneins (MTs) constitute a universal family of cysteine-rich, low-molecular-weight proteins with a high metal-binding capacity. They have been related to multiple biological processes, among which homeostasis of essential metal ions (Zn^{II} and Cu^{I}), and protection against toxic metal ions (i.e. Cd^{II}, Pb^{II}) appear as most relevant.[1] Almost all kinds of organisms contain multiple MT isoforms, normally homologous proteins that exhibit either similar or highly different preferences for divalent vs. Monovalent metal ion binding.[2,3] To date, there is no information about the molecular basis that determines when an MT peptide will yield well-folded, stable complexes with a determined metal ion, although this is a keystone to understand MT structure/function relationships, their physiological function, and their differentiation pattern through evolution. The best-known paradigm of highly similar MT peptides with fully conserved coordinating Cys residues, but nevertheless exhibiting opposite metal preferences, is offered by the Roman snail (*Helix pomatia*) MT system.

This pulmonate mollusk synthesizes two MT isoforms, which show clear and distinct metal specificity: the Cd-specific isoform, HpCdMT, involved in Cd binding and detoxification within the digestive tissues of the snail,[4] and the Cu-isoform, HpCuMT, which is only expressed in the rhogocyte cell type, where it seems to play a role associated with hemocyanin synthesis.[5] In a previous work, we showed how the two *H. pomatia* MT isoforms achieved their metal binding specificity by amino acid sequence diversification.[6] Since the two HpMTs exhibit a full conservation of the coordinating Cys positions (Table 1), it remains clear that the intercalating residues must be those that determine their intrinsic and extremely distinct metal binding behavior towards divalent (Zn^{II} and Cd^{II}) or monovalent (Cu^{I}) metal ions. Therefore, it is crucial to ascertain the role of the non-Cys residues of MT in metal ion coordination, and among them we centered our attention on the His present at position 38 of the Cu-specific HpMT peptide. Histidine contribution to metal-MT coordination is currently well established,[3,7–9] after being first reported in the cyanobacterial SmtA[10] and the wheat E_c-1 proteins.[11]

However, both these cases, and others involving animal MTs (*C.elegans* MT1[12] and chicken MT[13]), implicate divalent metal ion coordination and MTs that have the character of Zn-thioneins.[3] No data are available regarding the possible role of His in Cu-thioneins. Significantly, neither spectrometric and spectroscopic studies,[14] nor the 3D structure determination[15] showed any influence of the His present in Cup1 in Cu-coordination. Thus, we consider especially relevant the current study. Here, the role of the unique His residue of the HpCuMT isoform (Table 1) has been tested through the analysis of the in vivo metal binding properties of a recombinantly synthesized HpCuMTAla mutant, and it has been compared with the corresponding HpCuMT wild type isoform. The results obtained suggest that the His residue in the HpCuMT peptide could be related with the facility to release Cu^{+} at certain physiological conditions in snail rhogocytes.

Results and Discussion

DNA sequencing of the HpCuMTAla coding construct confirmed the presence of the His/Ala codon substitution,

* Prof. Dr. M. Capdevila
E-Mail: merce.capdevila@uab.cat
[a] Departament de Química, Facultat de Ciències
Universitat Autònoma de Barcelona
08193 Cerdanyola del Vallès, Barcelona, Spain
[b] Departament de Genètica, Facultat de Biologia
Universitat de Barcelona
Avda. Diagonal 643
08028 Barcelona, Spain
[c] Current address: Centro de Estudios Fotosintéticos y Bioquímicos, CONICET
Suipacha 531
2000 Rosario, Argentina
[d] Institute of Zoology
University of Innsbruck
Technikerstraße 25
6020 Innsbruck, Austria
[‡] These two authors contributed equally to this work..
Supporting information for this article is available on the WWW under http://dx.doi.org/10.1002/zaac.201300053 or from the author.

Table 1. Sequence alignment of the (1) *H. pomatia* HpCdMT, (2) HpCuMT and (3) HpCuMTAla mutant (His38 → Ala). (*Note*: the initial GS residues are the consequence of the recombinant construct used for protein synthesis).

```
1)GSGKGKGEKCTSACRSEPCQCGSKCQCGEGCTCAACKTCNCTSDGCKCGKECTGPDSCKCGSSCSCK
2)GS..GRGKNCGGACNSNPCSCGNDCKCGAGCNCDRCSSCHCSNDDCKCGSQCTGSGSCKCGSACGCK
3)GS..GRGKNCGGACNSNPCSCGNDCKCGAGCNCDRCSSCACSNDDCKCGSQCTGSGSCKCGSACGCK
```

and SDS-PAGE gels of total protein extracts from pGEX*HpCuMTAla*-transformed BL-21 *E. coli* cells showed the presence of a band of the expected size for the recombinant protein. Homogeneous metal-HpCuMTAla preparations (final concentrations of 2.00×10^{-4} M, 1.69×10^{-4} M and 0.75(regular)/0.64(low) $\times 10^{-4}$ M for Zn-, Cd- and Cu complexes, respectively) were obtained from 5-L cultures. Acidification of the Zn-HpCuMTAla preparation yielded the corresponding apo-form, with a molecular mass of 6194.2 Da, in accordance with the calculated theoretical value (6195.6). This confirmed both the identity and the integrity of the recombinant HpCuMTAla polypeptide (Table 1).

First, the HpCuMTAla metal binding ability for the noncognate metal ions (i.e. Zn^{II} and Cd^{II}), was analyzed. Synthesis in Zn-enriched cultures gave rise to several Zn-containing species, with major Zn_6- and Zn_5-HpCuMTAla complexes, which suggested a low in vivo preference for Zn^{II} coordination (Figure 1A). The CD spectrum of these preparations was also indicative of a poor folding degree (Figure 1C). Since these results were practically coincident with those described for HpCuMT,[6] it was concluded that the His38 residue did not play a major role in Zn-coordination.

A similar situation was found for the Cd^{II} binding features. In this case, the synthesis of HpCuMTAla in Cd^{II}-rich media always rendered highly heterogeneous preparations, including both sulfide-devoid and sulfide-containing complexes. The major species recovered were, Cd_7-, Cd_8- and Cd_9S-HpCuMTAla, which is again coincident with those rendered by HpCuMT (Figure 1B). The CD of this sample (Figure 1D) fully corroborated the presence of Cd_xS-HpCuMTAla species, with absorptions at ca. 250 nm corresponding to the Cd-SCys chromophores, and the signals at ca. 280 nm associated with the presence of sulfide ligands bound to Cd^{2+}.[16] Again, as the absence of His38 in the mutant form did not apparently alter the Cd^{II} coordination abilities of the HpCuMT isoform, it can be proposed that His does not play a significant role in the divalent metal ion binding to this copper-specific MT form.

On the other hand, the synthesis of HpCuMTAla in Cu-supplemented cultures, grown either at regular or low aeration conditions (determining regular and high cell copper content, respectively) revealed interesting differences between the mutated and wild-type isoforms. Under normal aeration, Cu-HpCuMTAla is synthesized as a major heterometallic M_{12}-, followed by M_{10}-HpCuMTAla complexes (M = Zn or Cu).

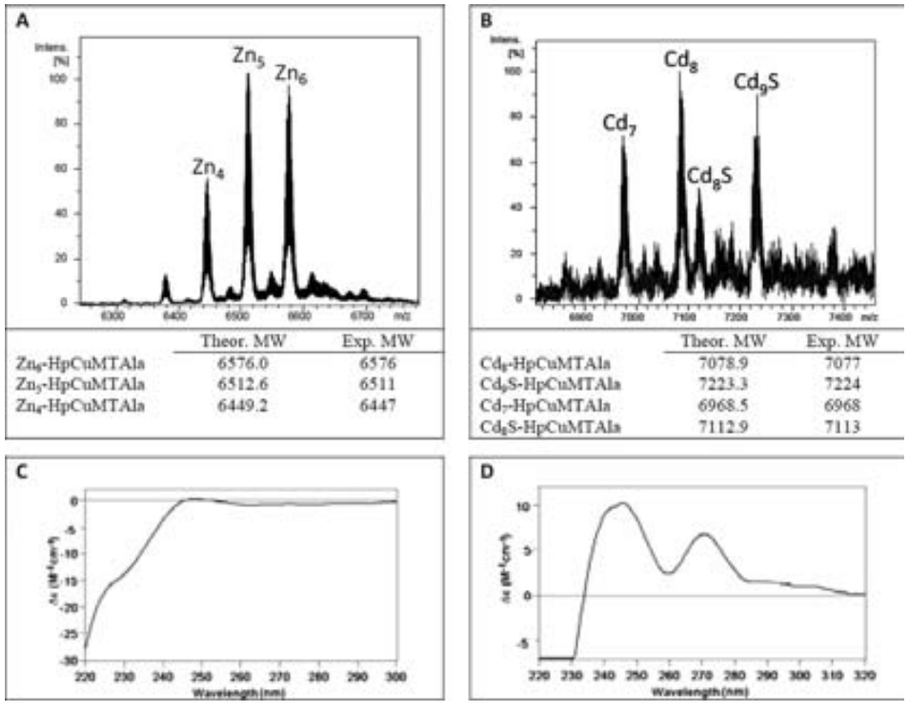

	Theor. MW	Exp. MW
Zn_6-HpCuMTAla	6576.0	6576
Zn_5-HpCuMTAla	6512.6	6511
Zn_4-HpCuMTAla	6449.2	6447

	Theor. MW	Exp. MW
Cd_8-HpCuMTAla	7078.9	7077
Cd_9S-HpCuMTAla	7223.3	7224
Cd_7-HpCuMTAla	6968.5	6968
Cd_8S-HpCuMTAla	7112.9	7113

Figure 1. Deconvoluted ESI-MS spectra, recorded at pH 7.0, of the recombinant preparations of HpCuMTAla in (A) Zn- and (B) Cd-enriched media. The error associated to the experimental MW values was always lower than 1%. CD spectra of the in vivo (C) Zn-HpCuMTAla and (D) Cd-HpCuMTAla preparations.

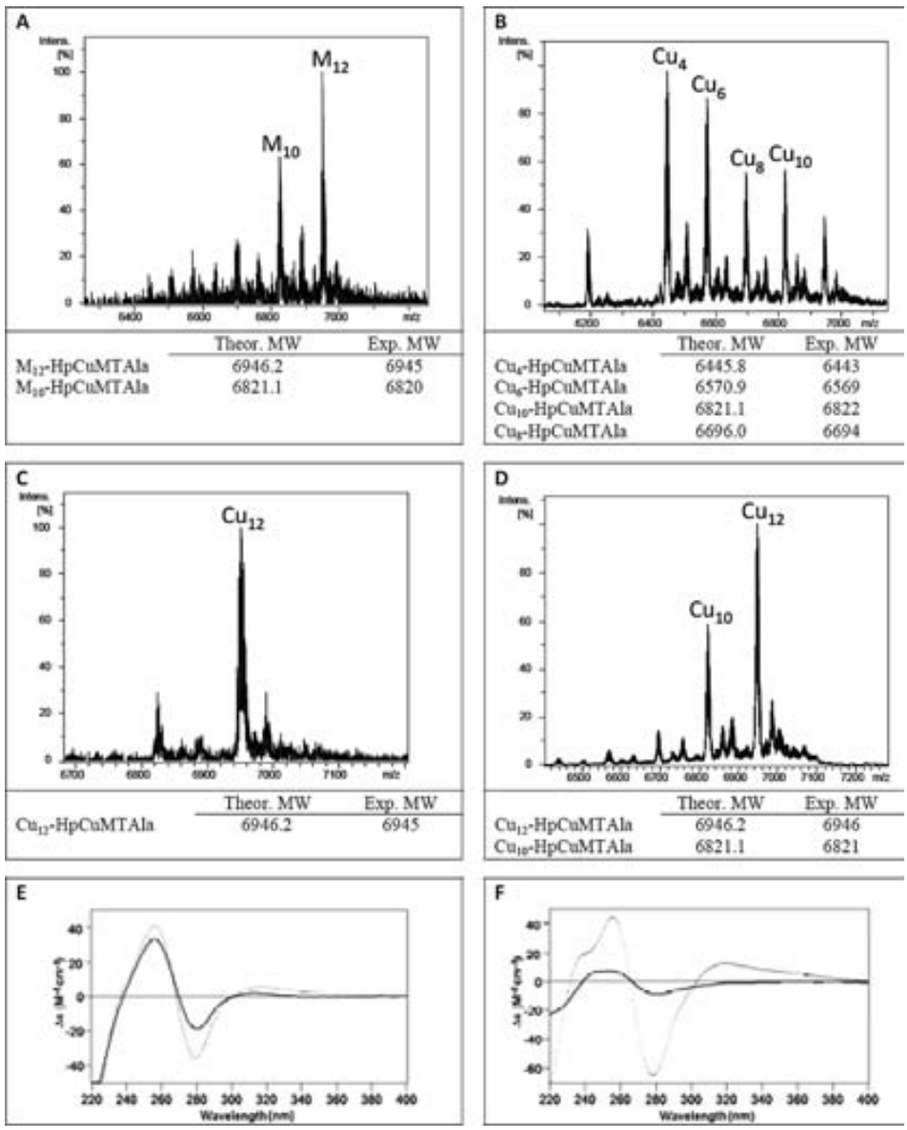

Figure 2. Deconvoluted ESI-MS spectra of the recombinant preparations of HpCuMTAla in Cu-enriched media under (A, B) regular or (C, D) low aeration conditions at (A, C) pH 7.0 and (B, D) pH 2.4. M stands for Zn+Cu, owing to the ESI-MS difficulties for discriminating between these two metal ions. The error associated with the experimental MW values was always lower than 1 %. CD spectra of the (E) Cu-HpCuMTAla and (F) Cu-HpCuMT preparations obtained at regular (solid) and low (doted) aeration conditions.

This is evidenced by the ESI-MS spectra of the corresponding preparations run at neutral and acidic pH (Figure 2A and Figure 2B, respectively) and the fact that ICP-AES measurements clearly indicated the presence of zinc in the sample (7Cu: 3Zn). The ESI-MS analysis at pH 2.4, which causes the loss of all Zn^{II} ions, but not regularly of Cu^{I}, revealed two peaks, corresponding to Cu_4- (major) and Cu_6-HpCuMTAla (minor) complexes. The most straightforward explanation for these results is that the M_{12}- and M_{10} complexes observed at neutral pH correspond to a mixture of hetero Cu_4Zn_x- and Cu_6Zn_y-HpCuMTAla species.

However, when the same MT peptide is synthesized under low aeration (i.e. high intracellular Cu), it folds into homonuclear, almost unique Cu_{12}-HpCuMTAla complexes, as revealed by the ESI-MS spectra (Figure 2C and Figure 2D) and the ICP-AES results that only report the presence of copper. The appearance of a second peak for Cu_{10}-HpCuMTAla in the acidic ESI-MS spectra is therefore probably explained if it is assumed that two of the Cu^{I} ions in the Cu_{12}- complex are bound too loosely to support the ionization conditions. CD spectra of the Cu preparations of the HpCuMT wild type and mutated forms (Figure 2E and Figure 2F) confirm the higher capacity of the Ala mutant to yield well folded complexes both at normal and high copper concentrations, while the wild type form only achieves this level of structuration when copper is high. It is worth remembering that under normal oxygenation of the cul-

tures, the wild-type HpCuMT produced a mixture of heterometallic M_{10}-, M_8-, M_6- and M_5- species, with a global equimolar Zn:Cu ratio, while under low aeration, it also rendered an almost unique Cu_{12}-HpCuMT species. Both Cu_{12}- species do seem to have the same stability at neutral pH. However that of the wild-type exhibited a higher instability than the mutant at the acidic ESI-MS conditions, yielding a Cu_{10}-HpCuMT peak (Figure S1, Supporting Information). Regardless of the reasons provoking these behaviors, it can be concluded that when coordinating Cu^I at normal conditions, HpCuMTAla folds into complexes with a higher Cu^I content than HpCuMT, and it forms more stable homonuclear Cu^I complexes where the Cu^I ions are more tightly bound.

Conclusions

All the results obtained suggest that, while the absence of His in HpCuMT has no effect on divalent metal ion coordination, it increases the Cu-binding abilities of this isoform. Thus, it is reasonable to postulate that the presence of His in HpCuMT could confer it with an optimal ability for copper binding as well as for copper release, a plasticity that would be essential for a putative role of HpCuMT in the transference of Cu^I to biomolecules that require it, as repeatedly hypothesized for haemocyanin synthesis in snail roghocytes.[5] Our data show that the metal binding properties of an MT peptide can be significantly changed by a mutation of one single amino acid, and support a role of His38 in the HpCuMT protein, probably enabling a controlled Cu^I release from the fully loaded Cu-HpCuMT complexes. There is no doubt that structural characterization of the Cu-HpCuMT complexes, which is under way, will significantly shed light on this singularity.

Experimental Section

Construction and Cloning of the cDNA Encoding the HpCuMTAla Site-directed Mutant

The site-directed His38Ala HpCuMT mutant (HpCuMTAla) was constructed by a two-step mutagenic PCR amplification using the wild-type HpCuMT cDNA as template.[6]

In the first step, the forward primer (5'TGCAGTTCTTGCGCTTGTTCCAAT 3') contained the mutated codon, and the reverse primer was the downstream primer (5'AGGCGTCGACTTGTCGTTTATTTGCAG 3') previously used for HpCuMT cloning.[6] PCR amplifications (x35) were performed following the cycle: 94 °C 30 s, 55 °C 30 s, and 72 °C 30 s, using Deep Vent (New England Biolabs) thermostable DNA polymerase. After purification, the resulting product was used as reverse megaprimer for the second PCR step, together with the forward primer previously used for HpCuMT amplification (5'ACAGGATCCGGACGAGGAAAGAACTGC 3'). In the final amplification product, the desired mutation had been introduced, and the flanking restriction sites (*Bam*HI and *Sal*I) allowed the in-frame cloning in the pGEX-4T-1 (Amersham GE Healthcare Bio-Sciences AB, Uppsala, Sweden) *E. coli* expression vector. All the DNA constructs were confirmed by automatic DNA sequencing (ABI 370, Perkin–Elmer Life Sciences), using BigDye Terminator (Applied Biosystems). DH5α was the *E. coli* host strain used for cloning and sequencing purposes, and thereafter, the expression plasmids were transformed into the *E. coli* protease-deficient strain BL21 for protein expression. To this end, *E. coli* LB cultures with 100 mg·mL^{-1} ampicillin were supplemented with: 300 μM $ZnCl_2$, $CdCl_2$, or 500 μM $CuSO_4$. Cu cultures were performed under two aeration conditions (regular and low) as described elsewhere.[17]

Purification and Analysis of the Metal-HpCuMTAla Complexes

All the metal-MT complex purifications were performed as reported in Ref. [6]. Metal-MT complexes were analyzed by ICP-AES, CD spectroscopy and ESI-TOF MS, as detailed in Ref. [8].

Supporting Information (see footnote on the first page of this article): Deconvoluted ESI-MS spectra of the recombinant preparations of HpCuMT in Cu-enriched media.

Acknowledgments

Work supported by the Spanish *Ministerio de Economía y Competitividad*, (grants BIO2012–39682-C02–01 and 02 respectively to SA and MC), and by the Austrian Science Foundation (grant P 23635-B20) to RD. Authors from Barcelona are members of the 2009SGR-1457 *Grup de Recerca de la Generalitat de Catalunya*. The Spanish and Austrian groups were also financed by *Acciones Integradas* grants HU2006–0027 (Spain) and ES 02/2007 (Austria). SPR received a pre-doctoral fellowship from the *Departament de Química, Universitat Autònoma de Barcelona*. We thank the *Centres Científics i Tecnològics (CCiT) de la Universitat de Barcelona* (ICP-AES, DNA sequencing) and the *Servei d'Anàlisi Química (SAQ) de la Universitat Autònoma de Barcelona* (CD, UV/Vis, ESI-MS) for allocating instrument time.

References

[1] M. Capdevila, R. Bofill, O. Palacios, S. Atrian, *Coord. Chem. Rev.* **2012**, *256*, 46–62.
[2] M. Capdevila, S. Atrian, *J. Biol. Inorg. Chem.* **2011**, *16*, 977–989.
[3] O. Palacios, S. Atrian, M. Capdevila, *J. Biol. Inorg. Chem.* **2011**, *16*, 991–1009.
[4] M. Chabicovsky, W. Klepal, R. Dallinger, *Environ. Toxicol. Chem.* **2004**, *23*, 648–655.
[5] R. Dallinger, M. Chabicovsky, E. Hödl, C. Prem, P. Hunziker, C. Manzl, *Am. J. Physiol.* **2005**, *189*, R1185–R1195.
[6] O. Palacios, A. Pagani, S. Pérez-Rafael, M. Egg, M. Höckner, A. Brandstätter, M. Capdevila, S. Atrian, R. Dallinger, *BMC Biology* **2011**, *9:4*.
[7] C. A. Blindauer, M. T. Razi, D. J. Campopiano, P. J. Sadler, *J. Biol. Inorg. Chem.* **2007**, *12*, 393–405.
[8] O. I. Leszczyszyn, R. Schmid, C. A. Blindauer, *Proteins* **2007**, *68*, 922–935.
[9] C. A. Blindauer, *J. Inorg. Biochem.* **2008**, *102*, 507–521.
[10] C. A. Blindauer, M. D. Harrison, J. A. Parkinson, A. K. Robinson, J. S. Cavet, N. J. Robinson, P. J. Sadler, *Proc. Natl. Acad. Sci. USA* **2001**, *98*, 9593–9598.
[11] E. A. Peroza, R. Schmucki, P. Guntert, E. Freisinger, O. Zerbe, *J. Mol. Biol.* **2009**, *387*, 207–218.
[12] R. Bofill, R. Orihuela, M. Romagosa, J. Domenech, S. Atrian, M. Capdevila, *FEBS J.* **2009**, *276*, 7040–7056.
[13] L. Villarreal, L. Tío, M. Capdevila, S. Atrian, *FEBS J.* **2006**, *273*, 523–535.
[14] R. Orihuela, F. Monteiro, A. Pagani, M. Capdevila, S. Atrian, *Chem. Eur. J.* **2010**, *16*, 12363–12372.

Special Issue

[15] V. Calderone, B. Dolderer, H. J. Hartmann, H. Echner, C. Luchinat, C. del Bianco, S. Mangani, U. Weset, *Proc. Natl. Acad. Sci. USA* **2005**, *102*, 51–56.
[16] M. Capdevila, J. Domenech, A. Pagani, L. Tio, L. Villarreal, S. Atrian, *Angew. Chem. Int. Ed.* **2005**, *44*, 4618–4622.
[17] A. Pagani, L. Villarreal, M. Capdevila, S. Atrian, *Mol. Microbiol.* **2007**, *63*, 256–269.

Received: January 30, 2013
Published Online: March 28, 2013

The role of histidine in a copper-specific metallothionein

Sílvia Pérez-Rafael, Ayelen Pagani, Òscar Palacios, Reinhard Dallinger, Mercè Capdevila, and Sílvia Atrian

SUPPLEMENTARY MATERIAL

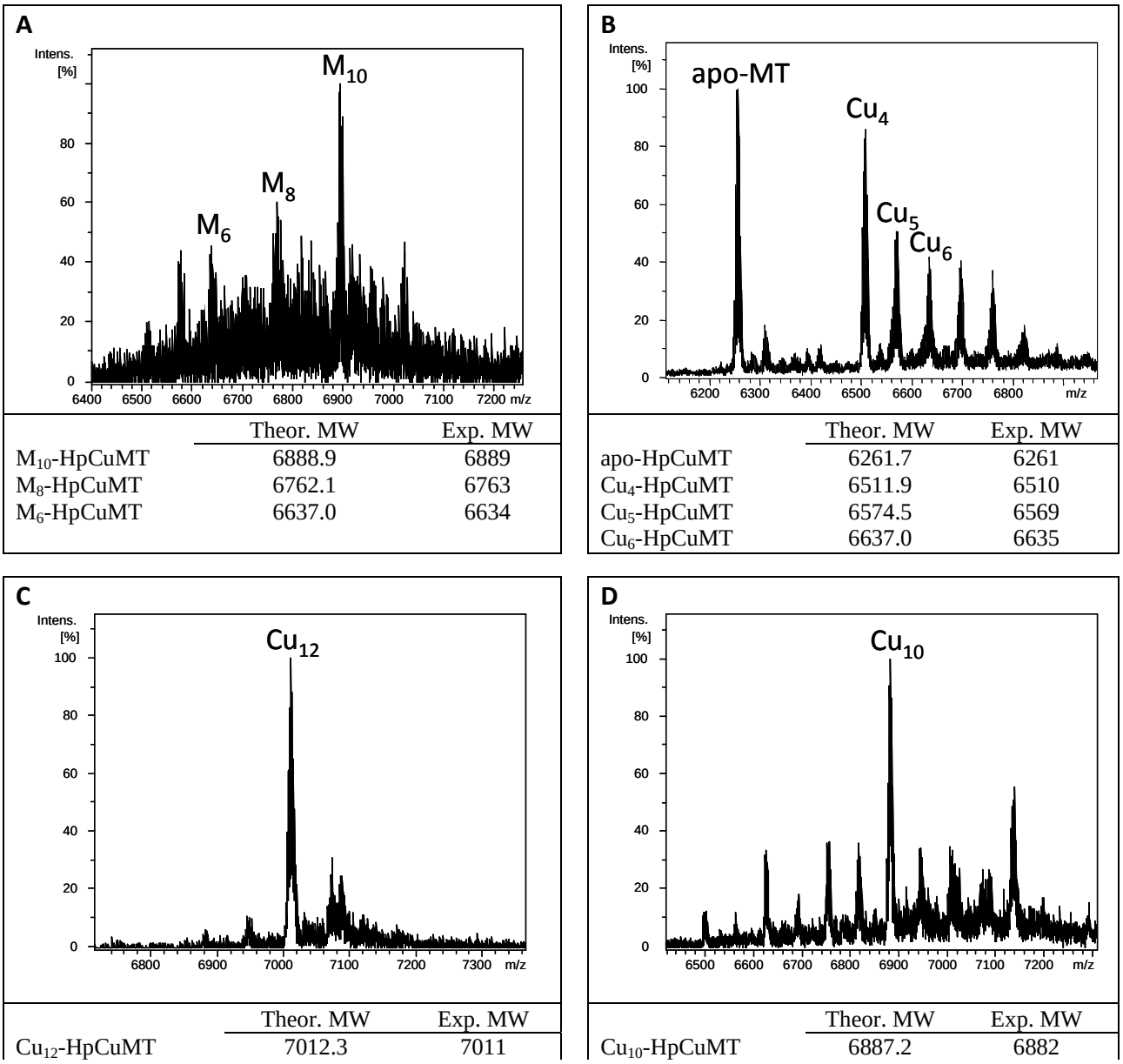

	Theor. MW	Exp. MW
M_{10}-HpCuMT	6888.9	6889
M_8-HpCuMT	6762.1	6763
M_6-HpCuMT	6637.0	6634

	Theor. MW	Exp. MW
apo-HpCuMT	6261.7	6261
Cu_4-HpCuMT	6511.9	6510
Cu_5-HpCuMT	6574.5	6569
Cu_6-HpCuMT	6637.0	6635

	Theor. MW	Exp. MW
Cu_{12}-HpCuMT	7012.3	7011

	Theor. MW	Exp. MW
Cu_{10}-HpCuMT	6887.2	6882

Figure S1. Deconvoluted ESI-MS spectra of the recombinant preparations of HpCuMT in Cu-enriched media under (A, B) regular or (C, D) low aeration conditions at (A, C) pH 7.0 and (B, D) pH 2.4. M stands for Zn+Cu, owing to the ESI-MS difficulties for discriminating between these two metal ions. The error associated with the experimental MW values was always lower than 1%.

III. ARTICLE 3:

Physiological relevance and contribution to metal balance of specific and non-specific metallothionein isoforms in the garden snail, *Cantareus aspersus*

Biometals, **(2011)**, 24, 1079-1092.

Biometals (2011) 24:1079–1092
DOI 10.1007/s10534-011-9466-x

Physiological relevance and contribution to metal balance of specific and non-specific Metallothionein isoforms in the garden snail, *Cantareus aspersus*

Martina Höckner · Karin Stefanon · Annette de Vaufleury · Freddy Monteiro · Sílvia Pérez-Rafael · Òscar Palacios · Mercè Capdevila · Sílvia Atrian · Reinhard Dallinger

Received: 11 February 2011 / Accepted: 17 May 2011 / Published online: 31 May 2011

Abstract Variable environmental availability of metal ions represents a constant challenge for most organisms, so that during evolution, they have optimised physiological and molecular mechanisms to cope with this particular requirement. Metallothioneins (MTs) are proteins that play a major role in metal homeostasis and as a reservoir. The MT gene/protein systems of terrestrial helicid snails are an invaluable model for the study of metal-binding features and MT isoform-specific functionality of these proteins. In the present study, we characterised three paralogous MT isogenes and their expressed products in the escargot (*Cantareus aspersus*). The metal-dependent transcriptional activation of the three isogenes was assessed using quantitative Real Time PCR. The metal-binding capacities of the three isoforms were studied by characterising the purified native complexes. All the data were analysed in relation to the trace element status of the animals after metal feeding. Two of the three *C. aspersus* MT (CaMT) isoforms appeared to be metal-specific, (CaCdMT and CaCuMT, for cadmium and copper respectively). A third isoform (CaCd/CuMT) was non-specific, since it was natively recovered as a mixed Cd/Cu complex. A specific role in Cd detoxification for CaCdMT was revealed, with a 80–90% contribution to the Cd balance in snails exposed to this metal. Conclusive data were also obtained for the CaCuMT isoform, which is involved in Cu homeostasis, sharing about 30–50% of the Cu balance of *C. aspersus*. No apparent metal-related physiological function was found for the third isoform (CaCd/CuMT), so its contribution to the metal balance of the escargot may be, if at all, of only marginal significance, but may enclose a major interest in evolutionary studies.

Keywords Cadmium · Copper · Zinc · Metallothionein · Mollusca · Pulmonata

Abbreviations

AAS	Atomic absorption spectrophotometry
CaMT	*C. aspersus* MT (global denomination)
CaCdMT	Cd-specific *C. aspersus* MT isoform
CaCuMT	Cu-specific *C. aspersus* MT isoform

M. Höckner · K. Stefanon · R. Dallinger (✉)
Institute of Zoology, University of Innsbruck, 6020 Innsbruck, Austria
e-mail: reinhard.dallinger@uibk.ac.at

A. de Vaufleury
Department of Chrono-Environment, University of Franche-Comté, 25030 Besançon Cedex, France

F. Monteiro · S. Atrian
Departament de Genètica, Facultat de Biologia, Universitat de Barcelona, 08028 Barcelona, Spain

S. Pérez-Rafael · Ò. Palacios · M. Capdevila
Departament de Química, Facultat de Ciències, Universitat Autònoma de Barcelona, 08193 Barcelona, Bellaterra, Spain

CaCd/CuMT	Mixed metal *C. aspersus* MT isoform
ESI-MS	Electrospray ionization mass spectrometry
ESI-TOF MS	Time-of-flight electrospray ionization mass spectrometry

Introduction

Fluctuating environmental availability of metallic trace elements represents a constant challenge for most organisms, which have to activate regulatory mechanisms to adjust and keep their internal trace element status within a physiologically tolerable range. This holds even more so because certain metal ions exert toxic effects at even very low concentrations, whereas other metals that are essential constituents of biomolecules cause adverse effects at high concentrations. Proteins playing an accommodating role in respect to these contrasting impacts are the so-called Metallothioneins (MTs). They belong to a ubiquitous, heterogeneous family of proteins with the ability to bind closed-shell metal ions via the sulphur atoms of their cysteine residues (Kägi and Kojima 1987; Sigel et al. 2009; Blindauer and Leszczyszyn 2010). In no animal group other than pulmonate molluscs, evolutionary differentiation brought about MT isoforms that possess such a strictly exclusive, sequence-based metal specificity (Palacios et al. 2011) being involved in contrasting metal-specific tasks such as cadmium detoxification, on the one hand, and homeostatic copper regulation, on the other (Dallinger et al. 1997). Hence, a number of pulmonate species has so far been shown to respond to environmental Cd exposure by synthesising an MT isoform loaded with high amounts of Cd (Dallinger et al. 1989). Its amino acid sequence has been elucidated for several species, including the Roman snail, *Helix pomatia* (Dallinger et al. 1993), the copse snail, *Arianta arbustorum* (Berger et al. 1995), and the escargot, *Cantareus aspersus* (Hispard et al. 2008). In accordance with its tissue-specific synthesis in digestive and excretory organs (Chabicovsky et al. 2003) and because of its protective effect against Cd, its function has been assigned to the detoxification of this metal ion (Manzl et al. 2004), and it was thus named CdMT. In contrast, a second MT type of isoforms, almost exclusively associated with Cu, have been characterised and named CuMTs (Dallinger et al. 1997). These are synthesised exclusively in the so-called rhogocytes, a specific molluscan cell type in which haemocyanin, the Cu-bearing respiratory pigment of snails, is synthesised (Chabicovsky et al. 2003). Consequently, a predominantly homeostatic function in connection with the supply of Cu for haemocyanin synthesis has been suggested (Dallinger et al. 2005). Recently, a third isoform was identified, first in *C. aspersus* (Hispard et al. 2008; Schuler et al. 2008) and then in other snail species (Palacios et al. 2011). This isoform exhibits no definite metal-specificity, since it was isolated from the midgut gland of Cd-exposed snails as a complex including both Cd and Cu, and was therefore named Cd/CuMT. Interestingly, the three MT protein sequences differ only in some of their non-Cys residues, signifying that these amino acids must be crucial in determining metal specificity of each isoform (Schuler et al. 2008; Palacios et al. 2011).

In the present work, we examine the role of the three MT isoforms in the accumulation and partitioning of metal ions (Cd^{2+}, Zn^{2+}, and Cu^{+}) in pulmonate tissues, using the edible snail, *C. aspersus* (the so-called escargot), as a study object. *C. aspersus* is one of the most common terrestrial pulmonate species, with an original distribution in Southern and Western Europe (Kerney and Cameron 1979) but nowadays widespread in many parts of the world owing to anthropochorous spreading (Guiller and Madec 2010). The significance of *C. aspersus* lies in its ecological impact for nutrient fluxes in the soil (Dallinger et al. 2001). Moreover, this species has been known as a pest organism in horticulture (Godan 1979) while at the same time being appreciated as the "edible snail" in gastronomy (Chevallier 1983). Therefore, a global acknowledgement of the biochemistry and physiology of metal uptake and regulation in this species is of general interest. This goal has been tackled here using different experimental approaches. Long-term metal exposure experiments yielded information about metal accumulation in the snail midgut gland and differential patterns of transcriptional induction for the three isogenes, depending on the metal surplus (Cd and Cu) applied. The three isoforms were purified and their metal load analysed quantitatively. In addition, their metal-binding abilities were assessed by mass spectrometric

analysis of the respective metal complexes obtained by recombinant synthesis in metal-supplemented *E. coli* cultures. Our data reveal that each of the three MT isoforms contributes specifically and differentially to the metal status in snail tissues, confirming the adaptational significance of the snail MT system for coping with different trace element availabilities under fluctuating (rapidly changing) environmental conditions.

Materials and methods

Animals and rearing conditions for control and metal exposure studies

Cantareus aspersus snails were from laboratory strains of the Department of Chrono-Environment of the University of Franche-Comté (Besançon, France). About 120 individuals were kept in plastic boxes on garden soil complemented with lime powder ($CaCO_3$) at 18°C and with a photoperiod of 12:12 h. Snails were fed every third day with commercially available lettuce (*Lactuca sativa*). For metal enrichment, lettuce leaves were soaked for 1 h in Titrisol standard dilutions of $CdCl_2$ or $CuCl_2$ (Merck, Darmstadt, Germany) made up to concentrations of 1 mg Cd^{2+} l^{-1} and 3 mg Cu^{2+} l^{-1}, respectively. Resulting concentrations of Cd and Cu in metal-enriched and untreated lettuce are summarised in Table 1. Another 35 individuals were fed on lettuce supplemented with Cd^{2+} or Cu^{2+}. Additionally, 40 animals fed on untreated lettuce were used as controls. On day 0, five individuals of the control group, and on days 1, 2, 3, 5, 8, 14, and 29, five snails of each group (control, Cd^{2+} and Cu^{2+}-exposed) were sampled for RNA isolation and tissue metal analyses. Finally, for MT protein purification, two groups of 30 animals each were kept in large plastic boxes and fed for 2 weeks either with uncontaminated (control diet) or Cd-enriched lettuce leaves prepared as described above. At the end of the feeding period, all snails were sacrificed by decapitation and processed for protein purification and characterisation.

RNA isolation and reverse transcription

After dissection, ~10 mg (fresh weight) of midgut gland tissue from each individual were removed for RNA isolation, whilst the remaining midgut gland and foot tissue were used to determine Cd and Cu concentrations as described below. Individual midgut gland aliquots were homogenised (Ultra Turrax T25, IKA, Staufen, Germany) in TRIzol® reagent and RNA was subsequently isolated according to a standard protocol (Sigma, Taufkirchen, Germany). The RiboGreen® RNA Quantitation Kit from Molecular Probes (Invitrogen, Karlsruhe, Germany) was used for quantification after DNase I (Fermentas, St. Leon-Rot, Germany) digestion. 450 ng of RNA per individual were subjected to cDNA synthesis (RevertAid™ H Minus M-MuLV Reverse Transcriptase, Fermentas) for subsequent isoform-specific PCR and quantitative Real Time PCR.

PCR amplification, cloning and sequencing of the cDNA of the MT isogenes

For amplification of *Cd-* and *CuMT* cDNAs, the following specific primers, designed after the *H. pomatia* orthologous sequences (Dallinger et al. 2004), were used:

CdMT-S: 5′-CTC CAT GGC AAC CAT GAG CGG AAA-3′
CdMT-AS: 5′-GCG TCG ACT TGT CCT GCG GTT ACT-3′

Table 1 Cd and Cu concentrations (means ± standard deviations; $n = 5$) in control, Cd, and Cu-enriched lettuce, measured by flame atomic absorption spectrophotometry and referred to dry weight

Metal treatment of feed	Metal concentration (μg/g)	
	Cd (μmol/g)	Cu (μmol/g)
Control lettuce	0.135 ± 0.169 (0.0012 ± 0.0015)	9.214 ± 1.970 (0.145 ± 0.031)
Cd-enriched	50.135 ± 12.253 (0.446 ± 0.109)	nd
Cu-enriched	nd	223.237 ± 46.516 (3.513 ± 0.732)

nd Not determined

CuMT-S: 5′-GTG ACC GAT GCA GTT CTT GCC ATT-3′
CuMT-AS: 5′-GCG TCG ACT TGT CGT TTA TTT GCA G-3′

PCR conditions were as follows: first denaturation at 94°C for 2 min, 39 cycles at 94°C for 20 s, 55°C for 10 s, 65°C for 40 s, and a final extension at 65°C for 10 min. Amplification of the *CdMT* cDNA from *C. aspersus* generated two PCR products of the same length, which, after cloning and sequencing, were distinguished as *CdMT* cDNA and *Cd/CuMT* cDNA. The SMART™ RACE cDNA Amplification Kit (Clontech Laboratories) was used for completion of both cDNA sequences. PCR products were cloned into pCR®4 vector (TOPO TA Cloning® Kit for Sequencing from Invitrogen) and sequenced using an AB 3130 genetic analyser (BigDye Terminator v3.1 Sequencing Kit, AB). Primer sequences for RACE PCR were as follows:

CdMT3-R-S: 5′-CAG GAG CGA GCC TTG CCA GTG TGG GAG-3′
CdMT5-R-AS: 5′-GCA AGT CTT GCA GGC GGC ACA TGT-3′
CuMT-3-R-S: 5′-TGT GAC CGA TGC AGT TCT TGC CAT TGT TCC-3′
CuMT-5-R-AS: 5′-ACT GCC ACA TTT GCA TGA TCC ACT TCC GGT-3′
CuMT-3-R (NGSP) S: 5′-TGA CGA CTG CAA GTG TGG TAG CCA ATG-3′
Cd/CuMT-3-R-S: 5′-CTA CTC CTG CCA ATG CAA CAA TGA CAC C-3′
Cd/CuMT 5-R AS: 5′-CCA GTG CGG CTA TGG GAG AGA GTG GTG A-3′

Touchdown PCR was performed using Advantage 2 polymerase (Clontech) with cycling parameters as follows: 5 cycles at 94°C for 30 s and 72°C for 3 min; 5 cycles at 94°C for 30 s, 70°C for 30 s, 72°C for 3 min; 30 cycles at 94°C for 30 s, 68°C for 30 s, 72°C for 3 min. Nested PCR was applied to amplify the *CuMT* cDNA using the following conditions: 39 cycles at 94°C for 30 s, 68°C for 30 s, 72°C for 3 min and a final extension at 72°C for 10 min. NGSP (see above) stands for nested gene specific primer.

Quantitative Real Time PCR

Quantitative Real Time PCR for the *Cd*-, *Cu*-, and *Cd/CuMT* cDNAs was performed on a 7500 Real Time PCR analyser (Applied Biosystems, Foster City, CA, USA) using Power SYBR Green. Amplicon plasmids were used to generate calibration curves for copy number analysis of Δct values for each isogene. Primers were designed with Primer Express 3.0 software (Applied Biosystems). Dissociation curves were used to elucidate the optimal primer concentrations. 2 µl cDNA were applied for Real Time detection PCR in a 20 µl approach (1× Power SYBR Green PCR Mastermix, 1× U-BSA, sense-, antisense primer). All transcripts had specific amplicon lengths (*CdMT*: 56 bp; CuMT: 74 bp; *Cd/CuMT*: 59 bp) and were amplified using the following concentrations and primers:

Cd-MTCa sense, 300 nM: 5’-GCC GCC TGT AAG ACT TGC A-3’;
Cd-MTCa antisense, 900 nM: 5’-CAC GCC TTG CCA CAC TTG-3’.
Cu-MTCa sense, 900 nM: 5’-AAC AGC AAC CCT TGC AAC TGT-3’
Cu-MTCa antisense, 900 nM: 5’-CGA GCA CTG CAT TGA TCA CAA-3’
CdCu-MT sense, 900 nM: 5’-TGT GGA GCC GGC TGT TCT-3’
CdCu-MT antisense, 300 nM: 5’-CAG GTG TCA TTG TTG CAT TGG-3’

Metal analysis

Cd and Cu concentrations in midgut gland tissues (samples taken on days 0, 3, 5, 8, 14, and 29) of each individual as well as in lettuce leaf aliquots were determined by flame atomic absorption spectrophotometry (AAS). After sample drying at 60°C and weight determination, digestion was achieved in 12 ml screw-capped polyethylene tubes (Greiner, Austria) with a mixture (1:1) of nitric acid (suprapure, Merck, Darmstadt, Germany) and deionised water in a heated aluminium digestion oven at 70°C until a clear solution was obtained. The samples were diluted to 11.5 ml with deionised water. Cd and Cu concentrations were measured in the flame of an atomic absorption instrument (model 2380, Perkin Elmer, Boston, MA, USA).

Purification of native MT isoforms by standard chromatography and HPLC

After the 14-day exposure treatment (see above), midgut glands of control and Cd-exposed snails were

pooled from five animals each and processed immediately for chromatography or otherwise stored at −80°C until further use. Pooled midgut gland samples (~3.0–3.5 g fresh weight) were homogenised in a threefold volume (v/w) of 25 mM Tris HCl buffer (pH 7.5) to which 100 mM NaCl, 5 mM 2-mercaptoethanol (Merck), and 0.1 mM phenylmethylsulfonyl fluoride (Merck) had been added. Homogenates were centrifuged for 1 h at 27,000×*g* in a high speed centrifuge (model RC 5C, Sorvall Instruments, Golden Valley, MN, USA). Resulting supernatants were purified in a step by step procedure by DEAE (diethylaminoethyl) cellulose extraction, gel permeation chromatography, ultrafiltration and reversed phase high performance liquid chromatography (RP-HPLC) (Berger et al. 1997). For gel permeation chromatography, samples were split into 6-ml aliquots and applied successively to a column (15 × 300 mm) packed with Sephacryl S-100 (GE Healthcare Europe GmbH, Munich, Germany), calibrated with a mixture of Blue Dextran (2000 kDa), chicken egg albumin (45 kDa), myoglobin (18.5 kDa), and vitamin B_{12} (1.35 kDa). After chromatography, metal concentrations (Cd, Cu and Zn) were measured in fractions by AAS and the presumed MT-containing fractions were pooled and concentrated by ultrafiltration (Amicon YM1, Beverly, MA, USA; 1 kDa cut-off). Subsequently, samples were further fractionated on an HPLC system (model 501, Waters, Milford, LA, USA) equipped with a multi-wavelength detector (model 490E; Waters), using a µBondapack C_{18} column (Waters). Elution was performed in a Tris HCl/acetonitrile gradient over 35 min (Hispard et al. 2008). Fractions were diluted with deionised water and analysed for metal concentrations (Cd, Zn, Cu) as described above.

Recombinant synthesis and purification of the metal-MT complexes

The cDNAs encoding each of the three *C. aspersus* isoforms, isolated as described in the previous section, were subcloned in the pGEX expression vector for recombinant synthesis of the corresponding proteins in *E. coli* BL21 cells, essentially as described for the *H. pomatia* MT isoforms (Palacios et al. 2011). Recombinant synthesis of CdMT, CuMT and Cd/CuMT was performed in metal supplemented LB medium (300 µM $CdCl_2$ or 500 µM $CuSO_4$), which allows the recovery of in vivo folded metal-MT complexes. Full analysis of all recombinant metal complexes of *C. aspersus* MT isoforms will be provided in a forthcoming publication.

Mass spectrometry analysis of recombinant metal-CaMT complexes

Molecular mass determination was performed by electrospray ionisation mass spectrometry equipped with a time-of-flight analyser (ESI-TOF MS) using a Micro Tof-Q Instrument, Bruker Daltonics Gmbh (Bremen, Germany) calibrated with NaI (200 ppm NaI in a 1:1 H_2O: isopropanol mixture), interfaced with a Series 1100 HPLC pump (Agilent Technologies) equipped with an autosampler, both controlled by the Compass Software. The experimental conditions for analysing proteins with Cd were: 20 µl of the sample were injected through a long PEEK tube (1.5 m × 0.18 mm i.d.) at 40 µl/min under the following conditions: capillary-counter-electrode voltage, 5.0 kV; desolvation temperature, 90–110°C; dry gas, 6 l/min. Spectra were collected throughout an m/z range from 800 to 2000. The proteins containing copper were analysed by injecting 20 µl of the 30 µl/min sample; capillary-counter-electrode voltage, 4.0 kV; desolvation temperature, 80°C; m/z range from 800 to 2000. The liquid carrier was a 90:10 mixture of 15 mM ammonium acetate and acetonitrile, pH 7.0. All samples were injected at least in duplicate to ensure reproducibility. In all cases, molecular masses were calculated according to the method reported by Fabris et al. (1996).

Statistics

Statistical analyses were performed using the software packages Statistica (version 8; StatSoft Inc., Tulsa, OK, USA) and Sigma Plot (version 11; Systat Software Inc., Chicago, IL, USA). Real Time PCR plots were tested by analysis of variance (ANOVA). In addition, differences between single values of different treatments (Cd or Cu-exposed versus controls) were analysed by means of the Mann–Whitney rank sum test. A *t*-test was applied for statistical comparison of Cd and Cu concentrations in midgut gland during metal exposure. In all cases, statistical significance was defined at $P \leq 0.05$.

Results and discussion

The three MT isoforms encoded in the *C. aspersus* genome

Figure 1 shows the amino acid sequences of the three MT isoforms from *C. aspersus*, as deduced from their respective cDNA sequences (GenBank accession numbers: CaCdMT, ABL73910; CaCuMT, ABM55268; CaCd/CuMT, ABM92276; Palacios et al. 2011). Upon alignment, it became evident that the three proteins share a high degree of similarity, particularly for the highly conserved cysteines and some amino acid positions flanking them. All isoform sequences largely match those of the orthologous MT isoforms in the Roman snail (*Helix pomatia*) (Fig. 1a), previously isolated and characterised from the midgut gland of *H. pomatia* (Dallinger et al. 1993, 1997; Berger et al. 1997). The third MT isoform (CaCd/CuMT), first identified in *C. aspersus* among all snail species (Schuler et al. 2008; Hispard et al. 2008), exhibits a sequence with intermediate peculiarities between those of CaCuMT and CaCdMT (Fig. 1a) and is largely similar to the corresponding isoform in *H. pomatia* which occurs in two allelic variants (Fig. 1b). It is worth remembering, however, that the designation as CaCd/CuMT has been ascribed to this isoform not from sequence features, but owing to the fact that it is natively recovered as a protein complex including Cd^{2+} and Cu^{+} ions simultaneously (Hispard et al. 2008). The occurrence of three MT isoforms with differential metal specificities and functions seems to be an evolutionary hallmark of this mollusc taxon (Palacios et al. 2011). Although it is obvious that all three MT isoforms must interact to maintain a physiological metal balance in their host, their particular contribution to the metal status of snails has so far not been elucidated.

Metal accumulation in *C. aspersus* snails

In the present study, garden snails were exposed to elevated Cd or Cu levels in the food over a long-term period of 29 days. During this time, metal accumulation and transcriptional activation of the three MT isoforms were assessed in the snail midgut gland,

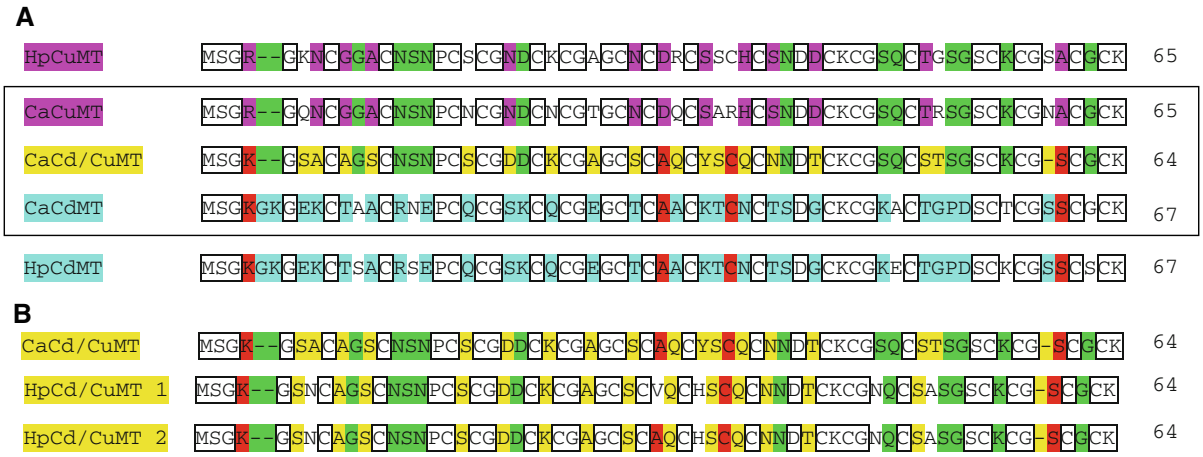

Fig. 1 **a** Amino acid sequence of three MT isoforms (in framed box) of *Cantareus aspersus*, featuring one peptide (CaCuMT) largely matching the Cu-specific isoform of *Helix pomatia* (HpCuMT) (above framed box), beside a second isoform (CaCdMT) with a high degree of similarity with the Cd-specific peptide from *Helix pomatia* (HpCdMT) (below framed box). In the middle of CaCuMT and CaCdMT (in framed box) a third isoform is shown (CaCd/CuMT) with an amino acid sequence sharing peculiarities with CaCuMT and CaCdMT. **b** Comparison of the CaCd/CuMT sequence or *C. aspersus* with two HpCd/CuMT sequences (allelic variants 1 and 2) from *H. pomatia*. Amino acids positions shared by all isoforms are framed. Identical amino acid positions shared only by part of the isoforms displayed are *colour*-underlayed as follows: *blue*, identical between CdMT isoforms (CaCdMT and HpCdMT); *pink*, identical between CuMT isoforms (CaCuMT and HpCuMT); *red*, identical between CdMT isoforms and CaCd/CuMT; *green*, identical between CuMT isoforms and CaCd/CuMT; *yellow*, only in CaCd/CuMT. The GenBank accession numbers of these sequences are EF178297.2 (CaCuMT), EF152281.1 (CaCdMT), and EF206312.1 (CaCd/CuMT). The GenBank accession numbers of the *Helix pomatia* MTs are: AF399741.1 (HpCuMT) AF399740.1 (HpCdMT), as well as ACY71053.1 (HpCd/CuMT allelic variant 1) and ACY71054.1 (HpCd/CuMT allelic variant 2)

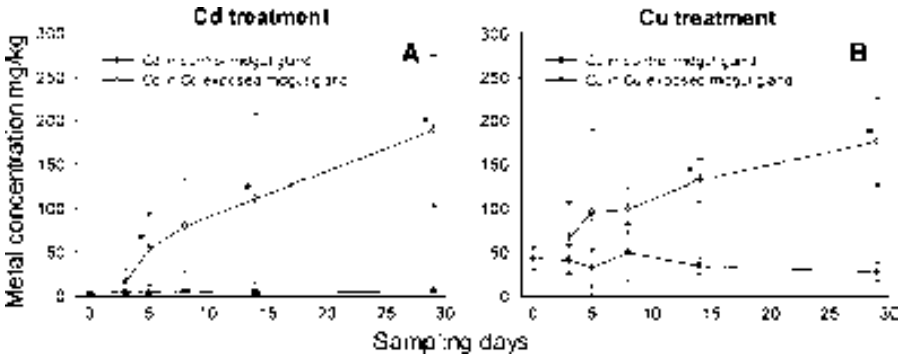

Fig. 2 Time course plot of (**a**) Cd concentration and (**b**) Cu concentration (mg/kg, dry weight) in midgut gland of control and Cd-exposed snails over 29 days. Significant differences of single values between controls and metal-exposed snails are marked by *small asterisks*. Means and two-sided standard deviations are shown for $n = 5$. The significance level for all statistical evaluations was set at $P \leq 0.05$)

since this organ accounts for most of the short and long-term metal accumulation in pulmonate snails (Dallinger and Wieser 1984; Hispard et al. 2008).

Cd was found steadily enriched in the midgut gland of Cd-exposed animals until the end of the feeding period, reaching maximum concentrations of more than 150 µg/g Cd. At the end of the exposure period, midgut gland Cd concentrations in exposed snails exceeded control levels by a factor of about 30 (Fig. 2a). In contrast to Cd, Cu uptake in the midgut gland of *C. aspersus* started from a considerably higher concentration level under control conditions (Fig. 2b) showing accumulation rates in metal-exposed individuals that are more restrained when compared to Cd accumulation. This observation coincides well with similar findings in other pulmonate snails (Dallinger and Wieser 1984) and reflects the fact that Cu is an essential trace element which has cellular concentration levels that are, to a certain extent, subject to a regime of intracellular regulation (Dallinger et al. 2005). In fact, significantly increased Cu concentrations were reached in the midgut gland of exposed snails only towards the end of the long-term feeding period, when Cu concentrations exceeded the respective control levels by a factor of 6 (Fig. 2b).

Transcription regulation of the *C. aspersus* MT isogenes

The long-term course of mRNA transcription of the *CdMT*, *CuMT* and *Cd/CuMT* genes in *C. aspersus* varied in an isoform and metal-specific manner, as shown by quantitative Real Time PCR results (Fig. 3). Already under control conditions, the basal mRNA transcription rates differed significantly between the three MT isogenes, showing the highest levels for *CdMT*, followed by intermediate levels of *CaCuMT*, and lowest values for *CaCd/CuMT* (Fig. 3). Results for gene induction are reported and discussed separately for each MT isoform.

Transcription of the CaCdMT gene

Upon Cd exposure, a significant induction of transcription was observed for *CaCdMT* (Fig. 3a), in contrast to the null response detected for the two other isogenes (Fig. 3b, c). This strong upregulation persisted until day 29, yielding mRNA copy numbers which ranged between 200,000 and 600,000, in contrast to the control group which showed copy numbers below 100,000. Interestingly, the *CaCdMT* induction rate reached a peak on day 8 of the feeding period (Fig. 3a). This may be due to the fact that at the beginning of Cd exposure, the concentration of free Cd^{2+} ions able to interact with the gene regulatory regions is higher than at later stages, when an increasing fraction of the metal ion is already bound to the CdMT protein. Overall, the transcriptional response of the *CdMT* gene in snails appears to proceed more slowly than in mammals, where highest induction peaks are observed few hours after Cd exposure, at least when injecting Cd (Swerdel and Cousins 1982). Furthermore, *MT gene* induction following intraperitoneal administration of Cd in a

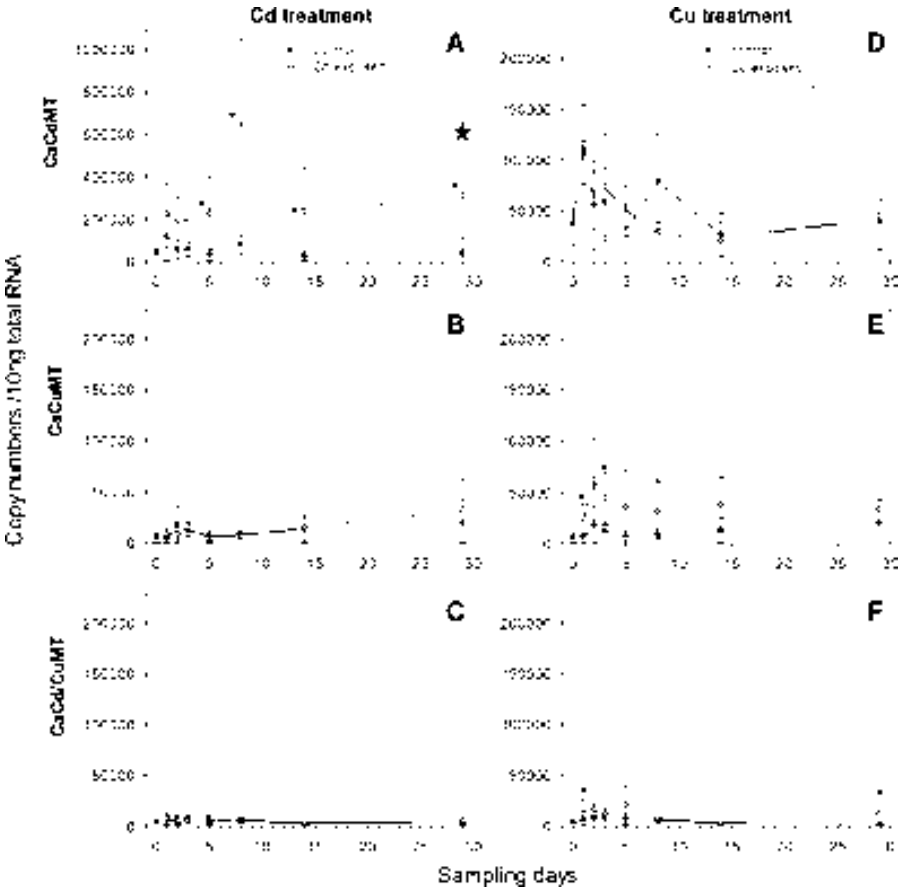

Fig. 3 Time course plots of quantitative Real Time PCR results of metal-dependent and control mRNA transcription (mRNA copy number/10 ng of total RNA) of *C. aspersus MT* isoform genes over 29 days after Cd-induction for: (**a**) *CaCdMT*, (**b**) *CaCuMT* and (**c**) *CaCd/CuMT*; and after Cu-induction for: (**d**) *CaCdMT*, (**e**) *CaCuMT*, and (**f**) *CaCd/CuMT*. Means and two-sided standard deviations are shown for $n = 3$–5 (mRNA copy numbers. Significant curves upon ANOVA are marked by a *large asterisk*. Significant differences of single values between controls and metal-exposed snails are marked by *small asterisks*. The significance level for all statistical evaluations was set at $P \leq 0.05$)

marine flatfish peaked in the liver after 4 days, and more rapidly in kidney and gills (George et al. 1996). This indicates that *MT* gene induction is tissue- and species-dependent, which may reflect differing molecular pathways and agents involved in such mechanisms (Höckner et al. 2009).

Conversely to Cd treatment, there was no induction of the *CaCdMT* gene by Cu exposure (Fig. 3d). These findings confirm that the *CaCdMT* gene of *C. aspersus* is upregulated specifically by Cd, which is consistent with the particularly important role ascribed to the CdMT protein upon Cd uptake through the feed (see below). Apart from its high response towards Cd, it cannot be excluded that *CaCdMT* may also be responsive to other, non-metallic cellular or environmental stressors, in a similar way that the orthologous gene in *H. pomatia* also exhibits a slight response towards non-metallic environmental stresses, such as desiccation (Egg et al. 2009).

Transcription of the CaCuMT gene

While there was no response of *CaCuMT* towards Cd, a slight transcriptional activation of this gene was observed after Cu intake (Fig. 3e). Although in Cu-exposed animals, the trend of transcription pattern over the course of time was not significant upon testing by ANOVA, some particular mRNA concentrations (i.e. those on days 1, 3 and 8) showed significant differences compared to the respective control values. However, in comparison with the strong responsiveness of the *CaCdMT* gene towards Cd, this occasional upregulation of the *CaCuMT* gene by Cu must be considered as very weak. Overall, this is consistent with the hypothesis that the main task of the *CaCuMT* isogene is not Cu detoxification, but rather the physiological homeostasis of this metal ion. In *H. pomatia*, the mRNA of the homologous gene is exclusively detected in rhogocytes, which are the cells where the Cu-bearing respiration pigment haemocyanin

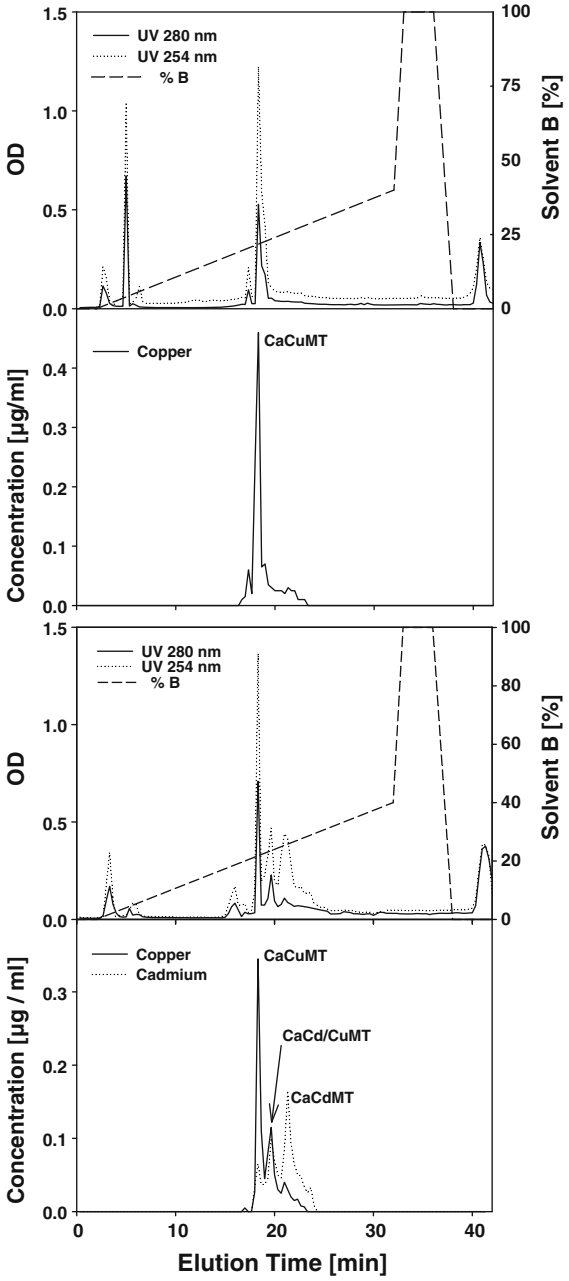

Fig. 4 Elution patterns of MT isoforms from cytosolic midgut gland homogenates of control (**a**, **b**) and Cd-exposed individuals of *C. aspersus* (**c**, **d**) upon RP-HPLC, obtained from ultrafiltrated protein extracts after initial anion exchange and gel permeation chromatography (see details in Materials and methods). **a** RP-HPLC elution profile (elution time, *x*-axis) of MT isoforms from control snail midgut glands showing the optical density (left *y*-axis) at 280 and 254 nm and the elution gradient (solvent B, right *y*-axis); (**b**) Cu concentrations in fractions of CaCuMT, measured by AAS. **c** RP-HPLC elution profile (elution time, *x*-axis) of MT isoforms from midgut glands of Cd-exposed snails showing the optical density (left *y*-axis) at 280 and 254 nm and the elution gradient (solvent B, right *y*-axis); (**d**) Cd and Cu concentrations in fractions of CaCuMT, CaCd/CuMT, and CaCdMT, measured by AAS

is synthesised. For this reason, HpCuMT has been suggested to serve in Cu donation to the nascent haemocyanin (Dallinger et al. 2005).

Transcription of the CaCd/CuMT gene

As shown by the Real Time PCR results, neither Cd nor Cu exposure induced the *CaCd/CuMT* gene (Fig. 3c, f). Noteworthy, and as for CuMT, in Cu-exposed snails a few mRNA copy number values appeared to be slightly elevated compared to the respective controls (Fig. 3f). The level of transcriptional activation of the *CaCd/CuMT* gene was the lowest observed among all three *C. aspersus MT* genes, which, together with the low rate of constitutive expression, suggests that its contribution to the overall metal balance in this species may be of only marginal significance.

Contribution of MT isoforms to metal binding in *C. aspersus*: purification of native metal-MT complexes

Midgut gland cytosol fractions of controls and Cd-exposed snails were examined for the presence of MT isoforms and their association with Cd, Cu and Zn. To this end, midgut gland homogenates were first separated into soluble and pellet fractions. The subcellular distribution analysis of Cd, Cu and Zn revealed that Cd was mainly present in the soluble cytosol (80–90%), whereas Cu and Zn were predominantly detected in pellet fractions (Cu: 60–80%; Zn: 80–85%), a distribution that is typical for the midgut gland of terrestrial pulmonate snails (Dallinger and Wieser 1984).

For MT purification, supernatants were consecutively applied to anion exchange and gel permeation chromatography, followed by ultrafiltration and RP-HPLC fractionation. As shown by the elution profiles of the final RP-HPLC step (Fig. 4), the presence of different isoforms, and the partitioning of metals among them, depended on the metal-feeding status of the animals (controls *vs.* Cd-exposed).

Control snails rendered practically one single MT peak showing a high absorption at 254 nm (Fig. 4a). Due to its exclusive Cu load and owing to its elution behaviour in comparison with the HpCuMT isoform (Berger et al. 1997; Dallinger et al. 2005), this peak was attributed to CaCuMT (Fig. 4b). The identification of this sequence as a CaCuMT isoform was corroborated by the fact that, upon recombinant synthesis in *E. coli* of the corresponding cDNA (Hispard et al. 2008), the resulting protein was a unique, homometallic Cu-loaded complex, a behaviour exhibited only by highly specific Cu-thioneins (Bofill et al. 2009). This isoform was equally detected in Cd-fed snails—without major changes in its abundance, elution time, Cu load, and Cu:Cd:Zn molar ratio (Fig. 4c, d; Table 2). The nearly exclusive Cu content of this isoform, and its independence of the state of Cd accumulation in the snail, corroborates the view that CaCuMT may be involved in the homeostatic regulation of Cu, rather than being responsible for detoxification processes (Dallinger et al. 2005; Hispard et al. 2008). This is in concordance with the observation that the transcription of *CaCuMT* in the midgut gland of *C. aspersus* does not vary as a function of supra-physiological exposure to Cd or Cu.

In addition to the CuMT isoform, the Cd-exposed snails exhibited two additional MT peaks that were not present in control animals. Both peaks showed an increased absorption at 254 nm (Fig. 4c) but differed with respect to their metal content (Fig. 4d). One of them was characterised by a clear preponderance of Cd over Cu, with a molar ratio of about 10 Cd:1 Cu and only traces of Zn (Table 2), and owing to this, it was identified as CaCdMT. The ability of this peptide to spontaneously form pure Cd complexes after recombinant expression in Cd-exposed *E. coli* cells is documented below. Interestingly, a considerable amount of *CaCdMT* mRNA had been detected in untreated snails (Fig. 3). This raises the question of why CaCdMT was not detectable in control animals at the protein level, in spite of conspicuously elevated basal mRNA concentrations. Several hypotheses could account for this apparent inconsistency, for example, that the lack of protein might be the result of inhibitory post-transcriptional regulatory mechanisms, or that, in the absence of metals, the peptide resulting from translation may be readily proteolysed in the cell, since apoMTs are known to be highly susceptible to degradation (Krezoski et al. 1988).

The second additional MT peak in the elution profile of Cd-exposed snails showed the simultaneous presence of Cd and Cu (Fig. 4d). In fact, due to this mixed metal-binding character, this isoform had been designated as CaCd/CuMT (Schuler et al. 2008; Hispard et al. 2008). The quantitative analysis of its metal content showed that Cd and Cu were present at a molar ratio of about [1 Cu:0.5 Cd], with only traces of Zn (Table 2). Its identity with the expression product of the corresponding gene (*CaCd/CuMT*) (Fig. 1) was confirmed by recombinant expression of the *CaCd/CuMT* cDNA in *E. coli*, which yields an MT peptide exhibiting non-specific metal-binding abilities, a behaviour sharply contrasting with the two metal-specific isoforms, as commented below. It is worth noting that Cd injection in marine crustaceans also yielded MT complexes including both Cd and Cu ions, as shown, for example, in the crab *C. pagurus* (Overnell and Trewhella 1979). This observation was also related to the special needs of these organisms for Cu.

Table 2 Metal content (mean ± standard deviation), expressed in μg and nmol (in brackets), in the CaCuMT, CaCdMT and CaCd/CuMT preparations obtained from control and Cd-exposed snails, as well as molar ratio (Cu:Cd:Zn) of the metal load in each case

	Metal content: μg (nmol)			Molar metal ratio
	Cu	Cd	Zn	(Cu:Cd:Zn)
Control animals				
CaCuMT	0.653 ± 0.195 (10.39)	0.000 (0)	0.012 ± 0.007 (0.18)	1:0:0.017
Cd-exposed animals				
CaCuMT	0.801 ± 0.115 (12.6)	0.087 ± 0.019 (0.77)	0.009 ± 0.001 (0.14)	1:0.06:0.011
CaCdMT	0.018 ± 0.005 (0.28)	0.316 ± 0.045 (2.81)	0.004 ± 0.002 (0.06)	1:10.03:0.18
CaCd/CuMT	0.255 ± 0.053 (4.01)	0.237 ± 0.029 (2.11)	0.005 ± 0.002 (0.08)	1:0.53:0.020

Metal contents are expressed as means and standard deviations from three repetitive elutions. Metal ratio is referred to Cu (=1)

Compared to MTs from other animal species, the *C. aspersus* native MT preparations were characterised by their remarkably poor content of Zn, even under physiological conditions (Fig. 4, Table 2) (Gehrig et al. 2000). Already in control snails, Zn was present in minor quantities in midgut gland cytosolic MT fractions and very low amounts, if any, were detectable in MT-containing fractions after gel permeation chromatography. Even less Zn, if at all, could be assessed in any of the three MT isoform peaks purified from Cd-treated snails (Table 2). Interestingly, low content or complete absence of Zn seems to be a consistent feature of pulmonate MTs and may be a consequence of the fact that in pulmonate midgut glands this metal ion is predominantly associated with granular fractions, where it may occur in a chemical form not suitable for MT binding (Dallinger et al. 1989). Therefore, the handling of essential Zn in pulmonate snails does not seem to be mediated primarily by MTs, which is concordant with the inability of Zn^{2+} to induce any of the three *C. aspersus* MT isoform genes. As shown before in this study, the snail CdMT isoform is synthesized at low basal levels in the absence of Cd^{2+}, when it may be present as Zn-loaded complexes, hardly detectable because of their low concentration. Most probably they are involved in stress-responsive functions (Egg et al. 2009) and therefore unlikely to play a major role for the Zn status in the snail organism.

Specificity of the metal-binding behaviour of the CaMT isoforms

We have recently shown that the *H. pomatia* metal-specific isoforms (HpCdMT and HpCuMT) exhibited a sequence-inherent property to form single, homometallic complexes when recombinantly synthesised in bacteria grown in media supplemented with their cognate metal and not vice versa (Palacios et al. 2011). Thus the properties of the metal-MT preparations resulting from recombinant synthesis can be considered an accurate test of MT metal-specificity. Consequently, we first characterised the products of expression of *CaCdMT* and *CaCuMT* in *E. coli* cells grown in cadmium and copper enriched media. In the former case, CaCdMT rendered a unique, homometallic cadmium complex as shown by the single ESI-MS peak of 7486.9 Da (corresponding to a Cd_6–CaCdMT complex) (Fig. 5a). In contrast, when recombinantly produced in the presence of Cu, CaCdMT is unable to form homometallic, unique complexes (manuscript in preparation). This is exactly the same result yielded by the orthologous HpCdMT, indicating that this feature of extreme Cd specificity may be shared by all pulmonate snail CdMT isoforms (Palacios et al. 2011).

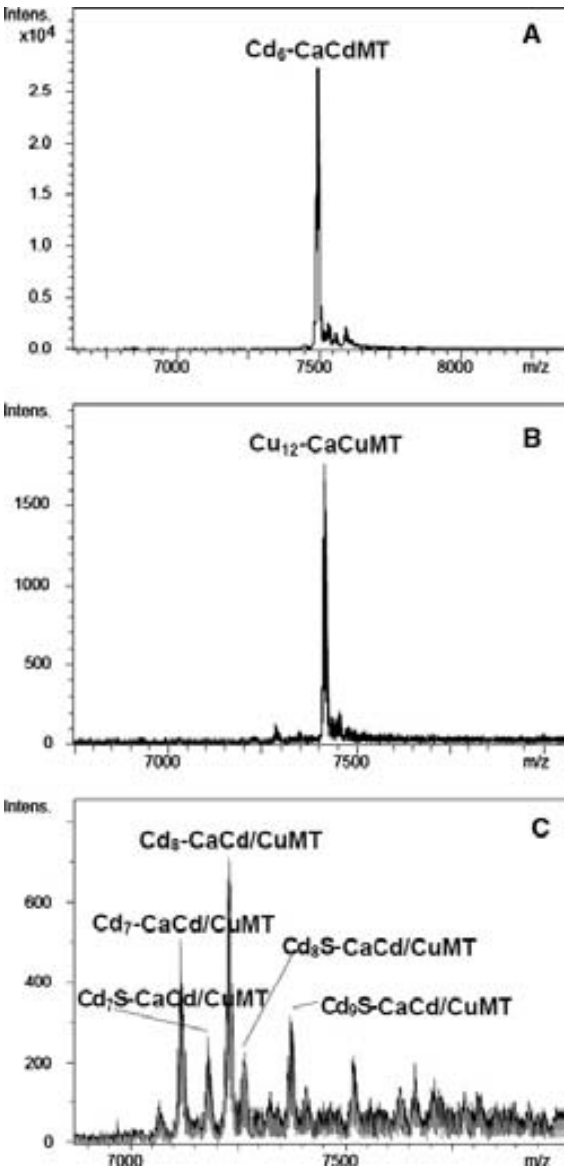

Fig. 5 Deconvoluted ESI-TOF MS spectra of different metal-MT complexes recombinantly synthesised: (**a**) CaCd-MT obtained from Cd-enriched *E. coli* cultures; (**b**) CaCuMT produced by Cu-enriched *E. coli* cultures; and (**c**) CaCd/CuMT produced by Cd-enriched *E. coli* cultures

On the other hand, when the *CaCuMT* gene was recombinantly expressed in *E. coli* under Cu surplus, the only recovered product was identified as a homometallic complex with a molecular mass of 7408.3 Da, corresponding to the Cu_{12}-CaCuMT species (Fig. 5b). In contrast, in this case, recombinant synthesis of this isoform with Cd or Zn produced variable mixtures of complexes with different stoichiometries, but never homometallic species (data not shown; manuscript in preparation). These results confirm the exceptional specificity of the CuMT isoform for Cu^{+}, which is also corroborated by its nearly exclusive Cu load when purified from Cd-exposed snails (Table 2). In fact, CaCuMT synthesis is not upregulated by Cu or other metals (Fig. 3b, e), as otherwise would be expected for a protein functioning as a Cu donor for haemocyanin synthesis (Dallinger et al. 2005).

The higher sequence similarity of the CaCd/CuMT isoform with CaCuMT than with CaCdMT (Fig. 1), led to the assumption that CaCd/CuMT and CaCuMT share a common ancestor in pulmonate snail origin (Palacios et al. 2011). A reflection of this close sequence resemblance is that both isoforms are natively recovered as Cu-containing complexes (homometallic or heterometallic) (Fig. 4; Table 2). But CaCd/CuMT is also associated with conspicuous amounts of Cd^{2+} at a molar ratio of [1 Cu:0.5 Cd] (Table 2), thus, in contrast to the specific CaCuMT isoform, CaCd/CuMT lacks metal specificity, either because it has not yet achieved this property or because it lost it during evolution. Indeed, the nature of the metal complexes formed by this isoform upon its recombinant synthesis under metal exposure indicates that CaCd/CuMT does not exhibit any definite metal specificity, since it gives rise to mixtures of metal:protein species with variable stoichiometries in the presence of either Cd^{2+} or Cu^{2+} (shown in Fig. 5c for the former). Furthermore, some of the Cd-species include S^{2-} ligands (Fig. 5c), which is a trait indicative of Cu-thionein character (Capdevila et al. 2005; Bofill et al. 2009; Orihuela et al. 2010). Concordantly, this isoform exhibits intermediate features regarding its induction pattern and synthesis. Hence, the *CaCd/CuMT* gene is clearly not inducible by metals, showing invariantly and extremely low mRNA levels in either control, Cu or Cd-exposed snails (Fig. 3c, f), reflecting the constitutive expression characteristics of *CuMT* genes. In contrast to this observation, a protein peak of this isoform was detectable by means of RP-HPLC in Cd-exposed snails (Fig. 4c, d), indicating that its synthesis or its formation may have been induced by the presence of Cd^{2+}. One possible explanation for these contradicting findings may be that in spite of the invariably low *CaCd/CuMT* mRNA concentration, a certain quantity of this isoform may yet be synthesised in Cd-exposed animals, so that the expressed protein can be stabilised by the presence of Cd in the corresponding complexes. The absolute amounts of this isoform in the snail may be very low. In other pulmonate species, this protein is not detectable at all after chromatographic isolation (cf. *H. pomatia*, Dallinger et al. 2005; Palacios et al. 2011). It is therefore suggested that exclusively in *C. aspersus*, CaCd/CuMT may function as a trapping molecule for excess traces of Cd and Cu during short-term events of acute exposure. Overall, its contribution to the trace element balance in the escargot may be of only marginal significance.

Conclusions

Cantareus aspersus possesses three MT isogenes: *CaCuMT*, *CaCdMT*, and *CaCd/CuMT*. As in other pulmonate snails, they have probably evolved by gene duplication from a common ancestor (Palacios et al. 2011). Only one (*CaCdMT*) of those genes is significantly upregulated by Cd, the other two genes (*CaCuMT* and *CaCd/CuMT*) are constitutively expressed and do not respond at all or only slightly to long-term Cd or Cu induction. The protein products of these genes are devoted to differential tasks, with two of them showing metal specificity for Cu (CaCuMT) or Cd (CaCdMT) and one non metal-specific isoform (CaCd/CuMT) natively binding Cd and Cu simultaneously. The CaCdMT protein binds most of the Cd absorbed by the snail tissues. Data of the present work and results from earlier studies (Hispard et al. 2008; Palacios et al. 2011) suggest that the CaCdMT isoform may account for 80–90% of the total Cd balance in snails exposed to this metal. In uncontaminated snails, this isoform is virtually absent or present at very low concentrations as a Zn complex (Egg et al. 2009). An important role for Cu balance and metabolism is attributed to the CaCuMT isoform, irrespective of whether snails are exposed to

contaminating Cu or not. This is due to the fact that the CaCuMT isoform is highly Cu-specific (see present study) binding a constant fraction of Cu absorbed by the snail tissues, mostly in rhogocytes (Dallinger et al. 2005). It is speculated that this MT-bound Cu may be available for the synthesis of the respiratory haemocyanin which represents the second significant Cu containing pool in most pulmonate snails. In addition, there are significant Cu pools present in granular cell fractions of rhogocytes, probably not in the form of a protein, and mainly in response to acute Cu exposure (Dallinger et al. 2005). Thus the share of CaCuMT in the total Cu metabolism of *C. aspersus* may be significant, although not sufficient to cover the Cu balance of the snail entirely. Its contribution to the Cu status of this species may range between 30 and 50%.

The contribution of the unspecific CaCd/CuMT isoform to the metal status of *C. aspersus* is obviously less important. This isoform may trap after Cd or Cu exposurea certain proportion of these metals. It is not present, however, under control conditions. Moreover, this isoform cannot normally be detected in other pulmonate species (Dallinger et al. 2005; Palacios et al. 2011). Because of these facts, it is suggested that its contribution to the metal status of *C. aspersus* may be low to negligible, this isoform possibly being more interesting from an evolutionary point of view. The CaCd/Cu sequence is more similar to that of CuMT isoforms than to CdMT snail isoforms. The corresponding gene is constitutively expressed, like most Cu-thionein genes, although Cd slightly enhances its transcription resulting in natively mixed Cd, Cu-complexes. Concordantly, recombinant analysis of its metal-binding behaviour reveals neither a genuine Cd- nor Cu-binding aptitude, even though some features, such as the production of sulfide-containing Cd-complexes when synthesised in cultures enriched with this metal ion, suggest a closer relationship of this isoform to Cu- than to Cd-thioneins (Bofill et al. 2009). In fact, a more detailed study (manuscript in preparation) of the structure/function relationship of this metal-binding peptide may elucidate the sequence determinants for metal specificity in MTs, i.e. which amino acids in what position favour the balance towards a Cd-thionein (divalent ion-thionein) or Cu-thionein.

Acknowledgments This work was supported by the Spanish Ministerio de Ciencia y Tecnología grants BIO2009-12513-C02-01 to S. Atrian, BIO2009-12513-C02-02 to M. Capdevila and project No. P19782-B02 from the Austrian Science Foundation to R. Dallinger. Collaboration between the Spanish and Austrian research groups was financed by the "Acciones Integradas" grants HU2006-0027 (Spain) and ES 02/2007 (Austria). Authors from the University of Innsbruck are members of "Centre of Molecular Biosciences Innsbruck" (CMBI). Authors from the Universitat Autònoma de Barcelona (UAB) and Universitat de Barcelona (UB) are members of a "Grups de Recerca de la Generalitat de Catalunya" (2009SGR-1457). We thank the Serveis Cientificotècnics of UB (GC-FPD, ICP-AES, DNA sequencing) and the Servei d'Anàlisi Química (SAQ) of UAB (CD, UV–vis, ESI-MS) for allocating instrument time.

References

Berger B, Hunziker PE, Hauer CR, Birchler N, Dallinger R (1995) Mass spectrometry and amino acid sequence of two cadmium-binding metallothionein isoforms from the terrestrial gastropod *Arianta arbustorum*. Biochem J 311:951–957

Berger B, Dallinger R, Gehrig P, Hunziker PE (1997) Primary structure of a copper-binding metallothionein isoform from mantle tissue of the terrestrial gastropod *Helix pomatia* L. Biochem J 328:219–224

Blindauer CA, Leszczyszyn OI (2010) Metallothioneins: unparalleled diversity in structures and functions for metal ion homeostasis and more. Nat Prod Rep 27:720–741

Bofill R, Capdevila M, Atrian S (2009) Independent metal-binding features of recombinant metallothioneins convergently draw a step gradation between Zn- and Cu-thioneins. Metallomics 1:229–234

Capdevila M, Domenech J, Pagani A, Tio L, Villarreal L, Atrian S (2005) Zn- and Cd-metallothionein recombinant species from the most diverse phyla contain sulfide (S^{2-}) ligands. Angew Chem Int Ed Eng 44:4618–4622

Chabicovsky M, Niederstaetter H, Thaler R, Hödl E, Parson W, Rossmanith W, Dallinger R (2003) Localisation and quantification of Cd- and Cu-specific metallothionein isoform mRNA in cells and organs of the terrestrial gastropod *Helix pomatia*. Toxicol Appl Pharmacol 190:25–36

Chevallier H (1983) Recherches appliquées pour l' élevage des escargots du genre *Helix*. J Moll Stud 49:27–30

Dallinger R, Wieser W (1984) Patterns of accumulation, distribution and liberation of Zn, Cu, Cd and Pb in different organs of the land snail *Helix pomatia* L. Comp Biochem Physiol 79C:117–124

Dallinger R, Berger B, Bauer-Hilty A (1989) Purification of cadmium-binding proteins from related species of terrestrial Helicidae (Gastropoda, Mollusca): a comparative study. Mol Cell Biochem 85:135–145

Dallinger R, Berger B, Hunziker P, Birchler N, Hauer C, Kägi JHR (1993) Purification and primary structure of snail metallothionein: similarity of the N-terminal sequence with histones H4 and H2A. Eur J Biochem 216:739–746

Dallinger R, Berger B, Hunziker PE, Kägi JHR (1997) Metallothionein in snail Cd and Cu metabolism. Nature (London) 388:237–238

Dallinger R, Berger B, Triebskorn R, Köhler HR (2001) Soil biology and ecotoxicology. In: Barker G (ed) Biology of terrestrial molluscs. CAB International, Wallingford, England, pp 489–525

Dallinger R, Chabicovsky M, Berger B (2004) Isoform-specific quantification of metallothionein in the terrestrial gastropod *Helix pomatia* I. Molecular, biochemical, and methodical background. Environ Toxicol Chem 23:890–901

Dallinger R, Chabicovsky M, Hödl E, Prem C, Hunziker P, Manzl C (2005) Copper in *Helix pomatia* (Gastropoda) is regulated by one single cell type: differently responsive metal pools in rhogocytes. Am J Physiol 189:R1185–R1195

Egg M, Höckner M, Chabicovsky M, Brandstätter A, Schuler D, Dallinger R (2009) Structural and bioinformatic analysis of the Roman snail Cd-Metallothionein gene uncovers molecular adaptation towards plasticity in coping with multifarious environmental stress. Mol Ecol 18: 2426–2443

Fabris D, Zaia J, Hathout Y, Fenselau C (1996) Retention of thiol protons in two classes of protein zinc coordination centers. J Am Chem Soc 118:12242–12243

Gehrig P, You C, Dallinger R, Gruber C, Brouwer M, Kägi JHR, Hunziker PE (2000) Electrospray ionization mass spectrometry of zinc, cadmium and copper metallothioneins: evidence for metal binding cooperativity. Prot Sci 9:395–402

George SG, Todd K, Wright J (1996) Regulation of metallothionein in teleosts: induction of MTmRNA and protein by cadmium in hepatic and extrahepatic tissues of a marine flatfish, the turbot (*Scophthalmus maximus*). Comp Biochem Physiol C Pharmacol Toxicol Endocrinol 113:109–115

Godan D (1979) Schadschnecken und ihre Bekämpfung. Ulmer, Stuttgart (Germany)

Guiller A, Madec L (2010) Historical biogeography of the land snail *Cornu aspersum*: a new scenario inferred from haplotype distribution in the Western Mediterranean basin. BMC Evol Biol 10:18

Hispard F, Schuler D, de Vaufleury A, Scheifler R, Badot PM, Dallinger R (2008) Metal distribution and metallothionein induction after cadmium exposure in the terrestrial snail *Helix aspersa* (Gastropoda, Pulmonata). Environ Toxicol Chem 27:1533–1542

Höckner M, Stefanon K, Schuler D, Fantur R, de Vaufleury A, Dallinger R (2009) Coping with cadmium exposure in various ways: the two helicid snails *Helix pomatia* and *Cantareus aspersus* share the metal transcription factor-2, but differ in promoter organization and transcription of their Cd-metallothionein genes. J Exp Zool A Ecol Genet Physiol 311:776–787

Kägi JHR, Kojima Y (1987) Chemistry and biochemistry of metallothionein. In: Kägi JHR, Kojima Y (eds) Metallothionein II. Exp Suppl 52. Birkhäuser Verlag, Basel, pp 25–61

Kerney MP, Cameron RAD (1979) A field guide of the land snails of Britain and North-west Europe. Wm. Collins & Sons, Glasgow

Krezoski SK, Villalobos J, Shaw CF, Petering DH (1988) Kinetic lability of zinc bound to metallothionein in Ehrlich cells. Biochem J 255:482–491

Manzl C, Krumschnabel G, Schwarzbaum PJ, Dallinger R (2004) Acute toxicity of cadmium and copper in hepatopancreas cells from the Roman snail (*Helix pomatia*). Comp Biochem Physiol C 138:45–52

Orihuela R, Monteiro F, Pagani A, Capdevila M, Atrian S (2010) Evidence of native metal-(S^{2-})-MT complexes confirmed by the analysis of Cup1 divalent metal ion binding properties. Chem A Eur J 16:2363–12372

Overnell J, Trewhella E (1979) Evidence for the natural occurrence of (cadmium, copper)-metallothionein in the crab *Cancer pagurus*. Comp Biochem Physiol 64C:69–76

Palacios O, Pagani A, Pérez-Rafael S, Egg M, Höckner M, Brandstätter A, Capdevila M, Atrian S, Dallinger R (2011) Shaping mechanisms of metal specificity in a family of metazoan metallothioneins: evolutionary differentiation of Mollusc MTs. BMC Biol 9:4

Schuler D, Dallinger R, Hispard F, De Vaufleury A (2008) Biochemical characterization of metallothionein isoforms in terrestrial snails: relationship between amino acid sequence and metal binding specificity. Comp Biochem Physiol 151A:S20

Sigel A, Sigel H, Sigel RKO (eds) (2009) Metal ions in life sciences; vol 5: metallothioneins and related chelators. Royal Society of Chemistry, Cambridge, UK

Swerdel MR, Cousins RJ (1982) Induction of kidney metallothionein and metallothionein messenger RNA by zinc and cadmium. J Nutr 112:801–809

IV. ARTICLE 4:

Differential ESI-MS behaviour of highly similar metallothioneins

Talanta, **(2011)**, 83, 1057-1061.

Talanta 83 (2011) 1057–1061

Contents lists available at ScienceDirect

Talanta

journal homepage: www.elsevier.com/locate/talanta

Short communication

Differential ESI-MS behaviour of highly similar metallothioneins

Sílvia Pérez-Rafael[a], Sílvia Atrian[b], Mercè Capdevila[a], Òscar Palacios[a,*]

[a] Departament de Química, Facultat de Ciències, Universitat Autònoma de Barcelona, 08193 Cerdanyola del Vallès, Barcelona, Spain
[b] Departament de Genètica, Facultat de Biologia, Universitat de Barcelona and IBUB (Institut de Biomedicina de la Universitat de Barcelona), 08028 Barcelona, Spain

ARTICLE INFO

Article history:
Received 30 July 2010
Received in revised form 25 October 2010
Accepted 29 October 2010
Available online 4 November 2010

Keywords:
Metallothionein
ESI-MS
Metal speciation
Protein quantification
Cornu aspersum
Helix pomatia

ABSTRACT

ESI-MS can only be accepted as a quantification method when using standards with a high resemblance to the analyte(s). Unfortunately, this is usually not applicable to metallothioneins (MTs), a superfamily of singular metal-binding cysteine-rich proteins, present in all living organisms, since the absence of suitable reference material due to the high diversity among metal–MT species precludes their quantification by molecular mass spectrometry. Even thus, it is widely assumed that the intensities of the ESI-MS peaks of similar species are directly correlated with their relative concentration in the sample, and this has been extended to the determination of different MT proteins coexisting in a sample.

Practically all organisms contain several MT isoforms, some of them exhibiting highly similar sequences, with conserved coordinating Cys residues. For the current analysis, we used as a model system the MT isoforms of two terrestrial snails (*Helix pomatia* and *Cornu aspersum*). Hence, distinct samples were prepared by mixing, at different molar ratios, the recombinant HpCuMT and HpCdMT isoforms from *H. pomatia*, or the recombinant CaCuMT, CaCdMT and CaCdCuMT isoforms from *C. aspersum*, and they were analyzed by ESI-MS both at neutral pH (for Zn-loaded MT forms) and at acidic pH (for the corresponding apo-forms). The results here presented reveal that the ESI-MS peak intensity of a single MT species strongly depends on its sensitivity to be ionized, and thus, on the presence or absence of metal ions bound. Furthermore, our data demonstrate that very similar MT isoforms of the same organism with similar pI (ranging from 7.9 to 8.3) can show a clear different sensitivity to ES ionization, something that cannot be readily predicted only by consideration of their amino acid content. In conclusion, even in this optimum case, deductions about quantity features of MT samples drawn from ESI-MS measurements should be carefully considered.

1. Introduction

Soft ionization molecular mass spectrometry, namely ESI-MS and MALDI-TOF MS, cannot be used for the quantification of different molecules present in a sample, because the intensity of the respective peaks that they yield in the MS spectra depends not only on their respective concentrations, but mainly on their behaviour as ionizable particles. However, in certain occasions, the use of suitable standards made possible the quantification of similar species [1–3]. When analyzing metalloproteins, the difficulties found for quantification purposes are more severe than in the case of other proteins, due to modifications of their pI and/or charge properties introduced by the presence of metal ions bound to the peptide chains. A very special, and highly illustrative case can be observed for metallothioneins.

Metallothioneins (MTs) are a singular superfamily of metal-binding, Cys-rich peptides, present in all living organisms [4,5]. In this case, the common absence of reference material and the high diversity among MT sequences, their promiscuity referring to metal – nature and number – load and other features of the metal–MT species makes virtually impossible to quantify the MT complexes present in a preparation by means of molecular MS. Despite this, many authors, including we among them, assume that the ratios between the peak intensities of similar metal–MT species in an ESI-MS spectrum bear a certain relation to their respective abundance in the sample [6–9]. But, can be this assumed for any MT system? How far can these assumptions be extended to any analysis conditions?

In this communication, we present a detailed overview of the response to ESI-MS of five highly similar MT isoforms, belonging to two terrestrial snails: *Helix pomatia* and *Cornu aspersum*. These organisms synthesize several MT isoforms, which show distinct metal specificity (for cadmium—CdMTs- and copper—CuMTs-binding) despite exhibiting highly similar sequences and full conservation of their Cys residues (Table 1) [10,11].

The use of recombinant techniques allows us to obtain the single protein desired in highly pure and concentrated solutions, and complexed with the desired metal ion. Precisely, in this work, the

* Corresponding author. Tel.: +34 93 5814532; fax: +34 93 5813101.
E-mail address: oscar.palacios@uab.cat (Ò. Palacios).

0039-9140/$ – see front matter © 2010 Elsevier B.V. All rights reserved.
doi:10.1016/j.talanta.2010.10.060

Table 1
Sequences of the recombinant metallothionein isoforms of *Helix pomatia* (HpMT: two isoforms, one specific for Cd and the other specific for Cu) and *Cornu aspersum* (CaMT: three isoforms, Cd, Cu and Cd/Cu without clear specificity) used in this work. The initial GS residues are a consequence of the expression system used, based on fusion protein synthesis and ulterior cleavage [13].

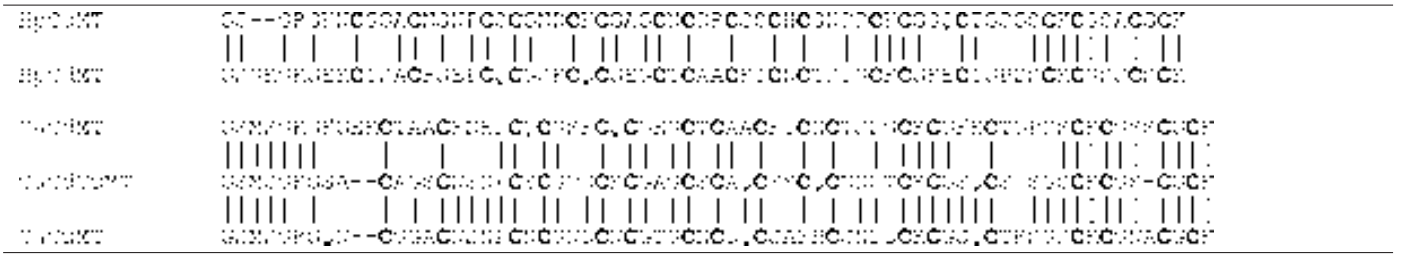

snail MT species produced by bacteria grown in Zn-enriched media have been considered. Our goal was the analysis of the ESI-TOF MS spectra recorded when mixing, at different molar ratios, the Zn-complexes of the several MTs of a same snail species, this is, HpCuMT and HpCdMT isoforms from *H. pomatia*, and CaCuMT, CaCdMT and CaCdCuMT isoforms from *C. aspersum*, both at neutral pH (for the analysis of the Zn-loaded MT form peaks) and at acidic pH (for the consideration of the corresponding apo-form signals).

2. Materials and methods

The Zn-complexes of HpCuMT, HpCdMT, CaCuMT, CaCdCuMT and CaCdMT were obtained following the recombinant methodology routinely used by this group [13], and already extensively applied to a considerable amount of MTs [14]. The full characterization of their metal-binding features will be the object of further reports (in preparation), so that this work only refers to the ESI-MS behaviour of their respective Zn-complexes.

The recombinantly expressed MT complexes were analyzed for element composition (S, Zn, Cd and Cu) by inductively coupled plasma atomic emission spectroscopy (ICP-AES) on a Polyscan 61E spectrometer (Thermo Jarrell Ash Corporation, Franklin, MA, USA) at appropriate wavelengths (S, 182.040 nm; Zn, 213.856 nm; Cd, 228.802 nm; Cu, 324.803 nm). Samples were prepared either at "conventional" (dilution with 2% HNO_3 (v/v)) [15], or at "acidic" (incubation in 1 M HCl at 65 °C for 5 min) conditions [16]. MT concentration in the recombinant preparations was calculated assuming that the only contribution to their S content was that made by the MT peptides. In all cases, the RSD in the concentration of S or Zn was lower than 5%, and the amounts of Cu and Cd were always lower than the detection limit.

Several experiments were run with samples at 3 different concentrations: 10, 50 and 100 μM of each protein, which covers the common range in agreement with the sensibility of the instrument. The spectra recorded at any concentration were mainly coincident, and for this reason, suppression of signal was not considered. The spectra shown in this work are those recorded at 100 μM, which showed better S/N ratio.

Molecular mass determination was performed by electrospray ionization mass spectrometry equipped with a time-of-flight analyzer (ESI-TOF MS) using a Micro Tof-Q Instrument (Bruker Daltonics Gmbh, Bremen, Germany) calibrated with NaI (200 ppm NaI in a 1:1 H_2O:isopropanol mixture), interfaced with an Series 1100 HPLC pump (Agilent Technologies) equipped with an autosampler, both controlled by the Compass Software. The experimental conditions for analyzing the samples were: 20 μL were injected through a PEEK long tube (1.5 m × 0.18 mm i.d.) at 40 μL/min under the following conditions: capillary-counterelectrode voltage, 5.0 kV; desolvation temperature, 90–110 °C; dry gas 6 L/min. Spectra were collected throughout an m/z range from 800 to 2000. The liquid carrier was a 95:5 mixture of 15 mM ammonium acetate and acetonitrile, for the analysis at pH 7.0, and for the analysis at acidic pH, a 95:5 mixture of 5 mM formic acid and acetonitrile adjusted at pH 2.4. All the samples were analyzed at least in duplicate to ensure reproducibility. In all cases, molecular masses were calculated according to the method in [17].

3. Results and discussion

The two terrestrial snails *H. pomatia* and *C. aspersum*, synthesize metal-specific MTs in different cell types and under different physiological requirements [10,11]. In Table 1, the sequences of all the peptides used in this work are compared through their Clustal X alignment [18]. It is worth noting the high similarity (more than 50% for all pairs) among all the sequences and the absolute conservation of their Cys residues (Table 2).

Once the five recombinant Zn–MT complexes had been synthesized, mixtures containing the isoforms of a same organism (*i.e.* Zn–HpCdMT plus Zn–HpCuMT; and Zn–CaCdMT plus Zn–CaCdCuMT and Zn–CaCuMT) at different molar ratios were prepared and analyzed by ESI-TOF MS at neutral and acidic (2.4) pH, to respectively obtain information about the Zn- and apo-forms present in the sample. In all cases, the ESI-MS spectra recorded from 800 to 2000 m/z units were deconvoluted in order to avoid the differences in intensity that can be observed among different charge states of the same mixture.

The spectra obtained for the mixture of *H. pomatia* isoforms (Zn–HpCdMT and Zn–HpCuMT) at neutral pH (Fig. 1) show that HpCdMT renders mainly a major peak, Zn_6–HpCdMT, together with minor signals corresponding to lower nuclearities, while the HpCuMT isoform yields three much more similar peaks identified as the Zn_6–HpCuMT, Zn_5–HpCuMT and Zn_4–HpCuMT species. However, the intensities observed for both Zn_6-species at 1:1 equimolar ratio clearly reveal a higher sensitivity of the Zn–HpCdMT preparation than that of Zn–HpCuMT to be ionized under our working conditions. Hence, when increasing the amount of the HpCuMT isoform, maintaining the concentration of HpCdMT at 50 μM, the intensity of the HpCuMT peak clearly increased but the ratio between both major peaks did not change in accordance with their relative abundance. In fact, it was necessary to raise the HpCuMT: HpCdMT ratio to nearly threefold to achieve the same ESI-MS intensity for both Zn_6-species. Interestingly, the intensity ratios between Zn_6–HpCuMT, Zn_5–HpCuMT and Zn_4–HpCuMT were constant along the mixtures.

Table 2
Analysis of the sequence similarities (identity) among the MT isoforms of each organism studied: *H. pomatia* and *C. aspersum*.

Identity	
Hp**Cu**MT *vs.* Hp**Cd**MT	56.9%
Ca**Cd**MT *vs.* Ca**Cu**MT	51.5%
Ca**Cd**MT *vs.* Ca**CdCu**MT	54.5%
Ca**Cu**MT *vs.* Ca**CdCu**MT	68.7%

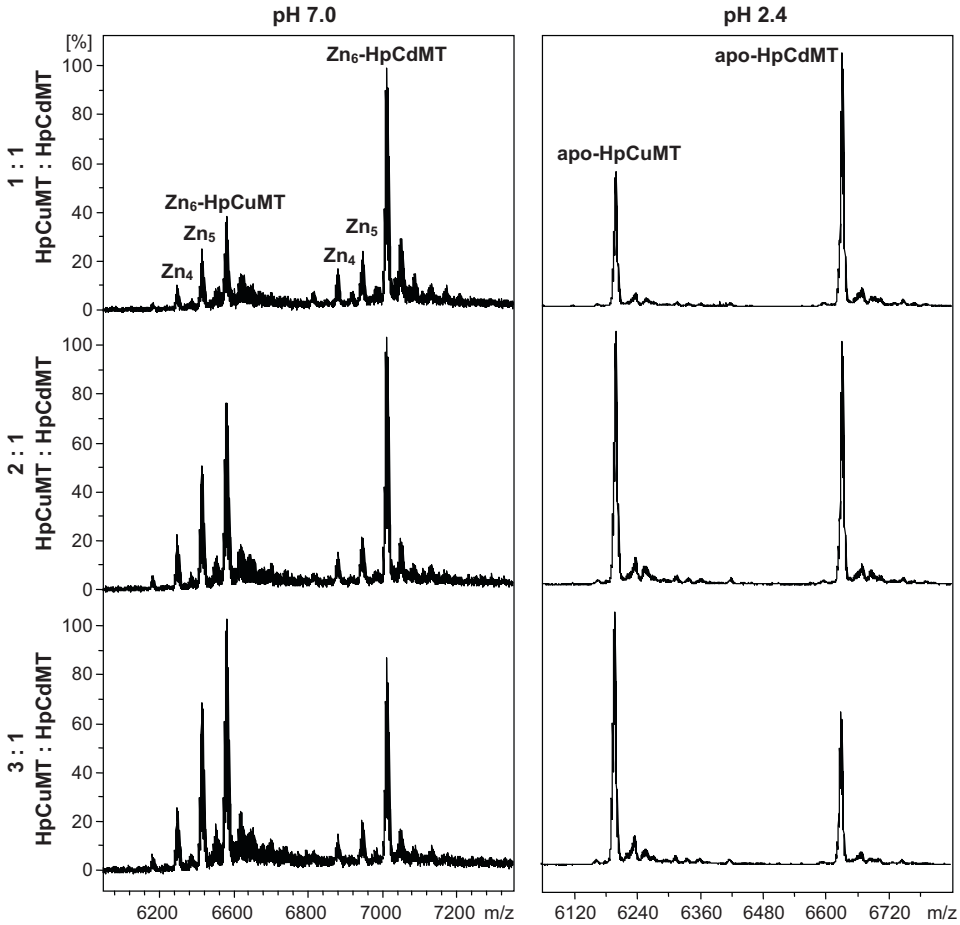

Fig. 1. Deconvoluted ESI-TOF MS spectra recorded both at pH 7.0 and at pH 2.4 for distinct mixtures of the preparations of the recombinant Zn-complexes of the HpCuMT and HpCdMT *Helix pomatia* MT isoforms at the indicated molar ratios. In all cases the starting material where the Zn complexes of the respective isoforms, which at acid pH render the corresponding apo-forms.

The same measurements run at acidic pH (Fig. 1) revealed that the propensity of the apo-HpCdMT peptide to ionization was also higher than that of HpCuMT, but interestingly, here only a 1:2 ratio was required to reach similar ESI-MS peak intensities. Therefore, again the ESI-MS intensity ratios between both apo-forms were not changing in proportion to their relative abundance in the sample.

Overall these results are consistent with a much higher sensitivity to be ionized of the Cd isoform (HpCdMT) of *H. pomatia* than the corresponding Cu isoform (HpCuMT) when analyzing either their Zn- or their apo-forms.

The mixture of the three *C. aspersum* isoform Zn–MT complexes (*i.e.* Zn–CaCdMT, Zn–CaCuMT and Zn–CaCdCuMT) at neutral pH (Fig. 2) informed about the different speciation yielded by each isoform. While Zn_6–CaCdMT was the clearly major species in the Zn–CaCdMT preparation, synthesis of the Cu- and the CdCuMT isoforms as Zn-complexes rendered mixtures of several metallated species. It is worth noting that the differences of the molecular masses of the 3 peptide apo-forms (Table 3) allow perfect identification in the spectra of the respective metal-loaded complexes. If only the major peak of each preparation is considered, it is observed that in the 1:1:1 equimolar mixture, Zn_6–CaCdMT yields a clearly higher intensity than the Zn_6–species of the other two isoforms. Doubling the molar ratios of Zn–CaCuMT and Zn–CaCdCuMT in relation to Zn–CaCdMT, produced a slight increase in the intensities of their peaks, although they were not proportionally doubled. In parallel to the observation for the HpMT isoforms (see above), a threefold CaCuMT:CaCdMT ratio was also required for both Zn_6-species to reach the same signal intensity in the spectra. Also as already observed for *H. pomatia*, the ESI-MS peak intensity ratios rendered by the Zn–MT complexes of the same isoform exhibiting different stoichiometry were constant in all the measurements.

The analysis at acidic pH of the mixtures of Zn–CaMT preparations at different ratios (Fig. 2) revealed that the apo-CaCdCuMT peptide exhibits a higher sensitivity to ionization than the corresponding Zn_6-species, at neutral pH. Thus, at the 1:1:1 equimolar conditions, both apo-CaCdCuMT and apo-CaCdMT showed similar ESI-MS peak intensities. Interestingly, the increase in the amount of CaCdCuMT in the mixture provoked a clear increase in the relative intensity of its signals, which was not as well observed in the case of CaCuMT. Finally apo-CaCuMT yielded the same peak intensity than apo-CaCdMT at a 2:1 molar ratio.

Therefore, and contrarily to the observations for the *H. pomatia* MT isoforms, not all the *C. aspersum* MT isoforms behaved equally as Zn-complexes (neutral) than as apo-peptides (acidic pH ESI-MS measurements), since CaCdCuMT showed a patently higher sensitivity to ionization at pH 2.4 than at pH 7.0.

The data obtained from the ESI-MS analysis of the apo-forms and the Zn-complexes corresponding to two *H. pomatia* and three *C. aspersum* MT isoforms suggest different lines of discussion. First, the ESI-MS ionization sensitivity of each MT peptide appears to vary depending to their metallation state, this is if they are in holo- or apo-form, although each MT isoform behaves differently to this respect. These disparities could be attributed to dissimilarities in their amino acid composition. However, the analysis of the sequence of each MT isoform (Table 3) reveals that they share

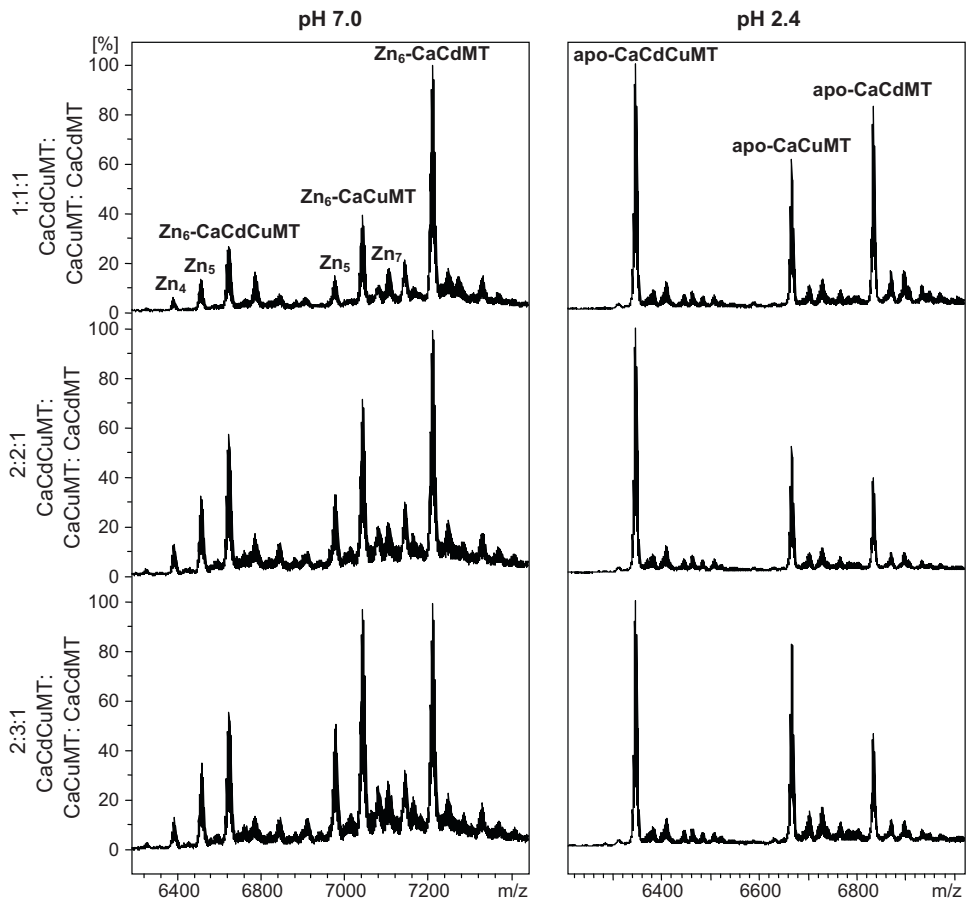

Fig. 2. Deconvoluted ESI-TOF MS spectra recorded both at pH 7.0 and at pH 2.4 for distinct mixtures of the CaCdMT, CaCdCuMT and CaCuMT *Cornu aspersum* MT isoforms at the indicated molar ratios. In all cases the starting material where the Zn complexes of the respective isoforms, which at acid pH render the corresponding apo-forms.

Table 3
Analysis of several features of the polypeptide chain of the different MT isoforms of *H. pomatia* and *C. aspersum* studied.

Protein	Molecular mass	Theoretical pI	Peptide length (C + H)	Polar aa (%)	Apolar aa (%)
Hp**Cu**MT	6261.92	8.13	65 (18 + 1)	16.9 ($4^-/7^+$)	24.6
Hp**Cd**MT	6625.54	8.29	67 (18 + 0)	23.9 ($6^-/10^+$)	20.9
Ca**Cu**MT	6658.29	7.91	67 (17 + 1)	14.9 ($4^-/6^+$)	22.4
Ca**CdCu**MT	6339.06	7.87	66 (18 + 0)	12.1 ($3^-/5^+$)	22.8
Ca**Cd**MT	6824.81	8.29	69 (18 + 0)	23.1 ($6^-/10^+$)	23.2

most of their features, the only significative differences arising from their content in polar amino acids, both acidic and basic ones. The higher percentage of polar amino acids of the HpCdMT sequence, around 24%, would ensure a higher ionization potential than for HpCuMT, at any conditions, as observed in our experiments (Fig. 1). Unfortunately, this reasoning cannot be used when considering the results obtained for CaCdCuMT: this peptide shows the lowest percentage of polar amino acids in its sequence, and it behaves at neutral pH similarly to CaCuMT, which exhibits also low amount of polar amino acids, but, unexpectedly, at acidic pH it shows always the highest ESI-MS intensities among the peaks observed. Consequently, the behaviour of CaCdCuMT does not correlate with the expected behaviour if only considering the amino acid sequence, namely the number of polar amino acids.

On the other hand, it is worthwhile to highlight that the metal–MT species of the same peptide but that differ in their metal content (for example, Zn_6–HpCuMT, Zn_5–HpCuMT and Zn_4–HpCuMT) preserve their relative ESI-MS peak intensities at any of the conditions assayed, thus confirming that the differential behaviour of a metal–MT complex depends on the nature of its peptide sequence more than in the relative metal load. Consequently, the mass data can afford a semi quantitative value for their determination.

4. Conclusions

The overall results allow reaching two main conclusions. First, it can be established that the electrospray ionization process of the MT molecules here studied clearly depends on their metallation state, *i.e.* if the proteins are analyzed at neutral pH (Zn-loaded forms) or at acidic pH (apo-forms).

Second, it can be deduced that every MT protein shows an individual and particular behaviour when ionized at certain conditions. Consequently, the intensities of the ESI-MS signals of distinct MT proteins, still if they are closely related isoforms of the same organism, cannot be directly related with their relative abundances in a sample, and this is correct even when these peptides or metal–MT complexes are analyzed under exactly the same conditions.

In spite of these two conclusions, we have also observed that the relative intensities of the ESI-MS peaks corresponding to differ-

ent species of the same protein that only differ in their metallation degree (metal–MT complexes of different stoichiometry) are maintained through the diverse experiments undertaken. Consequently, we can also state that peak intensities of similar species of the same MT peptide can be related with their relative abundance in the solution.

Acknowledgements

This work was supported by *Spanish Ministerio de Ciencia y Tecnología* grants BIO2009-12513-C02-01 to S. Atrian and BIO2009-12513-C02-02 to M. Capdevila. The authors of this work are recognized as a "Grup de Recerca" by the "Generalitat de Catalunya", ref. 2009SGR-1457. We thank the *Serveis Científico-Tècnics de la Universitat de Barcelona* and the *Servei d'Anàlisi Química (SAQ) de la Universitat Autònoma de Barcelona* for allocating ICP-AES and ESI-MS instrument time, respectively. We are also grateful to Reinhard Dallinger (University of Innsbruck, Austria) for the cDNA clones of the MTs included in this work and to Ayelen Pagani and Freddy Monteiro (Universitat de Barcelona) for MT syntheses.

Appendix A. Supplementary data

Supplementary data associated with this article can be found, in the online version, at doi:10.1016/j.talanta.2010.10.060.

References

[1] L. Shan, K. Jaffe, S. Li, L. Davis, J. Chromatogr. B 864 (2008) 22–28.
[2] J.J. Berzas Nevado, G. Castañeda Peñalvo, V. Rodríguez Robledo, G. Vargas Martínez, Talanta 79 (2009) 1238–1246.
[3] Y. Jiao, M. Su, M. Chen, W. Jia, Y. Chou, Z. Huang, N. Yang, W. Tong, J. Pharm. Biomed. Anal. 3 (2007) 1804–1807.
[4] A. Sigel, H. Sigel, R.K.O. Sigel (Eds.), Metal ions in Life Sciences; v 5: Metallothioneins and Related Chelators, Royal Society of Chemistry, Cambridge, UK, 2009, pp. 1–514.
[5] C.A. Blindauer, O.I. Leszczyszyn, Nat. Prod. Rep. 27 (2010) 720–741.
[6] H. Chassaigne, R. Lobinski, Anal. Chem. 70 (1998) 2536–2543.
[7] M.J. Stillman, D. Thomasa, C. Trevithick, X. Guob, M. Siu, J. Inorg. Biochem. 79 (2000) 11–19.
[8] L. Banci, I. Bertini, S. Ciofi-Baffoni, T. Kozyreva, K. Zovo, P. Palumaa, Nature 465 (2010) 645–650.
[9] R. Orihuela, F. Monteiro, A. Pagani, M. Capdevila, S. Atrian, Chem. Eur. J., in press.
[10] R. Dallinger, B. Berger, P.E. Hunziker, J.H.R. Kägi, Nature 388 (1997) 237–238.
[11] F. Hispard, D. Schuler, A. de Vaufleury, R. Scheifler, P. Badot, R. Dallinger, Environ. Toxicol. Chem. 27 (2009) 1533–1542.
[13] M. Capdevila, N. Cols, N. Romero-Isart, R. Gonzalez-Duarte, S. Atrian, P. Gonzalez-Duarte, Cell. Mol. Life Sci. 53 (1997) 157–166.
[14] R. Bofill, M. Capdevila, S. Atrian, Metallomics 1 (2009) 229–234.
[15] J. Bongers, C.D. Walton, D.E. Richardson, J.U. Bell, Anal. Chem. 60 (1988) 2683–2686.
[16] M. Capdevila, J. Domènech, A. Pagani, L. Tío, L. Villarreal, S. Atrian, Angew. Chem. Int. Ed. 44 (2005) 4618–4622.
[17] X. Yu, M. Wojciechowski, C. Fenselau, Anal. Chem. 65 (1993) 1355–1359.
[18] M.A. Larkin, G. Blackshields, N.P. Brown, R. Chenna, P.A. McGettigan, H. McWilliam, F. Valentin, I.M. Wallace, A. Wilm, R. Lopez, J.D. Thompson, T.J. Gibson, D.G. Higgins, Bioinformatics 23 (2007) 2947–2948.

Examples of ESI-TOF MS spectra:

Cornu aspersum,3:2:1 ratios, 100 uM, pH 2.4

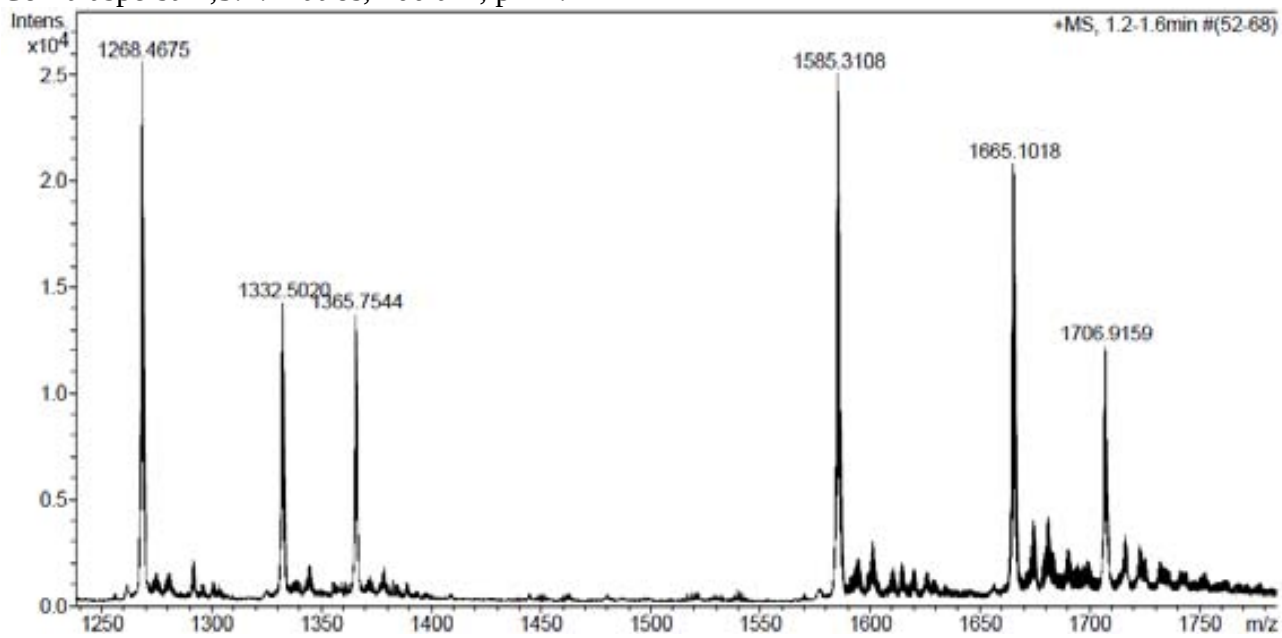

Helix pomatia, 1:1 ratio, 100 uM, pH 7

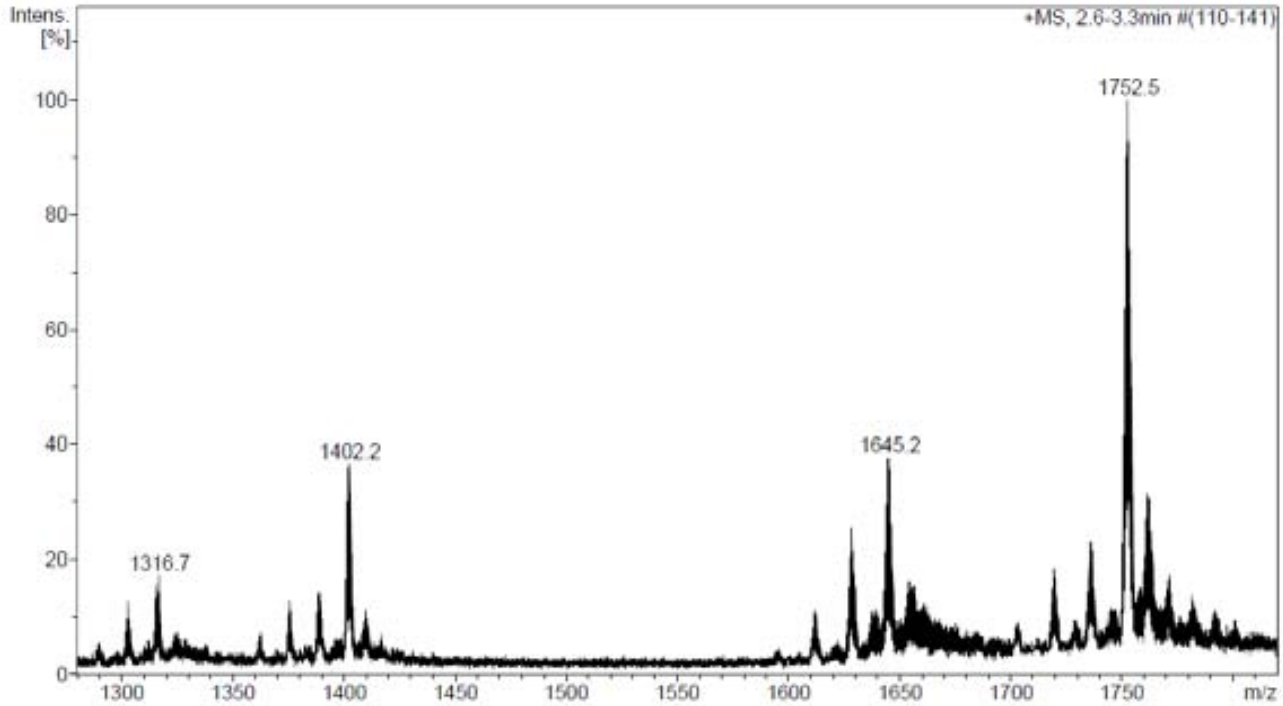

Helix pomatia, 2:1 ratio, 100 uM, pH 2.4

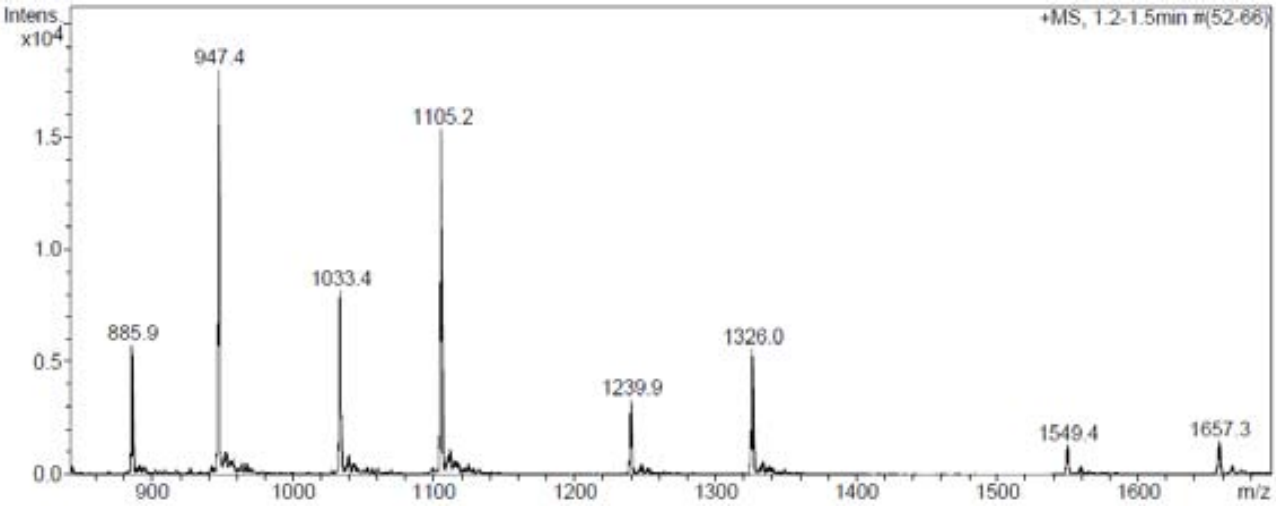

Helix pomatia, 2:1 ratio, 100 uM, pH 7

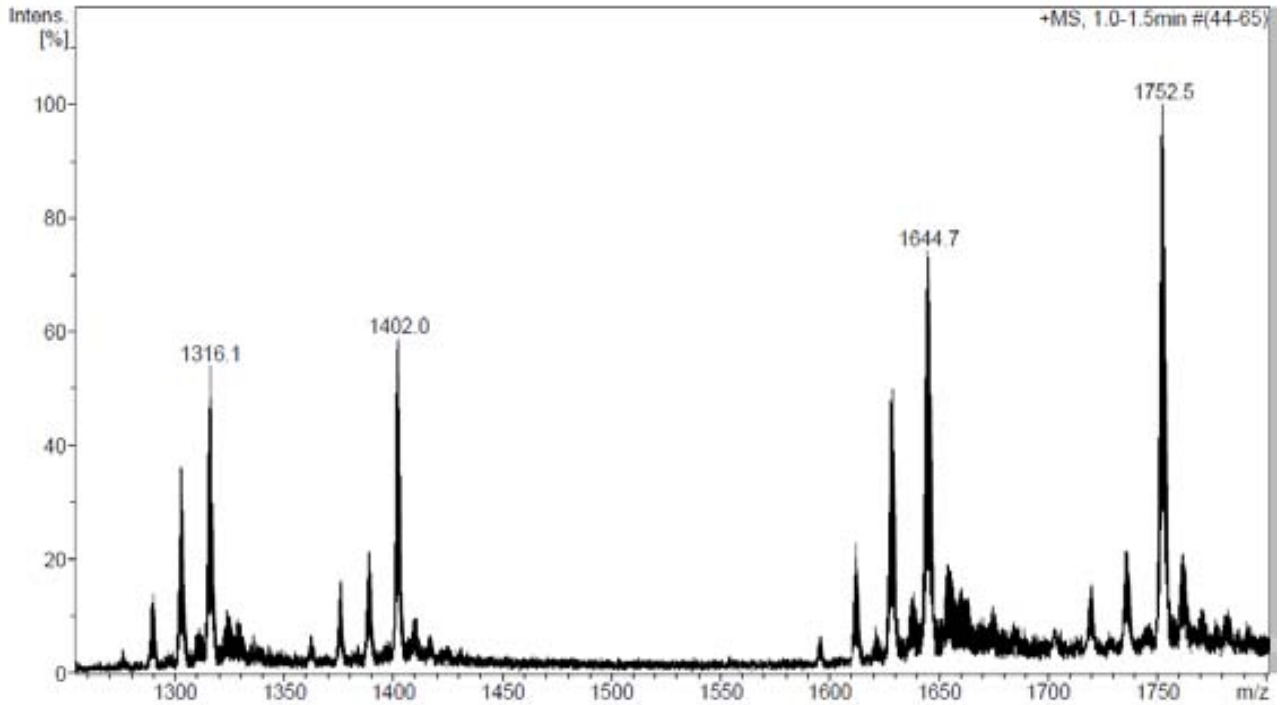

Cornu aspersum, 3:2:1 ratio, 100 uM, pH 7

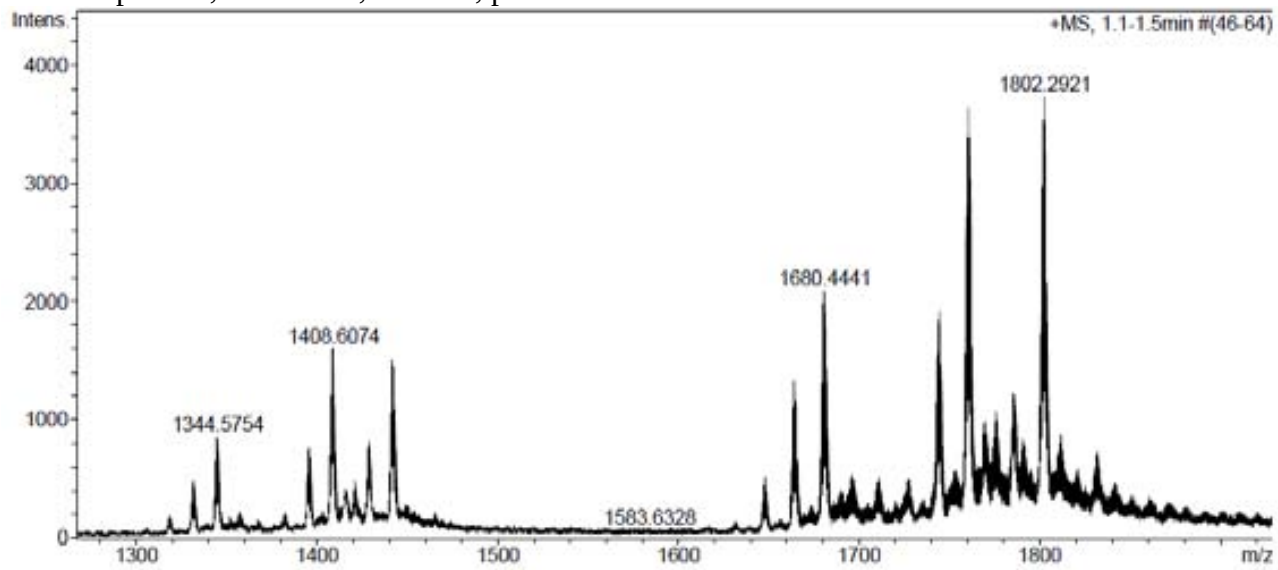

Cornu aspersum, 1:1:1 ratio, 100 uM, pH 2.4

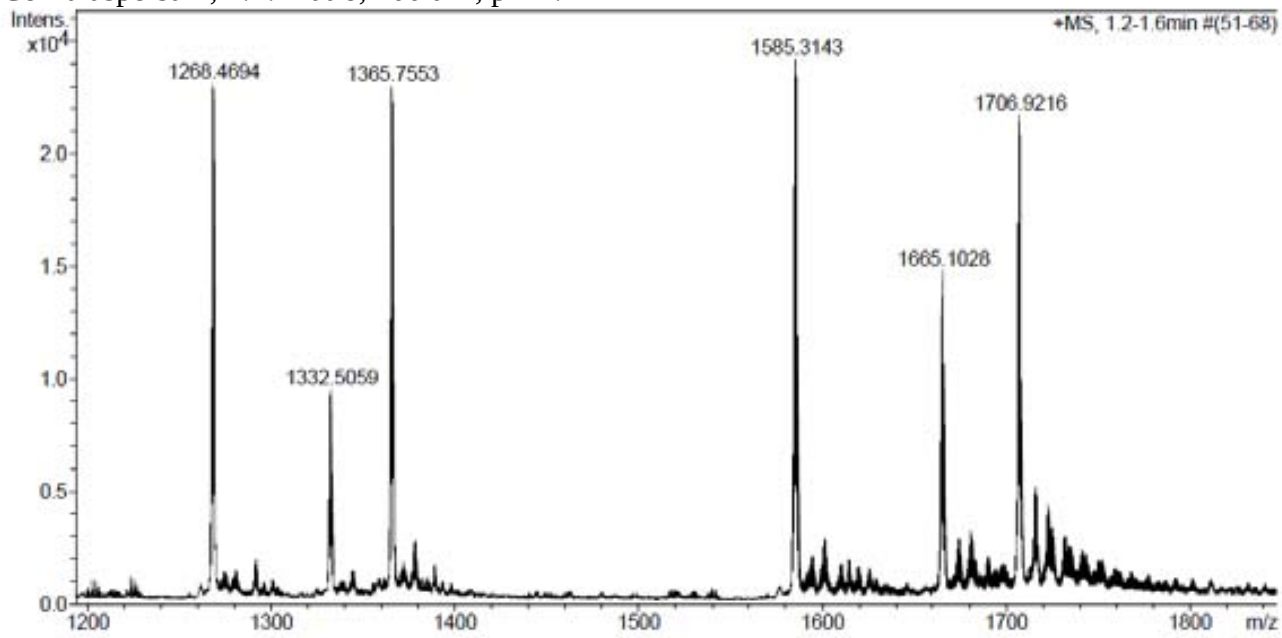

V. ARTICLE 5:

The metal binding abilities of *Megathura crenulata* metallothionein (McMT) in the frame of Gastropoda MTs

Journal of Inorganic Biochemistry, **(2011)**, 108, 84-90.

Journal of Inorganic Biochemistry 108 (2012) 84–90

Contents lists available at SciVerse ScienceDirect

Journal of Inorganic Biochemistry

journal homepage: www.elsevier.com/locate/jinorgbio

The metal binding abilities of *Megathura crenulata* metallothionein (McMT) in the frame of Gastropoda MTs

Sílvia Pérez-Rafael [a], Andreas Mezger [b], Bernhard Lieb [c], Reinhard Dallinger [d], Mercè Capdevila [a,*], Òscar Palacios [a], Sílvia Atrian [b]

[a] Departament de Química, Facultat de Ciències, Universitat Autònoma de Barcelona, 08193 Cerdanyola del Vallès, Barcelona, Spain
[b] Departament de Genètica, Facultat de Biologia, Universitat de Barcelona, Av. Diagonal 645, 08028 Barcelona, Spain
[c] Institute of Zoology, Johannes Gutenberg University of Mainz, 55099-Mainz, Germany
[d] Institute of Zoology, University of Innsbruck, A-6020 Innsbruck, Austria

ARTICLE INFO

Article history:
Received 27 May 2011
Received in revised form 13 November 2011
Accepted 14 November 2011
Available online 3 December 2011

Keywords:
Cadmium
Copper
Zinc
Metallothionein
Gastropoda
Evolution

ABSTRACT

Metallothioneins (MTs) are proteins that play a major role in metal homeostasis and/or detoxification in all kind of organisms. The MT gene/protein system of gastropod molluscs provides an invaluable model to study the diversification mechanisms that have enabled MTs to achieve metal-binding specificity through evolution. Most pulmonate gastropods, particularly terrestrial snails, harbor three paralogous isogenes encoding three MT isoforms with different metal binding preferences: the highly specific CdMT and CuMT isoforms, for cadmium and copper respectively, and the unspecific Cd/CuMT isoform. *Megathura crenulata* is a non-pulmonate gastropod in which only one MT isogene has so far been reported. In order to elucidate the metal binding character of the corresponding peptide (McMT), it has been recombinantly synthesized in the presence of Cd^{2+}, Zn^{2+} or Cu^{2+}, and the corresponding metal complexes have been analyzed using electrospray mass spectrometry, and CD and UV–visible spectroscopy. The metal-binding traits exhibited by McMT revealed that it is an unspecific MT, similarly to the pulmonate Cd/CuMT isoforms. This is in full concordance with the protein sequence distance analysis in relation to other gastropod MTs.

1. Introduction

Metallothioneins (MTs) are a super-family of small proteins, ubiquitous and probably polyphyletic, which coordinate heavy-metal ions through the metal-thiolate bonds established by their abundant cysteine residues [1]. Since their discovery in 1957 [2], metallothioneins have been the object of a great deal of studies in quite distinct areas of research (from biology and chemistry to medicine, toxicology and environmental sciences). Besides their role in different stress responses, as heavy metal chelators and/or free radical scavengers, MTs appear to be involved in physiological Zn and Cu homeostasis. This associates them with multiple processes [3], specific to each different group of organisms considered, and depending on their particular physiological needs. In particular, the extraordinary multiplication and diversification of MT isoforms along all the branches of the tree of life can be related to their ability to adapt and be useful for a great diversity of functions [4].

Gastropoda pulmonates constitute one of the most species-rich classes within the phylum of Mollusca in which divergent functional roles have been identified for their MT isoforms [5], so much so that these functions are thought to have driven the evolutionary differentiation of the corresponding peptides [6]. Particularly in the gastropod group of pulmonate snails, the members of the MT family exhibit a unique combination of two valuable properties which make this system a prime example for studies of evolutionary protein diversification: their isoforms are extremely specialized for binding distinct metal ions while exhibiting an extremely high sequence similarity (*cf.* Fig. 1). Pulmonates (*Helix pomatia*, *Cantareus aspersus* and *Biomphalaria glabrata*) synthesize three MT isoforms (CuMT, CdMT and Cd/CuMT) that are respectively isolated from native sources as homometallic Cu(I)- or Cd(II)-, or heterometallic Cu(I),Cd(II)-complexes. In accordance with their metal binding features, they have been assigned different metal-specific physiological roles. Hence, the CuMT isoforms, constitutively produced, are associated with the homeostasis of essential Cu, to secure it for haemocyanin biosynthesis [7], while the CdMT inducible isoforms play a role in the detoxification of non-essential, harmful Cd(II) [8]. On the other hand, the Cd/CuMT isoforms are natively isolated as complexes including both Cd(II) and Cu(I) simultaneously, although they are synthesized at minimal levels [9]. The fine-tuning of these metal-binding specificities seems to have been achieved by specific conditions of cellular environments (*i.e.* oxygen shielding of the homometallic Cu-HpCuMT species), and also by a coordinated evolution of the gene expression regulatory mechanisms, which ensures that transcription occurs only when and where it is needed [6]. Finally, it is worth noting that the analysis of

* Corresponding author. Tel.: +34 935813323; fax +34 93 5813101.
E-mail address: merce.capdevila@uab.cat (M. Capdevila).

0162-0134/$ – see front matter © 2011 Elsevier Inc. All rights reserved.
doi:10.1016/j.jinorgbio.2011.11.025

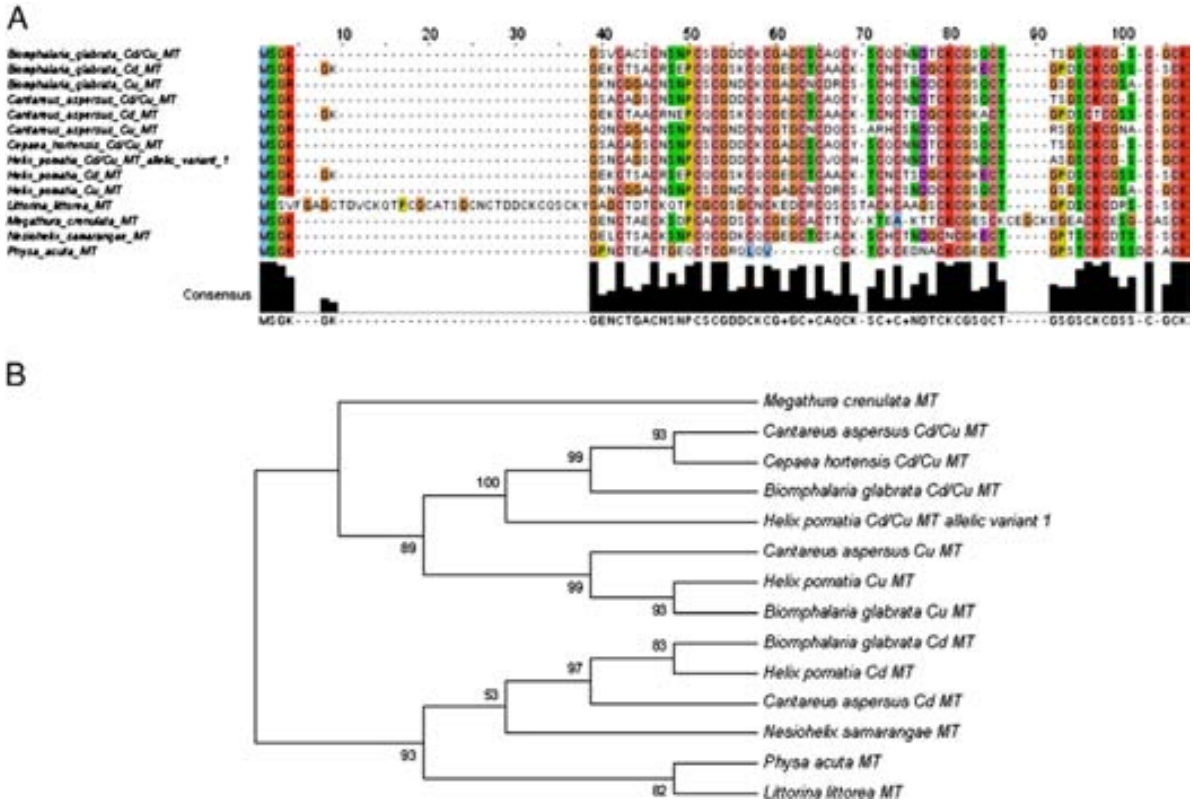

Fig. 1. (A) Multiple sequence alignment of all known Gastropoda MT proteins, performed as described in Materials and methods. (B) The Neighbor-joining phylogenetic tree of the sequence alignment, shown in (A), was constructed with a bootstrapping value of ×1000. The NCBI accession numbers of these sequences are as follows: *H. pomatia* CdMT, AAK84863; *H. pomatia* CuMT, AAK84864; *H. pomatia* Cd/CuMT, ACY71053; *B. glabrata* CdMT, ACS91928; *B. glabrata* CuMT, ACS91927; *B. glabrata* Cd/CuMT, ACS91929; *C. aspersus* CdMT, ABL73910; *C. aspersus* CuMT, ABM55268; *C. aspersus* Cd/CuMT, ABM92276; *N. samarangae* CdMT, ACC17831; *M. crenulata* MT, AAM51554; *L. littorea* MT, AAK56498; *C. hortensis*, ACX71837; *P. acuta*, ADB29127.

these MT protein sequence similarities clearly shows that the three pulmonate MT subfamilies share a common root in relation to other gastropod MTs, and that the Cd/CuMT and CuMT forms have likely evolved from a unique ancestor, clearly segregated from the CdMT line [6].

In this scenario, a question that clearly arises is the situation of the MT system in non-pulmonate gastropods, in which no polymorphism has been reported. Especially interesting is the case of *Megathura crenulata* (giant keyhole limpet), a marine gastropod belonging to the family of Fissurellids, which is greatly studied because its haemocyanin is used as an hapten carrier and immune stimulant. More precisely, the cDNA encoding for one *M. crenulata* MT (McMT) was isolated in 2003 [10] during a study aimed at identifying haemocyanin-encoding sequences. No sequencing or annotation has been performed for the *M. crenulata* genome, and therefore the existence of other MT genes cannot be completely ruled out. However, at present there is no further evidence of other at least significantly expressed MT isogenes in this organism. From protein sequence considerations, McMT has been proposed as closely related to *H. pomatia* CuMT, HpCuMT, but also exhibiting some features related to the HpCdMT isoform [10]. However, these hypotheses have never been analyzed through the characterization of the metal coordinating properties of the McMT polypeptide.

Some years ago, our group proposed a new criterion for the functional classification of MTs based on the analysis of the ability of a MT peptide to yield unique, well-folded, homometallic complexes when coordinating either divalent metal ions (Zn(II) and Cd(II)) or monovalent metal ions (Cu(I)). This classification initially considered two MT categories, namely Zn-thioneins (or divalent metal ion-thioneins) *vs*. Cu-thioneins [11], but later on, it was expanded to a step-wise gradation between extreme, or genuine, Zn-(divalent metal-ions) and Cu-thioneins [12]. It is worth noting that protein distance trees fully reproduced the Zn-/Cu-thionein clustering resulting from our experimental criterion, which suggests that the MT amino acid sequences, even of distant, clearly non-homologous forms, somehow enclose the determinants for their metal ion type preference (cysteine pattern distribution, number and kind of intercalating residues, total peptide lengths). The application of these criteria to pulmonate MT isoforms yielded exemplary results for both CdMT and CuMT isoforms of *H. pomatia* [6] and *C. aspersus* [13]. Also concordantly, the Cd/CuMT isoform of *C. aspersus* (CaCd/CuMT) exhibited a mixture of metal-binding properties [13], which points to an intermediate, polyvalent metal-binding character. More specifically, this behavior was observed for MTs of other organisms, such as the yeast Crs5 [14] and the mammalian MT4 isoform [15], two non-extreme Cu-thioneins [12].

Therefore, and in view of the lack of studies on the coordination capabilities of the McMT protein, we decided to characterize its metal binding abilities by recombinant expression of its cDNA in *E. coli* cells grown in Zn(II), Cd(II) or Cu(II) enriched media, and subsequent characterization of the corresponding metal complexes [6], and the consideration of some clue features, such as the presence/absence of S^{2-} ligands in the recovered Cd(II)-MT species [16], or the equivalence of the results obtained in the copper-supplemented cultures depending on the aeration degree [14]. All our results allow the evaluation of the distinctive features of Zn- *vs*. those of Cu-thioneins [12], which furthermore yield results totally concordant with the analyzed position in protein similarity trees.

2. Experimental

2.1. McMT expression plasmid construction

The cDNA coding for the *M. crenulata* metallothionein McMT was initially inserted into the TopoTA-vector (Invitrogen). For the

synthesis of McMT as a GST-fusion protein, the corresponding coding sequence was subcloned into the *Bam*HI/*Xho*I sites of the pGEX-4T2 expression vector (General Electric-Health Care). These two restriction sites, as well as a final TGA translation stop codon, were respectively added to the 5′ and 3′ ends of the cDNA sequence present in TopoTA, by PCR amplification, using this plasmid as template and the following oligonucleotides as primers: 5′-CGCGGATC-CATGTCGGGCAAAGGAGAAAAC-3′ (upstream) and 5′-TAGCCTC-GAGTCACTTGCACGCACATCC-3′ (downstream). The 30-cycle amplification reaction was performed with the thermo resistant DNA polymerase Proof-Start Polymerase (Qiagen) under the following conditions: 30 s at 95 °C (denaturation), 30 s at 55 °C (annealing) and 30 s at 72 °C (elongation). The final product was analyzed by 1% agarose gel electrophoresis/ethidium bromide staining; and the band with the expected size was excised (QIAEX II Gel Extraction Kit, Qiagen). The extracted DNA and the pGEX-4T-1 vector were digested with *Bam*HI and *Xho*I, and after the ligation reaction (DNA Ligation Kit 2.1, Takara Bio Inc.), the recombinant plasmids were transformed into *E. coli DH5α* for integrity and identity analysis, and into the *E. coli* BL21 protease deficient strain for protein synthesis. DNA sequence was determined using the Big Dye Terminator 3.1 Cycle Sequencing Kit (Applied Biosystems) in an Applied Biosystems ABIPRISM 310 Automatic Sequencer.

2.2. Recombinant synthesis and purification of the metal-McMT complexes

The McMT-GST fusion polypeptides were biosynthesized in 3 L cultures of transformed *E. coli* cells (BL21 strain). Expression was induced with isopropyl ß-D-thiogalactopyranoside (IPTG) and cultures were supplemented with 500 μM $CuSO_4$, 300 μM $ZnCl_2$ or 300 μM $CdCl_2$, final concentrations, and they were allowed to grow for a further 3 h. Cu-supplemented cultures were grown either under normal aeration conditions (1 L of media in a 2-L Erlenmeyer flask, at 250 rpm) or under low oxygen conditions (1.5-L of media in a 2 L-Erlenmeyer flask, at 150 rpm) [14]. Total protein extract was prepared from these cells as previously described in [17]. Metal complexes were recovered from the McMT-GST fusion constructs by thrombin cleavage and batch-affinity chromatography using Glutathione-Sepharose 4B (General Electric HC). After concentration using Centriprep Microcon 3 (Amicon), the metal complexes were finally purified through FPLC in a Superdex75 column (General Electric HC) equilibrated with 50 mM Tris–HCl, pH 7.5. Selected fractions were confirmed by 15% SDS-PAGE and kept at −80 °C until further use. All procedures were performed using Ar (pure grade 5.6) saturated buffers, and all syntheses were performed at least twice to ensure reproducibility. Further details on the purification procedure can be found in [17]. As a consequence of the cloning requirements, the dipeptide Gly–Ser was present at the N-terminus of the McMT polypeptides; however, this had previously been shown not to alter the MT metal-binding capacities [18]. Hence, the sequence of the recombinantly synthesized McMT was GSMSGKGENCTAECKSDPCACGDSCK CGEGCACTTCVKTEAKTTCKC GESCKCEGCKEGEACKCESGCASCK, with an average calculated molecular mass of 7203.19 Da.

2.3. In vitro Zn-, Cd- and Cu-binding studies of McMT

The titrations of the Zn-McMT preparation with Cd(II) or Cu(I) at pH 7 were carried out following the methodology previously described [17–19], using $CdCl_2$ or $[Cu(CH_3CN)_4]ClO_4$ solutions, respectively. The *in vitro* acidification/reneutralization experiments were also performed by adapting the procedure reported in [20]. Essentially, 10–20 μM preparations of the *in vivo* synthesized Cd-McMT were acidified from neutral (7.0) to acid pH (1.0) with HCl, kept at pH 1.0 for 20 min and subsequently reneutralized to pH 7.0 with NaOH. CD and UV–vis spectra (see below) were recorded at different pH throughout the acidification/reneutralization procedure, both immediately after acid or base addition and 10 min later, always with identical results. During all experiments strict oxygen-free conditions were maintained by saturating all the solutions with Ar.

2.4. Spectroscopic analyses of the metal-McMT complexes

The S, Zn, Cd and Cu content of the Zn-, Cd- and Cu-McMT preparations was analyzed by means of Inductively Coupled Plasma Atomic Emission Spectroscopy (ICP-AES) in a Polyscan 61E (Thermo Jarrell Ash) spectrometer, measuring S at 182.040 nm, Zn at 213.856 nm, Cd at 228.802 and Cu at 324.803 nm. Samples were treated as in [21], but were alternatively incubated in 1 M HCl at 65 °C for 15 min prior to measurements in order to eliminate possible traces of labile sulfide ions, as otherwise described in [16]. Protein concentrations were calculated from the *acid* ICP-AES sulfur measure, assuming that all S atoms were contributed by the McMT peptide. A Jasco spectropolarimeter (Model J-715) interfaced to a computer (J700 software) was used for CD measurements at a constant temperature of 25 °C maintained by a Peltier PTC-351S apparatus. Electronic absorption measurements were performed on an HP-8453 Diode array UV–visible spectrophotometer. All spectra were recorded with 1-cm capped quartz cuvettes, corrected for the dilution effects and processed using the GRAMS 32 program.

2.5. ElectroSpray ionization mass spectrometry analyses of the metal-McMT complexes

MW determinations were performed by electrospray ionization time-of-flight mass spectrometry (ESI-TOF MS) on a Micro Tof-Q instrument (Bruker) interfaced with a Series 1200 HPLC Agilent pump, equipped with an autosampler, all of which were controlled by the Compass Software. Calibration was attained with 0.2 g NaI dissolved in 100 mL of a 1:1 H_2O:isopropanol mixture. Samples containing McMT complexes with divalent metal ions were analyzed under the following conditions: 20 μL of protein solution injected through a PEEK (polyether heteroketone) column (1.5 m × 0.18 mm i.d.), at 40 μL min^{-1}; capillary counter-electrode voltage 5 kV; desolvation temperature 90–110 °C; dry gas 6 L min^{-1}; spectra collection range 800–2500 m/z. The carrier buffer was a 5:95 mixture of acetonitrile: ammonium acetate/ammonia (15 mm, pH 7.0). Alternatively, the Cu-McMT samples were analyzed as follows: (20 μL) of protein solution injected at 40 μL min^{-1}; capillary counter-electrode voltage 3.5 kV; lens counter-electrode voltage 4 kV; dry temperature 80 °C; dry gas 6 L min^{-1}. Here, the carrier was a 10:90 mixture of acetonitrile:ammonium acetate, 15 mM, pH 7.0. For analysis of apo-McMT and Cu-McMT preparations at acidic pH, 20 μL of the corresponding sample were injected under the same conditions described previously, but using a 5:95 mixture of acetonitrile:formic acid pH 2.4, as liquid carrier, which caused the complete demetalation of the peptides loaded with Zn(II) or Cd(II) but kept the Cu(I) ions bound to the protein.

2.6. Phylogenetic and protein distance analysis

The protein sequences of 14 mollusc MTs were obtained from the GenBank Database at NCBI. Sequence alignments were performed using the T-Coffee web service [22] and the corresponding results were edited and analyzed using Jalview [23] selecting the ClustalW color scheme. Protein alignments were then loaded onto the MEGA 4 software package [24] to construct the corresponding phylogenetic trees using the neighbor-joining method and the Kimura 2-parameter substitution model [25]. Bootstrapping (1000 replications) was also calculated as statistical support for all the nodes on the tree [26].

3. Results and discussion

3.1. Phylogenetic and protein distance analysis of McMT

The McMT protein is patently homologous to the other known gastropoda MTs (Fig. 1). Specifically, the number and residues of Cys residues are completely conserved. The previous analysis of the cDNA-deduced McMT sequence [10] already pointed to the peculiar insertion of 5 residues in the C-terminal moiety of the McMT that is unique among all gastropoda MTs reported to date (Fig. 1A). In this work, we have further analyzed the similarity between all these MTs. From the construction of the corresponding protein sequence distance tree (Fig. 1B), it is evident is that in the snail species in which 3 MT isoforms are known (the pulmonates *H. pomatia*, *C. aspersus* and *B. glabrata*), the peptides cluster together according to their metal specificities (Cd/CuMTs, CuMTs and CdMTs), showing that the generation of the isoform *triplicity* precedes the speciation event of pulmonates. There are 4 species from which only one MT isoform has so far been reported. Three of them group within the CdMT branch: the pulmonates *Physa acuta* and *Nesiohelix samarangae* MTs and the non-pulmonate *Littorina littorea* MT. Only the latter has been investigated with respect to its function, which has been shown to be related to freezing and anoxia stress reactions [27]. This coincides with the implication in the response to multiple stressors reported for snail CdMTs [28]. Otherwise, the non-pulmonate *M. crenulata* MT clusters within the group of Cd/CuMTs and CuMTs. This result is fully consistent with the previous observation that the McMT sequence is more similar to those of pulmonate snail CuMTs than to the corresponding CdMT isoforms, although sharing some of the features typical of the later [10]. In fact, the partial resemblance to CdMTs then reported is here shown to be a resemblance to the ambivalent Cd/CuMT isoforms, which had not been discovered at that time, since McMT appears clustered in the tree with the Cd/CuMT and CuMT dicotomic branch, and not with CdMTs (Fig. 1B).

3.2. Identity and integrity of the recombinant McMT polypeptide

DNA sequencing confirmed that the pGEX-McMT expression plasmid included no nucleotide substitutions, and that the cDNA was cloned in the correct frame after the GST coding sequence. The identity, purity and integrity of the recombinant McMT was confirmed by ESI-MS analysis of its apo-form, obtained by acidification at pH 2.4 of the complexes synthesized in Zn-enriched cultures (Zn-McMT). Hence, a unique peak of 7203.0 Da was detected (data not shown), in accordance with a theoretical MW of 7203.2 Da calculated for the recombinant McMT peptide including N-terminal Gly and Ser residues derived from the GST-fusion construct (Fig. 2E).

3.3. Zn-binding abilities of McMT

The recombinant synthesis of McMT in Zn-supplemented *E. coli* cultures produced a major Zn_6-McMT complex, together with minor Zn_5- and Zn_4-McMT species (Fig. 2A). These results are very similar to those reported for the synthesis at equivalent conditions of the *H. pomatia* (HpCdMT) [6] and *C. aspersus* (CaCdMT) [13] Cd-specific MT isoforms. However, the CD spectrum of the Zn-McMT preparation shows an unusual fingerprint, with two maxima at 230 and 245 nm (Fig. 3A). To our knowledge, only the recombinant Zn-βckMT peptide (β domain of chicken MT) afforded a similar CD fingerprint (Fig. 3C). In this case, it was shown that the 230 nm absorption could not be attributed to the presence of additional ligands (sulfide or/and chloride), so it was finally ascribed to protein conformation contributions at high wavelengths [29].

3.4. Cd-binding abilities of McMT

When *in vivo* synthesized by Cd-supplemented *E. coli* cells, McMT rendered a major (Cd_6-McMT) and also three minor species: Cd_7-, Cd_6S_1- and Cd_6S_2-McMT (Fig. 2B). The presence of S^{2-}-containing complexes in these samples was further confirmed by two additional results. First, by the difference between the conventional and acidic ICP-AES protein concentration measurements (0.080 mM *vs*. 0.071 mM, respectively) [16]. And second, by the CD absorption at *ca.* 290 nm characteristic of the Cd-S^{2-} chromophores [16] (spectra in red/gray of Fig. 3A). CD absorptions attributable to the presence of sulfide ligands at such high wavelengths have also been observed in the case of the yeast Cd-Crs5 recombinant preparations [16,30] (Fig. 3D). It is worth noting that the CD signals of the recombinant Cd-McMT preparation evolved with time, entailing an increase of the *ca.* 290 nm absorptions (contributed by the Cd-S^{2-} chromophores) and the concomitant decrease of the band at 250 nm (corresponding to the Cd-SCys chromophores) (Fig. 3B). This is a characteristic behavior of the Cd-loaded complexes of genuine Cu-thioneins, which we have already reported for the paradigmatic yeast Cup1 [31].

Cd-McMT complexes were obtained *in vitro* by two different procedures: (a) Cd(II) titration of Zn-McMT, and (b) acidification plus subsequent reneutralization of recombinant Cd-McMT. The full set of results of these two procedures is available as Supplementary Information (Fig. S1 and S2, respectively).

In the Zn(II)/Cd(II) McMT titration experiment (Fig. S1), the species obtained after the addition of 6 Cd(II) eq to the initial Zn_6-McMT are equivalent to those present in the recombinant Cd-McMT preparation, according to the ESI-MS results. Contrarily, the CD fingerprint of the titrated sample only slightly reproduces the *ca.* 250-nm region absorptions (Fig. 3A). The addition of Na_2S (Aldrich sodium sulfide nonahydrate, more that 99.99% metal free) to the titration solution, after the 6-Cd(II)-eq step, afforded a CD spectrum more closely resembling that of the *in vivo* Cd-McMT preparation, especially because the 290-nm absorption was partially recovered, this attributable to the reconstruction of some S^{2-}-containing Cd(II)-McMT complexes (Fig. 3A). Finally, it is worth noting that the addition of further Cd(II) to Zn(II)-McMT promoted the formation of species with higher Cd(II) content, in contrast with the behavior of HpCdMT and CaCdMT, for which the addition of excess Cd(II) did not alter the metal-MT speciation [6 and 13, respectively].

The second *in vitro* approach was the acidification to pH 1.0 of the Cd-McMT preparation, in order to remove the acid-labile S^{2-} ligands as $H_2S_{(g)}$, with further reneutralization to pH 7.0 to recover the Cd-McMT forms refolded in the absence of sulfide ligands. This procedure yielded a mixture of species, from Cd_3- to Cd_7-McMT (ESI-MS data in Fig. S2), which exhibited CD spectra different from those of the *in vivo* Cd-McMT preparation, in this case, even after the addition of S^{2-} anions to the reneutralized solution (Fig. 3B).

Overall, although McMT renders major $M(II)_6$-McMT species when binding divalent metal ions (*i.e.* Zn_6-McMT and Cd_6-McMT), the presence of a subpopulation of S^{2-}-containing complexes in the Cd-McMT preparations, exhibiting all the typical features of the Cd-complexes formed by MTs with Cu-thionein character [16], precludes the classification of McMT as a genuine divalent metal ion-preferring thionein. These results rather suggest an *intermediate* metal-binding specificity [12], and are fully comparable to those of the pulmonate mixed CaCd/CuMT isoforms when synthesized in a Cd(II)-rich media [13].

3.5. Cu-binding abilities of McMT

McMT was recombinantly produced in the presence of Cu(II) surplus under normal and low aeration, since we have already shown how bacterial culture oxygenation can affect the metal content of

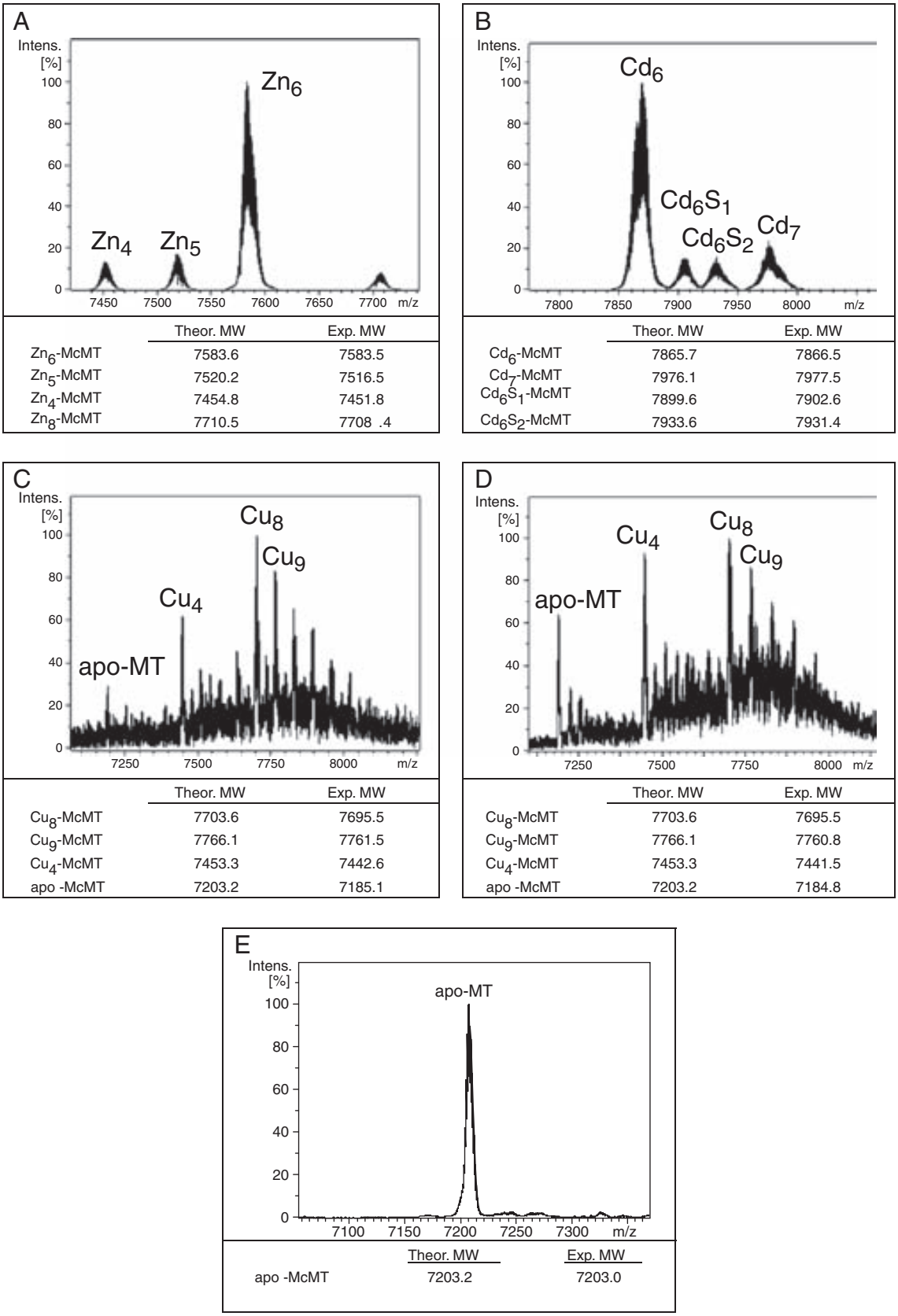

	Theor. MW	Exp. MW
Zn_6-McMT	7583.6	7583.5
Zn_5-McMT	7520.2	7516.5
Zn_4-McMT	7454.8	7451.8
Zn_8-McMT	7710.5	7708 .4

	Theor. MW	Exp. MW
Cd_6-McMT	7865.7	7866.5
Cd_7-McMT	7976.1	7977.5
Cd_6S_1-McMT	7899.6	7902.6
Cd_6S_2-McMT	7933.6	7931.4

	Theor. MW	Exp. MW
Cu_8-McMT	7703.6	7695.5
Cu_9-McMT	7766.1	7761.5
Cu_4-McMT	7453.3	7442.6
apo -McMT	7203.2	7185.1

	Theor. MW	Exp. MW
Cu_8-McMT	7703.6	7695.5
Cu_9-McMT	7766.1	7760.8
Cu_4-McMT	7453.3	7441.5
apo -McMT	7203.2	7184.8

	Theor. MW	Exp. MW
apo -McMT	7203.2	7203.0

Fig. 2. Deconvoluted ESI-MS spectra corresponding to the *in vivo* recombinant synthesis of McMT in (A) Zn-, (B) Cd-, and Cu-enriched media at (C) normal, (D) low aeration conditions (E) apo-form. The (C) and (D) spectra were exactly the same at pH 7.0 and at pH 2.4, therefore confirming the homonuclear nature of all the Cu-McMT complexes. The error associated with the experimental MW values was always lower than 1%, which allows a perfect correlation with the theoretical MW.

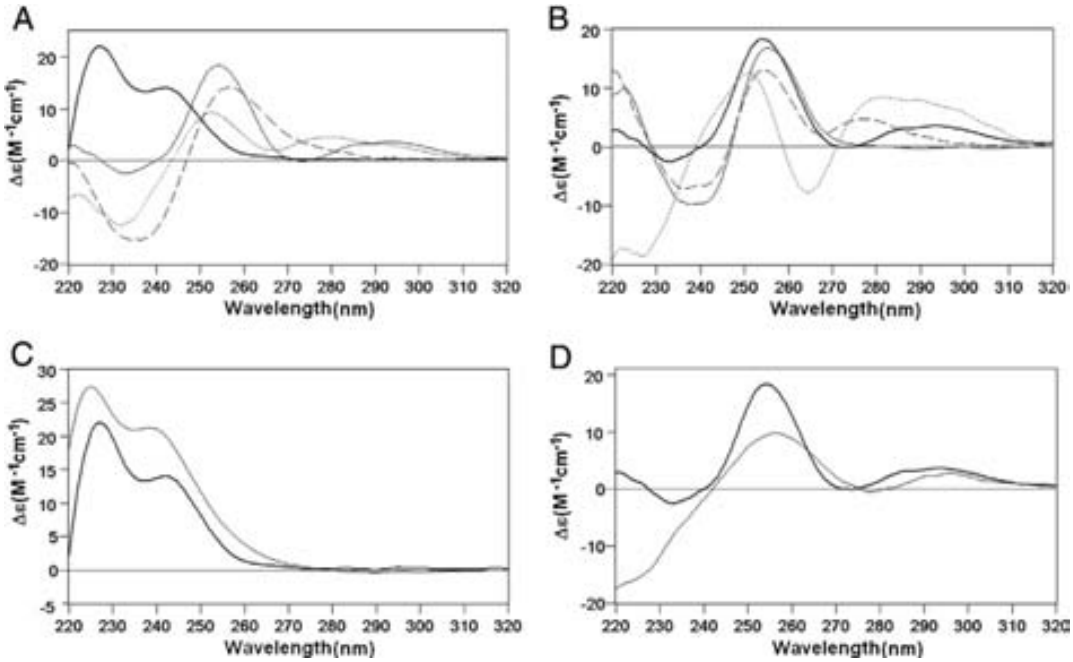

Fig. 3. CD spectra of distinct McMT preparations: (A) *in vivo* obtained Zn-McMT (solid black) and Cd-McMT (gray) preparations, and *in vitro* generated Cd-McMT preparations by addition of 6 Cd(II) eq (dashed) and 6 Cd(II) eq plus 2 S2− eq (dotted) to the *in vivo* Zn-McMT preparation; (B) *in vivo* Cd-McMT preparation before (solid black) and after acidification subsequent reneutralization of this sample (gray), the addition of 2 S2− eq to this reconstituted sample gave rise to the dashed spectrum and the dotted spectrum was recorded after 16 days evolution of the *in vivo* Cd-McMT preparation; (C) *in vivo* obtained Zn-McMT 18 (black) and Zn-βckMT (gray) preparations; (D) *in vivo* obtained Cd-McMT (black) and Cd-Crs5 (gray) preparations.

the complexes produced in these conditions [14,12]. In our current case, both McMT syntheses yielded practically identical results, if evaluated through the metal-MT species identified by ESI-MS both at pH 7 and pH 2 (Fig. 2C and D), and their respective CD spectra (Fig. 4). Hence, a mixture of several homometallic Cu(I)-McMT complexes, with Cu_8- as the major species, together with other minor homometallic species, even including the presence of apo-McMT, was observed.

The *in vitro* replacement of Zn(II) by Cu(I) in Zn_6-McMT allowed, after the addition of 10–12 Cu(I) equivalents, the reproduction of the features exhibited by the recombinant Cu-McMT preparations (*cf.* ESI-MS and CD data in Fig. 4 and Fig. S3). Interestingly, further addition of Cu(I) to the solution promoted the decrease of the CD signal intensity owing to metal release of the complexes, generating the corresponding apo-McMT peptides. This result could explain why apo-McMT is detected in the recombinant preparations of McMT obtained from Cu(II)-enriched cultures, as they would point to a clear instability of the Cu-McMT complexes in front of Cu(I) excess, either in an *in vivo* or *in vitro* environment.

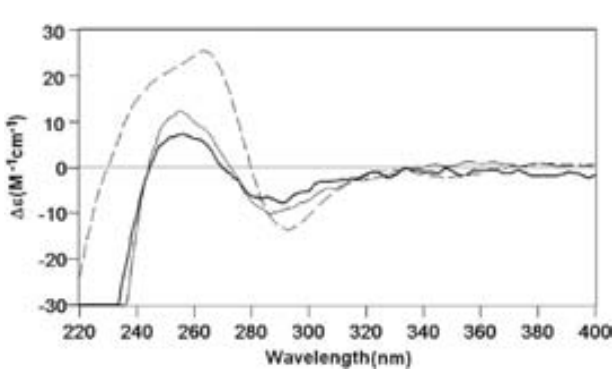

Fig. 4. CD spectra corresponding to the recombinant preparations of McMT in Cu-enriched media at normal (black) and low (gray) aeration conditions. The normalized CD spectrum in dashed corresponds to the addition of 10 Cu(I) eq to the *in vivo* Zn-McMT preparation.

Overall, the features of the McMT-Cu(I) coordination, especially the capacity to yield homometallic Cu(I)-complexes, correspond to a Cu-thionein, but the mixture of species recovered, as well as the low intensity of their CD signals, are far from matching those of genuine Cu-thioneins, resembling those reported for some clear Zn-thionein character [12].

4. Conclusions

The specificity for metal binding of McMT has been assessed according to the criteria previously applied to multiple MT isoforms of a diverse range of organisms [12], and recently to two pulmonate snail species [6,13]. McMT does not exhibit any definite metal specificity, rather behaving as the mixed Cd/Cu snail MT isoforms [6]. Hence, on the one hand, coordination of divalent metal ions (Zn(II) or Cd(II)) does not follow the model of genuine Zn- or Cd-thioneins, mainly because when McMT is biosynthesized in their surplus, it exhibits most of the typical features of Cu-thioneins when coordinating divalent metal ions [12,31]. Precisely, the corresponding Cd-McMT preparations include S^{2-}-containing complexes, this fact accounting for their time-evolving CD spectra, and for the impossibility to reproduce their spectroscopic features by *in vitro* preparation strategies (neither by Zn(II)/Cd(II) replacement or Cd-McMT denaturation/reconstitution reactions). On the other hand, despite McMT displays some typical characteristics of a Cu-thionein when synthesized in copper supplemented media, such as homometallic Cu(I)-species formation in both normal and low aeration culture conditions, these complexes exhibit a high instability, poor chiroptical properties, and they unfold in the presence of surplus copper concentration.

It is worth to note that this experimentally determined lack of metal specifity is fully concordant with the position of the McMT sequence in the protein distance trees, where it clusters with the Cd/Cu pulmonate MT isoforms. From the perspective of possible biological functions, the described metal binding peculiarities suggest that

McMT would be able to perform the diverse physiological functions that specific MTs carry out in pulmonate snails: cadmium detoxification as a CdMT, basal zinc metabolism and other stress (mainly oxidative stress) scavenging as a Zn-thionein, together with copper handing in relation to haemocyanin synthesis, as a Cu-thionein. At this point it should be remembered that the McMT transcript was precisely recovered when trying to isolate haemocyanin encoding mRNAs, and therefore the corresponding proteins are simultaneously present in time and localization in the limpet, something that is indicative of putative functional association.

Supplementary materials related to this article can be found online at doi:10.1016/j.jinorgbio.2011.11.025.

Abbreviations

MT	metallothionein
CaXMT	*C. aspersus* MT isoforms
HpXMT	*H. pomatia* MT isoforms
McMT	*M. crenulata* MT
CdMT	Cd-specific MT isoform
CuMT	Cu-specific MT isoform
Cd/CuMT	mixed metal MT isoform
ESI-MS	electrospray ionization mass spectrometry
ESI-TOF MS	electrospray ionization time-of-flight mass spectrometry

Acknowledgments

This work was financially supported by grants from the Spanish *Ministerio de Ciencia e Innovación* for the projects: BIO2009-12513-C02-01 (S. Atrian), and BIO2009-12513-C02-02 (M. Capdevila). These coordinated projects were co-financed by the European Union, through the FEDER program. The authors are members of the "Grup de Recerca de la Generalitat de Catalunya" ref. 2009SGR-1457. Cooperation with Innsbruck was financed by a grant (project no. P19782-B02) from the Austrian Science Foundation to R. Dallinger and by the "Acciones Integradas" grants HU2006-0027 (Spain) and ES 02/2007 (Austria). We are deeply grateful to Maria Guirola, from the Genetics Department of the *Universitat de Barcelona*, for her assistance in the protein distance tree calculations. We thank the *Serveis Científico-Tècnics de la Universitat de Barcelona* and the *Servei d'Anàlisi Química (SAQ) de la Universitat Autònoma de Barcelona* for allocating DNA sequencing, ICP-AES, CD, UV–vis and ESI-MS instrument time.

References

[1] Metallothioneins and Related Chelators, in: A. Sigel, H. Sigel, R.K.O. Sigel (Eds.), Metal Ions in Life Sciences, vol. 5, Royal Society of Chemistry, Cambridge, U.K, 2009.
[2] M. Margoshes, B.L. Vallee, J. Am. Chem. Soc. 79 (1957) 4813–4814.
[3] R.D. Palmiter, Proc Nat. Acad. Sci. U. S. A. 95 (1998) 8428–8430.
[4] M. Capdevila, S. Atrian, J. Biol. Inorg. Chem. 16 (2011) 991–1009.
[5] R. Dallinger, B. Berger, P. Hunziker, J.H.R. Kägi, Nature 388 (1997) 237–238.
[6] O. Palacios, A. Pagani, S. Perez-Rafael, M. Egg, M. Höckner, A. Brandstätter, M. Capdevila, S. Atrian, R. Dallinger, BMC Biol. 9 (2011) 4.
[7] R. Dallinger, M. Chabicovsky, E. Hödl, C. Prem, P. Hunziker, C. Manzl, Am. J. Physiol. 189 (2005) R1185–R1195.
[8] R. Dallinger, B. Berger, A. Bauer-Hilty, Mol. Cell. Biochem. 85 (1989) 135–145.
[9] F. Hispard, D. Schuler, A. de Vaufleury, R. Scheifler, P.M. Badot, R. Dallinger, Environ. Toxicol. Chem. 27 (2008) 1533–1542.
[10] B. Lieb, Comp. Biochem. Physiol. C 134 (2003) 131–137.
[11] M. Valls, R. Bofill, R. Gonzalez-Duarte, P. Gonzalez-Duarte, M. Capdevila, S. Atrian, J. Biol. Chem. 276 (2001) 32835–32843.
[12] R. Bofill, M. Capdevila, S. Atrian, Metallomics 1 (2009) 229–234.
[13] M. Höckner, K. Stefanon, A. de Vaufleury, F. Monteiro, S. Pérez-Rafael, O. Palacios, M. Capdevila, S. Atrian, R. Dallinger, Biometals (2011), doi:10.1007/s10534-011-9466-x.
[14] A. Pagani, L. Villarreal, M. Capdevila, S. Atrian, Mol. Microbiol. 63 (2007) 256–269.
[15] L. Tío, L. Villarreal, S. Atrian, M. Capdevila, J. Biol. Chem. 279 (2004) 24403–24413.
[16] M. Capdevila, J. Domenech, A. Pagani, L. Tio, L. Villarreal, S. Atrian, Angew. Chem. Int. Ed. Engl. 44 (2005) 4618–4622.
[17] M. Capdevila, N. Cols, N. Romero-Isart, R. González-Duarte, S. Atrian, P. González-Duarte, Cell. Mol. Life Sci. 53 (1997) 681–688.
[18] N. Cols, N. Romero-Isart, M. Capdevila, B. Oliva, P. Gonzàlez-Duarte, R. Gonzàlez-Duarte, S. Atrian, J. Inorg. Biochem. 68 (1997) 157–166.
[19] R. Bofill, O. Palacios, M. Capdevila, N. Cols, R. Gonzàlez-Duarte, S. Atrian, P. Gonzàlez-Duarte, J. Inorg. Biochem. 73 (1999) 57–64.
[20] J. Domenech, R. Orihuela, G. Mir, M. Molinas, S. Atrian, M. Capdevila, J. Biol. Inorg. Chem. 12 (2007) 867–882.
[21] J. Bongers, C.D. Walton, D.E. Richardson, J.U. Bell, Anal. Chem. 60 (1988) 2683–2686.
[22] C. Notredame, D. Higgins, J. Heringa, J. Mol. Biol. 302 (2000) 205–217.
[23] A.M. Waterhouse, J.B. Procter, D.M.A. Martin, M. Clamp, G.J. Barton, Bioinformatics 25 (2009) 1189–1191.
[24] K. Tamura, J. Dudley, M. Nei, S. Kumar, Mol. Biol. Evol. 24 (2007) 1596–1599.
[25] M. Kimura, J. Mol. Evol. 16 (1980) 111–120.
[26] J. Felsenstein, Evolution 39 (1985) 783–791.
[27] T.E. English, K.B. Storey, J. Exp. Biol. 206 (2003) 2517–2524.
[28] M. Egg, M. Höckner, A. Brandstätter, D. Schuler, R. Dallinger, Mol. Ecol. 18 (2009) 2426–2443.
[29] L. Villarreal, L. Tío, M. Capdevila, S. Atrian, FEBS J. 273 (2006) 523–535.
[30] A. Pagani, L. Villarreal, M. Capdevila, S. Atrian, Mol. Microbiol. 63 (2007) 256–269.
[31] R. Orihuela, F. Monteiro, A. Pagani, M. Capdevila, S. Atrian, Chem. A Eur. J. 16 (2010) 2363–12372.

The metal binding abilities of *Megathura crenulata* metallothionein (McMT) in the frame of Gastropoda MTs

S. Pérez-Rafael, A. Mezger , B. Lieb, R. Dallinger, M. Capdevila, Ò. Palacios, S. Atrian

The following material is available as supplementary figures in the on line version of this article:

Fig. S1 : Spectroscopic and ESI-MS data of the Cd(II) titration of a recombinant Zn-McMT 20 μM preparation.

Fig. S2 : Acidification, renaturalization and sulphide addition to a recombinant Cd-McMT 20 μM preparation.

Fig. S3 : Spectroscopic and ESI-MS data of the Cu(I) titration of a recombinant Zn-McMT 20 μM preparation. The ESI-MS data recorded after 14 Cu(I) eq added were identical as those showed for 14 Cu(I) eq added.

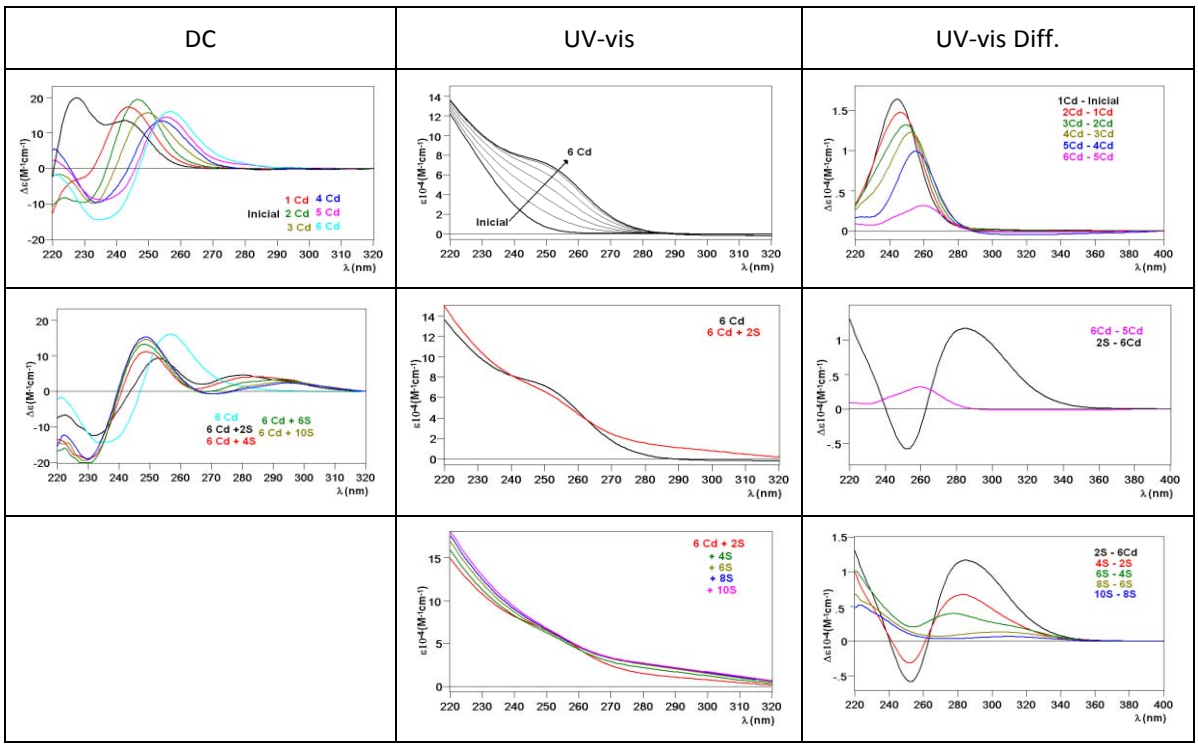

Eq of Cd(II) added	ESI-MS spectra at pH 7.0	Eq of Cd(II) added	ESI-MS spectra at pH 7.0
3 eq	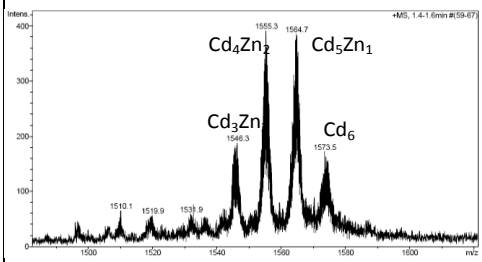	**6 eq**	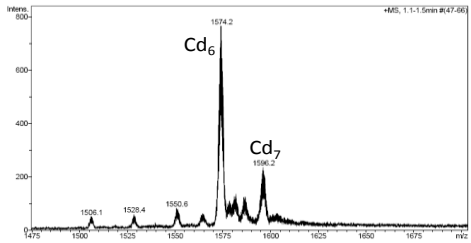
2 S^{2-}	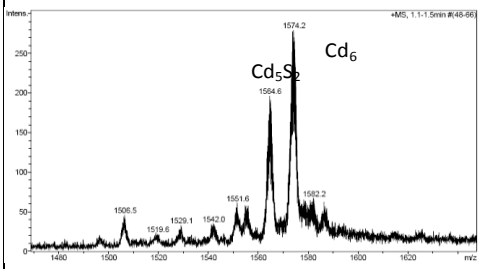	**4 S^{2-}**	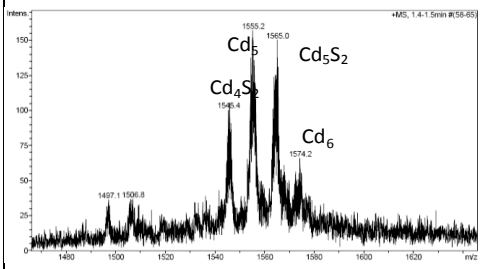
8 S^{2-}	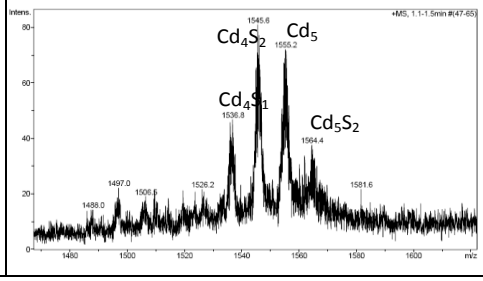	**10 S^{2-}**	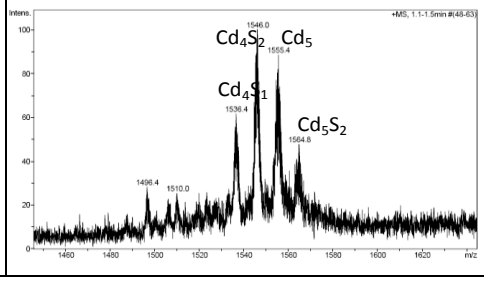

Fig. S1 : Spectroscopic and ESI-MS data of the Cd(II) titration of a recombinant Zn-McMT 20 μM preparation.

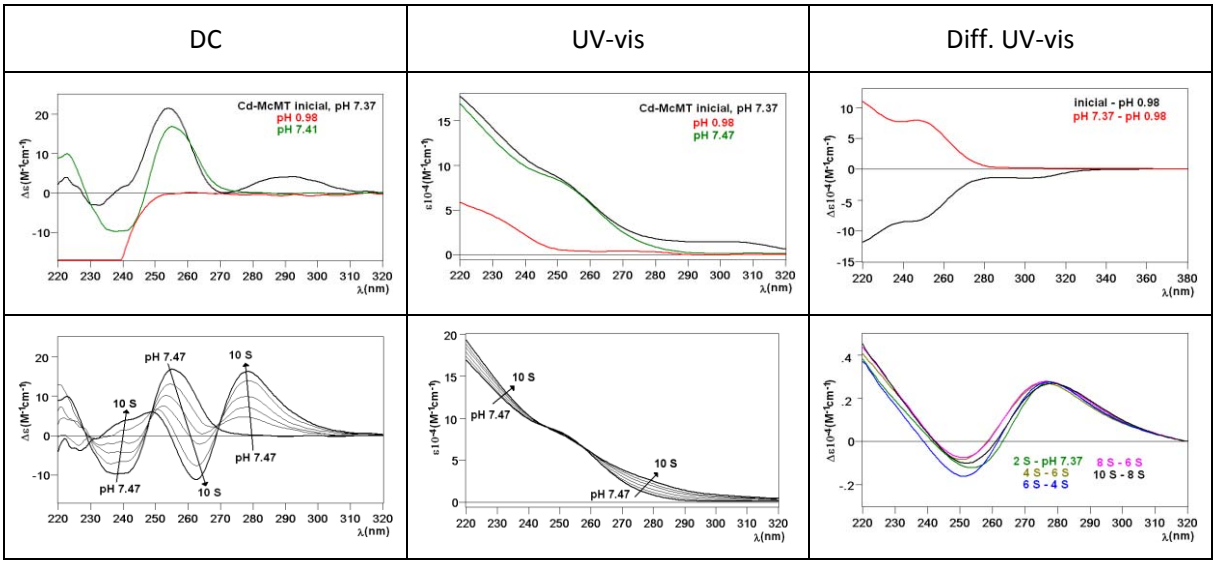

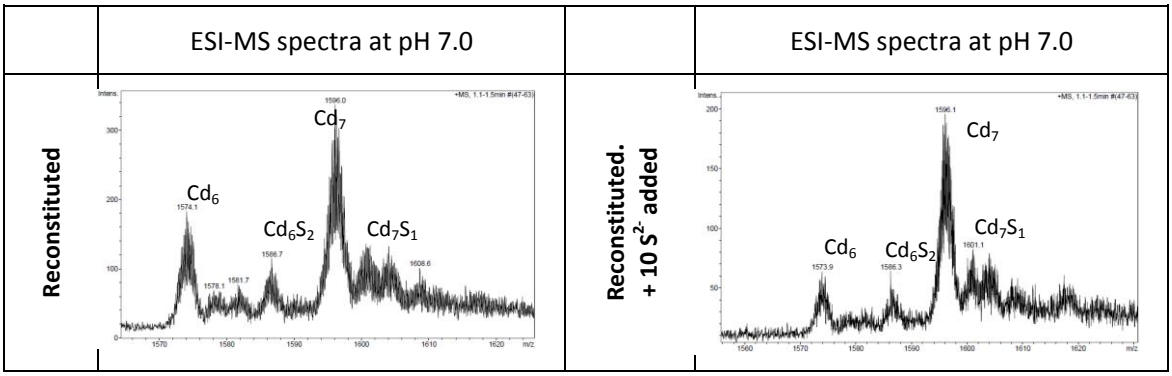

Fig. S2 : Acidification, renaturalization and sulphide addition to a recombinant Cd-McMT 20 μM preparation.

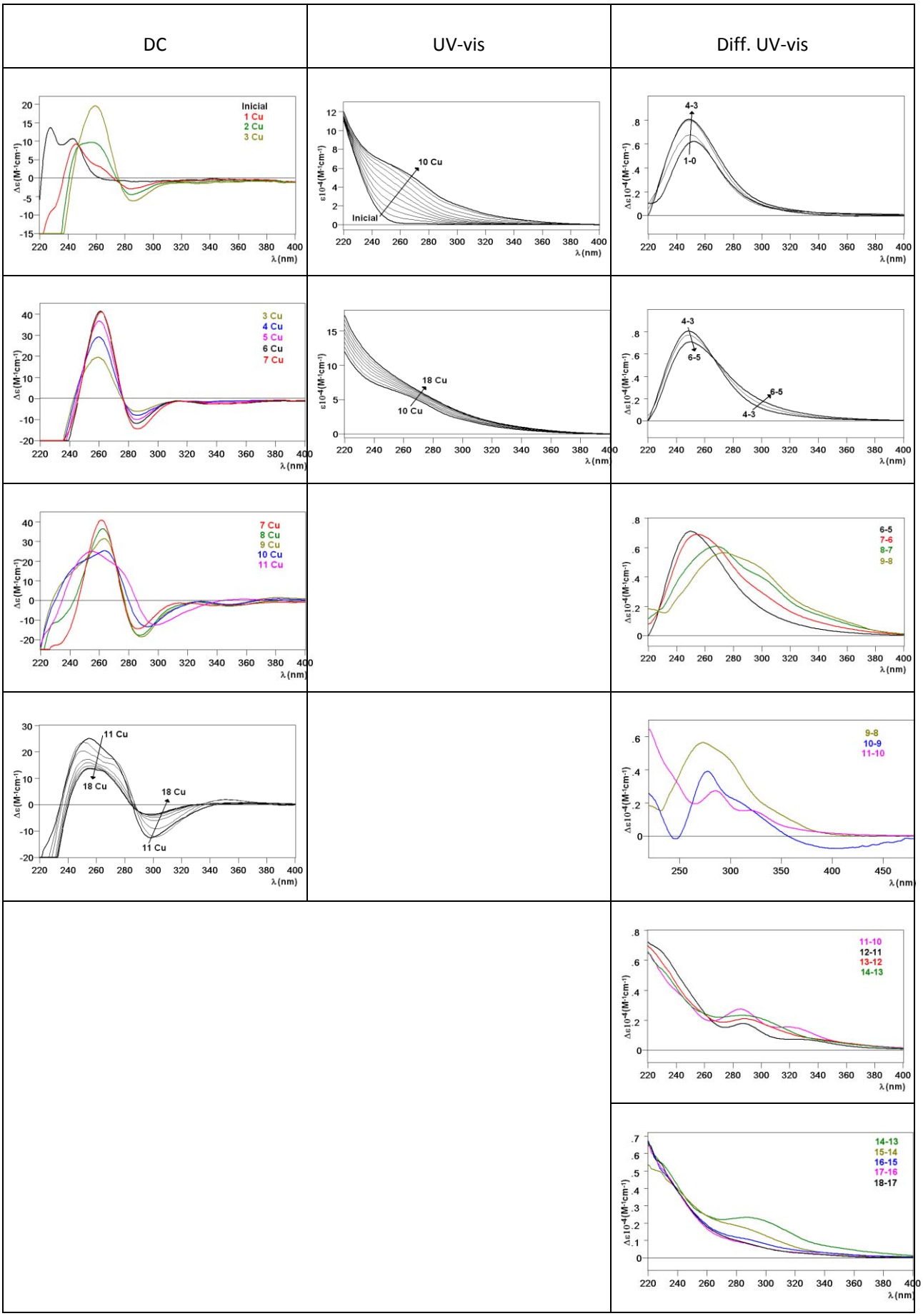

Fig. S3 : continues next page

Cu(I) eq added	ESI-MS spectra at pH 7.0	ESI-MS spectra at pH 2.4
2 eq	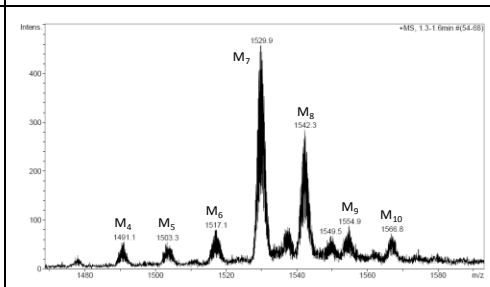	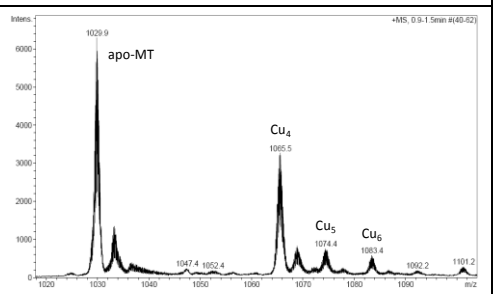
4 eq	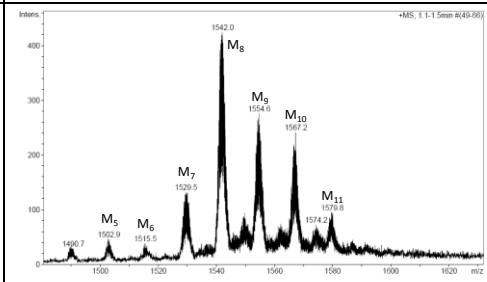	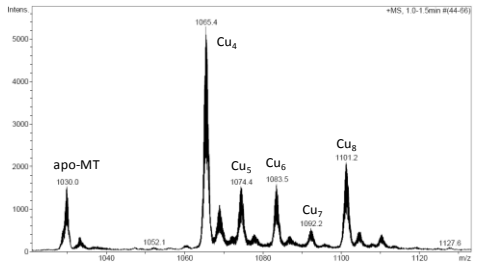
8 eq	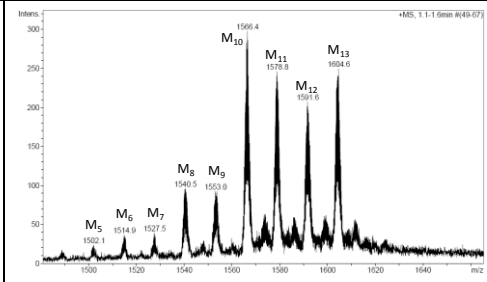	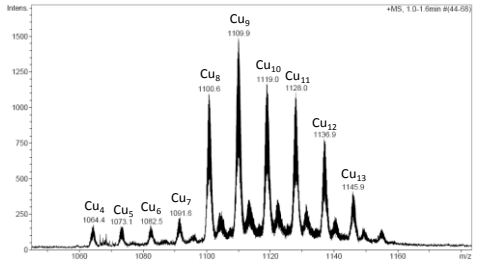
10 eq	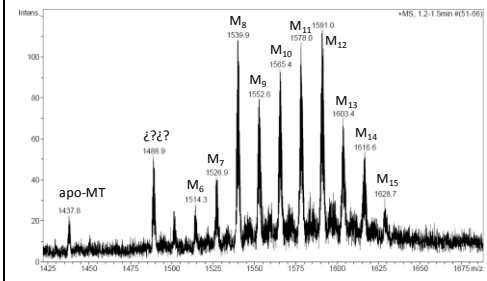	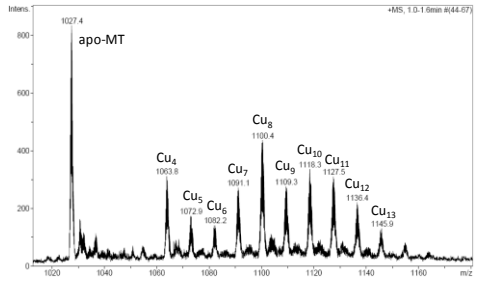
12 eq	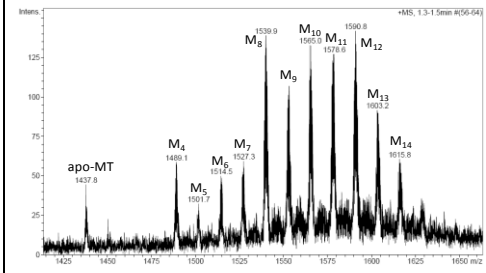	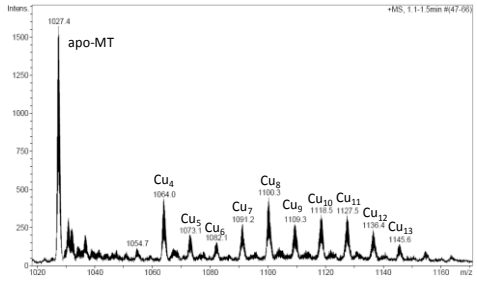
14 eq	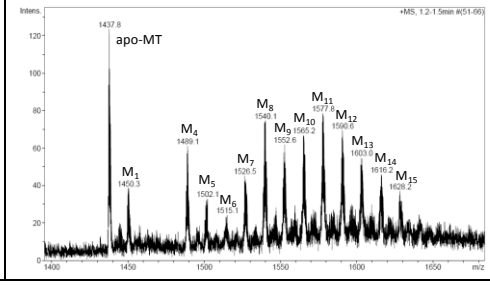	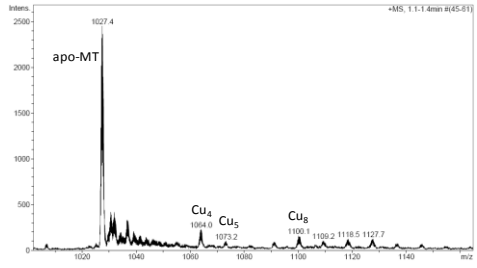

Fig. S3 : Spectroscopic and ESI-MS data of the Cu(I) titration of a recombinant Zn-McMT 20 µM preparation. The ESI-MS data recorded after 14 Cu(I) eq added were identical as those showed for 14 Cu(I) eq added.

VI. ARTICLE 6:

Metal Dealing at the Origin of the Chordata Phylum: The Metallothionein System and Metal Overload Response in *Amphioxus*

PLOS ONE, **(2012)**, 7, e43299.

Metal Dealing at the Origin of the Chordata Phylum: The Metallothionein System and Metal Overload Response in *Amphioxus*

Maria Guirola[1], **Sílvia Pérez-Rafael[2]**, **Mercè Capdevila[2]**, **Òscar Palacios[2]**, **Sílvia Atrian[1]***

1 Departament de Genètica, Facultat de Biologia, Universitat de Barcelona, Barcelona, Spain, **2** Departament de Química, Facultat de Ciències, Universitat Autònoma de Barcelona, Barcelona, Spain

Abstract

Non-vertebrate chordates, specifically amphioxus, are considered of the utmost interest for gaining insight into the evolutionary trends, i.e. differentiation and specialization, of gene/protein systems. In this work, MTs (metallothioneins), the most important metal binding proteins, are characterized for the first time in the cephalochordate subphylum at both gene and protein level, together with the main features defining the amphioxus response to cadmium and copper overload. Two MT genes (*BfMT1* and *BfMT2*) have been identified in a contiguous region of the genome, as well as several ARE (antioxidant response element) and MRE (metal response element) located upstream the transcribed region. Their corresponding cDNAs exhibit identical sequence in the two lancelet species (*B. floridae* and *B. lanceolatum*), *BfMT2* cDNA resulting from an alternative splicing event. BfMT1 is a polyvalent metal binding peptide that coordinates any of the studied metal ions (Zn, Cd or Cu) rendering complexes stable enough to last in physiological environments, which is fully concordant with the constitutive expression of its gene, and therefore, with a metal homeostasis housekeeping role. On the contrary, BfMT2 exhibits a clear ability to coordinate Cd(II) ions, while it is absolutely unable to fold into stable Cu (I) complexes, even as mixed species. This identifies it as an essential detoxification agent, which is consequently only induced in emergency situations. The cephalochordate MTs are not directly related to vertebrate MTs, neither by gene structure, protein similarity nor metal-binding behavior of the encoded peptides. The closest relative is the echinoderm MT, which confirm proposed phylogenetic relationships between these two groups. The current findings support the existence in most organisms of two types of MTs as for their metal binding preferences, devoted to different biological functions: multivalent MTs for housekeeping roles, and specialized MTs that evolve either as Cd-thioneins or Cu-thioneins, according to the ecophysiological needs of each kind of organisms.

Citation: Guirola M, Pérez-Rafael S, Capdevila M, Palacios Ò, Atrian S (2012) Metal Dealing at the Origin of the Chordata Phylum: The Metallothionein System and Metal Overload Response in *Amphioxus*. PLoS ONE 7(8): e43299. doi:10.1371/journal.pone.0043299

Editor: Fanis Missirlis, Queen Mary University of London, United Kingdom

Received May 21, 2012; **Accepted** July 19, 2012; **Published** August 14, 2012

Funding: This work was supported by the Spanish ''Ministerio de Ciencia e Innovación'' (MICINN) grants BIO2009-12513-C02-01 to Silvia Atrian and BIO2009-12513-C02-02 to Merce Capdevila. These coordinated projects were co-financed by the European Union, through the ''Fondo Europeo de Desarrollo Regional'' (FEDER) program. The authors from the Universitat de Barcelona and the Universitat Autònoma de Barcelona are members of the 2009SGR-1457 ''Grup de Recerca de la Generalitat de Catalunya''. Maria Guirola is recipient of an ''Ministerio de Asuntos Exteriores-Agencia Española de Cooperación Internacional para el Desarrollo'' (MAE-AECID) fellowship for PhD studies in Spain. The funders had no role in study design, data collection and analysis, decision to publish, or preparation of the manuscript.

Competing Interests: The authors have declared that no competing interests exist.

* E-mail: satrian@ub.edu

These authors contributed equally to this work.

Introduction

Metallothioneins (MTs) constitute a heterogeneous superfamily of ubiquitously occurring, low molecular weight, cysteine rich proteins, which coordinate divalent (Zn^{2+}, Cd^{2+}) or monovalent (Cu^{+}) metal ions through metal-thiolate bonds that impose a definite polypeptide folding (see [1,2] for recent revisions). No single biological role has been assigned to these peptides, but, instead, several functions have been proposed [3], ranging from toxic metal protection to physiological metal homeostasis, and also including free radical scavenging, oxidative stress protection, antiapoptotic defense and control of the redox status of the cell. Another fascinating *black hole* in knowledge of MT is their origin and functional differentiation through evolution. Although a polyphyletic origin has been proposed [4], their evolutionary history is particularly hard to interpret by means of standard molecular evolution criteria.

Vertebrate MTs are grouped in the *Family 1* of the taxonomy-based Binz and Kägi's MT classification [5], available at www.bioc.unizh.ch/mtpage/classif.html, therefore including all the isoforms identified in mammals, birds, reptiles, amphibians and fishes. These MTs are 60- to 68- amino acid long polypeptides, encompassing 20 cysteines (19 of which are totally conserved). They fold into two structural domains upon divalent metal ion coordination, namely the ß-domain (N-terminal moiety) and the α–domain (C-terminal moiety), connected by a hinge with a low number of residues. Vertebrate MT encoding genes are composed of three exons and two introns of variable lengths, but interrupting the coding regions at conserved positions. MT polymorphism is constant from fishes to mammals, which exhibit a four-member

cluster (MT1 to MT4) [6], with differences in gene (*i.e.* gene expression pattern) and protein level (*i.e.* isoform metal binding preferences) [7]. Avian MTs, the closest mammalian relatives, exhibit less polymorphism, with two isoforms identified in chicken [8]. Their genes share the same exon/intron structure as mammalian *MTs*, and they are regulated by similar stimuli including metal overdose and oxidative stress [8,9,10]. CkMT1 (chicken MT1) isoform is able to bind divalent and monovalent metal ions with an intermediate affinity between those observed for mammalian MT1 (classified as a Zn-thionein) and MT4 (Cu-thionein) [9]. All the fish MT genes and proteins reported up to date also share the same structural and functional features described for mammalian MTs [11]. A single MT has been described so far in amphibians, with a gene structure more similar to avian than to mammals and whose expression is inducible by zinc, copper and cadmium [12]. Finally, little information is available regarding the MT system in reptiles, although some isoforms have been identified that bear a strong similarity to avian MTs, including preservation of cysteine alignment and structure [13]. All this information has drawn a fairly clear picture of the evolution of the MT system inside the vertebrate subphyla (*cf.* http://www.bioc.unizh.ch/mtpage/trees.html), but there is still no clue about the point (or points) of origin of MT molecular diversification of vertebrate MTs regarding other organism groups. Besides vertebrates, the chordata phylum comprises two further subphyla: cephalochordates (the lancelets or amphioxus) and tunicates (previously urochordates, the sea-squints). The privileged position of these groups in the *tree of life* has been highly relevant for their use in studies of the molecular phylogeny and genome evolution of chordate/vertebrate organisms [14,15,16]. Hence, the study of genome evolution from the two prochordate groups to chordates revealed a final quadruplication in vertebrates, but most of the resulting duplicated genes were apparently lost and severe rearrangements, worsened by a high number of trans-position events, are likely to blur the evolutionary transition to vertebrates [17]. In fact, the situation is so unclear that the relationship between the prochordate taxa and vertebrates is still a matter of much debate [18].

Precisely regarding the MT system in non-vertebrate chordates, very little information is available at present. Among tunicates, two mRNA from *Herdmania curvata* are annotated as MT-like in Gene Bank (AY314949 and AY314939 accession numbers), and more recently an MT gene (*CiMT-1*) has been characterized in *Ciona intestinalis* [19]. Like vertebrate MTs, *CiMT-1* is composed of three exons and two introns, but only two of its exons comprise coding stretches, so that the encoded MT peptide is the shortest currently known in deuterostomes. The corresponding protein still retains the characteristic 30% cysteine content, although showing very little similarity with other reported MTs. Exposure to cadmium induces the expression of CiMT-1, but the presence of various putative response elements in the promoter region suggests that the transcription of the gene could be activated by other stimuli [19]. For cephalochordates, no information was available on any MT aspect at the beginning of this study, except for an annotated ORF in amphioxus (*Branchiostoma floridae*), predicted as a putative MT.

Since we consider that the knowledge of non-vertebrate chordates, specifically of amphioxus, is of the outmost interest for understanding and gaining insight into the evolutionary trends of the MT proteins, we have undertaken a study of the lancelet MT system, exploiting the recently completed amphioxus genome information [16]. Hence, we here report the first identification and characterization of two different amphioxus MT genes/proteins (BfMT1 and BfMT2), including the characterization of the gene structure and their metal induction pattern, the metal binding behavior of the encoded peptides and also the first characterization of the response of lancelets to metal intoxication. *BfMT1* appears to be an essentially constitutive gene, *BfMT2* is a clear inducible gene. The consideration of the Cd and Cu transcription regulation trends for the two genes, as well as of the metal binding behavior of both recombinantly synthesized peptides converge in the hypothesis that the serve very different purposes in the amphioxus organisms. BfMT1 is a polyvalent metal binding peptide, able to coordinate any of the studied metal ions (Zn, Cd or Cu), rendering complexes stable enough to last in physiological environments, which is fully concordant with the constitutive character of its encoding gene, and therefore, with a metal homeostasis housekeeping role. On the contrary, BfMT2 exhibits an clear ability to coordinate Cd(II) ions, while it is absolutely unable to fold into stable complexes under Cu(I) surplus, even as

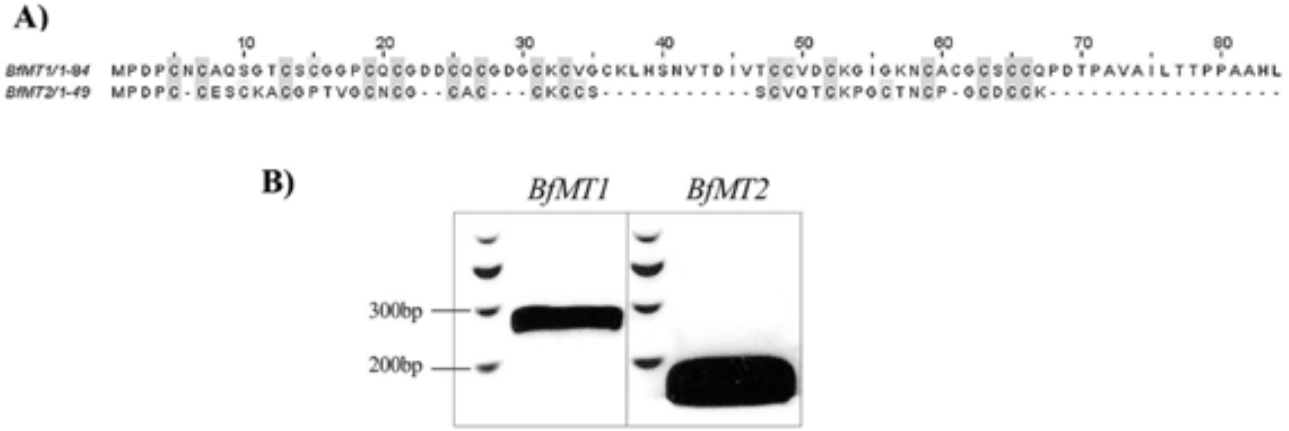

Figure 1. Protein sequences deduced of both identified Amphioxus metallothionein genes, which are patently transcribed in adult organisms. (**A**) Aligned protein sequences of the two identified amphioxus MTs, BfMT1 and BfMT2, *in silico* translated from the rbfeg037o01 and bfne062f22 cDNA clones, respectively. Cysteine residues are highlighted in gray. Alignment was performed using the T-Coffee software. (**B**) RT-PCR amplification of BfMT1 and BfMT2 cDNA using adult *B. lanceolatum* total mRNA as a template. Both band sizes corresponded to that expected for the respective coding sequences (255 bp for BfMT1 and 150 bp for BfMT2). The amplified cDNAs were cloned, and their sequences were verified as exact matches with respect to the *B. floridae* library cDNA clones.
doi:10.1371/journal.pone.0043299.g001

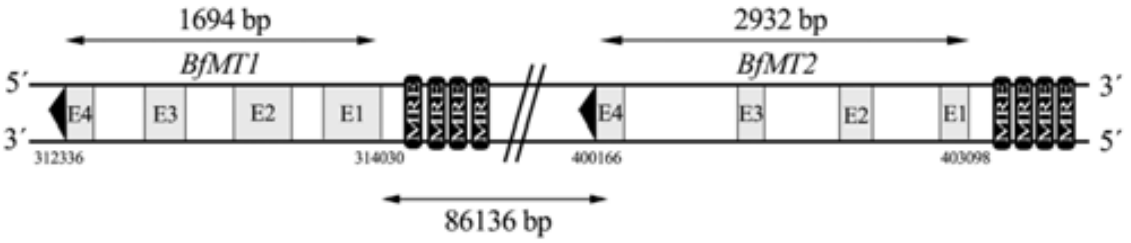

Figure 2. The genomic localization, orientation and structure of the *BfMT1* and *BfMT2* genes coincide in a 100-Kb region of the *B. floridae* genome. Both are located in the negative strand of the *B. floridae* genome scaffold 398. Exact location in pair bases with respect to the scaffold sequence is represented below each gene. The distance between both genes, as well as their size, are also indicated. Exons are shown in gray, and numbered E1 to E4. Black arrows indicate the transcription direction and the metal response elements (MREs) identified in the promoter regions are represented as black boxes.
doi:10.1371/journal.pone.0043299.g002

mixed Zn, Cu species. This is compatible with an essential cadmium detoxification role, which is consequently only induced in emergency situations. Notably, the Cd and Cu internal accumulation in metal treated organism fully confirms this metal binding behavior. A comprehensive consideration of all their features suggests interesting hypotheses not only for MT differentiation and specialization through evolution, but also for the phylogenetic relationship between cephalochordates and their surrounding taxa.

Materials and Methods

Bioinformatics methods for identification and analysis of MT genes in the amphioxus genome

Accession to the Florida lancelet species (*Branchiostoma floridae*) genome data (v1.0) was via the corresponding platform of the DOE Joint Genome Institute (http://genome.jgi-psf.org/Brafl1/Brafl1.home.html). The genome was first analyzed to find putative metallothionein genes that had already been annotated. Further homology searches were performed using BLAST and the NCBI and UNIPROT databases [20], applying one MT sequence from each of the 15 MT families in Kägi's classification as the query (*cf.* www.bioc.unizh.ch/mtpage/classif.html). The *in silico* translated putative MT sequences were characterized by using the bioinformatic facilities of the EBI-SRS platform [21], the main objective being the identification of metal binding functional motifs by using the PROSITE algorithm [22]. Furthermore, a scan was made of the BLOCKS database to identify the most highly conserved regions of protein families contained in the identified sequences [23]. Finally, the Metal Detector (v1.0) software (http://metaldetector.dsi.unifi.it/v1.0/) [24] was used to predict the metal binding capacity of the Cys and His residues in the selected sequences, as well as the DIANNA web server [25] which also predicts the most likely bound metal. To search for *cis* gene expression control elements (MRE and ARE) and TATA boxes of the putative *MT* genes, a 1000-bp region upstream of their predicted transcription initiation site was screened using the transcription element search system (TESS), available online at http://www.cbil.upenn.edu/cgi-bin/tess/tess. Gene structure schemes were drawn with the gene structure display server [26] at http://gsds.cbi.pku.edu.cn/.

Construction of amphioxus MT expression vectors

The coding sequences of the putative *MT* genes identified *in silico* were used to perform a BLAST search of the *Branchiostoma floridae* cDNA database (http://amphioxus.icob.sinica.edu.tw/) [27]. After analyzing all the retrieved ESTs and cDNAs, two clones including the full sequences encoding two non-homologous MTs were selected for recombinant expression: clone rbfeg037o01, for one *Branchiostoma floridae* MT sequence (*BfMT1*), and clone bfne062f22, including the second MT sequence (*BfMT2*). These clones were kindly provided by the Center for Genetic Resource Information at the Japanese National Institute of Genetics, in Mishima, Japan. The *BfMT1* and *BfMT2* coding regions were PCR-amplified from these clones, using as primers: BfMT1 upstream 5′-AAAGGATCCATGCCTGATCCCTGCAACTGTGCA-3′; BfMT1 downstream 5′-AAGCTCGAGTTACAGGTGAGCCGCTGGAG-3′; BfMT2 upstream 5′-AAAGGATCCATGCCAGACCCCTGTTGTGAG-3′; and BfMT2 downstream 5′- AAGCTCGAGTCACTTGCAGCAGTCACAACC-3′. This reaction introduced a *Bam*HI restriction site (underlined) before the ATG initiation codon, and a *XhoI* site (underlined) after the stop codon, of the BfMT coding regions. PCR conditions used were in accordance with the recommendations for the Expand High Fidelity PCR System (Roche) and the annealing step was performed at 55°C. The PCR products were isolated from 2% agarose gels, digested with *BamH*I–*Xho*I (New England Biolabs), and directionally inserted in the pGEX-4T-1 expression vector (GE Healthcare) for the synthesis of GST (glutathione-S-transferase) fusion proteins (*i.e.*, GST-BfMT1 and GST-BfMT2). Ligations were performed using the TAKARA DNA ligation kit (v2.1) (Takara Shuzo Co), and the ligation mixtures were used to transform both *E. coli* DH5α and BL21 cells. The *GST-BfMT1* and *GST-BfMT2* constructs were automatically sequenced (Applied Biosystems Abiprism 310, PerkinElmer) using the BigDye terminator v3.1 kit (ABI Biosystems).

Preparation of recombinant and *in vitro*-constituted metal-MT complexes

For recombinant synthesis of the metal-BfMT complexes, the pGEX–BfMT1 and pGEX–BfMT2 plasmids were transformed into the *E. coli* BL21 protease-deficient strain. Recombinant bacteria grown under metal supplemented conditions (300 μM $ZnCl_2$, 300 μM $CdCl_2$, or 500 μM $CuSO_4$) and fusion protein purifications were carried out essentially as previously described [28,29,30]. At the end, the MT-containing fractions eluted from an FPLC Superdex 75 column (GE-Healthcare) in 50 mM Tris-HCl buffer pH 7.0, were pooled, aliquoted and stored at −80°C under argon atmosphere until required. *In vitro* metal-MT binding studies were performed through metal replacement and denaturation experiments. Titrations of the Zn-BfMT1 and Zn-BfMT2 preparations with Cd(II) or Cu(I) at pH 7 were performed as described earlier [28,29,31] using $CdCl_2$ or $[Cu(CH_3CN)_4]$-ClO_4 solutions, respectively. The *in vitro* acidification/reneutralization experiments were adapted from [32]. Mainly, 10–20 μM

A)

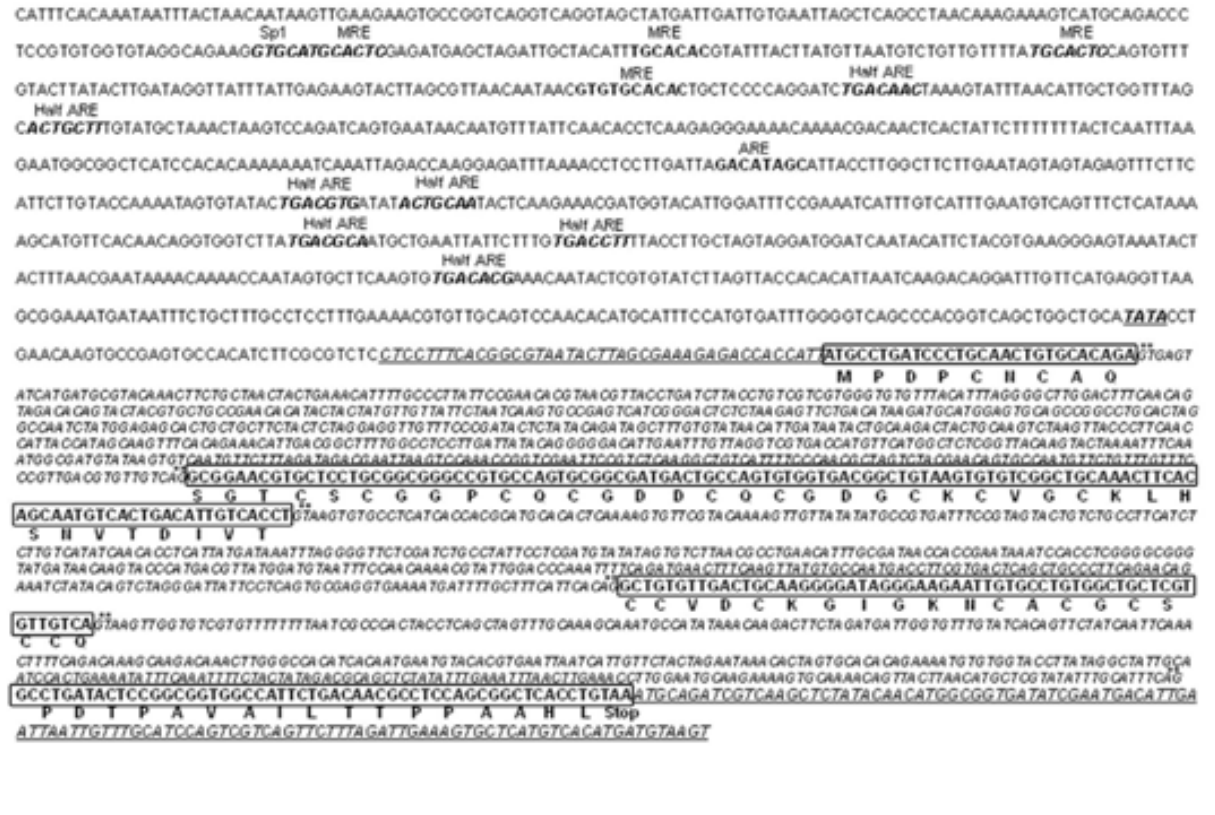
Sp1
MRE
MRE
MRE
MRE
Half ARE
Half ARE
ARE
Half ARE
Half ARE
Half ARE
Half ARE
Half ARE
M P D P C H C A Q
S G T C S C G G P C Q C G D D C Q C G D G C K C V G C K L H
S H V T D I V T
C C V D C K G I G K H C A C G C S
C C Q
GCCTGATACTCCGGCGGTGGCCATTCTGACAACGCCTCCAGCGGCTCACCTGTAA
P D T P A V A I L T T P P A A H L Stop

B)


ARE
ARE
MRE
MRE
MRE
MRE
M P D P
C C S A C E G C S S T C H K C S C D C C K
C C A S C K A C G P T A D C S C G C A C C K
C C A S C D G C K S S C T S C S C
D C C K Stop

Figure 3. The analysis of the *BfMT1* and *BfMT2* genomic sequences identify all the elements of these genes. Promoter regions (-1 kb) are included and the *in silico* identified regulatory sequences (MRE and ARE) are highlighted in bold. 5′and 3′UTR regions, corresponding to the cDNA sequences of the cDNA clones, are included and represented in italics and underlined. Coding sequences are boxed in their corresponding exons and translated protein sequences are included below each exon.
doi:10.1371/journal.pone.0043299.g003

preparations of the recombinantly synthesized metal-complexes were acidified from neutral (7.0) to acid pH (1.0) with HCl, kept at pH 1.0 for 20 min and subsequently reneutralized to pH 7.0 with NaOH. CD (circular dichroism) and UV–vis spectra were recorded at different pH throughout the acidification/reneutralization procedure, both immediately after acid or base addition, and 10 min later. During all experiments strict oxygen-free conditions were maintained by saturating the solutions with argon. All the *in vitro*-obtained metal-MT samples were analyzed following the same rationale as for the recombinant preparations.

Characterization of the metal-MT complexes

Metal content (S, Zn, Cd and Cu) of the purified metal-MT complexes was analyzed by means of ICP-AES (inductively coupled plasma atomic emission spectroscopy) in a Polyscan 61E (Thermo Jarrell Ash) spectrometer, measuring S at 182.040 nm, Zn at 213.856 nm, Cd at 228.802 and Cu at 324.803 nm. Samples were treated as in [33], and were alternatively incubated in 1 M HCl at 65 °C for 15 min prior to measurements to eliminate possible traces of labile sulfide ions, as otherwise described in [34]. Protein concentration was calculated from the acid ICP-AES sulfur measure, assuming that in this case, all S atoms are contributed by the MT peptide. CD measurements were performed by using a Jasco spectropolarimeter (model J-715) interfaced to a computer (J700 software) maintaining a constant temperature of 25 °C using a Peltier PTC-351S apparatus. Electronic absorption measurements were performed on an HP-8453 Diode array UV–visible spectrophotometer. All spectra were recorded with 1–cm capped quartz cuvettes, corrected for the dilution effects and processed using the GRAMS 32 program.

ESI-MS (electrospray ionization mass spectrometry) analyses of the metal-MT complexes

Electrospray ionization time-of-flight mass spectrometry (ESI-TOF MS) was applied to assess the molecular mass of the metal-BfMT1 and metal-BfMT2 complexes. The equipment used was a Micro Tof-Q instrument (Bruker) interfaced with a Series 1200 HPLC Agilent pump, equipped with an autosampler, which were controlled using the Compass Software. Calibration was attained with 0.2 g of NaI dissolved in 100 mL of a 1:1 H_2O:isopropanol mixture. Samples containing MT complexes with divalent metal ions were analyzed under the following conditions: 20 μL of protein solution injected through a PEEK (polyether heteroketone) column (1.5 m × 0.18 mm i.d.), at 40 μL min^{-1}; capillary counter-electrode voltage 5 kV; desolvation temperature 90–110 °C; dry gas 6 L min^{-1}; spectra collection range 800–2500 m/z. The carrier buffer was a 5:95 mixture of acetonitrile:ammonium acetate/ammonia (15 mM, pH 7.0). Alternatively, the Cu-BfMT1 and Cu-BfMT2 samples were analyzed as follows: 20 μL of protein solution injected at 40 μL min^{-1}; capillary counter-electrode voltage 3.5 kV; lens counter-electrode voltage 4 kV; dry temperature 80 °C; dry gas 6 L min^{-1}. Here, the carrier was a 10:90 mixture of acetonitrile:ammonium acetate, 15 mM, pH 7.0. For analysis of apo-BfMT1, apo-BfMT2, Cu-BfMT1 and Cu-BfMT2 preparations at acid pH, 20 μL of the corresponding samples were injected under the same conditions described previously, but using a 5:95 mixture of acetonitrile:-formic acid pH 2.4, as liquid carrier, which caused the complete demetalation of the peptides loaded with Zn(II) or Cd(II) but kept the Cu(I) ions bound to the protein.

DEPC (diethyl pyrocarbonate) protein modification assays

Covalent modification experiments with DEPC were performed essentially as described in [35]. A fresh DEPC solution in absolute ethanol (DEPC:ethanol 1:200 v/v) was allowed to react with a 100 μL solution of the metal-MT complexes (ranging from 0.2×10−4 to 2.1×10−4 M) in 50 mM Tris-HCl buffer, pH 7.0, for 20 min at room temperature. The resulting DEPC:protein ratios used were 7:1 for Zn(II)- and Cd(II)-BfMT1. After incubation, all samples were immediately analyzed by ESI-TOF MS, under the conditions described above.

Analysis of expression of amphioxus MT genes

To test the expression of both *BfMT1* and *BfMT2* genes, and to determine the main gene regulation features, some organisms of

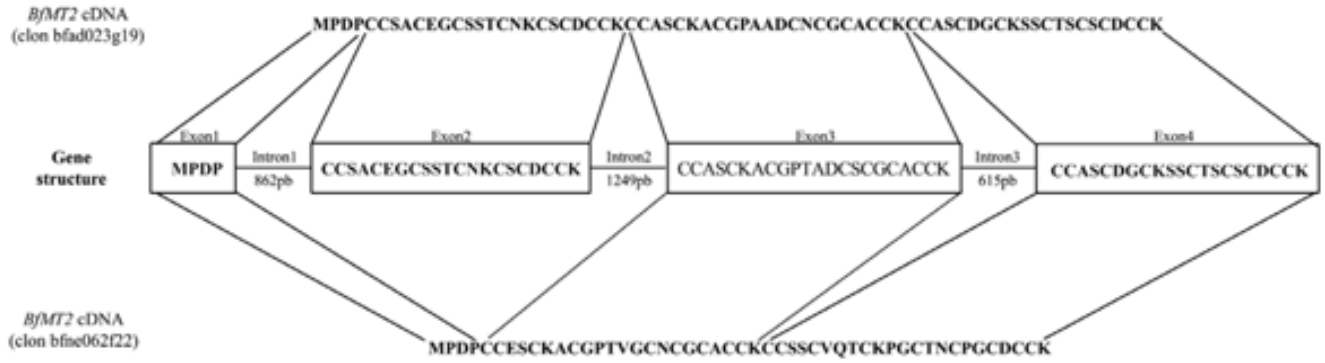

Figure 4. *BfMT2* transcription proceeds through alternative splicing patterns. Schematic representation of the *BfMT2* gene structure and the protein sequence corresponding to each exon (in the centre), and the protein sequences for each alternative cDNA. *BfMT2* coding sequence used for translation was extracted from the NCBI Databank and corresponds to *B. floridae* strain S238N-H82. cDNA clone sequences were extracted and obtained from the *B. floridae* cDNA Database.
doi:10.1371/journal.pone.0043299.g004

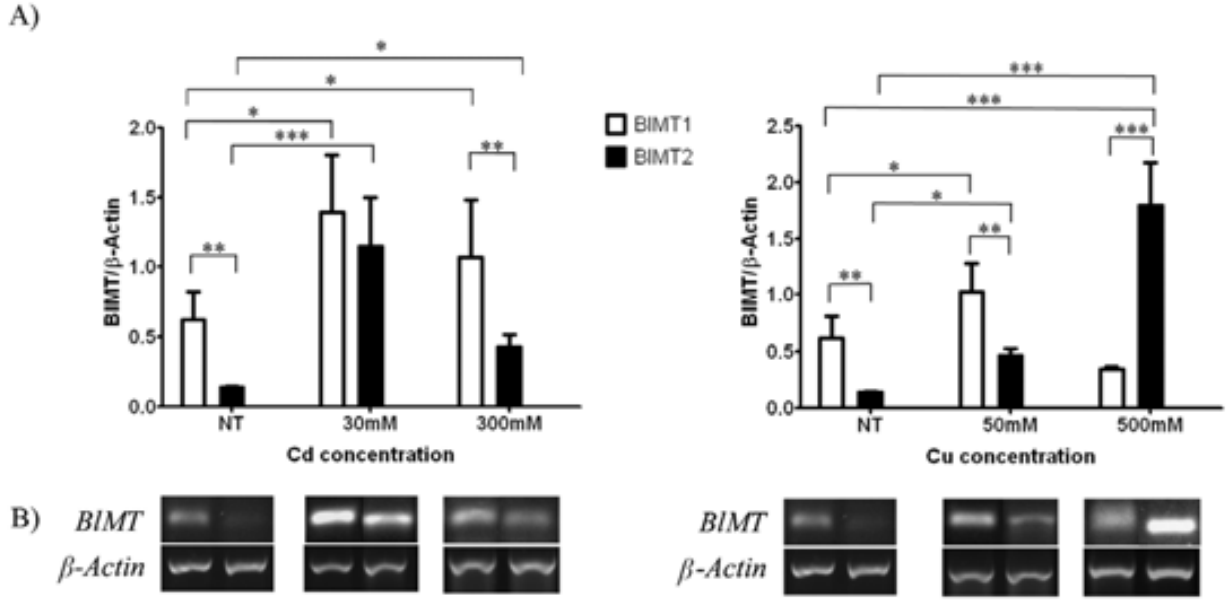

Figure 5. *BlMT1* is essentially constitutive, while *BlMT2* is an inducible gene, as revealed in metal and non-metal treated *B. lanceolatum* organisms. (**A**) Semi quantification by RT-PCR of transcription rates under Cu and Cd supplementation, and statistical comparison. Data for each gene and condition is normalized by the corresponding value for the constitutive gene *β-actin*, previously homogenized between organisms and groups. Data represent mean and standard deviation of six organisms. Significance was assessed using the Newman-Keuls statistical test. Stars denote statistical significance as follows: * as equivalent to a significance of $P<0.05$, ** equivalent to $P<0.01$, and *** to $P<0.001$. B) Best examples of RT-PCR bands representing the results observed in A). NT stands for non-treated organisms.
doi:10.1371/journal.pone.0043299.g005

the European lancelet species (*Branchiostoma lanceolatum*) were kindly offered by Dr. Hector Escriva, from the *Observatoire Océanologique* in Banyuls-sur-Mer, France. For RNA purification, whole organisms were treated with the RNALater solution (Qiagen), and the total RNA was extracted by using the RNeasy Mini Kit (Qiagen), and cleansed from DNA contamination by DNAase digestion. Purified RNA was quantified and stored at −80°C until use. The Qiagen OneStep RT-PCR Kit was used for reverse transcription of 1 μg of total RNA, using the same specific oligonucleotides designed for cloning purposes. Final PCR products were sequenced as described previously. To semi-quantify the transcription rates of the *BfMT1* and *BfMT2* genes in *B. lanceolatum*, several of the sea-collected organisms were washed in sterile PBSx1 buffer and grouped for metal treatment: a solution of $CdCl_2$ at 0.03 mM, 0.3 mM or 3 mM; or a solution of $CuSO_4$ at 0.05 mM, 0.5 mM or 5 mM, final concentrations. A non-treated group was also maintained to obtain the corresponding control values. The corresponding metal salts were added onto the reconstituted Reef Crystals (Aquarium Systems) as synthetic sea water, and the treatment lasted for two days. After 48 h, all organisms were washed and total RNA was extracted as previously described. Semi quantitative RT-PCR was performed using the same RT-PCR Kit, on 30 ng of total RNA as template. Actin was used as conserved housekeeping gene to check for an equal retrotranscription rate among samples. PCR reactions were loaded onto a 1.5% agarose gel and bands were quantified by using the QuantityOne v.22 software from BioRad. Data are shown as the ratio of band intensities in relation to the corresponding actin. Statistical analysis was performed by using the GraphPad Prism 5 software (La Jolla, USA).

Metal content measurements in amphioxus organisms

After incubation for two days in the metal-supplemented sea water medium described for the semi quantitative RT-PCR experiment, some organisms from each treatment condition were used to measure total body metal content. We evaluated not only total Cd and Cu contents, but also Zn and Fe, to ascertain possible metabolic relations. The organisms were washed with miliQ water, dried at 95°C, weighted, and finally decomposed in 1 ml of Trace Metal Grade (Fisher) nitric acid by heating at 80°C for 1 hour. After cooling to room temperature, samples were transferred to 15 ml asks, the volume was adjusted to 10.0 ml with Milli-Q water, and the total metal content of the samples measured by ICP-AES, as previously described for MT preparations. Control experiments without organisms were run in parallel to determine the background metal content in all the solutions used. All glassware and plasticware was acid-washed overnight with 10% nitric acid prior to use. Results are shown as total metal content normalized in relation to the dry weight of each organism. Statistical analysis was performed by using the GraphPad Prism 5 software (La Jolla, USA).

Phylogenetic analysis

The set of MT sequences used to perform the phylogenetic analysis was selected by choosing one MT from each subfamily considered in the classification published in the Metallothionein Homepage (http://www.bioc.unizh.ch/mtpage/MT.html). Sequences were extracted from the UNIPROT website (http://www.uniprot.org/). Multiple sequence alignments were performed using the TCOFFEE web service at http://tcoffee.vital-it.ch/cgi-bin/Tcoffee/tcoffee_cgi/index.cgi [36], and stored in a *.PHY format, to be further used to construct the corresponding phylogenetic trees by the Maximum Likelihood algorithm (PHYLIP software package) [37]. Genetic distances were calculated using the Kimura 2-parameter method [38] and statistical support for nodes on the tree was evaluated using bootstrapping (1000 replications) [39].

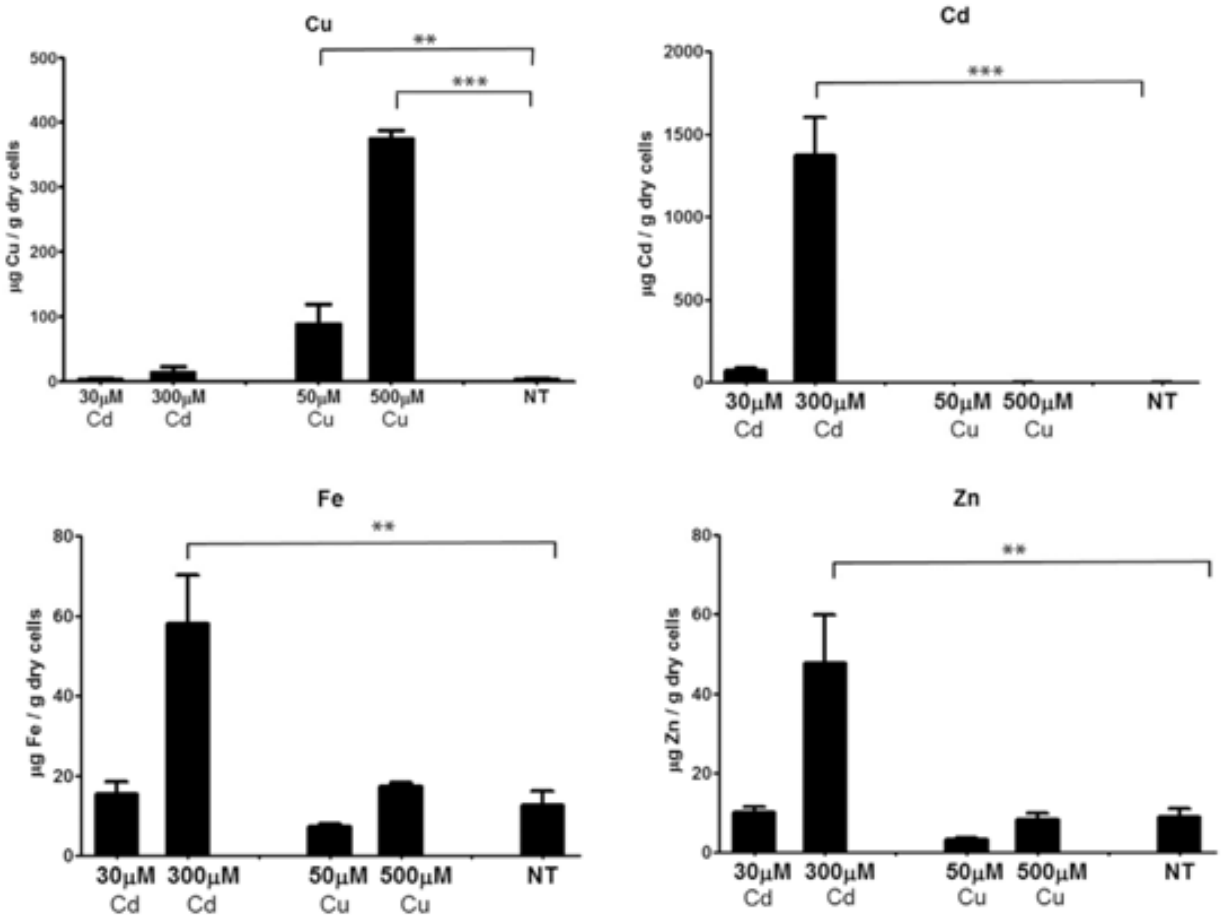

Figure 6. ICP-measured Cd and Cu accumulation in treated lancelets follow different patterns. *B. lanceolatum* organisms were treated with two different concentrations of Cd or Cu, or non-metal treated (NT). Data is represented as mean and standard deviation of six organisms per group. Statistical significance is represented as ** equivalent to $P<0.01$, and *** to $P<0.001$ according to the Newman-Keuls statistical test.
doi:10.1371/journal.pone.0043299.g006

Results and Discussion

The amphioxus genome includes two linked genes coding for rather dissimilar metallothionein isoforms: BfMT1 and BfMT2

The estimated size of the genome of *Branchiostoma floridae* is approximately 575 Mb contained in 19 chromosomes. Although it has been completely sequenced and annotated [16], the assignment of contigs to the physical chromosome map is not yet finished, which introduces some uncertainty to the studies of gene identification and localization in this organism. The examination of annotated *B. floridae* genes revealed only one sequence encoding a putative MT protein (ID 129939), hereinafter called BfMT1, already reported in a recent study on tunicate MTs [19]. Additionally a totally unpredicted ORF, coding for a second putative MT isoform (called BfMT2), was further identified after several homology searches (BLAST) using the cDNAs of members of different MT families as queries [5]. The predicted BfMT1 and BfMT2 protein sequences (Figure 1A) coincide with the general features of MTs, *i.e.* short, low molecular weight and cysteine-rich peptides, containing the PROSITE Cys-rich profile (ID PS50311). When submitting the BfMT1 sequence to a BLOCKS analysis, the signatures of the mollusk MT (PR00875), vertebrate MT (PR00860), and Diptera (*Drosophila*) MT (PR00872) families were identified (*E-value*$<$*3.6e-05*). On the other hand, the signature of crustacean MTs (PR00858) (with an *E-value* $=$ *6.2e-05*), as well as other less significant MT signatures, were identified in the BfMT2 sequence. Finally, the Metal Detector algorithm predicted that 60% of cysteines in BfMT1 and 42.1% in BfMT2 sequences were able to bind metals with a probability higher than 0.6, these results agreeing with those obtained by the DIANNA web server for the prediction of metal binding sites. Before continuing our study, we decided to test whether the two BfMT1 and BfMT2 ORFs were indeed *real genes*, by checking the presence of the respective transcripts in lancelet organisms. To this end, we used the European *Branchiostoma lanceolatum* species, which is available from the near Mediterranean coast. Hence, RT-PCR assays were performed on total mRNA isolated from recently-captured organisms, by using isoform specific primers. A single band was obtained in each case, corresponding to the expected size deduced from the position of the primers in the *BfMT1* and *BfMT2* cDNA sequences (255 bp and 150 bp respectively, Figure 1B). This showed that both ORFs were transcribed to mature mRNAs in *B. lanceolatum*, and therefore that both *BfMT1* and *BfMT2* can be considered as functional genes. The corresponding PCR products were purified, cloned and sequenced. Their sequences fully matched those of the cDNA initially retrieved from the *in silico* searches in the *B. floridae* data bank, and thus these results also served to verify the identity of the BfMT1 and BfMT2 protein sequence between the two *Branchiostoma* species. While this

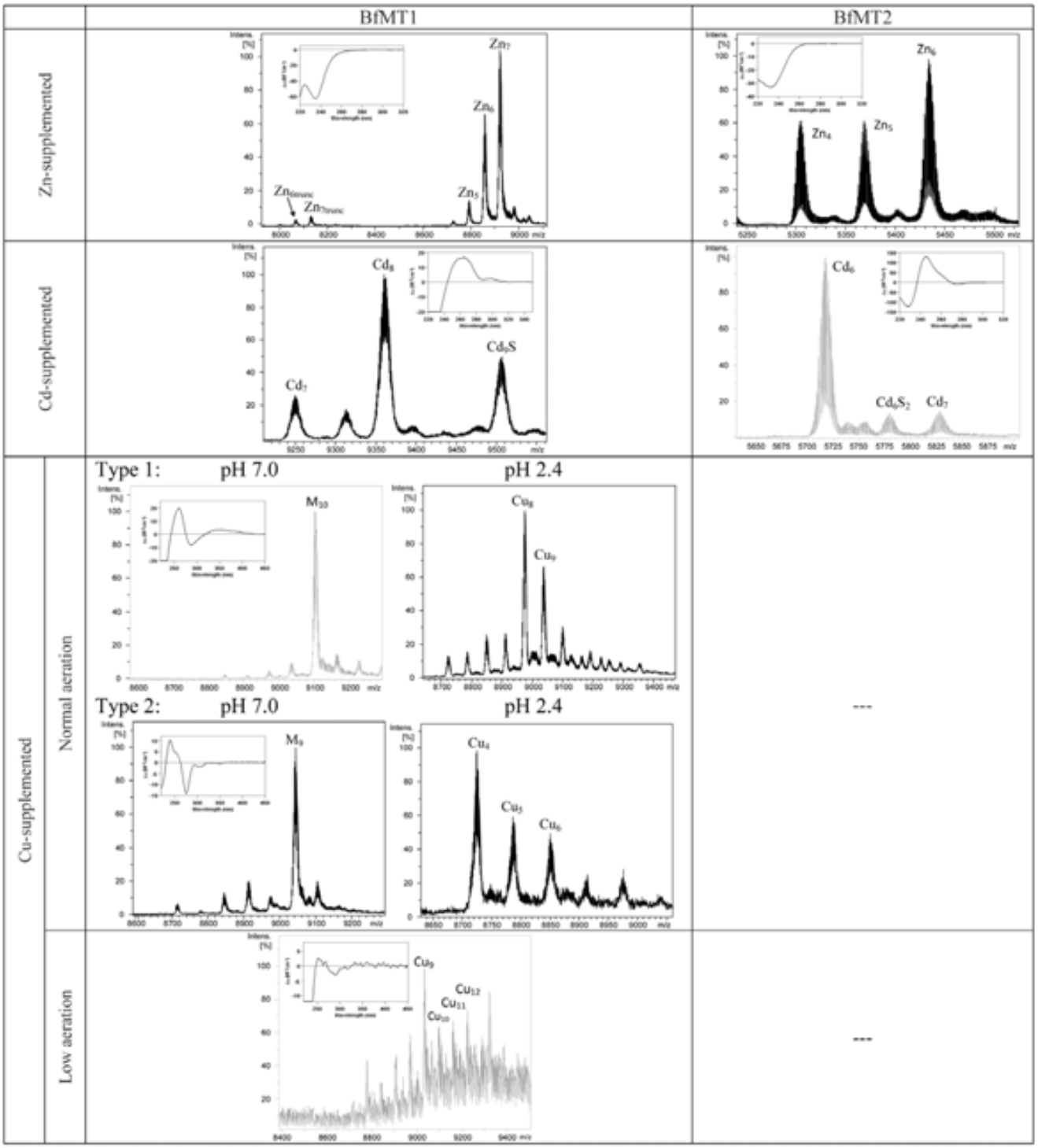

Figure 7. The BfMT1 and BfMT2 peptides exhibit different metal binding abilities. Deconvoluted ESI-MS spectra, at neutral pH, corresponding to the BfMT1 and BfMT2 recombinant syntheses, obtained from bacterial cultures grown in Zn-, Cd- and Cu-supplemented. Insets correspond to the CD fingerprint of each preparation. The ESI-MS spectra at pH 2.4 is also included for the Cu-BfMT preparations obtained under normal aeration conditions of the cultures.
doi:10.1371/journal.pone.0043299.g007

manuscript was under revision, the *B. lanceolatum* transcriptome first release, obtained by shotgun assembly, was published [40]. In Fig. S1, we include the sequence of the BLAST retrieved clones, putatively correspondent to BlMT1 and BlMT2 cDNAs in this lancelet species.

The amphioxus MT genes exhibit different structure and transcript processing patterns, which include alternative splicing for BfMT2

The location of the two *BfMT* genes in the amphioxus genome indicates a linked position in the *B. floridae* genome, in the negative

Table 1. Analytical characterization of the recombinant preparations of the Zn-, Cd- and Cu-complexes yielded by BfMT1 and BfMT2.

	Zn	Cd	Cu	
			Normal aeration	**Low aeration**
BfMT1			Type 1:	
		2.6 10^{-4} M	0.57 10^{-4} M	0.19 10^{-4} M
		(1.0 10^{-4} M)	2.7 Zn/MT	11.9 Cu/MT
	1.7 10^{-4} M		5.1 Cu/MT	
	5.8 Zn/MT		Type 2:	
		4.4 Cd/MT	0.55 10^{-4} M	
		(10.3 Cd/MT)	1.8 Zn/MT	
			8.0 Cu/MT	
BfMT2		2.4 10^{-4} M	–	–
	2.6 10^{-4} M	(0.9 10^{-4} M)	–	–
	5.0 Zn/MT	3.3 Cd/MT	–	–
		(7.6 Cd/MT)	–	–

In all cases the Zn, Cd, Cu and S content was measured by ICP-AES but only detectable contents are shown. The protein concentration values and Cd/MT ratios shown in parenthesis correspond to those measured by acid ICP-AES.
doi:10.1371/journal.pone.0043299.t001

strand of scaffold #398. Exact locations are [312336–314030] for *BfMT1* and [400166–403098] for BfMT2 (Figure 2). The identification of the complete *BfMT2* structure was only possible when working with the NCBI genome data, since in the original amphioxus genome platform (DOE Joint Genome Institute), almost all the corresponding region was of undetermined sequence, showing strong evidences of the presence of transposable elements, which are extremely common in amphioxus [17]. This situation may explain why this gene has remained undetected until now. The full sequence of both genes, as well as that of the flanking regions, is shown in Figure 3. BfMT1, expanding through almost 1.7 kpb in the genome, is composed of 4 exons separated by 3 introns, of 653−, 414−, and 372-bp. The first and last exons comprise respective 5′ and 3′ UTRs of regular length. Significantly, a considerable number of transcription factor binding elements could be identified *in silico*, comprising putative metal response elements (MRE), antioxidant response elements (ARE) and TATA box, which predict a gene regulation pattern similar to that of vertebrate *MT* genes. *BfMT2* also has a 4-exon/3-intron structure, but since the *BfMT2* introns are considerably longer (862 bp, 1249 bp and 615 bp) than those of *BfMT1,* the entire gene is considerably more extended in the genome. Most surprising, however, was the observation that the *BfMT2* cDNA sequence retrieved from the amphioxus data bank (bfne062f22 clon) did not correspond to the *canonical* cDNA expected from the splicing of the three *BfMT2* introns, but was the result of an alternate splicing pattern that skips exon 2 (*cf.* Figure 4). Only some small discrepancies between the sequence of the bfne062f22 cDNA and that of the predicted [exon1-exon3-exon4] sequence were observed, which are perfectly accountable due to natural variability between the different lancelet populations used as sources for these data. In fact, a thorough search of the *B. floridae* genome failed to identify any other possible coding region for BfMT2. An analysis of the presence of clones corresponding to the long mRNA in the cDNA databank readily suggests it can be considered an extremely rare transcript, since only a single clon (#rbfad023g19) out of the total of 132066 retrieved clones. This is concordant with the fact that no PCR product was amplified in the RT-PCR assay shown in Figure 1, which was performed by using primers corresponding to exons 1 and 4. Conversely, the number of clones for the short BfMT2 mRNA (that corresponding to bfne062f22), amounted to 90, being mostly abundant in the egg and adult stages (24 and 32, respectively). Overall, it seems plausible to assume that this short transcript, encoding for an MT peptide, is the most prominent product of the BfMT2 gene. Several MREs and AREs, but no canonical TATA box, could also be predicted in the 5′ *BfMT2* promoter region, as also shown in Figure 2. To support the functionality of these MREs, the *B. floridae* genome platform was searched for the presence of a putative MTF-1 coding gene, which we were able to locate in scaffold #418, using as a query the sequence of the zebra fish MTF-1 (*D. rerio)*. The corresponding product, ID 155422, is annotated as a nucleic acid (MRE), zinc ion binding protein including the corresponding zinc-finger motifs, to be considered a canonical MTF-1 transcription factor.

The two amphioxus MT genes are distinctly expressed at non-induced conditions and they are distinctly regulated by cadmium and copper ions

To investigate the response of both amphioxus MT genes to metal exposure, several organisms of the *B. lanceolatum* species were treated with different concentrations either of $CdCl_2$ or $CuSO_4$. As there was no previous reference for metal treatment for amphioxus, three metal concentrations ranging between two orders of magnitude (0.03-to-3 mM Cd and 0.05-to-5 mM Cu) were first assayed in order to determine sub-lethal conditions. All organisms kept at the highest metal concentration died within one day, and therefore *MT* transcriptional activity data were evaluated by semi-quantitative PCR from the other conditions, as well as from non-treated animals for basal expression information. *BlMT1* and *BlMT2* transcription patterns are already different in the absence of metal supplementation, since while *BlMT1* shows a significant constitutive expression rate, *BlMT2* transcripts are almost undetectable (Figure 5). Cadmium is a very good *BlMT1* inducer, since at both concentrations assayed (30 and 300 μM) the mRNA abundance approximately doubles that of the control conditions. But *BlMT2* is even more responsive to Cd, because this metal ion provokes, at 30 μM, an eight fold increase in the gene transcription rate in comparison with the control group ($P<0.1$) and threefold for Cd 300 mM ($P<0.5$). Treatment with copper did not significantly increase the number of *BlMT1* transcripts ($P>0.5$) at either of the two tested concentrations (Figure 5), while surprisingly, it proved to be a very strong inducer of *BlMT2*, specially in 500 μM Cu-treated organisms, where a 12 fold increase was observed in comparison with the background expression ($P<0.01$). Overall, it is clear that in physiological conditions, the *BlMT1* gene is constitutively transcribed, in contrast to *BlMT2,* which remains practically silent. Cadmium treatment induces both gene expressions, although at a much more pronounced rate for *BlMT2*. The less pronounced induction capacity, or even repression effect, of high cadmium concentrations has been observed before in metal response studies carried out with other model organisms, such as that for *C. elegans* MT genes [41], and is attributable to the inhibitory transcription activity of Cd (II) ions [42]. Copper has little effect on *BlMT1* transcription, but in contrast, it provokes a significant increase in *BlMT2* mRNA accumulation. However, this trend can be related to the BlMT2 peptide copper-binding incapacity, as discussed later in this study. In this scenario, the unbound Cu(I) ions would remain free in the organism and therefore continue to induce gene

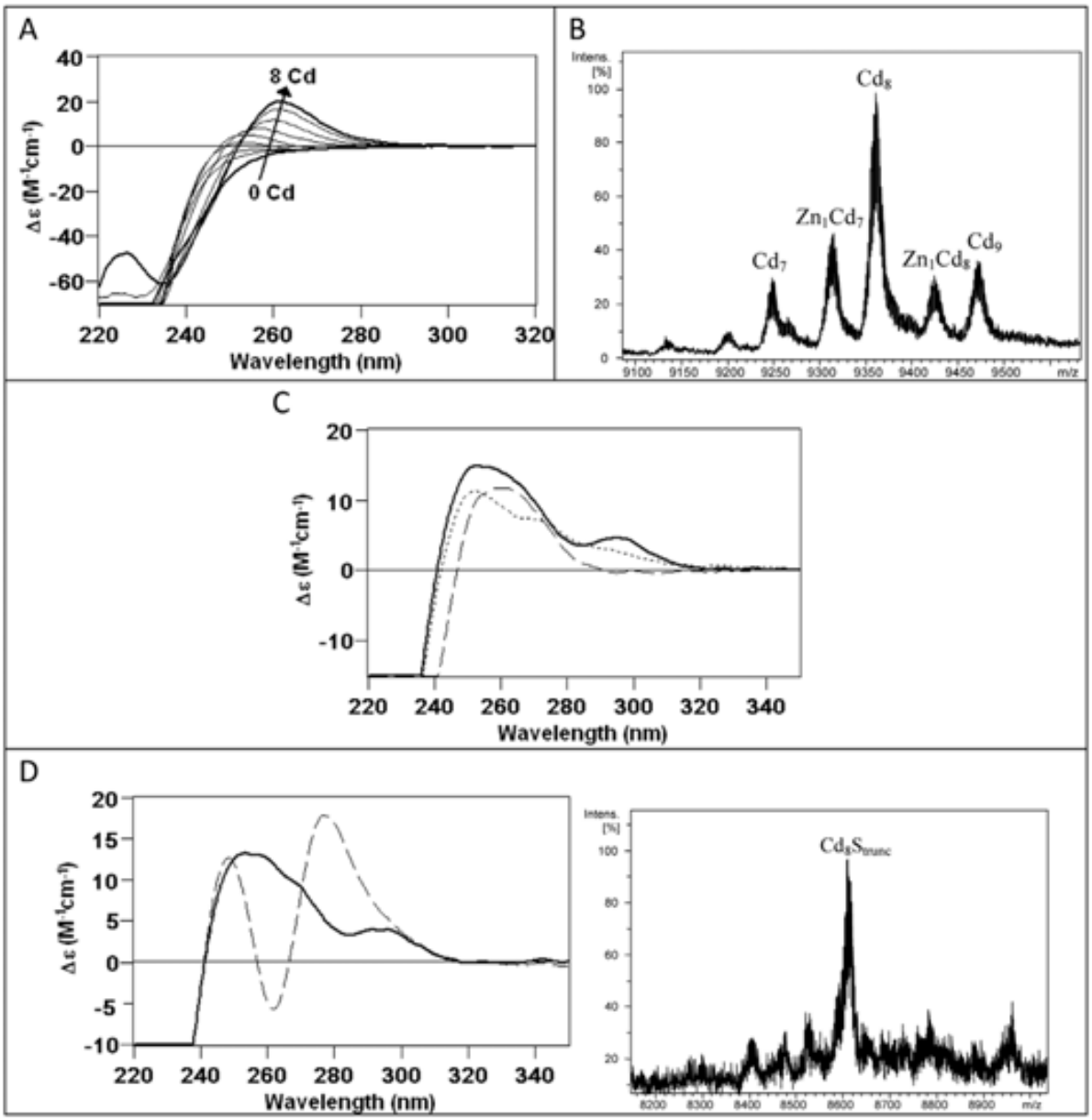

Figure 8. The *in vitro* Cd(II) binding abilities of BfMT1 points to a partial preference for divalent metal ion coordination. (A) CD corresponding to the titration of a 10 μM solution of Zn-BfMT1 with Cd(II) at pH 7.0 until 8 Cd(II) eq added (B) Deconvoluted ESI-MS spectrum of an aliquot corresponding to the addition of 8 Cd(II) eq to Zn-BfMT1. (C) Comparison of the CD spectra of the recombinant Cd-BfMT1 preparation (solid line), the acidified and reneutralized sample (dashed line), and the latter after the addition of 4 S^{2-} equivalents (dotted line). (D) Comparison of the CD spectra of the Cd-BfMT1 sample before (solid line) and after (dashed line) 28-days of evolution under inert atmosphere and ESI-MS spectrum of the final sample.
doi:10.1371/journal.pone.0043299.g008

expression, through the identified MRE elements. The experimentally observed response to metal induction for both BfMT genes fully agrees with the functionality of the multiple MREs identified in the promoter regions of the respective genes, as reported in the *in silico* analysis section (*cf.* Figure 3).

The amphioxus metal homeostasis is disrupted by cadmium and copper overload in a different way

Metal accumulation was measured in lancelets exposed (or non-exposed) to Cd or Cu in the same experimental conditions as for the transcriptional pattern studies reported in the previous section. Besides Cu and Cd, Fe and Zn contents were also measured to assess whether there was any significant interrelation between the pathways ensuring the homeostasis of these metals, as established in relevant model organisms, such as yeast [43]. All the results are summarized in Figure 6. Cadmium accumulation was readily evident in Cd-intoxicated animals, reaching maximum concentrations of 71.26 μM Cd/g dry weigh after 30 μM Cd treatment, and even 1373.99 μM Cd/g dry weigh for 300-μM Cd doses. As expected, no cadmium was accumulated in control or in Cu-treated organisms. These results are indicative of a notable disruption of the Cd homeostasis mechanisms in high Cd conditions, which is in concordance with the *MT* gene repressor effect described in the preceding section, and with a parallel

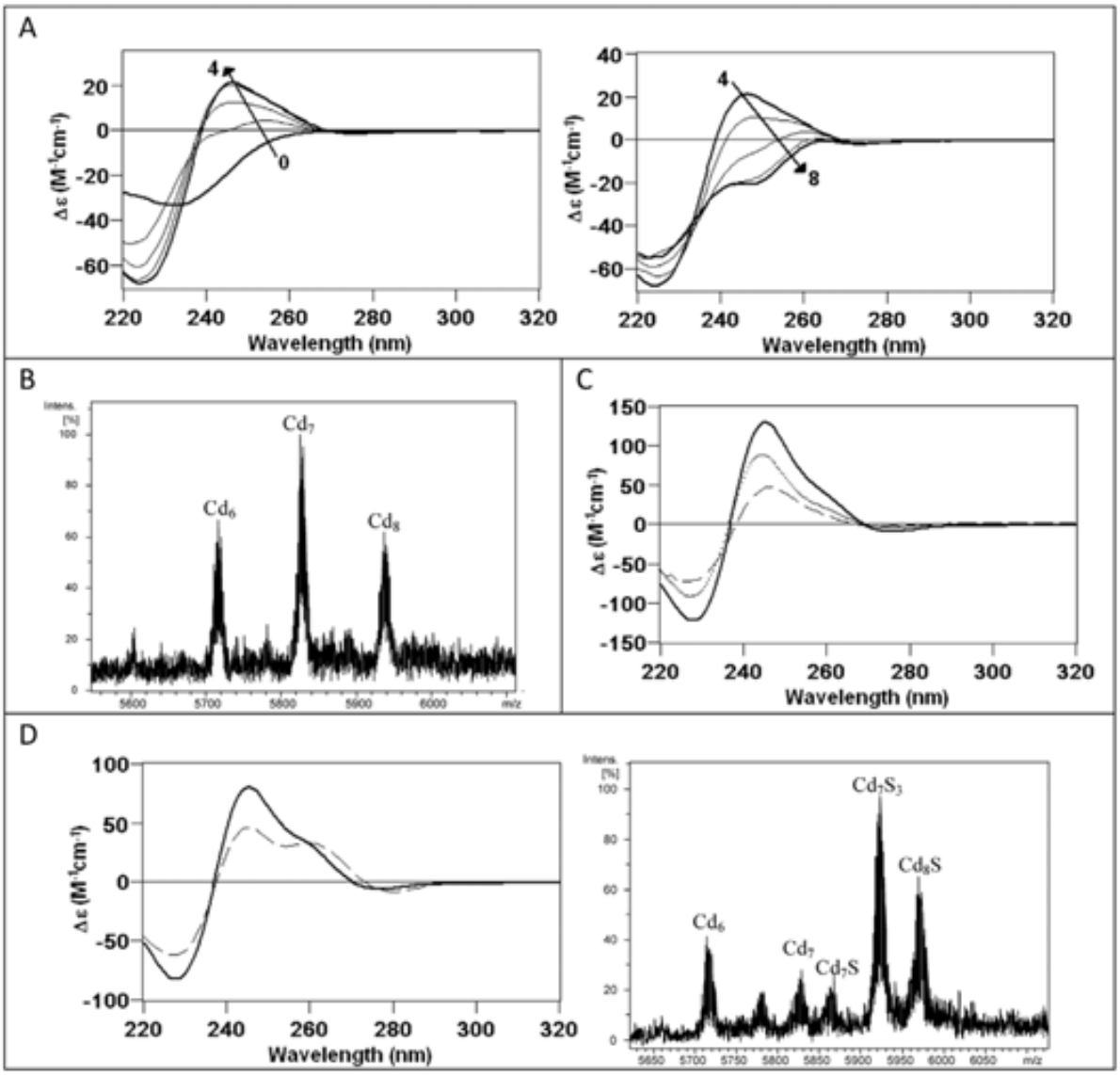

Figure 9. The *in vitro* Cd(II) binding abilities of BfMT2 points to a partial preference for divalent metal ion coordination. (A) CD corresponding to the titration of a 10 μM solution of Zn-BfMT2 with Cd(II) at pH 7.0 from 0 to 4 and from 4 to 8 Cd(II) eq added. (B) Deconvoluted ESI-MS spectrum of an aliquot corresponding to the addition of 8 Cd(II) eq to Zn-BfMT2. (C) Comparison of the CD spectra of the recombinant Cd-BfMT2 preparation (solid line), the acidified and reneutralized sample (dashed line), and the latter after the addition of 4 sulfide equivalents (dotted line). (D) Comparison of the CD spectra of the Cd-BfMT2 sample before (solid line) and after (dashed line) 28-days of evolution under inert atmosphere and ESI-MS spectrum of the final sample.
doi:10.1371/journal.pone.0043299.g009

phenomenon reported for MT-null *C. elegans* mutants [44]. Significantly, 300 μM Cd also deregulates internal Zn and Fe levels, which increase exponentially ($P<0.01$) in comparison to the non-treated organisms, while at a lower Cd dose (30 μM), there is no significant alteration of any physiological metal content (Zn, Cu. Fe). This leads to the hypothesis that the decrease in both MT gene expression levels would severely impair global metal homeostasis under heavy Cd intoxication conditions. On the other hand, Cu overload, at any concentration, has a poor effect on Zn and Fe contents, which remain as in control animals. Conversely, the internal pools for copper are significantly higher, in this case also with a much more drastic accumulation behavior also at the lower assayed concentration (50 μM).

The recombinant synthesis of the BfMT1 and BfMT2 proteins

DNA sequencing of the BfMT1 and BfMT2 coding segments in the pGEX expression constructs ruled out the presence of any artifactual nucleotide substitution. Furthermore, SDS-PAGE analyses of total protein extracts from the transformed BL21 cells showed the presence of bands corresponding to the expected GST-BfMT1 and GST-BfMT2 sizes (data not shown). Homogeneous metal-BfMT1 and metal-BfMT2 preparations were obtained from 5-L *E. coli* cultures at final concentrations ranging from 2.6×10^{-4} M for divalent metal ions to 0.2×10^{-4} M for Cu complexes. Acidification of the Zn-BfMT complexes yielded the corresponding apo-forms, with molecular masses of 8476.2 Da for BfMT1 and 5053.0 Da for BfMT2, fully concordant with the

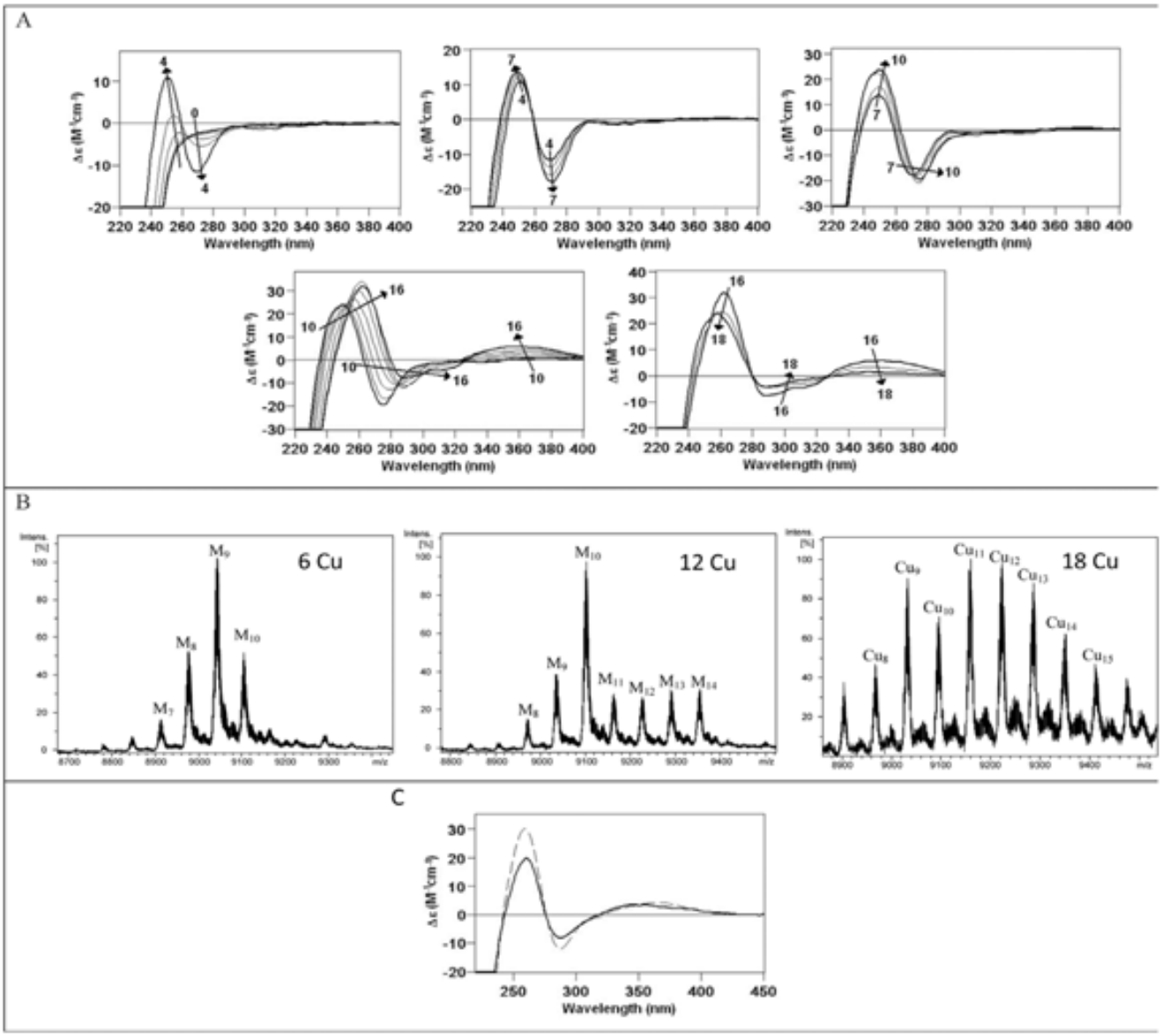

Figure 10. The *in vitro* Cu(I) binding abilities of BfMT peptides shows the preference of BfMT1 *vs.* BfMT2 to coordinate this metal ion. (A) CD corresponding to the titration of a 10 µM solution of Zn-BfMT1 with Cu(I) at pH 7.0 until 18 Cu(I) eq added. The arrows show the number of Cu(I) eq added at each stage of the titration. (B) Deconvoluted ESI-MS spectrum of several aliquots extracted from the solution at 6, 12, and 18 Cu(I) eq added to Zn-BfMT1. (C) Comparison of the CD spectra of the recombinant Cu-BfMT2 preparation (solid line), and that of the Zn-BfMT1 sample after the addition of 12 Cu(I) eq (dashed line).
doi:10.1371/journal.pone.0043299.g010

calculated average theoretical values (8476.7 Da and 5053.9 Da, respectively) for the synthesized products. This confirmed both the identity and purity of the recombinant polypeptides.

The Zn-binding abilities of BfMT1 and BfMT2 points to an intermediate Zn-/Cu-thionein character for both isoforms

The recombinant synthesis of BfMT1 and BfMT2 in Zn-supplemented *E.coli* cultures rendered a mixture of Zn-complexes of different stoichiometries (Figure 7). For BfMT1, the major species was Zn_7-BfMT1, with the significant presence of lower amounts of the Zn_6- and Zn_5-BfMT1 complexes. Conversely, for the BfMT2 isoform, a major Zn_6-BfMT2 species was accompanied by minor equimolar Zn_5- and Zn_4-BfMT2 complexes. These results match well the mean Zn-per-protein content calculated from ICP-AES measurements (Table 1), and are in accordance with the number of putative coordinating residues in their peptide sequences: 19 Cys and 2 His in BfMT1 and 18 Cys in BfMT2 (*cf.* Figure 1). The CD spectra of both preparations were practically silent in the corresponding spectral region (*ca.* 240 nm for Zn-Cys chromophores), this suggesting a poor folding degree of the clusters formed about the metal ions (Figure 7). Interestingly, the ESI-MS spectrum of the Zn-BfMT1 preparation revealed the presence of very minor peaks, which could be unambiguously identified as resulting from a BfMT1 truncated form, after the loss of the eight C-terminal protein residues (*i.e.* TTPPAAHL). Curiously, the corresponding Zn-complexes exhibit the same stoichiometries (Zn_7-, Zn_6- and Zn_5-) as those of the whole peptide, which indicates that this minor posttranslational event does not

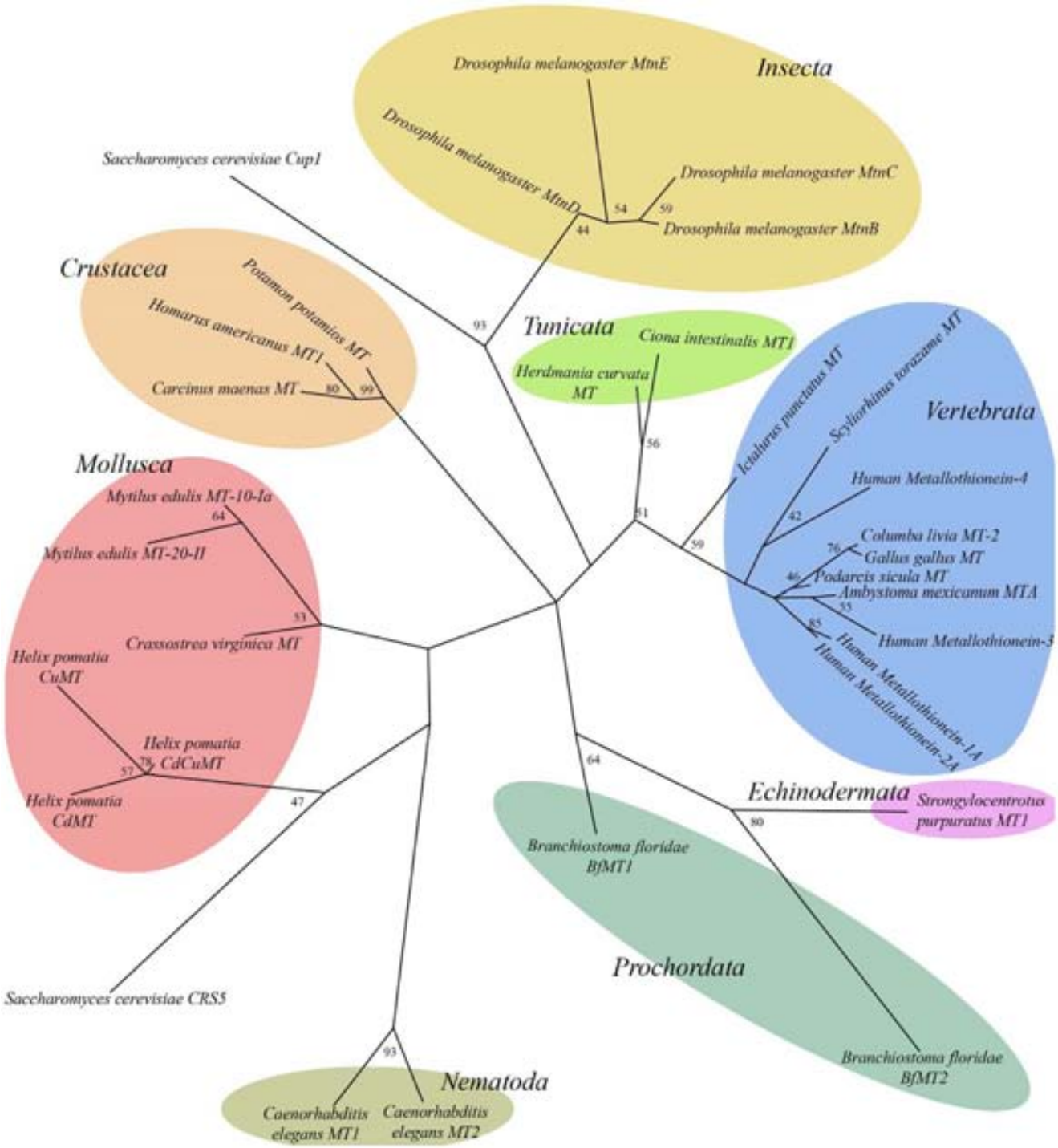

Figure 11. Protein distance analysis of MTs from organisms of different taxa positions *Branchiostoma* MTs at the base of vertebrates and close to Echinoderm MTs. The Maximum Likelihood tree was obtained by the Phylip method, and the corresponding bootstrap values (in percentages) obtained are included. Sequences and their Uniprot IDs are: Human MT-1A (P04731), Human MT-2A (P02795), Human MT-3 (P25713), Human MT-4 (P47944), *Gallus gallus* MT (P68497), *Columba livia* MT-2 (P15787), *Podarcis sicula* MT (Q708T3), *Ictalurus punctatus* MT (O93571), *Scyliorhinus torazame* MT (Q6J1T3), *Ambystoma mexicanum* MTA (O42152), *Mytilus edulis* 10 Ia (P80246), *Crassostrea virginica* MT (P23038), *Mytilus edulis* MT-20-II (P80252), *Helix pomatia* CdCuMT (D1LZJ8), *Helix pomatia* CdMT (P33187), *Helix pomatia* CuMT (P55947), *Homarus americanus* MT1 (P29499), *Carcinus maenas* MT (P55948), *Potamon potamios* MT (P55952), *Drosophila melanogaster* MtnB (P11956), *Drosophila melanogaster* MtnC (Q9VDN2), *Drosophila melanogaster* MtnD (Q8I9B4), *Caenorhabditis elegans* MT1 (P17511), *Caenorhabditis elegans* MT2 (P17512), *Saccharomyces cerevisiae* Cup1 (P0CX80), *Saccharomyces cerevisiae* CRS5 (P41902). The following sequences were obtained from GeneBank: *Strongylocentrotus purpuratus* MT1 (AAA30061.1), *Ciona intestinalis* MT1 (ACN32211.2), *Herdmania curvata* MT (AY314949.1). *Drosophila melanogaster* MtnE sequence was obtained from FlyBase (FlyBaseID: FBpp0293071).
doi:10.1371/journal.pone.0043299.g011

affect the coordinating capacity of BfMT1, and indirectly suggests that the His residue in the penultimate position does not participate in zinc binding. Histidine participation in BfMT1 metal coordination was also ruled out through DEPC-modification experiments, which indicated that neither of the two His residues present in BfMT1 was involved in Zn-binding (data not shown).

Concerning the observed minor truncation of BfMT1, it is noteworthy that a similar event has been observed for *C. elegans* CeMT1, produced under equivalent conditions. These two peptides have in common a C-terminal region devoid of cysteines, and with a similar amino acid composition. Interestingly a revision of our previous CeMT1 MS data [35] revealed a truncation of the three final residues of its metal-complexes, this suggesting the susceptibility of these free peptide tails to endoproteolysis.

The Cd-binding abilities of BfMT1 and BfMT2 indicates a preference of BfMT2 over BfMT1 for cadmium dealing

The biosynthesis of the BfMT1 and BfMT2 isoforms in Cd-supplemented bacterial cultures revealed much more significant differences between their metal binding properties. Hence, BfMT1 rendered a mixture of many species, the two most abundant being, in this order, Cd_8-, Cd_9S- and Cd_7-BfMT1 in this order (Figure 7). Among the minor peaks, many species of high Cd content and containing sulfide ligands could be envisaged. The important presence of S^{2-}-containing complexes in this sample was confirmed by two independent results: first, the discrepancy between the Cd-per-MT contents measured by normal and acid ICP-AES results (Table 1); and second, the CD spectra of the Cd-BfMT1 preparation exhibiting the typical absorptions due to the Cd-S^{2-} bonds at *ca.* 300 nm, besides a broad signal centered at 250–260 nm contributed by the $Cd(SCys)_4$ chromophores [34]. In marked contrast with these results, the folding of the BfMT2 peptide ensuing Cd coordination practically yielded a single Cd_6-BfMT2 species. Only very minor species could be detected, corresponding to Cd_7- and Cd_6S_2-BfMT2 (Figure 7). The latter would account for the only slight divergence between normal and acid ICP measurements) and the fact that the CD spectrum showed the typical fingerprint attributable to tetrahedral $Cd(SCys)_4$ chromophore absorbing at *ca.* 250 nm, and only a minor absorption at (-) 275 nm. The presence of S^{2-}-containing complexes in the preparation of both Cd-BfMT1 and Cd-BfMT2 preparations prompted us to analyzed whether their CD fingerprints evolved over time, a phenomenon that we have previously reported for preparations of the yeast Cd-Cup1, containing a significant proportion of S^{2-}-containing complexes [45]. The main changes are observed for the Cd-BfMT1 CD fingerprint, in which the initial broad signal evolves to form two new narrower signals *ca.* 250 and 275 nm while maintaining the absorption at *ca.* 300 nm (contributed by the Cd-S^{2-} chromophores) (Figure 8D). Interestingly, while the more important CD variations are associated to the Cd-BfMT1 preparation, the more important speciation changes over time are observed for Cd-BfMT2. The former, which starts from a mixture of species with a major full Cd_8-BfMT1 complex, ends in a truncated Cd_8S-BfMT1 form. On the contrary, the single Cd_6-BfMT2 species ends as a mixture of sulfide-containing cadmium complexes of the protein (Figure 8D).

In vitro Cd-binding behavior of the BfMT isoforms was analyzed by two different approaches: (i) Cd(II) titration of the Zn-BfMT preparations, and (ii) acidification plus subsequent reneutralization of the recombinant Cd-BfMT samples. The Cd(II) titration of Zn-BfMT1 shows a point of saturation in the UV-vis, CD and ESI-MS spectra for 8 Cd^{2+} equivalents added (Figure 8A). Although further Cd^{2+} equivalent addition provokes losses in the intensity of CD and UV-vis spectra, the speciation obtained at this point remains constant, including a mixture of several Cd_x- and Zn, Cd-BfMT1 species, with major Cd_8-BfMT1, as revealed by the ESI-MS results (Figure 8B). As expected from the important contribution of the S^{2-}-containing species to the recombinant Cd-BfMT1 preparation, its CD spectrum is not obtained at the end of the Zn(II)/Cd(II) replacement reaction, but the addition of several S^{2-} equivalents to the resulting mixture after the Cd(II) titration clearly indicated the incorporation of these ligands into the Cd-BfMT1 complexes, although neither the CD fingerprint nor the speciation of the recombinant preparation can be reproduced *in vitro*. When the recombinant Cd-BfMT1 preparation was acidified, reneutralized and several S^{2-} eq were added, a CD fingerprint and a fairly similar speciation to that of the initial sample was obtained (Figure 8C). All these results highlight the importance of the S^{2-} ligands in the formation of an important subset of Cd-BfMT1 complexes under *in vivo* conditions.

In all the steps of the Zn(II)/Cd(II) replacement reaction in the Zn-BfMT2 preparation (Figure 9A), the species obtained correspond to a mixture of Cd_6-, Cd_7- and Cd_8-BfMT2 (Figure 9B). The CD spectra show an absorption *ca.* 245 nm for 4 eq of Cd^{2+} added and after the addition of more equivalents this signal fades to eventually render an absorption at *ca* (-) 250 nm. Neither the CD nor the ESI-MS results at any point of the titration reproduced the features of the *in vivo* Cd-BfMT2 preparations. Similar results to those achieved after the acidification, reneutralization and sulfide addition to the Cd-BfMT1 preparations were achieved for those of BfMT2. Figure 9C shows the CD spectra of the initial recombinant Cd-BfMT2 sample together with that obtained after reneutralization and how the addition of S^{2-} anions allows restoration of the initial CD fingerprint. ESI-MS data (not shown) also indicates that the initial speciation is recovered after S^{2-} addition.

Overall results obtained for cadmium-binding converge in the classification of BfMT1 as an MT poorly competent peptide for Cd(II) coordination, as its recombinant synthesis by Cd-supplemented *E. coli* cells yields a mixture of species, including a subpopulation of complexes with sulfide ligands. This behavior is accompanied by other features typical of MT peptides of Cu-thionein character [7], and mainly derived from the substantial presence of S^{2-} anions in the preparations, such as the evolution of the CD spectra over time, and the inability of the final stage of the Zn/Cd titration, and also of the denaturalization/renaturalization process, to reproduce the fingerprint and stoichiometry of the recombinant sample. Although BfMT2 is not completely free of these features, they are considerably less pronounced than for BfMT1, and it can therefore be assumed that BfMT2 is much closer to an optimized MT for divalent metal ion binding.

Cu-binding abilities of BfMT1 and BfMT2: the essential inability of BfMT2 for copper binding

BfMT1 and BfMT2 recombinant synthesis in the presence of Cu(II) surplus was assayed under normal and low aeration conditions, since we previously showed how bacterial culture oxygenation can affect the metal content of the complexes produced in these conditions [30]. Although we invariably failed to recover any BfMT2 product from Cu-supplemented cultures, the Cu-BfMT1 syntheses rendered some interesting results that allowed characterization of the purified samples. In normal oxygenation conditions, BfMT1 yielded different types of preparations, namely Cu-preparations of type 1 and type 2. Both types were constituted by mixtures of Cu, Zn-BfMT1 species in which an M_9- (Type 1) or M_{10}-BfMT1 (Type 2) (M = Zn+Cu)

were the major species, as shown by the ESI-MS analyses at pH 7 (Figure 7). Mass measurements at pH 2.4 revealed that the M_{10}-complexes of type 2 were in fact mainly Cu_8Zn_2- species, in accordance with the ICP results (Table 1). On the contrary, a mixture of major Cu_4Zn_5-, and minor Cu_5Zn_4- plus Cu_6Zn_3-BfMT1 complexes, would account for the detected type 1 M_9-aggregates. In contrast, low oxygenation conditions yielded a mixture of homometallic Cu-BfMT1 species ranging from Cu_9- to Cu_{12}-BfMT1 (Figure 7 and Table 1). Interestingly, regular oxygenation type 2 preparations render the most intense and well-defined CD spectra (Figure 7); the CD fingerprint of type 1 productions is also well defined but less intense, while that of the low-aerated productions is practically silent. This suggests that the presence of Zn(II) ions in type 1 and 2 preparations would be crucial for the building of a well-folded structure to the corresponding complexes.

The *in vitro* Zn(II)/Cu(I) replacement studies in Zn-BfMT1 (Figure 10A) afforded the typical CD signals observed when Cu(I) binds to MTs [30,46]. Interestingly, at different stages of this Zn/Cu replacement process, CD fingerprints and speciations analogous to those obtained in the *in vivo* productions are obtained. Hence, the addition of 4 and 6 Cu(I) eq gives rise to a mixture of species in which M_9- is the major one, like in type 1 productions, although both samples do not share the same CD fingerprint. Addition of 12 Cu(I) eq makes M_{10}- the major species of a mixture that shows a CD envelope similar to that of the type 2 productions (Figure 10C). Finally, excess Cu(I) addition to this solution affords mixtures of homometallic Cu_7- to Cu_{15} complexes, which are somewhat similar to the results for the low-oxygenation syntheses. This is exactly the same situation that we described for the Zn(II)/Cu(I) titration of the yeast Crs5 MT [30]. The fact is that different stages of the replacement reaction reproduce the results of different recombinant productions, which in turn correspond to different copper availably conditions. Therefore this behavior suggests a copper-binding peptide that can cope with different physiological conditions yielding equally stable complexes.

On the other hand, the *in vitro* replacement of Zn(II)/Cu(I) in Zn-BfMT2 revealed some clues for understanding the impossibility of recovering recombinant Cu-BfMT2 complexes from the corresponding *E. coli* cells grown in copper supplemented cultures. When successive Cu(I) equivalents were added to the Zn-BfMT2 preparation, the UV-vis and ESI-MS spectra recorded at different steps unequivocally showed that Cu(I) was being bound to the peptide at increasing ratios, but the CD fingerprint remained practically silent (data not shown), which suggested a complete lack of structured folding. Significantly, exposure of the Zn(II)-BfMT2 complexes to Cu(I) caused the progressive generation of a highly complex mixture of heteronuclear (Zn(II), Cu(I)) and homonuclear (Cu(I)) species, also comprising apo-BfMT2, which evolved into the major form from 18 eq Cu(I) added on. Thus, it is reasonable to assume that the failure to reach a minimally folded state when coordinating Cu(I) ions leads to complete proteolysis inside the bacteria producing cells, a phenomenon that we have reported before for the mollusc *Megathura crenulata* [47] and the *Drosophila* MtnE MT isoforms [48], although only for the attempts to synthesize them from low-aerated (i.e. high intracellular copper) Cu-enriched cultures.

As this point, and admitting the obvious fact that BfMT2 is unsuitable as Cu-thionein, it is worth considering that BfMT1, although far from being optimal for Cu(I) coordination, presents the typical features of a partial Cu-thionein MT [7], since it is able to render homometallic Cu-complexes when recombinantly synthesized in highly Cu-enriched cells (*i.e.* cultured in Cu-supplemented media at low aeration), this adding up to its poor Cd-binding character, as discussed earlier.

Phylogenetic and evolutionary studies places amphioxus MTs in the same echinoderm branch

Homology searches by performing BLAST in the UNIPROT database clearly show that both BfMT1 and BfMT2 protein sequences (sharing only 26.2% identity) clearly differ in sequence to other MTs, not being directly alignable to the vertebrate isoform peptides. Therefore there is a no clear lineage connecting any cephalochordate MT with the vertebrate MT prototype sequence. This is in concordance with the reported observation that most of the gene copies emerging from the large scale genome duplications on the vertebrate stem were lost, so that the relationship between non-vertebrate and vertebrate genomes is not always straightforward [16]. A protein distance similarity tree (Figure 11) shows the different positions of both amphioxus MTs, while revealing further interesting evolutionary relationships. First, it is worth noting that both cephalochordate (*Branchiostoma*) MTs are much more distant, and appear in a separate tree branch than the two tunicate (*Ciona* and *Hermania*) MTs. Interestingly, the tunicate MTs are situated in the "vertebrate branch", close to the MTs of some fish (*Ictalurus* and *Scyliorhinus*), the most primitive vertebrates. Contrarily, the amphioxus MT group with the sea urchin isoform, at a greater distance of the vertebrate counterparts. This is in major concordance with the alternative hypothesis of a close relationship between amphioxus and echinoderms, leaving the tunicates close to vertebrates [18], which was proposed some years ago as opposed to the classic view that placed the Cephalochordates as close precursors of vertebrates.

Conclusions

At least two genes encoding metallothionein peptides, here named *BfMT1* and *BfMT2*, are present, in tandem disposition, in the *B. floridae* genome. They have similar gene structures (4 exons interrupted by 3 exons) and exhibit an equivalent number of expression response elements (MREs and AREs), in their upstream DNA region. One gene encoding a putative MTF-1 has also been identified in the genome that is very similar to the MTF1 sequence in fishes, which supports the putative functionality of these MREs. ESTs and cDNA corresponding to both *BfMT* genes were retrieved from the *B. floridae* data banks, and RT-PCR experiments revealed that both transcripts were also present in the *B. lanceolatum* species, sharing a complete sequence identity. Surprisingly, both genes follow rather different expression strategies and patterns. *BfMT1* cDNA is composed of the four exon sequences; while *BfMT2* cDNA results from an alternate splicing that skips exon 2. The full length *BfMT2* cDNA would also be present in lancelets, but in extremely small amounts. *BlMT1* and *BlMT2* mRNA accumulation rates under Cd and Cu exposure also reveal very different metal responses: *BlMT1* is constitutively transcribed at considerable levels, and in control conditions, *BlMT2* is practically silent. Although metal treatment induces an enhanced synthesis of both isoforms, the relative response of *BlMT2* is much higher than that of *BfMT1*, and therefore while *BlMT1* can be considered an essentially constitutive gene, *BlMT2* is clearly inducible. The consideration of the Cd and Cu transcription regulation trends for the two genes, as well as the metal binding behavior of both recombinantly synthesized peptides converge in the hypothesis that they serve very different purposes in the amphioxus organisms. BfMT1 is a polyvalent metal binding peptide, able to coordinate any of the studied metal ions (Zn, Cd or Cu), rendering complexes stable enough to endure in

physiological environments, which is fully concordant with the constitutive character of their encoding gene, and therefore, with a metal homeostasis housekeeping role. On the contrary, BfMT2 exhibits a clear ability to coordinate Cd(II) ions, while it is absolutely unable to fold into stable complexes under Cu(I) surplus, even as mixed Zn, Cu species. This is compatible with an essential cadmium detoxification role, which is consequently only induced in emergency situations. Notably, the Cd and Cu internal accumulation in metal treated organisms fully confirms this metal binding behavior, as discussed in the corresponding result sections. It is sensible to presume that there may be gene expression and/or metal binding differences between MT homologous isoforms of different lancelet species (*B. floridae* vs. *B. lanceolatum*). But it is worth noting that in the cases of MT polymorphic systems belonging to close species that we have previously analyzed, *e.g.* the pulmonate snails MTs, there are significant differences between the features of the several isoforms encoded in a same genome (paralogs), but MT isoforms of the same type (ortologs) exhibit extremely equivalent properties [49,50]. This will presumably be the same case in the two lancelet species.

The key question of the metal specificity of different MT isoforms has been analyzed in depth in several model organisms exhibiting polymorphic MT systems. Molluscs (pulmonate gastropoda) and nematodes (*C. elegans*) are optimal for comparative purposes (Figure 11). Other interesting taxa, with somewhat opposing MT systems in terms of metal preferences, are vertebrates and the baker's yeast, also included in the tree shown in Figure 11. Different situations are encountered in these groups. In the *Helix pomatia* [49] and *Cantareus aspersus* [50] snails, there are three MT isoforms, one with a polyvalent behavior, and the other two having evolved into extreme metal specificities: one highly inducible, for Cd detoxification, and the other rather constitutive, for Cu metabolism mainly linked to the needs of their hemocyanin respiratory pigment. Neither of the two reported MTs in the nematode *C. elegans* exhibits a Cu-thionein character, but the two CeMT peptides still exhibit different metal binding behaviors: being CeMT1, encoded from a somewhat constitutive gene and showing better Zn(II) binding abilities, being mostly associated to a housekeeping metal metabolism role; while a detoxification function is attributed to CeMT2, which is mainly synthesized after Cd induction, and which in turn shows better coordination behavior for this metal ion [35,44].

None of the four MT isoforms present in mammals exhibits a clear Cu-thionein character, although the most putatively primitive, MT4, is clearly more prone to Cu-binding that the others [46]. Finally, the two highly dissimilar yeast MTs (Cup1 and Crs5) are of Cu-thionein character, but the extreme specificity for copper binding of Cup1 [45] is changed to a more subtle preference for Crs5 [30], compatible with a mixed metal metabolism role. A fairly comprehensive picture of MT differentiation in different taxa seems to emerge from these considerations. On the one hand, there are MT isoforms with somewhat polyvalent metal binding abilities, able to form physiologically stable complexes with all kinds of the considered metal ions (mainly the physiological Zn and Cu), without exhibiting any clear metal preference, and which are encoded in a constitutive, or poorly inducible, pattern. These isoforms always appear at the root of the branches in phylogenetic or protein distance trees (*cf.* Figure 11), and are best exemplified by yeast Crs5, snail Cd/Cu MTs, *C. elegans* MT1 or vertebrate MT4. Then, in each group of organisms, highly specialized MT isoforms, optimized for the handling of a specific metal ion, would have evolved to fulfill specific metabolic needs or cope with intoxication threads, according to the specific conditions of their habitats. On the one hand, metal-responsive MTs would have emerged as defense peptides against metal surplus, synthesized from clear metal-inducible genes, as found for the Cd-MT snail isoforms and the Cup1 yeast MT. On the other hand, MT specific isoforms related to special basic metabolic needs would have remained constitutive, as is the case with the Cu-MT forms in snails. This kind of specialization pattern would easily account for the tremendous heterogeneity among metallothionein peptides [4], as each differentiation event would have been highly specific and independent in each branch of the tree of life, and starting from different *substrate* peptides. However, since the main determinant of MT metal specificity has been identified as its protein sequence, this including both the number and position of the coordinating residues (mainly Cys) and also the nature of the intercalating amino acids [49], it is not surprising that similar amino acid motifs are detected for MT peptides converging in a preference for the same metal ion, as has been long reported [51]. And this is also precisely what we observe for the two characterized BfMT isoforms that lancelets synthesize: an MT isoform for general metal handling (BfMT1), and a specialized form devoted to metal (eventually cadmium) defense (BfMT2). Precisely, BfMT1 appears in a position in the tree in Figure 11 that is closer to the common central link of all MTs, while the most specialized BfMT2 is in a longer (therefore distant) branch, which is concordant with the above proposed evolutionary scenario.

Supporting Information

Figure S1 Sequences of the *B. lanceolatum* BlMT1 and BlMT2 cDNAs. This data were deposited in the NCBI Transcriptome Shotgun Assembly (TSA) database, as reported while the current manuscript was under revision [40].
(DOC)

Acknowledgments

We are grateful to the Center for Genetic Resource Information of the Japanese National Institute of Genetics, in Mishima (Japan) for providing us with amphioxus cDNA clones from their libraries. We thank the *Serveis Científico-Tècnics de la Universitat de Barcelona* and the *Servei d'Anàlisi Química de la Universitat Autònoma de Barcelona* for allocating instrument time.

Author Contributions

Conceived and designed the experiments: MC ÒP SA. Performed the experiments: MG SP-R ÒP. Analyzed the data: MG SP-R MC ÒP SA. Contributed reagents/materials/analysis tools: MC ÒP SA. Wrote the paper: MC SA.

References

1. Sigel A, Sigel H, Sigel RKO (2009) Metal ions in Life Sciences; v 5: Metallothioneins and Related Chelators Cambridge: Royal Society of Chemistry, 514 p.
2. Capdevila M, Bofill R, Palacios O, Atrian S. (2012) State-of-the-art of metallothioneins at the beginning of the 21st century. Coord Chem Rev 256: 46–62.
3. Vasak M, Hasler DW (2000) Metallothioneins: new functional and structural insights. Curr Opin Chem Biol 4: 177–183.
4. Capdevila M, Atrian S (2011) Metallothionein protein evolution: a miniassay. J Biol Inorg Chem 16: 977–989.
5. Binz PA, Kägi JHR (1999) Metallothionein: Molecular evolution and classification. In: Klaassen C, editor. Metallothionein IV. Basel: Birkhäuser Verlag, 7–13.
6. Vasák M, Meloni G (2011) Chemistry and biology of mammalians metallothioneins. J Biol Inorg Chem 17: 1067–1078.

7. Bofill R, Capdevila M, Atrian S (2009) Independent metal-binding features of recombinant metallothioneins convergently draw a step gradation between Zn- and Cu-thioneins. Metallomics 1: 229–234.
8. Villarreal L, Tio L, Capdevila M, Atrian S (2006) Comparative metal binding and genomic analysis of the avian (chicken) and mammalian metallothionein. FEBS J 273: 523–535.
9. Andrews GK, Fernando LP, Moore KL, Dalton TP, Sobieski RJ (1996) Avian metallothioneins: structure, regulation and evolution. J Nutr 126: 17S–23S.
10. Nam DH, Kim EY, Iwata H, Tanabe S (2007) Molecular characterization of two metallothionein isoforms in avian species: evolutionary history, tissue distribution profile, and expression associated with metal accumulation. Comp Biochem Physiol C Toxicol Pharmacol 145: 295–305.
11. Vergani L (2009) Metallothioneins in aquatic organisms:fish, crustaceans, molluscs and echinoderms. In Sigel A, Sigel H, Sigel, RKO, editors. Metal ions in Life Sciences; v 5: Metallothioneins and Related Chelators. Cambridge: Royal Society of Chemistry, 199–238.
12. Muller JP, Wouters-Tyrou D, Erraiss NE, Vedel M, Touzet N, et al. (1993) Molecular cloning and expression of a metallothionein mRNA in Xenopus laevis. DNA Cell Biol 12: 341–349.
13. Riggio M, Trinchella F, Filosa S, Parisi E, Scudiero R (2003) Accumulation of zinc, copper, and metallothionein mRNA in lizard ovary proceeds without a concomitant increase in metallothionein content. Mol Reprod Dev 66: 374–382.
14. Schubert M, Escriva H, Xavier-Neto J, Laudet V (2006) Amphioxus and tunicates as evolutionary model systems. TRENDS Ecol Evol 5: 269–277.
15. Cañestro C, Bassham S, Postlethwait JH (2003) Seeing chordate evolution through the Ciona genome sequence. Genome Biol 4: 208.
16. Putnam NH, Butts T, Ferrier DE, Furlong RF, Hellsten U, et al. (2008) The amphioxus genome and the evolution of the chordate karyotype. Nature 19: 1064–1071.
17. Cañestro C, Albalat R (2012) Transposon diversity is higher in amphioxus than in vertebrates: functional and evolutionary inferences. Brief Funct Genomics 11: 131–141.
18. Delsuc F, Brinkmann H, Chourrout D, Philippe H (2007)Tunicates and not cephalochordates are the closest living relatives of vertebrates. Nature 439: 965–968.
19. Franchi N, Boldrin F, Ballarin L, Piccinni E (2010) CiMT-1, an unusual chordate metallothionein gene in *Ciona intestinalis* genome: structure and expression studies. J Exp Zool 315: 90–100.
20. Magrane M and the UniProt consortium (2011) UniProt Knowledgebase: a hub of integrated protein data. Database 2011, article ID bar009.
21. Zdobnov EM, Lopez R, Apweiler R, Etzold T (2002)The EBI SRS server-new features. Bioinformatics 18: 368–73.
22. Sigrist CJA, Cerutti L, de Castro E, Langendijk-Genevaux PS, Bulliard V, et al. (2010) PROSITE, a protein domain database for functional characterization and annotation. Nucl Acids Res 38: 161–166.
23. Henikoff JG, Pietrokovski S, McCallum CM, Henikoff S (2000) Blocks-based methods for detecting protein homology. Electrophoresis 21: 1700–1706.
24. Lippi M, Passerini A, Punta M, Rost B, Frasconi P (2008) MetalDetector: a web server for predicting metal-binding sites and disulfide bridges in proteins from sequence. Bioinformatics 24: 2094–2095.
25. Ferre F, Clote P (2006) DiANNA 1.1: an extension of the DiANNA web server for ternary cysteine classification. Nucl Acids Res 1: 82–185.
26. Guo AY, Zhu QH, Chen X, Luo JC: GSDS (2007) a gene structure display server. Yi Chuan 29: 1023–1026.
27. Yu JK, Wang MC, Shin-I T, Kohara Y, Holland LZ, et al. (2008) A cDNA resource for the cephalochordate amphioxus Branchiostoma floridae. Dev Genes Evol 218: 723–727.
28. Capdevila M, Cols N, Romero-Isart N, González-Duarte R, Atrian S, et al. (1997) Recombinant synthesis of mouse Zn3-ß and Zn4-α metallothionein 1 domains and characterization of their cadmium(II) binding capacity. Cell Mol Life Sci 53: 681–688.
29. Cols N, Romero-Isart N, Capdevila M, Oliva B, Gonzàlez-Duarte P, et al. (1997) Binding of excess cadmium(II) to Cd7-metallothionein from recombinant mouse Zn7-metallothionein 1. UV-VIS absorption and circular dichroism studies and theoretical location approach by surface accessibility analysis. J Inorg Biochem 68: 157–166.
30. Pagani A, Villarreal L, Capdevila M, Atrian S (2007) The *Saccharomyces cerevisiae* Crs5 metallothionein metal-binding abilities and its role in the response to zinc overload. J Mol Microbiol 63: 256–269.
31. Bofill R, Palacios O, Capdevila M, Cols N, Gonzalez-Duarte R, et al. (1999) A new insight into the Ag^+ and Cu^+ binding sites in the metallothionein beta domain. J Inorg Biochem 73: 57–64.
32. Domenech J, Orihuela R, Mir M, Molinas S, Atrian S, et al. (2007) The Cd(II)-binding abilities of recombinant *Quercus suber* metallothionein: bridging the gap between phytochelatins and metallothioneins. J Biol Inorg Chem 12: 867–882.
33. Bongers J, Walton CD, Richardson DE, Bell JU (1988) Micromolar protein concentrations and metalloprotein stoichiometries obtained by inductively coupled plasma atomic emission spectrometric determination of sulfur. Anal Chem. 60: 2683–2686.
34. Capdevila M, Domenech J, Pagani A, Tio L, Villarreal L, et al. (2005) Zn- and Cd-metallothionein recombinant species from the most diverse phyla may contain sulfide (S^{2-}) ligands. Angew Chem Int Ed Engl 44:4618–4622.
35. Bofill R, Orihuela R, Romagosa M, Domenech J, Atrian S, et al. (2009) *Caenorhabditis elegans* metallothionein isoform specificity-metal binding abilities and the role of histidine in CeMT1 and CeMT2. FEBS J 276:7040–7056.
36. Notredame C, Higgins D, Heringa J (2000) T-Coffee: A novel method for fast and accurate multiple sequence alignment. J Mol Biol 302: 205–217.
37. Felsenstein J: PHYLIP: Phylogenetic inference package, version 3.6. 2002, Department of Genome Sciences, University of Washington, Seattle, WA, USA
38. Kimura M (1980) A simple method for estimating evolutionary rates of base substitutions through comparative studies of nucleotide sequences. J Mol Evol 16: 111–120.
39. Felsenstein J (1985) Confidence limits on phylogenies: an approach using the bootstrap. Evolution 39: 783–791.
40. Ouilon S, Bertrand S, Belgacem MR, Le Petillon Y, Escriva H (2012) Sequencing and analysis of the Mediterranean amphioxus (*Branchiostoma lanceolatum*) transcriptome. PLoS ONE 7: e36554.
41. Barsyte D, Lovejoy DA, Lithgow GJ (2001) Longevity and heavy metal resistance in daf-2 and age-1 long-lived mutants of Caenorhabditis elegans. FASEB J 15:627–34.
42. Cohen M, Lotta D, Coogan T, Costa M (1900) Mechanisms of metal carcinogenesis: the reactions of metals with nucleic acids. In Biological Effects of Heavy Metals. Foulkes EC, editor. CRC Press; 19–75.
43. Pagani A, Casamayor A, Serrano R, Atrian S, Ariño J (2007) Disruption of iron homeostasis in Saccharomyces cerevisiae by high zinc levels: a genome-wide study. Mol Microbiol 65: 521–537.
44. Zeitoun-Ghandour S, Charnock JM, Hodson ME, Leszczyszyn OI, Blindauer CA, et al. (2010) The two Caenorhabditis elegans metallothioneins (CeMT-1 and CeMT-2) discriminate between essential zinc and toxic cadmium. FEBS J 277: 2531–2542.
45. Orihuela R, Monteiro F, Pagani A, Capdevila M, Atrian S (2010) Evidence of native metal-S^{2-}-metallothionein complexes confirmed by the analysis of Cup1 divalent-metal-ion binding properties. Chem Eur J 16: 12363–12372.
46. Tio L, Villarreal L, Atrian S, Capdevila M (2004) Functional differentiation in the mammalian metallothionein gene family: metal binding features of mouse MT4 and comparison with its paralog MT1. J Biol Chem 279: 24403–24413.
47. Pérez-Rafael S, Mezger A, Lieb B, Dallinger R, Capdevila M, et al. (2012) The metal binding abilities of Megathura crenulata metallothionein (McMT) in the frame of Gastropoda MTs. J Inorg Biochem 108: 84–90.
48. Pérez-Rafael S, Kurz A, Guirola M, Capdevila M, Palacios O, et al. (2012) Is MtnE, the fifth Drosophila metallothionein, functionally distinct from the other members of this polymorphic protein family? Metallomics 4: 342–349.
49. Palacios O. Pagani A, Pérez-Rafael S, Egg M, Höckner M, et al. (2011) How Metazoan Metallothioneins achieved Metal Specificity: Evolutionary Differentiation in the Mollusc MT Gene Families. BMC Biol 9: 4.
50. Höckner M, Stefanon K, de Vaufleury A, Monteiro F, Pérez-Rafael S, et al. (2011) Physiological relevance and contribution to metal balance of specific and non-specific Metallothionein isoforms in the garden snail, *Cantareus aspersus*. Biometals 24: 1079–1092.
51. Valls M, Bofill R, Gonzàlez-Duarte R, Gonzàlez-Duarte P, Capdevila M, et al. (2001) A New Insight into Metallothionein (MT) Classification and Evolution. J Biol Chem 276: 32835–32843.

Supplementary Figure S1.

The *B. lanceolatum* transcriptome (TSA assembly, NCBI Bioproject PRJNA82409 [40]) was searched with BLAST for BfMT1 and BfMT2 homologous cDNAs. The JT862963 (A) and JT862963 (B) transcripts were respectively identified as putatively coding for BlMT1- and BlMT2-like (long version) proteins. Similarity guarantees the homology between the two isoforms in the two species, but heterogeneity in the information provided by different genome and EST projects (as observed for the *B. floridae*), isoform multiplicity and above all, the complexity of the amphioxus MT genes and coding regions renders the information presented below as definitely provisional, in the absence the *B. lanceolatum* genome sequence.

(A)

```
JT862963        GTATGCCTGATCCCTGCAACTGTGCTCAGAGCGGTGCGTGCTCCTGTAACGGACTGTGCC 60
BfMT1           --ATGCCTGATCCCTGCAACTGTGCACAGAGCGGAACGTGCTCCTGCGGCGGGCCGTGCC 58
                  ************************:********:.********** ..***.* *****

JT862963        AGTGCGGTGATGACTGCCAGTGTGGTGACGGCTGTAAATGTGTCGGCTGCAAACTTCACG 120
BfMT1           AGTGCGGCGATGACTGCCAGTGTGGTGACGGCTGTAAGTGTGTCGGCTGCAAACTTCACA 118
                ******* ******************************.********************.

JT862963        GCAACGTCGACGTCGCTCTCACCTGTTGTGGCACCTGCACGGGGATAGGGAAGAACTGTG 180
BfMT1           GCAATGTCACTGACATTGTCACCTGCTGTGTTGACTGCAAGGGGATAGGGAAGAATTGTG 178
                **** ***.. *:*. * ******* ****  ..*****.*************** ****

JT862963        CCTGTGGATGCTCGTGTTGCCAGCCCGACGTTCCAGCCGTGACCGTGCTGACAACGCCTC 240
BfMT1           CCTGTGGCTGCTCGTGTTGTCAGCCTGATACTCCGGCGGTGGCCATTCTGACAACGCCTC 238
                *******.*********** ***** ** . ***.** ***.**.* *************

JT862963        CAGCGGCTCACCTGTAAATTGCAGATCGTAAAACCCCATATAACATGGTCTGCCTTGTGG 300
BfMT1           CAGCGGCTCACCTGTAA------------------------------------------- 255
                *****************

JT862963        AATGACGTCATGTAGTTACATTTAGTCATCTGATCGTTACATTGGAATTCATTATGTCAC 360
BfMT1           ------------------------------------------------------------


JT862963        CTGTTTCCCTGT 372
BfMT1           ------------
```

```
JT862963p       MPDPCNCAQSGACSCNGLCQCGDDCQCGDGCKCVGCKLHGNVDVALTCCGTCTGIGKNCA 60
BfMT1           MPDPCNCAQSGTCSCGGPCQCGDDCQCGDGCKCVGCKLHSNVTDIVTCCVDCKGIGKNCA 60
                ***********:***.* *********************.**   :***  *.*******

JT862963p       CGCSCCQPDVPAVTVLTTPPAAHL 84
BfMT1           CGCSCCQPDTPAVAILTTPPAAHL 84
                *********.***::*********
```

(B)

```
JT872034        GGCACAATCAGTATAAAGCATGGAGCACTGGACACGTCGTCATTTTCCTGCTACGCCACA 60
BfMT2_L         ------------------------------------------------------------

JT872034        GCGCCCTTTGTGTTCGTGACTGTCCCAGACGCTACGAGAAAAGACTGACAAGATGCCAGA 120
BfMT2_L         -------TTGTGTTCGTGACCGCCCAAGACACTACGAGGAAAGACTGACAAGATGCCAGA 53
                        ************* * **.****.*******.********************

JT872034        CCCCTGCTGCTCTGCCTGTACTGGATGCTCCACCTCCTGCAAGTCATGTAACTGTGACTG 180
BfMT2_L         TCCCTGCTGTTCCGCTTGTGAGGGATGCTCCAGCACCTGTAACAAATGTAGCTGTGACTG 113
                ******** ** ** ***.. ********** *:**** ** :.*****.*********

JT872034        CTGCAAGTGTTGTGCCTCTTGCACTGGCTGCAGCCCC---AACTGCAACTCATGTGGCTG 237
BfMT2_L         CTGCAAGTGTTGTGCCTCTTGCAAGGCCTGTGGTCCCGCAGCCGACTGCAACTGTGGCTG 173
                ************************. * *** .* ***   ..* .*:.*:..********

JT872034        TGACTGCTGCAAGTGCTGTGCCTCGTGTGACGGTTGCAAGTCTGGCTGCACCAGCTGTAG 297
BfMT2_L         TGCCTGCTGCAAATGCTGTGCCTCTTGTGATGGATGCAAGTCTAGCTGCACCAGCTGTAG 233
                **.*********.*********** ***** **:*********.****************

JT872034        CTGTGACTGCTGCAAATGAAGGGAAGCAG--ACAAGTACCACAG-------GAG-ACTGC 347
BfMT2_L         CTGTGACTGCTGCAAGTAAGGAGAGACAATCACCAATACCACAGATCTATAGAGGACTGT 293
                ***************.*.*.*.**..**.  **.*.********       *** ****

JT872034        AGCGGACTGGCCAGAATGGACATCAA------CAACACC--GTACATTCCAATACCTAGC 399
BfMT2_L         GGCAGACTGGCTAGTATGGACATCAATGCTATCAGCACCTTGTACATTCCATTATCAAGC 353
                .**.******* **:***********      **.****  **********:** *:***

JT872034        TGGCATGTTATGTTAG--AAGCTTAGCTTTTAATTAT-----------------CTTATA 440
BfMT2_L         CGGAATGTTGTAAAAGCATAGCTTATGTTTCAGTGATGACGTCACAGAGGAAAGCATTTA 413
                 **.*****.*.::**  :******  *** *.* **                 *:*:**

JT872034        TATTACTAT-----TAGTGATACCTGCTACG--CAGTGAAGGATTG--ATGTCT------ 485
BfMT2_L         AATGTCTATGGTGATAGCTAAGCTTGCATTTTTAAGTCTAAGTATCTTCTGTCTGTCCTT 473
                :** :****     ***  *:.* ***::    .*** :*.*::*   .*****

JT872034        ------ATTGTGATGGCACAGCATGCATGCATTTTCAAGTTTAAGTATTTTTCTGTCCTT 539
BfMT2_L         TTAGAATTTATGAATGGAAAAAGAGTAATCAGTATTAAAAAGATGTTTTATTCACATATT 533
                      :**.***: * *.*...:* *: ** *:* **.:: *:**:**:***: : .**

JT872034        ------TTAAAAATCATTTCTGAGATAAAGGAAATC--GGTGTTCAAAATGTTATT-CAG 590
BfMT2_L         GAGTACTATCTACTTAAATGTAAAGCAGAAGATTTCTTGGAGATATAGAAATTATTGAAA 593
                      *::.:*.* *::* *.*.. *.*.**::**  **:*:*.:*.*:.***** .*.

JT872034        ATGAATTCTAGAATTCTCAAATAT------ 614
BfMT2_L         GTGCACTTTATTTTTTTAAAAAGTTGAATG 623
                .**.* * ** ::** *.***:.*


JT872034p       MPDPCCSACTGCSTSCKSCNCDCCKCCASCTGCSP--NCNSCGCDCCKCCASCDG-CKSG 57
BfMT2_L         MPDPCCSACEGCSSTCNKCSCDCCKCCESCKACGPTVGCN-CGCACCKCCSSCVQTCKPG 59
                ********* ***::*:.*.******* **..*.*  .** *** *****:**   **.*

JT872034p       CTSCS-CDCCK 67
BfMT2_L         CTNCPGCDCCK 70
                **.*. *****
```

VII. ARTICLE 7:

Is MtnE, the fifth *Drosophila* metallothionein, functionally distinct from the other members of this polymorphic protein family?

Metallomics, **(2012)**, 4, 342-349.

Metallomics

Cite this: *Metallomics*, 2012, **4**, 342–349

www.rsc.org/metallomics

PAPER

Is MtnE, the fifth *Drosophila* metallothionein, functionally distinct from the other members of this polymorphic protein family?†

Sílvia Pérez-Rafael,‡[a] Antje Kurz,‡[b] Maria Guirola,[b] Mercè Capdevila,[a] Òscar Palacios[a] and Sílvia Atrian*[b]

Received 10th December 2011, Accepted 3rd February 2012
DOI: 10.1039/c2mt00182a

Metallothioneins (MTs) are a super-family of small, Cys-rich, non-homologous proteins that bind metal ions through the formation of metal–thiolate bonds. Although universally ubiquitous, they exhibit distinct metal-binding preferences, either for divalent (Zn-thioneins) or monovalent (Cu-thioneins) metal ions. *Drosophila* constitutes a bizarre exception, since it is currently the only case of metazoans synthesizing only Cu-thioneins, which are similar to the paradigmatic yeast Cup1 protein. Until recently, the *Drosophila* MT system was assumed to be composed of 4 isoforms (*MtnA, MtnB, MtnC* and *MtnD*), all of them responsive to heavy metal load through the dMTF1 transcription factor. The significance of this polymorphism has been analyzed in depth both at genomic and proteomic levels. Singularly, a fifth MT isoform was recently annotated and named MtnE. The analysis of the *MtnE* expression pattern revealed some differential traits with regard to the other MTs. We analyze here the peculiarities of the metal binding abilities of the MtnE polypeptide and compare them with those of the other *Drosophila* MTs determined through the same rationale. Characterization by ESI-MS spectrometry and CD and UV-visible spectrophotometry of the Zn(II)–, Cd(II)– and Cu(I)–MtnE complexes obtained by recombinant synthesis demonstrates that MtnE is the least metal-specific isoform of the *Drosophila* MTs, and therefore it could play a role when/where a *broad spectrum* of metal coordination abilities are advantageous in terms of physiological needs.

1. Introduction

Metallothioneins (MTs) are a super-family of small, non-homologous, metalloproteins that fold about multinuclear metal clusters owing to the formation of metal–thiolate bonds, which occur as a result of their high Cys content (recently reviewed).[1] MTs are universal and ubiquitous, but exhibit distinct metal-binding preferences, either for divalent or monovalent metal ions. This allows their differentiation not only in extreme Zn- and Cu-thioneins,[2] but also in a step-wise gradation of MTs that show a continuum of metal binding behaviors.[3,4] The molecular basis of the observed metal specificity of MTs is not yet well-known, although it is a keystone to understand their structure/function relationship, their physiological function and their differentiation pattern through evolution.[5] In fact, another noteworthy feature of MTs is that they are polymorphic in almost all the taxa of organisms analyzed up to now, a polymorphism that is also difficult to interpret because in many cases it does not correlate with a functional differentiation of the multiple MT forms.[6] In animal phyla, three situations are globally encountered. First, most organisms exhibit different MT isoforms with little or no appreciable differentiation and specialization in their functions and metal-binding preferences, although variations in metal selectivity can exist to some degree. In this case, MTs predominantly exhibit a preference for divalent metal ions, although some isoforms could show better abilities to coordinate monovalent metal ions than the others (*i.e.* a partial copper-thionein character). Vertebrate, and among them, the four mammalian MT isoforms, are the best example of this type of polymorphism.[7] Second, some organisms exhibit MT isoforms with totally differentiated metal-binding preferences, which therefore are easily assignable to specific physiological purposes. These are ideal cases for studying the molecular basis of metal-binding selectivity in MT polypeptides, as they comprise well-differentiated Cd- and Cu-specific isoforms, which are highly similar in the protein sequence. Illustrative examples of this case are the MT systems of pulmonate snails,[4,8] the *Tetrahymena* genus[9] and crustacea.[10] Finally, Cu-thioneins as unique MTs have been reported in a few organisms. These are fungi and yeasts,[11] and exceptionally diptera insecta.[12]

[a] *Departament de Química, Facultat de Ciències, Universitat Autònoma de Barcelona, 08193 Cerdanyola del Vallès, Barcelona, Spain*
[b] *Departament de Genètica, Facultat de Biologia, Universitat de Barcelona, Av. Diagonal 645, 08028 Barcelona, Spain. E-mail: satrian@ub.edu; Fax: +34 934034420; Tel: +34 934021501*

† Electronic supplementary information (ESI) available. See DOI: 10.1039/c2mt00182a

‡ These two authors contributed equally to this work.

In fact *Drosophila*, as a model for diptera, is an exceptional case, as it is the unique metazoan organism synthesizing only Cu-thioneins, similar to the yeast (*S. cerevisiae*) Cup1 paradigmatic Cu-thionein. *D. melanogaster* genome had been reported to contain four *MT* genes (*MtnA*, *MtnB*, *MtnC and MtnD*),[13] which are clustered in the same genomic region, probably arising from amplifying duplications.[12] Recently, this has been shown for all twelve *Drosophila* species whose genome is fully sequenced.[14] The main isoforms, MtnA and MtnB, are peptides 40- and 43-amino acid long, respectively, comprising 10 and 12 cysteines. MtnC and MtnD probably arise from MtnB duplications, and they seem to play a minor role in flies. Expression of the four genes is dependent on dMTF-1, a transcriptional activator homologous to the mammalian MTF-1.[15] Major MT synthesis is observed in the digestive tract of larvae and adults, mainly in the midgut, although with some spatial distribution differences between *MtnA* and *MtnB*. Minor *Mtn* gene expression takes place in salivary glands, ventricula, Malpighian tubules and hemocytes. Invariably, metal induction increases the rate of MT synthesis, the best response being obtained for copper, followed by cadmium, and a very poor response for zinc, so that a definitive role of *D. melanogaster* in copper metabolism (from ingesta to distribution, storage, delivery and detoxification in the organism) as well as in cadmium tolerance (by digestive assimilation blockage) is envisaged. At the protein level, all four *Drosophila* MT isoforms exhibit overlapping, yet distinct properties for the coordination of different heavy metals, as the stoichiometric, spectrometric and spectroscopic features of the copper and cadmium complexes with MtnA and MtnB correlate well with a greater stability of copper–MtnA and cadmium–MtnB. Additionally, MtnC and MtnD display lower copper and cadmium binding capabilities compared to either MtnA or MtnB, which can mainly be explained by the intrinsic instability of the complexes.[16]

Surprisingly, early this year a fifth MT family member was uncovered in the *D. melanogaster* genome through sequence analysis in Prof. Schaffner's lab (University of Zürich). It was subsequently named MtnE, and in fact corresponds to the orphan CG42872 ORF in the FlyBase annotation of the *D. melanogaster* genome. The *D. melanogaster MtnE* gene has recently been characterized at the structural and expression level.[17] It is located inside the MtnB-like cluster of genes, between *MtnB* and *MtnD*, and it is encoded in the opposite strand of the closest *MtnD* gene, so they share a tail-to-tail expression sense. The MtnE coding region is interrupted by a short-type intron, and it encodes a MT polypeptide that can be perfectly aligned to the other MtnB-like proteins (*cf.* Fig. 1). Significantly, in the genomics survey of the MT family in twelve *Drosophila* species,[14] not only the presence of this new *MtnE* gene was confirmed in all the cases, but also identical chromosomal localization—inside the MtnB-like cluster—and gene architecture identical to that described in *D. melanogaster*. As in the other *Mtn* genes, *MtnE* expression is regulated by the metal-regulatory transcription factor 1 (dMTF-1), acting by binding to metal-response elements (MRE), which in this case and due to the peculiar gene divergent situation, is shared with *MtnD*. Consequently, MtnE is synthesized in response to both physiological (zinc or copper) and xenobiotic (cadmium, mercury or silver) heavy metal ions.[17] These authors show that monovalent metal cations (*i.e.* copper and silver) induce higher *MtnE* transcription levels than divalent metal cations, while this expression is always more elevated than for *MtnD*. The tissue expression pattern is similar to that exhibited by the other *Drosophila* MT genes, predominantly significant in the intestine of larvae raised on copper-, but also in cadmium-supplemented food.

Fig. 1 Multiple sequence alignment of all reported *Drosophila melanogaster* MT isoforms, performed as described in Materials and methods.

It has been suggested that MtnE might complement the function of the other MT proteins in *Drosophila*. To gain a deeper insight into the MtnE putative functionality, we present here the characterization of this MT peptide at the protein level, through the study of its amino acid sequence trends and its metal binding abilities, which are compared with those of the other four members of the *Drosophila* MT family. A combination of this information with the previously reported data at the gene level should provide new clues for the functional assignment of MtnE and for interpretation of the MT polymorphism present in the *Drosophila* genus.

2. Experimental

2.1. MtnE cDNA cloning in the pGEX-4T1 expression vector

The *MtnE* cDNA was inserted into the pGEX-4T2 expression vector (GE Healthcare) to obtain the corresponding product as a GST-fusion protein. The MtnE coding sequence was subcloned into the *BamH*I/*Sal*I sites of the vector, which allows the presence of a thrombin digestion site just preceding the region corresponding to the MtnE peptide in the fusion construct. As explained in the next section, this will allow the recovery and analysis of the MtnE peptide devoid of the GST tag. The two restriction sites were, respectively, added to the 5′ and 3′ ends of the cDNA sequence by PCR amplification, using the following oligonucleotides as primers: 5′-CCCGGATCCATGCCTTGCAAG-3′ (forward) and 5′-CCCGTCGACTCACTTGGCCTG-3′ (reverse). This cloning procedure was performed for us in Prof. W. Schaffner's lab (University of Zurich) following our indications. The MtnE–pGEX clone was sequenced in our premises using the Big Dye Terminator 3.1 Cycle Sequencing Kit (Applied Biosystems) in an Applied Biosystems ABIPRISM 310 Automatic Sequencer.

2.2. Recombinant synthesis and purification of Zn–, Cd– and Cu–MtnE and preparation of *in vitro*-substituted complexes

The MtnE–GST fusion polypeptides were biosynthesized in 5 L cultures of transformed *E. coli* cells (BL21 strain). Expression was induced with isopropyl β-D-thiogalactopyranoside (IPTG) and cultures were supplemented with 500 μM $CuSO_4$, 300 μM $ZnCl_2$ or 300 μM $CdCl_2$, final concentrations, and they were allowed to grow for a further 3 h. Cu-supplemented cultures were grown either under normal aeration conditions (1 L of media in a 2 L Erlenmeyer flask, at 250 rpm) or under low oxygen conditions (1.5 L of media in a 2 L Erlenmeyer flask, at 150 rpm),

since different results have been reported for some MTs depending on the aeration conditions of the cultures.[18] The total protein extract was prepared from these cells as previously described for the MtnA and MtnB *Drosophila* MT isoforms.[19,20] Metal complexes were recovered from the MtnE–GST fusion constructs by thrombin cleavage and batch-affinity chromatography using Glutathione-Sepharose 4B (General Electric HC). After concentration using Centriprep Microcon 3 (Amicon), the metal complexes were finally purified through FPLC in a Superdex75 column (General Electric HC) equilibrated with 50 mM Tris–HCl, pH 7.5. Selected fractions were confirmed by 15% SDS-PAGE and kept at −80 °C until further use. All procedures were performed using Ar (pure grade 5.6) saturated buffers, and all syntheses were performed at least twice to ensure reproducibility. As a consequence of the cloning requirements, the dipeptide Gly-Ser was present at the N-terminus of the MtnE polypeptides; however, this had previously been shown not to alter the MT metal-binding capacities.[21] *In vitro*-substituted Cd–MtnE and Cu–MtnE complexes were obtained by titration of the Zn–MtnE preparation with Cd(II) or Cu(I) at pH 7, using $CdCl_2$ or $[Cu(CH_3CN)_4]ClO_4$ solutions, respectively, as previously described.[21,22] During all experiments strict oxygen-free conditions were maintained by saturating all the solutions with Ar.

2.3. Spectroscopic analyses of the metal–MtnE complexes

The S, Zn, Cd and Cu content of the Zn–, Cd– and Cu–MtnE preparations was analyzed by means of Inductively Coupled Plasma Atomic Emission Spectroscopy (ICP-AES) in a Polyscan 61E (Thermo Jarrell Ash) spectrometer, measuring S at 182.040 nm, Zn at 213.856 nm, Cd at 228.802 and Cu at 324.803 nm. Samples were treated as previously described,[23] but were alternatively incubated in 1 M HCl at 65 °C for 15 min prior to measurements in order to eliminate possible traces of labile sulfide ions, as otherwise described for S^{2-}-containing metal–MT complexes.[24] Protein concentrations were calculated from the *acid* ICP-AES sulfur results, assuming that all S atoms were contributed by the MT peptide. A Jasco spectropolarimeter (Model J-715) interfaced to a computer (J700 software) was used for CD measurements at a constant temperature of 25 °C maintained by a Peltier PTC-351S apparatus. Electronic absorption measurements were performed on an HP-8453 diode array UV-visible spectrophotometer. All spectra were recorded with 1 cm capped quartz cuvettes, corrected for dilution effects and processed using the GRAMS 32 program.

2.4. ElectroSpray Ionization Mass Spectrometry (ESI-MS) analyses of the metal–MtnE complexes

Electrospray ionization time-of-flight mass spectrometry (ESI-TOF MS) was applied to assess the molecular mass of the metal–MtnE complexes. The equipment used was a Micro Tof-Q instrument (Bruker) interfaced with a Series 1200 HPLC Agilent pump, equipped with an autosampler, all of them controlled by the Compass Software. Calibration was attained with 0.2 g of NaI dissolved in 100 mL of a 1 : 1 H_2O : isopropanol mixture. Samples containing MtnE complexes with divalent metal ions were analyzed under the following conditions: 20 μL of protein solution injected through a PEEK (polyether heteroketone) column (1.5 m × 0.18 mm id), at 40 μL min^{-1}; capillary counter-electrode voltage 5 kV; desolvation temperature 90–110 °C; dry gas 6 L min^{-1}; spectra collection range 800–2500 m/z. The carrier buffer was a 5 : 95 mixture of acetonitrile : ammonium acetate/ammonia (15 mM, pH 7.0). Alternatively, the Cu–MtnE samples were analyzed as follows: 20 μL of protein solution injected at 40 μL min^{-1}; capillary counter-electrode voltage 3.5 kV; lens counter-electrode voltage 4 kV; dry temperature 80 °C; dry gas 6 L min^{-1}. Here, the carrier was a 10 : 90 mixture of acetonitrile : ammonium acetate, 15 mM, pH 7.0. For analysis of apo-MtnE and Cu–MtnE preparations at acidic pH, 20 μL of the corresponding sample were injected under the same conditions described previously, but using a 5 : 95 mixture of acetonitrile : formic acid, pH 2.4, as liquid carrier, which caused the complete demetalation of the peptides loaded with Zn(II) or Cd(II) but kept the Cu(I) ions bound to the protein.

3. Results and discussion

3.1. The MtnE peptide

DNA sequencing of the MtnE coding portion in the expression construct ruled out the presence of any artifactual nucleotide substitution. The SDS-PAGE of total protein extracts from pGEX–*MtnE*-transformed BL-21 cells showed the presence of a band of the GST–MtnE expected size (approx. 31 kDa). Homogeneous metal–MtnE preparations (final concentration of 2.1×10^{-4} M for Zn–MtnE, 0.2×10^{-4} M for Cd–MtnE, and 1.0×10^{-4} M for Cu–MtnE) were obtained from 5 L *E. coli* cultures. Acidification of the Zn–MtnE complexes yielded the corresponding apo-form, with a molecular mass of 4131.6 Da in accordance with the calculated average theoretical value (4132.4) for the synthesized product. This confirmed both the identity and integrity of the recombinant MtnE polypeptide (Fig. 1).

The analysis of the MtnE protein sequence revealed unique features when compared to the other four isoforms. First, the whole alignment clearly demonstrates that MtnE belongs to the MtnB-like isoforms, constituting the MtnB-like cluster with MtnB, MtnC and MtnD. This is confirmed by the close genomic situation of the corresponding encoding genes,[17] which is fully consistent with duplication events followed by chromosomal rearrangements as an explanation of their origin.[12] But significantly, the number of cysteines, the residues responsible for the formation of metal–thiolate bonds in metal–MT clusters, is 10 (as in the MtnA isoform) and not 12 as typical of the MtnB-like family, owing to the replacement of Cys23 and Cys31 with Gly and Ala respectively (*cf.* Fig. 1). Therefore, MtnA and MtnE share the same number of Cys, but some at different positions, which poses the question concerning how sequence traits (number *vs.* position of coordinating residues) may influence the metal-binding abilities of an MT peptide.

3.2. Zn and Cd binding abilities of MtnE

The MtnE polypeptide produced by Zn-supplemented *E. coli* cells mainly folded into Zn_3–MtnE complexes (*cf.* the major peak in the ESI-MS spectrum shown in Fig. 2A and Table S1, ESI†), although some minor Zn_4–MtnE species, together with

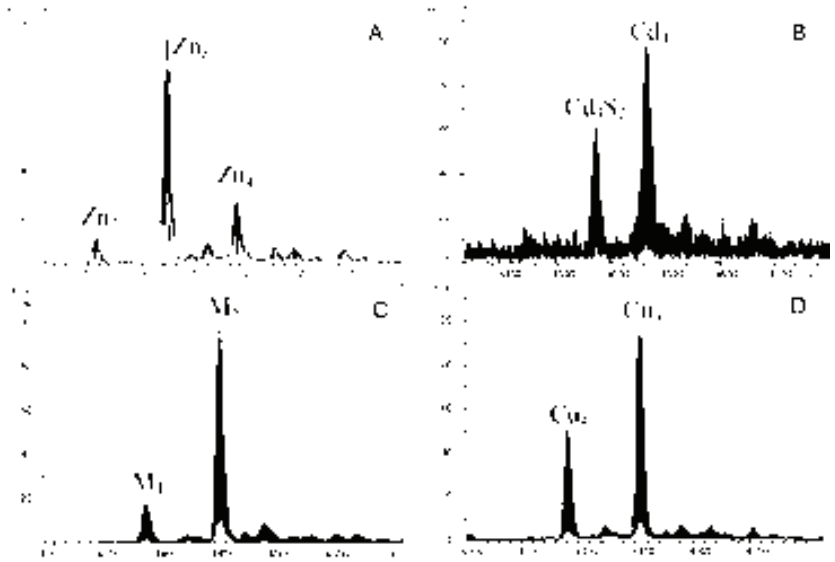

Fig. 2 Deconvoluted ESI-MS spectra corresponding to the *in vivo* preparations of MtnE from bacterial cultures grown in (A) Zn-, (B) Cd- and (C and D) Cu-supplemented media under normal aeration conditions, in this case, analyzed at (C) neutral pH and (D) pH 2.4.

frequent NH_4 adducts, were also detected in the corresponding preparations. These samples were almost silent to CD (Fig. 3A), a common feature among the Zn-complexes of the other *Drosophila* MT isoforms.[16] Interestingly, acidification and reneutralization of these samples reversed the abundance ratios between the Zn_3– and Zn_4–MtnE species, without changes in the CD spectra (data not shown).

The synthesis of MtnE in Cd-supplemented media rendered two main species (according to ICP-AES and ESI-TOF-MS data): Cd_4–MtnE as the major complex and Cd_3S_2–MtnE, with an ESI-MS peak about half of the intensity of the former (Fig. 2B and Table S1, ESI†). The presence of sulfide-containing species was confirmed by the corresponding ICP measurements, in which the S content proved to be significantly different depending on whether or not the sample had been subjected to acid treatment prior to analysis.[24] Additionally, the recombinant Cd–MtnE preparation exhibited the typical CD profile of samples including species with both Cd–SCys and Cd–S^{2-} binding motifs, absorbing at *ca.* 250 nm and *ca.* 300 nm respectively (Fig. 3B).[24] These CD features suggest a specific folding around the Cd(II) ions different from that observed in the other *Drosophila* MT isoforms (*cf.* Fig. 3B).

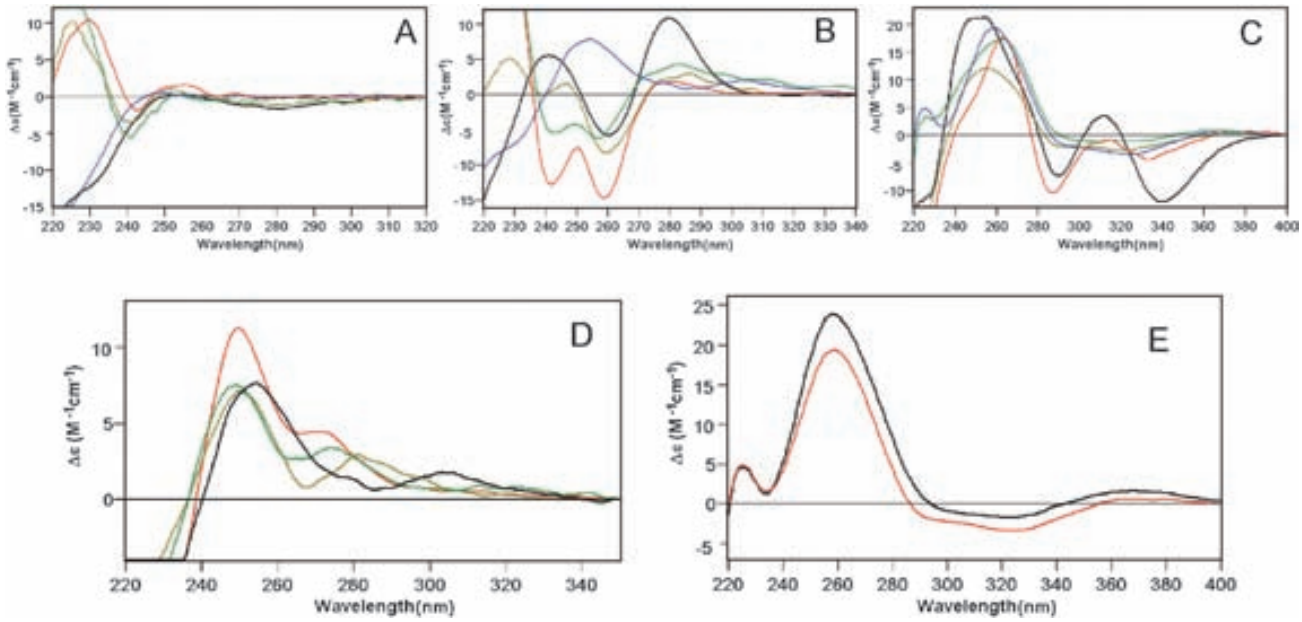

Fig. 3 CD spectra of the five *D. melanogaster* MT isoform preparations obtained from (A) Zn-, (B) Cd-, and (C) Cu-supplemented bacterial cultures. Colors in A, B and C correspond to: MtnA (black), MtnB (red), MtnC (green), MtnD (khaki), and MtnE (blue). (D) Comparison of the CD spectra of the *in vivo* Cd–MtnE preparation (black), Zn–MtnE + 4 Cd(II) eq. (red), *in vivo* Cd–MtnE after acidification/reneutralization (green) and after addition of 2 eq. of Na_2S (khaki). (E) Comparison of the CD spectra of the *in vivo* Cu–MtnE preparation obtained under normal aeration conditions (red) with the CD spectra recorded after addition of 6 Cu(I) eq. to Zn–MtnE (black) at neutral pH.

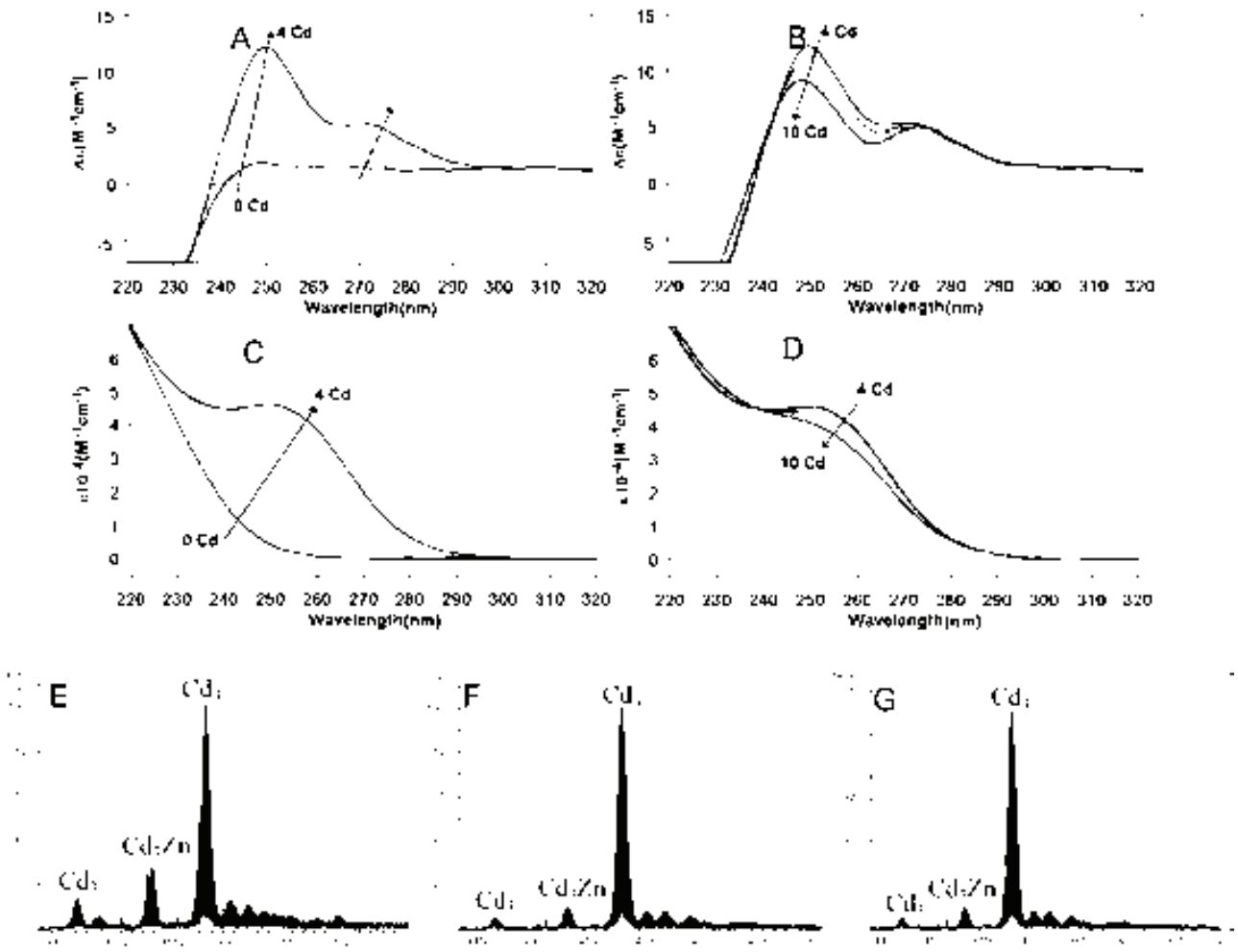

Fig. 4 CD (A, B) and UV-vis spectra (C, D) corresponding to the titration of a 20 μM solution of the Zn–MtnE preparation with $CdCl_2$ at neutral pH after the addition of (A, C) up to 4 Cd(II) eq. and (B, D) up to 10 Cd(II) eq. (E–G) Deconvoluted ESI-MS spectra corresponding to aliquots extracted at different stages of the titration of a 20 μM solution of Zn–MtnE with $CdCl_2$ at neutral pH after the addition of (E) 3, (F) 5 and (G) and 10 Cd(II) eq.

The results of the Zn(II)/Cd(II) displacement reaction in MtnE (Fig. 4 and Table S1, ESI†) confirmed the assignment made for the *in vivo*-folded Cd–MtnE complexes, since the spectroscopic features saturated for 4 Cd(II) eq. added to Zn–MtnE yielding a CD fingerprint with absorptions centered at *ca.* 250 nm and *ca.* 270 nm. From this point, and even after 10 Cd(II) eq. were added, the CD spectrum showed no further significant evolution. Consequently, the CD envelop of the Cd–MtnE species resulting from the Zn(II)/Cd(II) replacement did not reproduce the absorption at 300 nm observed in the *in vivo* Cd–MtnE (Fig. 3D) and attributed to the Cd–S^{2-} chromophores. The shoulder at *ca.* 270 nm, which could be a consequence of a minor presence of Cd–S^{2-} bonds,[24] might be attributed to an undetectable presence of S^{2-} ligands in the Zn–MtnE preparation, low enough to impair generating the CD features (*i.e.* number and type of chromophores) of those Cd–S^{2-} entities conformed in the *in vivo* Cd–MtnE preparations. ESI-MS analyses of the Zn(II)/Cd(II) replacement products on MtnE, at 3, 5 and 10 Cd(II) eq. added (Fig. 4E–G and Table S1, ESI†), revealed a Cd_4–MtnE stoichiometry similar to that of the recombinant preparation, although the presence of a minor Cd_3Zn_1–MtnE species, instead of the Cd_3S_2–MtnE detected *in vivo*, is observed. Under a high excess of Cd(II), Cd_4–MtnE was revealed as the most favored species, and in no case complexes exceeding four Cd(II) ions were detected. Significantly, a Zn(II) ion appeared as reluctant to Cd(II) replacement in a subpopulation of complexes, which did not change ESI-MS intensity beyond 5 Cd(II) eq. added, and clearly persisted even at 10 eq. Cd(II) added (Fig. 4G and Table S1, ESI†). Finally, in order to confirm the participation of S^{2-} ligands in the species present in recombinant Cd–MtnE preparation, this was acidified to pH lower than 1, to liberate the putatively present acid-labile S^{2-} ligands, and it was afterwards reneutralized. The resulting species exhibited a close CD profile to those registered during the Cd(II) titration of the Zn–MtnE preparation (Fig. 3D). Here, the subsequent addition of S^{2-} anions to the sample promoted a slight red shift of the 270 nm absorption without reaching the CD features of the *in vivo* sample. Therefore, it can be stated that the characteristic chromophores, of the *in vivo* Cd–MtnE complexes, are only formed *in vivo* when enough S^{2-} is available in the surrounding media.

3.3. Cu binding abilities of MtnE

We routinely perform two kinds of Cu-supplemented cultures, at standard and at low aeration, due to the observed influence

of this factor on the *E. coli* copper internal levels, which in turn could determine the composition of the synthesized Cu-complexes.[18] Unfortunately, the three attempts at purification of MtnE from bacterial cultures grown under low aeration conditions were unsuccessful. On the contrary, the productions carried out at regular aeration yielded preparations, which were readily analyzed by CD and ESI-MS. The CD profile of Cu–MtnE closely resembles those recorded for the other *D. melanogaster* Cu–MT preparations (Fig. 3C), especially MtnC and MtnD, thus suggesting a similar folding of all of them when binding Cu(I) *in vivo*. The mass spectra of the Cu–MtnE sample run at neutral pH exhibited a clear major peak corresponding to a M_5–MtnE complex (Fig. 2C and Table S1, ESI†), and a minor peak, attributable to M_4–MtnE species (namely Cu_4–MtnE when analyzing the isotopic pattern of the peak), where M can be either Zn(II) or Cu(I), due to the proximity of their atomic mass. When the sample was analyzed at pH 2.4, which causes the loss of all Zn(II) ions but not of Cu(I) from the complexes, two peaks corresponding to the homonuclear Cu_5–MtnE (major) and Cu_4–MtnE (minor) complexes were observed (Fig. 2D and Table S1, ESI†), the relative intensity of which had clearly varied. The most straightforward explanation for these results is that the M_5–MtnE peak observed at neutral pH corresponds to a mixture of homonuclear Cu_5–MtnE complex and heteronuclear Cu_4Zn_1–MtnE species, which is consistent with the ICP-AES results for the total metal content of the preparations (4.7 Cu : 0.8 Zn).

The stepwise addition of Cu(I) to Zn–MtnE renders interesting information on the Cu(I) binding abilities of this *Drosophila* MT isoform. Initially, below 6 Cu(I) eq. added, the Zn(II)/Cu(I) displacement process takes place both isosbestically and isodichroically, therefore suggesting a cooperative metal replacement reaction. This hypothesis is confirmed by the ESI-MS data, which reveals that the major Zn_3–MtnE species is directly converted into the Cu_4– and Cu_5–MtnE complexes. These increase their abundance with the incoming Cu(I), while the Zn_3- (pH 7)/apo- (pH 2.4) disappears (Fig. 5 and Table S1, ESI†). Exactly for 6 Cu(I) eq. added, the *in vitro* experiment perfectly reproduces the features observed for the recombinant Cu–MtnE preparation, namely the same CD fingerprint (Fig. 3E), and the same speciation (Fig. 2C, D and Fig. 5 and Table S1, ESI†). Significantly, the addition of further Cu(I) equivalents causes a loss of the CD signals, which is compatible with an unfolding of the Cu–MtnE complexes. This is readily evident for more

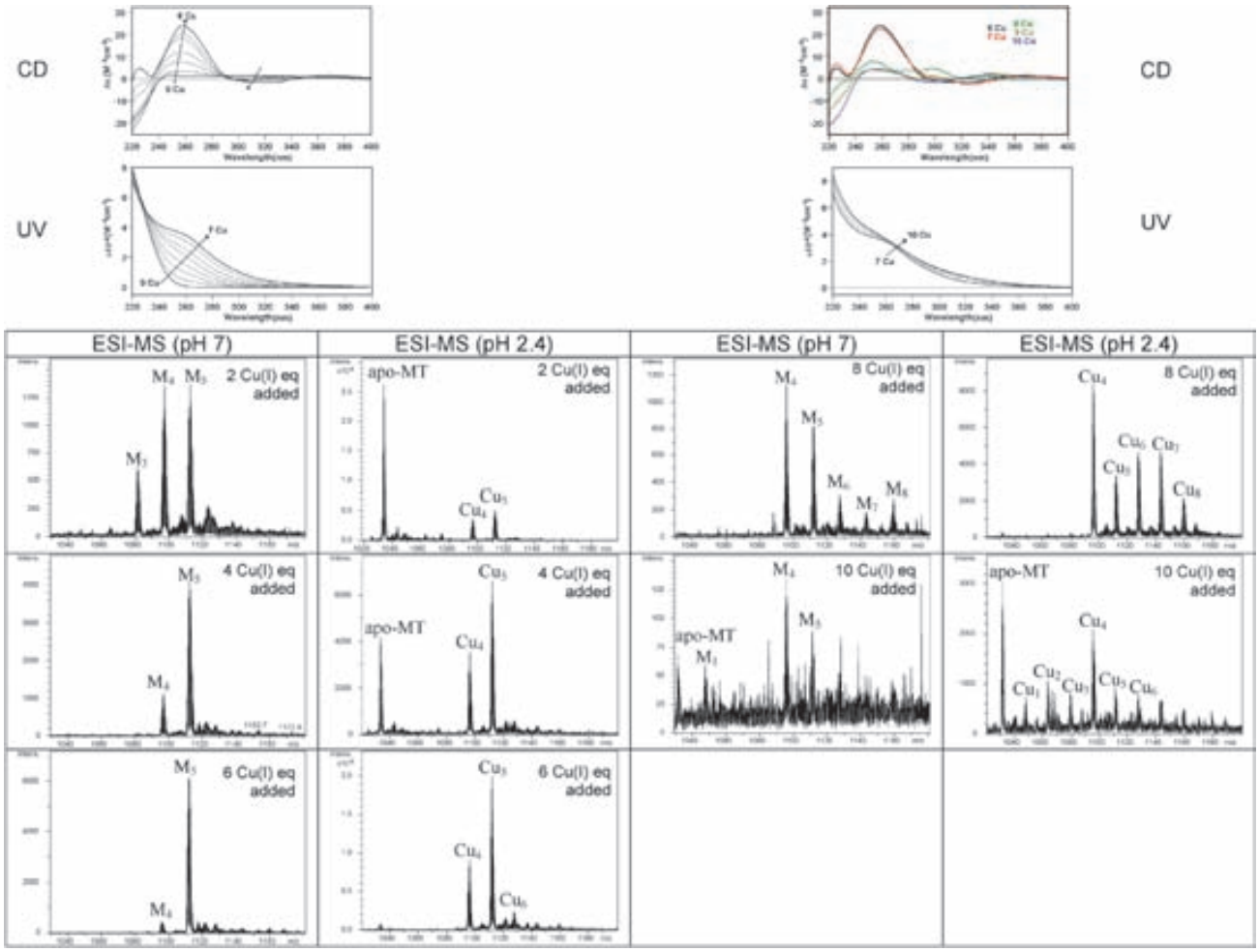

Fig. 5 CD and UV-vis spectroscopic features obtained from the titration of a 20 μM solution of the Zn–MtnE preparation with Cu(I) at neutral pH and ESI-MS data obtained at different stages of this titration, both at neutral and acidic pH. The +3 charge state is shown for pH 7 while the +4 charge state is shown for pH 2.4.

than 8 Cu(I) eq. added (Fig. 5 and Table S1, ESI†). At this step, the ESI-MS results show that after total conversion of Zn_3– into Cu_4– and Cu_5–MtnE, these latter species evolve to become complexes of higher Cu-to-MT stoichiometry (Cu_6– to Cu_8–MtnE), and afterwards to unfolded apo-MtnE. This observation fully explains the impossibility of recovering Cu–MtnE complexes from the bacterial cells grown at low-aerated cultures, and therefore with high levels of internal Cu(I) ions. Significantly, the same effect has been recently described for the mollusc *Megathura crenulata* MT.[25]

4. Conclusions: consideration of MtnE metal binding features in the context of the *Drosophila* MT system

The characterization of *MtnE at* the gene level[17] already highlighted some differential expression features of this fifth member of the *Drosophila* MT system. Significantly, its transcription appeared enhanced in response to a wide range of metals (silver, mercury and zinc) and not only to cadmium and copper, and also its expression in L1 larvae reached values equivalent to those for *MtnB*, and much higher than those for *MtnC* and *MtnD*, considered as subsidiary forms. All these data support not only the fact that *MtnE* is an active gene, but also that the corresponding product may carry out specific functions in the organisms, at least during some developmental stages. The conservation of the MtnE sequence among 12 *Drosophila* species adds further support to functional significance.[14]

The global consideration of MtnE metal binding features analyzed in this work enables it to be classified as a copper-thionein of intermediate (*i.e.* non-extreme) character.[3] In fact, and for several reasons discussed herein, it could be considered the metallothionein with the least Cu-thionein character among all the *Drosophila* MT peptides. It is worth remembering that the MtnB-like isoforms were already characterized as "less Cu-preferent" than MtnA[16] but MtnE is even more distant from MtnA in metal-ion preferences than the rest of their close relatives.

Zn(II) coordination appears to proceed differently whether considering the species rendered by the *in vivo* coordination of Zn(II) to the peptide (Zn_3–MtnE as major species) or the *in vitro* folding of the MtnE apo-form about Zn(II) (major Zn_4–MtnE). This could be easily explained assuming that Zn(II) binding to MtnE may begin even before the end of the translation process, thus preventing the formation of the fourth metal coordination site, if it is contributed by cysteines situated far in the polypeptide sequence. The *in vivo* Zn(II) binding capacity of MtnE is lower than that of the other MtnB-like isoforms (*cf.* Table 1), which was to be expected due to the lack of 2 out of the 12 Cys of these isoforms, but it is also lower than that of MtnA, an MT also with 10 Cys. These observations once again confirm that the number of putatively binding residues (cysteines) is not the only determinant for metal ion coordination, but that the location of these amino acids in the MT sequence as well as their situation in precise motifs are also important. Hence, 8 out of the 10 Cys of MtnA are in four Cys-X-Cys motifs, while in the MtnE this motif is present only once. In fact, two Cys-X-Cys motifs are lost in MtnE owing to the Cys/Gly and Cys/Ala replacements in its sequence. These MtnE sequence features may be related to the singularity exhibited by this peptide in relation to what could be denominated the "fourth divalent metal site". The Cd(II) coordination ability of MtnE yielded further information about it. The Cd(II) binding capacity of MtnE allows a major Cd_4–MtnE species, but this stoichiometry is never exceeded as was the case for the other MtnB-like MTs (*cf.* Table 1).[12] Conversely, a significant Cd_3S_2–MtnE species is produced *in vivo*, thus with an equivalent stoichiometry to that of the Zn_3–MtnE species, but with the support of additional ligands: two sulfide anions. Therefore again, the coordination of the fourth divalent metal ion (here Cd(II)) seems to exhibit a peculiar behavior, which is supported by further experimental observations such as: (i) the maintenance of a subpopulation of Cd_1–MtnE species even after the

Table 1 Comparison of the metal-binding features of the five *Drosophila* metallothionein peptides. Metal content and major species of the MtnA–, MtnB–, MtnC–, MtnD– and MtnE–metal (in bold) complexes recovered from recombinant synthesis in transformed *E. coli* cultures. Data for MTs other than MtnE were first published in the following references: MtnA,[19] MtnB,[20] and MtnC and MtnD[16]

	Zn (300 μM final)				
Supplemented metal in culture	MtnA	MtnB	MtnC	MtnD	**MtnE**
Metal/Mtn content[a]	3.5 Zn	3.7 Zn	3.9 Zn	3.8 Zn	**3.3 Zn**
Metal–Mtn species[b]	$Zn_4 > Zn_3$	$Zn_4 > Zn_5$	$Zn_4 > Zn_5$	$Zn_4 > Zn_5$	$\mathbf{Zn_3 \gg Zn_4}$
	Cd (300 μM final)				
Supplemented metal in culture	MtnA	MtnB	MtnC	MtnD	**MtnE**
Metal/Mtn content[a]	3.8 Cd	4.1 Cd	2.3 Cd	2.0 Cd	**4.69 Cd**
Metal–Mtn species[b]	$Cd_4 > Cd_3 \approx Cd_4S_2$	$Cd_4 \approx Cd_4S > Cd_5 \approx Cd_5S$	$Cd_4 > Cd_5$	Cd_5	$\mathbf{Cd_4 > Cd_3S_2}$
	Cu (500 μM final)				
Supplemented metal in culture	MtnA	MtnB	MtnC	MtnD	**MtnE**
Metal/Mtn content[a]	7.0 Cu	8.9 Cu	4.2 Cu	5.3 Cu	**4.7 Cu/0.8 Zn**
Metal–Mtn species[b]	$Cu_8 > Cu_7$	$Cu_9 > Cu_8$	$Cu_5 > Cu_6$	$Cu_5 > Cu_6$	$\mathbf{Cu_5 > Cu_4Zn_1 > Cu_4}$

[a] Metal per Mtn molar ratio calculated from the zinc, cadmium and copper and sulfur content measured by acid ICP-AES. The four elements were quantified in all the samples, but only detectable contents are shown in the table. [b] Metal per Mtn molar ratio calculated from the difference between holo- and apoprotein molecular masses, obtained from ESI-MS.

acidification of the recombinant Cd–MtnE sample at pH 2.0 (data not shown); (ii) the persistence of a Zn_1Cd_3–MtnE species at the end of the Zn(II)/Cd(II) exchange process; and (iii) the fact that the highest degree of folding for the Cd(II)–MtnE complexes was reached after the addition of 3 to 4 Cd(II) eq. to Zn(II)–MtnE.

Although assuming the Cu-thionein character of the MtnE peptide conferred by its ability to fold into homometallic copper-complexes, the first striking feature is its diminished Cu-binding capacity in relation to the main isoforms (MtnA and MtnB), showing Cu-to-MT stoichiometries similar to those observed for the secondary MtnC and MtnD forms (*cf.* Table 1). Furthermore, the Cu–MtnE preparations show the unmistakable presence of heterometallic species (Cu_4Zn_1–MtnE) accompanying the major Cu_5–MtnE, and a notable instability towards excess Cu(I), which results in the unfolding of the protein. The analysis of the sequence of the MtnB-like peptides renders no obvious conclusions for the radically different Cu-coordination behavior of MtnE in relation to MtnB, the only apparent putative reason being the presence of a bulky amino acid at position 15 in MtnB (Gln) which is a Thr or Gly in the other cases, and a positive charge contributed by Lys25, which is absent in MtnC, MtnD and MtnE. Finally, the presence of a significant portion of complexes including one Zn(II) ion when MtnE is synthesized by Cu-supplemented bacteria could also support the role of the 4th divalent metal site.

To conclude, the study of the metal binding abilities of MtnE allows a clear differentiation not only from MtnA (the most pronounced "Cu-thionein" *Drosophila* MT), but also from its closest paralogues (MtnB-like MTs), with a diminished Cu coordination capacity and a particular site for the allocation of a divalent metal ion, which could remain deeply buried in view of its reluctance to be exchanged. In view of these features, MtnE would be the *Drosophila* MT with a broadest metal ion binding capacity (*i.e.* the less specific) and this nicely correlates with some observations made at the gene level study. Precisely, MtnE is more widely expressed in flies than the other isoforms, and it is also less responsive to copper induction.[17] Therefore, the *MtnE* expression profile, especially outstanding in the late-embryo and larval stages, could serve the need for a "broad spectrum metal-preferent MT peptide".

Acknowledgements

This work was supported by the Spanish "Ministerio de Ciencia e Innovación" (MICINN) grants BIO2009-12513-C02-01 to S. A. and BIO2009-12513-C02-02 to M. C. These coordinated projects were co-financed by the European Union, through the FEDER program. The authors from the *Universitat de Barcelona* and the *Universitat Autònoma de Barcelona* are members of the 2009SGR-1457 "*Grup de Recerca de la Generalitat de Catalunya*". M. G. is recipient of a MAE-AECID fellowship, and A. K. was recipient of a *Leonardo da Vinci* grant covering the expenses of her stay in the *Universitat de Barcelona* lab. We are deeply grateful to W. Schaffner and O. Georgiev (University of Zurich) for, respectively, informing us of the existence of the *MtnE* gene, and for performing the cloning of its cDNA into the vector used in this work. We thank the *Serveis Científico-Tècnics de la Universitat de Barcelona* and the *Servei d'Anàlisi Química de la Universitat Autònoma de Barcelona* for allocating instrument time.

References

1 M. Capdevila, R. Bofill, O. Palacios and S. Atrian, *Coord. Chem. Rev.*, 2012, **256**, 46–52.
2 M. Valls, R. Bofill, R. Gonzalez-Duarte, P. Gonzalez-Duarte, M. Capdevila and S. Atrian, *J. Biol. Chem.*, 2001, **276**, 32835–32843.
3 R. Bofill, M. Capdevila and S. Atrian, *Metallomics*, 2009, **1**, 229–234.
4 O. Palacios, A. Pagani, S. Perez-Rafael, M. Egg, M. Höckner, A. Brandstätter, M. Capdevila, S. Atrian and R. Dallinger, *BMC Biol.*, 2011, **9**, 4.
5 O. Palacios, S. Atrian and M. Capdevila, *JBIC, J. Biol. Inorg. Chem.*, 2011, **16**, 991–1009.
6 M. Capdevila and S. Atrian, *JBIC, J. Biol. Inorg. Chem.*, 2011, **16**, 977–989.
7 M. Vasak and G. Meloni, *JBIC, J. Biol. Inorg. Chem.*, 2011, **16**, 1067–1078.
8 M. Höecker, R. Dallinger and R. Stürzenbaum, *JBIC, J. Biol. Inorg. Chem.*, 2011, **16**, 1057–1065.
9 J. C. Gutierrez, F. Amaro, S. Diaz, P. de Francisco, L. L. Cubas and A. Martín-Gonzalez, *JBIC, J. Biol. Inorg. Chem.*, 2011, **16**, 1025–1034.
10 L. Vergani, in *Metal Ions in Life Sciences: Metallothioneins and Related Chelators*, ed. A. Sigel, H. Sigel and R. K. O. Sigel, RSC Publishing, Cambridge, UK, 2009, vol. 5, pp. 199–238.
11 B. Dolderer, H. J. Hartmann and U. Weser, in *Metal Ions in Life Sciences: Metallothioneins and Related Chelators*, ed. A. Sigel, H. Sigel and R. K. O. Sigel, RSC Publishing, Cambridge, UK, 2009, vol. 5, pp. 83–106.
12 S. Atrian, in *Metal Ions in Life Sciences: Metallothioneins and Related Chelators*, ed. A. Sigel, H. Sigel and R. K. O. Sigel, RSC Publishing, Cambridge, UK, 2009, vol. 5, pp. 155–181.
13 D. Egli, H. Yepiskoposyan, A. Selvaraj, K. Balamurugan, R. Rajaram, A. Simons, G. Multhaup, S. Mettler, A. Vardanyan, O. Georgiev and W. Schaffner, *Mol. Cell. Biol.*, 2006, **26**, 2686–2696.
14 M. Guirola, Y. Naranjo, M. Capdevila and S. Atrian, *J. Inorg. Biochem.*, 2011, **105**, 1050–1059.
15 K. Balamurugan and W. Schaffner, in *Metal Ions in Life Sciences: Metallothioneins and Related Chelators*, ed. A. Sigel, H. Sigel and R. K. O. Sigel, RSC Publishing, Cambridge, UK, 2009, vol. 5, pp. 31–49.
16 D. Egli, J. Domenech, A. Selvaraj, K. Balamurugan, H. Hua, M. Capdevila, O. Georgiev, W. Schaffner and S. Atrian, *Genes Cells*, 2006, **11**, 647–658.
17 L. Atanesyan, V. Günther, S. E. Celniker, O. Georgiev and W. Schaffner, *JBIC, J. Biol. Inorg. Chem.*, 2011, **16**, 1047–1056.
18 A. Pagani, L. Villarreal, M. Capdevila and S. Atrian, *Mol. Microbiol.*, 2007, **63**, 256–269.
19 M. Valls, R. Bofill, N. Romero-Isart, R. Gonzalez-Duarte, J. Abian, M. Carrascal, P. Gonzalez-Duarte, M. Capdevila and S. Atrian, *FEBS Lett.*, 2000, **467**, 189–194.
20 J. Domenech, O. Palacios, L. Villarreal, P. Gonzalez-Duarte, M. Capdevila and S. Atrian, *FEBS Lett.*, 2003, **533**, 72–78.
21 N. Cols, N. Romero-Isart, M. Capdevila, B. Oliva, P. Gonzàlez-Duarte, R. Gonzàlez-Duarte and S. Atrian, *J. Inorg. Biochem.*, 1997, **68**, 157–166.
22 R. Bofill, O. Palacios, M. Capdevila, N. Cols, R. González-Duarte, S. Atrian and P. González-Duarte, *J. Inorg. Biochem.*, 1999, **73**, 57–64.
23 J. Bongers, C. D. Walton, D. E. Richardson and J. U. Bell, *Anal. Chem.*, 1988, **60**, 2683–2686.
24 M. Capdevila, J. Domenech, A. Pagani, L. Tio, L. Villarreal and S. Atrian, *Angew. Chem., Int. Ed.*, 2005, **44**, 4618–4622.
25 S. Pérez-Rafael, A. Mezger, B. Lieb, R. Dallinger, M. Capdevila, O. Palacios and S. Atrian, *J. Inorg. Biochem.*, 2011, DOI: 10.1016/j.jinorgbio.2011.11.025.

Is MtnE, the fifth *Drosophila* metallothionein, functionally distinct from the other members of this polymorphic protein family?

Sílvia Pérez-Rafael, Antje Kurz , Maria Guirola, Mercè Capdevila, Òscar Palacios, Sílvia Atrian

Supplementary material for the manuscript:

Table S1. Experimental *vs.* theoretical molecular masses of the species identified from the ESI-MS spectra shown in Figs. 2, 4 and 5. The error associated to the measurements is always lower than 0.2 % of the molecular mass. M means Cu and/or Zn, as they cannot be distinguished by means of standard ESI-MS).
* Theoretical mass of the Cu-MT species.

Figure	Species (M-MT)	Experimental mass	Theoretical mass
2.A	Zn_3-MT	4322.5	4323.0
	Zn_4-MT	4385.4	4386.4
	Zn_2-MT	4260.3	4259.6
2.B	Cd_4-MT	4574.9	4574.4
	Cd_3S_2-MT	4526.9	4527.4
2.C	M_5-MT	4444.3	4445.5*
	M_4-MT	4382.2	4382.9*
2.D	Cu_5-MT	4444.2	4445.5
	Cu_4-MT	4382.4	4382.9
4.E	Cd_4-MT	4574.0	4574.4
	Cd_3Zn-MT	4526.8	4527.4
	Cd_3-MT	4461.8	4464.0
4.F	Cd_4-MT	4574.8	4574.4
	Cd_3Zn-MT	4526.0	4527.4
	Cd_3-MT	4462.8	4464.0
4.G	Cd_4-MT	4574.0	4574.4
	Cd_3Zn-MT	4526.0	4527.4
	Cd_3-MT	4462.0	4464.0
5 (2 Cu(I) eq added pH 7)	M_5-MT	4444.8	4445.5*
	M_4-MT	4384.8	4382.9*
	M_3-MT	4321.2	4320.4*
5 (2 Cu(I) eq added pH 2.4)	apo-MT	4131.6	4132.8
	Cu_5-MT	4444.4	4445.5
	Cu_4-MT	4381.2	4382.9
5 4 Cu(I) eq added pH 7)	M_5-MT	4444.0	4445.5*
	M_4-MT	4382.8	4382.9*
5 (4 Cu(I) eq added pH 2.4)	Cu_5-MT	4444.4	4445.5
	apo-MT	4132.8	4132.8
	Cu_4-MT	4381.2	4382.9
5 (6 Cu(I) eq added pH 7)	M_5-MT	4442.8	4445.5*
	M_4-MT	4381.0	4382.9*
5 (6 Cu(I) eq added pH 2.4)	Cu_5-MT	4444.2	4445.5
	Cu_4-MT	4380.2	4382.9
	Cu_6-MT	4506.2	4508.0
5 (8 Cu(I) eq added pH 7)	M_4-MT	4379.8	4382.9*
	M_5-MT	4443.8	4445.5*
	M_6-MT	4506.8	4508.0*
	M_8-MT	4632.8	4633.1*
	M_7-MT	4567.6	4570.6*
5 (8 Cu(I) eq added pH 2.4)	Cu_4-MT	4380.4	4382.9
	Cu_6-MT	4507.4	4508.0
	Cu_7-MT	4569.0	4570.6
	Cu_5-MT	4444.2	4445.5
	Cu_8-MT	4633.0	4633.1
5 (10 Cu(I) eq added pH 7)	M_4-MT	4379.2	4382.9*
	M_5-MT	4443.0	4445.5*
	apo-MT	4132.0	4132.8
	M_1-MT	4189.2	4195.3*
5 (10 Cu(I) eq added pH 2.4)	apo-MT	4132.8	4132.8
	Cu_4-MT	4380.2	4382.9
	Cu_2-MT	4255.4	4257.8
	Cu_5-MT	4442.4	4445.5
	Cu_3-MT	4319.6	4320.4
	Cu_1-MT	4191.4	4195.3